THE UNIVERSITY OF CAPE TOWN

Nonlinear Behaviour of Pulsating White Dwarfs

Thesis Presented for the Degree of
DOCTOR OF PHILOSOPHY
in the Department of Astronomy
UNIVERSITY OF CAPE TOWN

François Vuille

May 1999

Acknowledgements

There were many people who somehow, somewhere, had a positive impact on my research, which helped me keep going and kept me sane. Besides buying them rounds at the nearest pub, I also want to take the opportunity here to express my heartfelt thanks to each of them.

To begin with, there are those of you who provided specific help, i.e. a direct scientific interaction. I am grateful to:

Darragh O'Donoghue, for his general supervision of the project. His thorough correction of my write-ups had an enormous impact on my understanding of stellar pulsations and on the quality of my English. He also taught me the art of analysing time series and provided me with his well-written Eagle code for this purpose, which rapidly became my most useful research tool. Darragh also arranged for me to meet several knowledgeable people in the field of pulsating white dwarfs, which turned out to be decidedly crucial when the project was half sinking.

Brian Warner, my co-supervisor, for having unexpectedly proposed this research project to me during my impromptu visit to the University of Cape Town while I was on vacation in South Africa. Brian supervised the logistic side of the project with his efficient and phlegmatic English aplomb.

Scot Kleinman, for having kindly provided me with the data on G29-38 without which there would have been no thesis.

Ed Nather for having provided me with the so fruitful Whole Earth Telescope data on GD358. The analysis of these data sets turned out to make up a major part of the

thesis.

Pawel Moskalik, who certainly is the person who helped me the most by sharing his understanding and knowledge of the nonlinear pulsations. He was always happy to answer my questions and generously agreed to read and comment on my write-ups. I am glad I finally had the chance to meet Pawel during a conference in Norway.

Scot Kleinman, for having invited me to visit him in Iowa and for having shared interest in my research for which he was always keen to give me advice. Scot has not only arranged for me to meet Ed Nather and Don Winget in Texas, but has also managed to obtain the necessary funding for me to travel to the States.

Marie-Jo Goupil who kindly invited me to the Observatoire de Paris to help in finding a direction for this rather challenging research project. Both my visits there have been fruitful in terms of the scientific feed-back I received from Marie-Jo.

Gilles Fontaine, for having taken the time, despite his hectically busy schedule, to answer in detail the numerous questions I have asked him by E-mail.

Pierre Brassard, for sharing interest in my research. The inter- action we had over the E-mail turned into a collaboration from which two publications came. It has been a pleasure working with Pierre, and I hope I will have a chance to meet him sometime.

Mike Montgomery and Paul Bradley, for having kindly provided me with their numerical models.

Atsuko Nitta for having kindly lent me her exciting data on GD358.

Ed Nather, Steve Kawaler, Don Winget, Joregeen Christensen-Dalsgaard, and Mike Montgomery, for very helpful discussions of the possibilities and limitations of the project.

Norman Morisson and Adrian Jongens, from the electrical engineering department for helpful discussions on Fourier analysis and harmonic distortions.

Such a long-term project has no chance of being completed without some necessary financial support. I am indebted to:

The University of Cape Town for having provided me with a 3-year bursary through its postgraduate scholarship office.

The Swiss National Fund of Research for having granted me a one-year "Bourse de Relève Jeune Chercheur" bursary, which financed my final year in Cape Town.

The "Fondation Annaheim" in Villeneuve, Switzerland, for having granted me a 3- year bursary which complemented the one from the University of Cape Town.

The American International Institute of Theoretical and Applied Physics, for having granted me an International Visitor Fund, which allowed me to visit Scot Kleinman and Steve Kawaler at Iowa Sate University, and Ed Nather and Don Winget at Texas State University.

Brian Warner, who dug into his research grant to help me visit Marie-Jo Goupil at the Observatoire de Paris.

The organising committee (in particular Janerik Solheim) of the 11th European Workshop on White Dwarfs, for having provided some financial support which allowed me to participate to this workshop held in Norway in June 1998.

Finally, there are all those people whose not less important implicit interaction allowed me to stay tuned with the outside world, and prevented me from falling into the "crazy scientist trap", despite the last few insane months. I want to thank:

My father, for his deep love of science and for his $upport during the long course of my studies.

My mother, for supporting me in my choice of becoming an astronomer, despite her own preference for astrology...

Don Kurtz for his intransigent views and his states of mind which definitely gave some life to our small department. His controversial opinions were unfortunately always delivered too fast for my poor English to be able to follow. By the time I had an answer ready, he would already be ten arguments ahead. Things will change since he has decided to learn French, which should finally give me some home game advantage!

Mike Feast, for his contagious, everlasting good humor.

Thony Fairall, for sharing insiders' jokes and for trusting me to teach part of his astronomy course while he was away.

Basil Mohamed, for having kept me updated on the rugby scores and for having taught me about fish, i.e. for having implicitly reminded me I was still living on Earth.

Thebe Medupe, Patrick Woudt, Yuri Anderson, Liza Van Zyl, and Sonja Vrielman, for having shared many good laughs amongst astronomy students.

My housemates (and nevertheless friends) Arthur and Mungo, for sharing a great social life.

I kept one person for the end because I could not find the necessary words to express all my gratitude to her. I still can't and never will be able to. Chantal has given me moral support when things were not going well, and confidence when things were going fine. Her love gave me the strength, obstinacy, and guts to complete this research. I am truly happy that she is now my fiancée, and fortunate to be her fiancé.

Abstract

Using a phenomenological approach, I have investigated the nonlinear properties of the pulsations of two white dwarfs, namely DA G29-38 and DB GD358. The data at my disposal comprised numerous single- and multi-sites time series photometric campaigns, including light curves from four Whole Earth Telescope runs conducted respectively in 1988 and 1992 on G29-38, and in 1990 and 1994 on GD358.

Thanks to their length and quality, several of these individual data sets have the beating between the excited eigenmodes resolved. Amplitude changes are nevertheless visible between these various amplitude spectra, suggesting the presence of intrinsic nonlinear processes. However, I showed that only when the spectral changes are drastic have time-dependent nonlinear phenomena to be invoked; no matter how long the data sets, mild seasonal amplitude variations can often be accounted for by beating between the eigenmodes and high order cross-frequencies when harmonic distortion is strong enough. From third order of perturbation, cross-frequencies naturally appear in the direct vicinity of the normal modes, which not only alter the simple eigenmultiplet structures thus rendering the mode identification more difficult, but also generate long and complex beating processes. In GD358, for instance, 153 such third order combination frequencies are expected to appear in the frequency range of each eigentriplet; a light curve spanning at least 9 months is thus necessary to resolve the period structure of this star.

Drastic spectral changes were nevertheless recorded in both G29-38 and GD358 which could not be accounted for by such high order beating processes. I could securely conclude that the pulsations of both these stars experience intrinsic amplitude variations on time-scales ranging from days to years, suggesting that different nonlinear processes dominate the evolution of the pulsations at different time.

G29-38 is a restless star; each time it has been observed, it presented a drastically different period spectrum. Although Kleinman et al. (1998) uncovered an underlying structure of recurrent g-modes, I could not find any periodic pattern in the appearance and disappearance of these modes, although some of them show indication of correlated evolution. Various considerations led to the conclusion that resonant mode coupling, although not strictly excludable, can probably not account for the observed spectral changes. Instead, I invoked the presence of some other nonlinear processes, possibly linked to the pulsation/convection interaction, that would directly affect the driving and the mode selection mechanism in a complex time-dependent manner.

GD358 is a much more stable pulsator. Its temporal spectrum obtained from the 1990 and 1994 WET campaigns look qualitatively very similar. A detailed mode identification has been performed on the 1994 data, which shows that its extremely rich period spectrum (over 70 identified multiplets) is entirely explained in terms of just 6 eigentriplets and their combination frequencies. In particular, this analysis revealed the presence of combination frequencies up to fourth order, i.e. frequencies that are the sum of four frequencies of parent modes.

However, a 1996 campaign on GD358 caught the star in a completely different pulsating state, where first only one, then two, eigenmodes were present, with amplitudes up to 10 times larger than that of any mode observed before. Also, the amplitude spectrum was clearly evolving on a daily time-scale; the fast decrease of the two excited modes allowed their decay rate to be measured, yielding values of $(0.97 \pm 0.12) \times 10^{-5}\,\mathrm{s}^{-1}$ and $(1.45 \pm 0.24) \times 10^{-5}\,\mathrm{s}^{-1}$. Theses quantities may represent linear damping rates, which would then represent the first such measurements in white dwarfs.

The phase spectra of G29-38 and GD358 have also been analysed, which represents the first such investigation for variable white dwarfs. Although the phase of the normal modes cannot be properly monitored from season to season because of inherent cycle count errors, the relative phase of the combination frequencies proved to be a useful measurement; virtually all the nonlinear frequencies identified over the years in the period spectra of these two stars are in phase with (or slightly in advance of) their parent normal modes. This strongly suggests that these harmonics and cross-frequencies owe their presence principally to harmonic distortion, that is to the inability of the stellar medium to respond linearly to the finite amplitude oscillatory perturbation. Other nonlinear processes, such as resonant

mode coupling, are only marginally responsible for these nonlinear peaks. Furthermore, I determined that the characteristic pulsating white dwarfs light curves, showing sharply peaked pulses with large flat bottoms in between, are direct consequences of the global phasing of the cross-frequencies, and can thus be considered as a signature of harmonic distortion.

The amplitude of these nonlinear frequencies relative to those of their parent modes ought to be similar when modes of the same spherical and azimuthal degrees (ℓ, m) are compared, as expected from the existing models of Brickhill (1992), Brassard et al. (1995), and Wu (1997). This property may help constrain the mode identification. Applied to G29-38 and GD358, it allowed the overall $\ell = 1$ identification to be confirmed, with a few exceptions which are thought to be $\ell = 2$ modes.

The quantitative comparison, in G29-38, of the relative amplitudes with those predicted by the above models, enabled the dominant harmonic distortion effects to be identified as being due to the nonlinear response of the convective flux to the pulsations, as predicted by Brickhill (1992) and Wu (1997). The nonlinear response of the emergent flux to the surface temperature variations, a process treated in the model of Brassard et al. (1995), seems to be negligible in comparison. These conclusions are also supported by the characteristic asymmetrical pulse shapes observed in the light curve, i.e. peaks with steep uphills and milder downhills, which are believed to reflect the hysteresis-type behaviour of the appearance and disappearance of the convection zone during the oscillatory flux perturbation.

Finally, various consideration led me to conclude that the pulsations are linearly driven, and that all the nonlinear features appearing in the light curve are generated afterwards, i.e. during the journey of the oscillatory perturbation to the stellar surface.

Important note

During the course of this thesis, I have written seven articles which have been submitted to scientific Journals. Due to some special circumstances, the Doctoral Degrees Board of the University of Cape Town has given me permission to use these publications as the core of my thesis, provided sufficient additional material is incorporated to clarify the details of the techniques used.

This thesis is thus built around seven publications which are reproduced in their original form as far as the content in concerned. In order to make the thesis a coherent whole, extra linking matter is inserted in between these different articles, where it is felt to be necessary. In keeping with the above requirement from the Doctoral Degrees Board, this additional material also comprises all the technical information relevant to the thesis, but which could not be included in the publications for conciseness and brevity reasons. A general introduction, as well as a conclusion have also been added as individual chapters. Although this overall structure might yield a certain redundancy in the information given, it is not significant as the scientific results reported in each paper are clearly distinguished from each other and do not at all suffer from redundant overlap.

The general layout of the seven publications has been adapted to that of the thesis, in order to make it a consistent whole. Depending on the context, the titles of these papers appear either as chapters or as sections of the thesis, and might have been slightly changed for coherency purposes. The different sections of the papers are then re-numbered accordingly as sections and subsections of the thesis. Although, the individual abstracts and bibliographies of each publications are kept, a general bibliographic section is found at end of the thesis. The cross-references to the publications which are part of the thesis have been replaced by the section numbers of where they appear; for instance the references

"Vuille *et al.* 1999" are replaced by "section 6.2", so that that the logical links between the different parts of the thesis become more explicit to the reader.

The seven articles used as the core of the thesis are listed below, together with their publication status, and their appearance position in the thesis.

- Vuille F., 1998, *Pulsating Stars*, JSAAI[1], 7, 28
  Appearance in the thesis: chapter 2.
- Vuille F., 1998, *Asteroseismology of Pulsating White Dwarfs*, JSAAI, 7, 40
  Appearance in the thesis: chapter 3.
- Vuille F., 1999, *Nonlinear Behaviour of Pulsating White Dwarf G29-38. I. Evolution of the Temporal Spectrum*, MNRAS[2], in press
  Appearance in the thesis: section 5.2.
- Vuille F., 1999, *Nonlinear Behaviour of Pulsating White Dwarf G29-38. II. Evolution of the Phase Spectrum*, MNRAS, in press
  Appearance in the thesis: section 5.3.
- Vuille F., Brassard P., 1999, *Nonlinear Behaviour of Pulsating White Dwarf G29-38. III. Relative Amplitude of the Cross-frequencies*, submitted to MNRAS May 1999.
  Appearance in the thesis: section 5.4.
- Vuille F., *et al.*[3], 1999, *Normal modes and discovery of high order combination frequencies in the DBV GD358*, submitted to MNRAS June 1999.
  Appearance in the thesis: section 6.2.
- Vuille F., Brassard P., 1999, *Nonlinear behaviour of the DB Variable GD358*, submitted to MNRAS June 1999
  Appearance in the thesis: section 6.3.

Being sole author in four out of these seven publications, and first author in the remaining three, my contribution to the research is thus clearly defined: all observations and

[1] Journal of the South African Acoustics Institute

[2] Monthly Notices of the Royal Astronomical Society

[3] See complete list of co-authors in section 6.1

reductions thereof were supplied to me and I carried out all the analyses, and wrote all the papers unaided. The specific contributions of the co-authors in the three multi-author papers will be made explicit in the introductory section of the respective chapters. I naturally also received feed-back and consent from the co-authors before actually submitting these articles. However, the remarks received were mainly about the form, especially the English, rather than about the scientific contents which did not provoke much controversy besides a few minor points. The work presented in this thesis which is not explicitly attributed to others can thus be entirely considered as my own, original, and unaided work, besides normal guidance from my supervisor, and kind advice from various astrophysicists working in the field[4].

[4]see acknowledgments section

Contents

List of Figures

Chapter 1

Introduction

1.1 Historical context

Besides a few references to supernovae, by the Arabs (1006), the Chinese (1054), and Tycho Brahe (1572), the first definite record of a variable star dates back to 1596, when Fabricius discovered the Mira o Ceti (Strohmeier 1972). This came surprisingly late in the history of astronomy, as, already in the Ancient Greek age, Hipparchus and Ptolemy started classifying all the visible stars to try and determine whether some new ones would appear in the celestial sky, and whether some of the visible ones would possibly increase or decrease in intensity (Ledoux & Walraven 1958).

Even though Fabricius' star triggered enthusiasm among astronomers, it did not, however, beget rapid subsequent discoveries, and only 16 and 22 stars were respectively referenced in Pigott's catalogue (1795), and Argelander's catalogue (1844). Although the total number of known variables was still very low, five classes of them were already discovered. Those were, chronologically, the Miras (1596), the eclipsing binaries (β Persei, by Montanari in 1667), the Cepheids (δ Cephei, by Goodricke in 1784), the irregulars (α Herculis, by Herschel in 1795), and the semi-regulars (R Scuti, by Pigott in 1795), amongst which four are intrinsic variables. A new era for the discovery of variable stars began with the advent of stellar photography, towards the end of the nineteenth century. From there on, the number of known variables basically doubled every decade from 700 in 1900, reaching

18791 in 1967 (Strohmeier 1972), amongst which not a single pulsating white dwarf.

Of course, at first, neither the origin of this variability was known, nor the distinction between the different classes of variables made. The first attempt to explain the variability by intrinsic stellar pulsations came from Ritter (1879, 1881). The idea was followed up analytically by Moulton (1909), who introduced interesting concepts, in particular that of nonradial pulsations, an idea which was unfortunately going to be completely abandoned for about four decades. The major pioneering work on stellar pulsation was carried out by Eddington (1918a, 1918b), who derived, from the fundamental set of hydrodynamic equations, a wave equation that describes the stellar oscillations throughout the star. He also conceptually addressed the issue of the stellar stability (Eddington 1917), i.e. how the oscillations are driven and where the energy that drives them originates. Although his wave equation, derived in the linear adiabatic framework, could not yield any clue about this phenomenon, it still showed that the relative amplitude of the oscillations decreases rapidly towards the center of the star, because the density is so high. He therefore discarded the process that generates energy at the center of the star, the nature of which was not known in those days, as a possible mechanism for the driving of the oscillation. Instead, he introduced the idea that the natural opacity of the atoms in an ionization zone might behave like a heat engine, which could drive and maintain oscillations. Keeping in mind that early this century, not only was nuclear burning not known, but the stars were thought to be made of heavy elements like iron, he could not determine the true nature of the instability, but he was still able to describe the manner in which it must operate.

In order to understand the observational properties of any class of pulsating stars, realistic stellar models must first be computed, as the latter provide the physical input to the dynamical equations that govern stellar pulsations. However, due to the complexity of the pulsation problem, and the difficulty of computing stellar models, it was only in the 1960s, with the advent of large electronic computers, that pulsation theory made its next significant step. With the aid of such machines, it became possible for astrophysicists to compute detailed tables of the physical properties of the matter in stars. Since the existence of the pulsations depends sensitively on the relative amount of driving and damping, the material properties must be known precisely even for a rough comparison of a calculated model with an actual star. In particular, tables of opacities are essential for understanding the pulsations, as the latter depend strongly on the changes in the opacity of ionization zone, as first suggested by Cox (1955). Computers were thus not directly

applied to the study of stellar pulsations, but were rather used as tools for building stellar models. Improvements in the construction of equilibrium models have directly resulted in significant theoretical progresses in our understanding of pulsations.

In constructing evolutionary models of pulsating stars, several parameters must be provided if we are to understand the variability observed. Besides obvious quantities such as the stellar mass, the effective temperature and the chemical composition, the models must also provide the constitutive physics. This not only encompasses an equation of state, that relates the different physical quantities to each other, but also the way all the physical processes such as radiative, convective, and conductive transfers are numerically handled. Not only is any treatment inevitably approximate, but the better the model, the more difficult its incorporation in the pulsational code, i.e. the more intricate the numerical calculation of the pulsations.

Early theoretical work was centered around linear adiabatic radial pulsations. This means that the motion takes place purely along the stellar radius, that the variations in all the physical properties remain small compared to the average values, and that each mass shell neither gains nor loses heat during the course of a cycle. These assumptions allowed the pulsation periods for radial oscillation to be reasonably accurately obtained, but could not yield any information as far as the existence, and stability of the modes are concerned. Only in the mid-1960s was the adiabatic assumption removed to be replaced by the true physical laws that rule the variations in the energy flow between mass shells (Baker & Kippenhahn 1962, 1965). The modern eigenvalue approach to the problem of linear nonadiabatic radial pulsations has produced a very good representation of small amplitude pulsations (Castor 1971, Iben 1971). Various studies have been conducted in this approximation that provided valuable information regarding the physical basis of the pulsations and the location of the instability strips in the HR diagram (Tuggle & Iben 1972, King *et al.* 1973).

In spite of the remarkable progress in the development of the theory of radial pulsations, the theoretical study of nonradial pulsations had had virtually no practical application. This was due to the fact that the latter formalism is much more intricate than the radial case, and that variable stars were only considered to oscillate radially, probably as a long term consequence of Eddington having ignored the nonradial case. However, for many stars observed in the 1960s and 1970s, it was believed, mostly for time-scale reasons,

that nonradial oscillations were responsible for their variability. This triggered rapid theoretical development in the field of nonradial pulsations, and in the mid-1970s, the full linear nonadiabatic nonradial problem were solved numerically for realistic stellar models (Christensen-Dalsgaard & Gough 1975). However, even in the linear adiabatic approximation, the mathematical nature of the nonradial problem precludes any simple, unambiguous, and completely reliable method for ordering or classifying nonradial modes of oscillations in arbitrarily complicated stellar models (Cox 1976).

It became rapidly clear that nonradial pulsations were ubiquitous among stars. Today they are believed to be responsible for the brightness variability in β-Cephei stars (Jerzykiewicz 1980), in line profile B stars (Smith 1980), in δ-Scuti stars (Breger 1980), in the sun (Hill 1980), in rapidly oscillating Ap stars (Kurtz 1990), and, of course, in pulsating white dwarfs (Osaki & Hansen 1973). Even though the latter represent today an excellent laboratory for the study of nonradial pulsations, they arrived extremely late in the history of stellar variability. Although some early theoretical investigations (Sauvenier-Goffin 1949) suggested the variability of compact pulsators, the intrinsic faintness of white dwarfs precluded their discoveries. Eventually, these theoretical suggestions prompted surveys of white dwarfs aimed at discovering high frequency variability, as they were originally foreseen to pulsate radially on time scales of a few seconds (Schatzman 1958).

At the same time as the first surveys searching for variability in the compact pulsators were reporting unsuccessful results (Lawrence, Ostriker, & Hesser 1967, Hesser, Ostriker, & Lawrence 1968, Willstrop 1969), Landolt (1968) discovered the first pulsating white dwarfs by accident. This discovery did not, however, attract much enthusiasm, as the main periodicity of about 12 minutes was about two orders of magnitude higher than those predicted at the time for white dwarfs (Faulkner & Gribbin 1968, Ostriker & Tassoul 1968), in keeping with the period-mean density relation based on radial oscillations (e.g. Cox & Giuli 1969). It was not even clear whether these variations represented pulsations at all, which led Warner & Nather (1970) to suggest that they could be caused by some sort of flare activity.

A much better data set on this star confirmed the periodicity at around 12.5 minutes (Warner & Nather 1972). In the mean time, two other white dwarfs were discovered to be variable with similar periods: G44-32, with eigenperiods of 10.0 and 13.7 min (Lasker &

Hesser 1969), and R548 with periods of 3.6 and 4.5 min (Lasker & Hesser 1971). Warner & Robinson (1972) were the first to assert that white dwarfs owed their variability to nonradial g-modes, rather than purely radial p-modes (see chapter 2). Their claim was based on various independent theoretical works that predicted nonradial pulsations for white dwarfs in the range 2-17 minutes (Chanmugam 1972, Baglin & Schatzman 1969, Harper & Rose 1970).

In the first half of the 1970s, high frequency variability was reported in a number of other compact objects, but with diverse character. Variations were indeed found in white dwarfs of all spectral type and colours (McGraw 1977), which implied that effective temperature was no indicator of the variability. The innovative introduction by Nather (1973) of the two-star high-speed photometer completely revolutionized the observations of compact variables, in the sense that it separated true intrinsic variables from spurious ones which only appeared variable due to observations made in non-photometric conditions. The use of this new technology directly led McGraw & Robinson (1976) to demonstrate that the compact variables that remained after the sorting out actually formed a highly homogenous class of pulsators, the DAV stars. This important work delimited a framework for future research, and allowed rapid subsequent progresses to be made in the "new field" of pulsating white dwarfs.

Confirmation that white dwarfs were indeed pulsating nonradially came from the observation of rotational splitting in R548 (Robinson, Nather, & McGraw 1976), where, due to the Coriolis force produced by the stellar rotation, the excited modes have their natural g-mode degeneracy lifted, and thus get split into multiplets of frequencies (see chapter 3). Other observational support for the g-mode interpretation came from the work by McGraw (1979) whose multicolour Strömgen high-speed photometric data suggested that the luminosity variations were due entirely to surface temperature variations, and not to radius changes. This was in direct agreement with the fact that, unlike the one of p-modes, g-modes have a predominantly horizontal displacement during the pulsations. This conclusion was reconfirmed with the multicolour photometric observation of the wings of the H_γ line of ZZ Cetis R548 (Robinson, Kepler, & Nather 1982) and G117-B15A (Kepler 1984a). The former very important paper by Robinson , Kepler, & Nather (1982) also gave a sound theoretical support to the contention that the luminosity changes are entirely due to surface temperature variations.

In the mean time, the first detailed theoretical investigation of the nonradial properties of pulsating white dwarfs were carried out by Osaki & Hansen (1973), and Brickhill (1975). These early investigations demonstrated that the low order g-modes, with periods of about 200 s, may account for the shorter periods present in some ZZ Cetis. These models could, however, not account for the long periods observed without having recourse to very high radial order modes. The first theoretical demonstrations of instability for nonradial modes with periods long enough to agree with the observed periods of the ZZ Cetis were by Dziembowski (1979) and Keeley (1979). The exact cause of the pulsations was, however, not known, although the so-called κ- and γ-mechanisms, which occur in partial ionization zones, were strongly suspected. This suspicion arose from the observation that the ZZ Cetis lie in the region of the HR diagram where the extrapolation of the Cepheids instability strip intersects the white dwarfs (McGraw & Robinson 1976).

All these contentions were confirmed by various groups in the early 80s (Dziembowski & Koester 1981, Dolez & Vauclair 1981, Winget 1981) that completed independently linear nonradial analyses of g-mode properties in compositionally stratified white dwarf models. Since then, it has been widely accepted that pulsating white dwarfs owed their variability to g-mode instability, although the existence of p- and r-mode instability strips is theoretically predicted, and the search for these modes is still on-going (Lindblom 1999).

Even though the overall understanding of white dwarf pulsations was quite satisfying by the early 1980s, two problems nevertheless remained. Firstly, the understanding of the nature of the filter mechanism that preferentially excites certain frequencies in the g-mode spectrum, often without driving some adjacent eigenmodes, was not understood. Secondly, the nonlinear question had not yet been tackled, which limited the applicability of existing models to low amplitude pulsators.

The first attempt to explain the mode selection problem came from the work of Winget, Van Horn & Hansen (1981), which introduced the concept of mode trapping (see chapter 3). This resonant process is today still accepted as the actual selection mechanism, although its understanding has remained qualitative. Theoreticians are thus not yet able to determine what mode should benefit from the driving. In particular, the relationship between the saturation mechanism, driving, and mode trapping is not at all understood. This was quite a pressing question, as even though the time averaged properties of the white dwarfs are homogeneous, their pulsation properties are not. Significant qualitative

differences distinguish the small amplitude pulsators from the large ones. While the former have very stable modes in both amplitude and frequency, showing sinusoidal light curves (e.g. Stover et al 1980, Kepler et al. 1982), the latter experience amplitude modulation, often with modes appearing and disappearing on time-scales of about a month. Their light curves depart from linearity, due to the presence in their period spectrum, of harmonics and cross-frequencies, as first identified by McGraw & Robinson (1975). It became the practice to classify the pulsating white dwarfs into two categories according to whether they showed linear or nonlinear behaviour, as determined by the appearance in their spectrum of harmonics and by the occurrence of amplitude modulation (Hansen 1980, Winget and Fontaine 1982).

Although nonlinear developments were badly needed to investigate and understand large amplitude pulsators, fully nonlinear, nonadiabatic, nonradial calculations of stellar pulsations have not yet been attempted by anyone. Only Deupree (1974, 1975) had taken some steps in this direction, with some encouraging results, but he assumed axisymmetric oscillations, which represents a special case of the most general kind of nonradial oscillations. The formalism for nonradial pulsation being so much more intricate than its radial counterpart, the former theory has always been lagging behind. While the nonlinear radial problem had already been tackled from the mid-1960s (Christy 1964, 1966), theorists were still busy in the mid-1970s with the linear nonadiabatic case for nonradial pulsations. The fully linear nonadiabatic nonradial calculations were eventually carried out independently by Christensen-Dalsgaard & Gough (1975), Dziembowski (1975), and Ando & Osaki (1975).

Even though early work on the nonlinear radial question used the completely unrealistic one-zone model (Baker 1966), these models still helped clarify certain qualitative aspects of the nonlinear oscillations, and led the way for further developments. New astute iterative techniques were developed, that allowed solutions to be obtained under some assumptions, such as strictly periodic oscillations (Von Sengbusch 1970, Stellingwerf 1974). Models were soon produced that described promisingly well the behaviour of nonlinear radial pulsators such as RR Lyrae (Stellingwerf 1975). However, these complex numerical computations all failed to produce any stable resonant behaviour (Simon, Cox & Hodson 1980), and thus could not address the very important question of modal interaction. Theoreticians eventually realised that the direct treatment of the nonlinear problem which consists in numerically integrating the full coupled thermodynamic and

thermal equations was hopelessly complicated, even in the 'much simpler' radial case.

An alternative approach was developed in the early 1980s, in particular by Dziembowski (1982), that borrowed a formalism commonly used in plasma physics. This perturbative method, called the amplitude equation (AE) formalism, consists in investigating dynamically the coupling between modes. The AEs are general and fundamental. For a given set of coupled modes, the time derivative of their respective amplitudes form a set of relatively simple coupled equations that can easily be solved once the input parameters entering these equations are known.

The advantage of the AEs is that they do not depend explicitly on the detailed structure of the star. This dependence is entirely hidden in the values of the nonlinear coupling coefficients which enter these equations. Furthermore, these coefficients can be derived ab initio for any given stellar model, although the actual calculations are extremely difficult, and have only been attempted in very limited ways for radial pulsators (Dziembowski 1982, Klapp, Goupil, & Buchler 1985). Alternatively, the values of the coupling coefficients can also be obtained numerically from the hydrodynamical nonlinear pulsation equations. Attempts have also been limited to radial pulsators such as RR Lyrae (Buchler & Kovács 1986), and Cepheids (Kowácz & Buchler 1989). Unfortunately direct numerical hydrodynamical calculations are not yet feasible for nonradial pulsations. Even if the coupling coefficient cannot be provided, AE formalism can still yield a qualitative description of the nonlinear processes such as modal saturation and amplitude modulation. However, for proper quantitative confrontation with the observations, the constitutive physics, i.e. the coupling coefficients of the AEs, must be provided.

Even though the AEs are easy to write down in their general form, a complete description of the pulsations in terms of these equations is useful, from a practical standpoint, only when the number of modes is small, or when certain groups of modes can be considered decoupled from others. AE formalism is, however, the only theoretical tool available at present to investigate mode coupling for nonradial oscillators. The original formalism developed by Dziembowski (1982) for radially pulsating stars was first generalised to the nonadiabatic case (Buchler & Goupil 1984), and then to the complete nonradial nonlinear nonadiabatic case by Goupil and Buchler (1994).

Resonances between pulsation frequencies are known to play an important role in the dynamics of classical variable stars. For nonradial pulsators, that exhibit a much denser

frequency spectrum, resonances are also expected to occur, and may play a significant role in mechanisms such as modal selection and amplitude saturation (Dziembowski 1993). Many white dwarfs were observed in the 1970s that showed amplitude spectra changing on a time-scale of weeks, and even from night to night (e.g. Robinson 1979, Fontaine *et al.* 1980). At first, these modal instabilities were attributed to mode coupling, for not only were theoreticians predicting these resonant processes to be significant in white dwarfs due mainly to the highly populated g-mode spectrum (Dziembowski 1979), but also because this would explain the systematic presence of numerous harmonics and combination frequencies whenever amplitude changes are occurring.

As the AE formalism was a newly born theory, enthusiasm was great to observe and analyse these amplitude modulations for qualitative comparison with theoretically predicted behaviours. Unfortunately, application of AE formalism to all the promising candidates for unstable pulsations had to be discarded on the grounds that their apparent spectral variations were in effect due to unresolved beating processes (Kepler, Robinson, & Nather 1983, Kepler 1984b, O'Donoghue 1988). For a long time observers would systematically report nonlinear behaviour of white dwarfs, whereas they were erroneously "overinterpreting undersampled data" (Winget 1988). To uncover possible genuine amplitude changes, resolved data sets were required. Unfortunately, such light curves are very difficult to obtain because the closely spaced frequencies, often due to rotational splitting, generate long period beating of up to several days and a single telescope cannot follow a star continuously for longer than an observing night.

The problem was shelved thanks to the advent of a new exciting field of research for white dwarfs, that drew attention away from nonlinear behaviour. It was slowly but surely realised that the period spectrum directly reflects the physical conditions of the stellar interior, as the pulsations involve the entire star, and not just its outermost layer. Asteroseismology, the use of the pulsations to probe the stellar interior, was born. Information was first obtained on the location of the blue edge of the DAV instability strip (Winget 1988, and reference therein). Based on the very important asymptotic calculations by Tassoul (1980), Kawaler (1988) then determined the mass of DOV PG1159-035 from the period spacing of the normal modes identified in its period spectrum. This first genuine asteroseismological results triggered enormous excitement, as it literally unveiled the untapped potential of this new technique (see chapter 3).

The rapid progress obtained in stellar seismology of compact pulsators was the result of a "combination of fortunate circumstances" (Winget 1988). First, their physical structure is very simple, as a direct result of the gravitational settling. Second, the amplitudes are often small enough to be treated in the framework of the linear theory, but large enough still to be observable. Third, the multi-periodic behaviour provides many independent clues to their underlying stellar structures. Fourth, the periods are short enough, as a result of their high density, so that many cycles can be observed per night, therefore possibly resolving the period structure of these stars.

Unfortunately, this enthusiastic impetus also got stopped prematurely, because the observed period spectra were too intricate for any secure analyses to be performed. In particular, the success of asteroseismology depends directly on our ability to identify, in the period spectrum, the normal modes excited, and label them correctly with their proper indices (k, ℓ, m) (see section 2.5). The difficulty lies not only in the labelling process itself (see section 6.2), but also in the fact that the spectra obtained are full of artifact frequencies and window effects (Nather *et al.* 1990) due to the daytime gaps in the data, that are difficult to distinguish from real normal modes.

The need for long and continuous data sets was thus not only an inherent need for the analysis of the nonlinear processes, but was also a requirement to resolve and clean the amplitude spectrum for asteroseismological purposes. This need was met by the advent of multi-site campaigns such as the Delta Scuti Network (e.g. Breger *et al.* 1995), the Stellar Photometric International (STEPHI; Michel *et al.* 1992), and especially the Whole Earth Telescope network (WET; Nather *et al.* 1990), that allows, in principle, to observe a star continuously for as long as one wishes.

1.2 Current context of the thesis

The 1990s have seen the advent of the multi-site campaigns. Basically all asteroseismological studies are nowadays conducted on light curves obtained from more than one telescope, widely distributed around the earth, in order to reduce as much as possible the gaps between the individual observing runs. The use of the large institutional telescope networks, such as the WET, is however costly in terms of people, observatories, and co-

ordination. Such campaigns are thus used wisely and parsimoniously. The targets are chosen according to the amount of meaningful information they are expected to yield. It is therefore not surprising that each new WET campaign is a success providing, thanks to the asteroseismological tool, wealth of information about the targeted star.

Unfortunately, at present, the field of asteroseismology is purely based on the linear adiabatic theory. This directly explains its success, but also sets its limitations. Even though the pulsation periods of the eigenmodes are well described by the linear theory, these are the sole quantities that the later formalism is able to provide. Therefore, all the information obtained on the star using asteroseismology is, at present, inherently rooted in the analysis of the sole oscillation frequencies identified. Although the amplitudes and phase of the eigenmodes and cross-frequencies, as well as their presence or absence, directly reflects the physical conditions inside the star, the present linear asteroseismology is of no use to extract any stellar parameters from these measurements.

This limitation comes from our poor understanding of the nonadiabatic and nonlinear processes undergone by the compact pulsators. From a nonadiabatic point of view, our comprehension of the mode selection mechanism is limited to some conceptual aspects such as that of mode trapping. The crucial relationship between the mode selection and the driving mechanisms is not at all understood at present, and these processes cannot yet be included in the theoretical models. From a nonlinear point of view, the exact origin of the harmonics and cross-frequencies often identified in the period spectra, and the nature of the saturation mechanism that limits the amplitudes to which the modes grow, are unknown. Various processes have been suggested, but it is not yet possible to determine which ones are actually taking place, or dominating over the others. Furthermore, their incorporation into the hydrodynamical equations of pulsation requires numerical computations that are not as yet feasible. Although very real, the nonlinear problem is not new. Its long lasting unsolved status has been deplored by numerous theoreticians, as illustrated by the few following words selected from the literature, and reproduced chronologically:

A. N. Cox & J. P. Cox (1967): "Unfortunately, the nonlinear nonadiabatic calculations are still lacking. "

R. F. Stellingwerf (1974): "The usual nonlinear approach has proven to be [computationally] extremely expensive"

J. P. Cox (1976): "To remove the assumption of linearity is likely to involve a major effort."

D. E. Winget & G. Fontaine (1982): "The lack of nonlinear nonradial calculations may be regarded as a major theoretical failure."

D. E. Winget (1988): "The period ratios observed in several of the compact pulsators have no simple explanation in terms of linear analysis of nonradial g-modes and cry out for nonradial calculations."

W. Unno et al (1989): "A number of theoretical problems remain to be studied, among them are nonlinear problems."

S. D. Kawaler & C. J. Hansen (1989): "Nonlinear calculations of nonradial pulsations of white dwarfs are intractable at present, whereas they have been part of the arsenal of tools used for many years in the study of purely radially pulsating Cepheids."

D. E. Winget (1991): "Clearly, our biggest theoretical weakness is in the area of nonlinear processes."

P. A. Bradley (1993): "Theoretical efforts in this [i.e. nonlinear] direction are still in their infancy."

W. A. Dziembowski (1993): "Nonlinear equations for stellar oscillations are very difficult to solve."

Gautschy & Saio (1996): "The nonlinear behaviour, however, is not so comprehensively understood."

J. R. Buchler, M.-J. Goupil, & C. J. Hansen (1997): "Unfortunately, [nonlinear] hydrodynamical computations are not yet possible for nonradial pulsators."

Phenomenological analyses of the nonlinear features observed in most pulsating white dwarfs have been conducted only in a very limited way. The existence of harmonics and combination frequencies in the amplitude spectra of pulsating white dwarfs has been known since McGraw & Robinson (1975), and it has mostly been believed that these frequencies owed their presence to resonant coupling with unstable eigenmodes. Some

recent analyses of WET observations however pointed out (e.g. Winget *et al.* 1994) that these nonlinear frequencies were probably too numerous all to be accounted for by independent resonances. Three models have been recently developed (Brickhill 1992a, 1992b, Brassard, Fontaine, & Wesemael 1995, Wu 1997) which explain the presence of these nonlinear frequencies as resulting from a natural distortion of the sinusoidal wave due to the nonlinear response of the stellar medium. Although these models yield qualitative and quantitative predictions, they have only been tested in a very limited way, but seemed to agree qualitatively well with the observations (Brickhill 1992b, Brassard *et al.* 1995, Wu 1997).

The 1990s have thus been marked on the one hand by significant theoretical progresses in the field of nonlinear pulsations, and on the other hand by the collection of high quality photometric data obtained from multi-site campaigns. The time is ripe to begin studying the nonlinear processes possibly undergone by the large amplitude pulsating white dwarfs. This study is important not only to obtain a better understanding of the stellar pulsations themselves, but also to make better use of the asteroseismological approach. As stated before, the only quantities used by the present asteroseismological techniques are the oscillation periods. However, it is important to try and extract all the information contained in the amplitude spectra of pulsating white dwarfs. This is the aim of the as yet unborn field of nonlinear asteroseismology.

1.3 Goal of the thesis

Summarised in one sentence, the aim of the present thesis is to study the nonlinear behaviour of pulsating white dwarfs, using a phenomenological approach. The idea is to extract, from given light curves, any possible information regarding the nonlinear processes in action. Questions such as "what are these processes?", "how do they work?", "on what time scales?", etc. will be addressed. As discussed earlier, undersampled data preclude any analysis, as genuine nonlinear behaviour would be confused with modulations generated by unresolved frequencies. Therefore, data of extremely good resolution is THE necessary pre-requisite for the feasibility of this project. I have been fortunate enough to be kindly provided with the best data of this kind available to date. These include in particular four light curves on the DAV G29-38 and the DBV GD358 obtained by

the Whole Earth Telescope. All the data will be presented in due course in the thesis. Together with this material, I have also been kindly provided with several useful scientific tools, such as a time series analysis program, as well as data from numerous numerical models[1].

With these data and tools in hand, I was feeling well equipped to extract some of the nonlinear secrets. Two types of nonlinearities are, or seem to be, observed in the amplitude spectra of pulsating white dwarfs. The first is the amplitude variations, whereby modes appear to vary in amplitude on time-scales reported to vary from days to seasons. The second is the definite presence of harmonics and cross-frequencies that affect the sinusoidal shape of the light curves. Two fundamental questions, specific to these processes, have never received any strictly satisfying answer, and will constitute the starting research points of this thesis:

- Can we detect any amplitude changes in the period spectrum which can with certainty not be explained by unresolved beating?

- What is the origin of the numerous nonlinear frequencies identified in the amplitude spectra of pulsating white dwarfs?

The outcome of these primary analyses will then determine the subsequent direction that the research will take. It can nevertheless be foreseen that the following fundamental questions will certainly be addressed:

- Can we find any recurrent pattern in the appearance and disappearance of modes?

- Can any specific resonant process be uncovered?

- Can any qualitative and/or quantitative comparison be made between the observed nonlinear features and those predicted by theoretical models?

- What is the saturation phenomenon that limits the amplitudes of the excited modes?

- What information about the star can potentially be obtained from the analysis of the nonlinear features, i.e. how fruitful can nonlinear asteroseismology possibly be?

[1] All the kind providers of these data sets, programs, and models are detailed in the acknowledgments section, at the beginning of this thesis, to which I refer the reader.

- Are the pulsations intrinsically linear or nonlinear?

1.4 Structure of the thesis

Chapters 2 and 3 are general introductions to, respectively, pulsating stars and asteroseismology of pulsating white dwarfs. Their purposes is to provide an indepth discussion of the scientific context in which this research project will be conducted.

Chapter 4 describes in some detail the analysis techniques used to carry out the research. It mainly presents the statistical and computational aspects of the time series analysis methods. This chapter also defines some important physical notions that are used throughout the thesis.

Chapters 5 and 6 represent the core of the research; they report on the nonlinear behaviour of two pulsating white dwarfs: the DAV G29-38 and the DBV GD358. Both these chapters bear more or less the same substructure, where mode identification is first performed, before analysing the evolution of the amplitude and phase spectra of these two stars.

Chapter 7 concludes the analysis; it summarises concisely the findings of the project, suggests directions for further research, and emphasises the aspects where specific efforts are most needed for progress to be made.

A bibliographical section, at the end of the thesis, lists alphabetically the references indicated throughout the thesis, and on which this research project is based.

General bibliography

In addition to the specific references indicated throughout this introduction, the following general literature has been widely consulted to acquire the historical knowledge necessary for the preparation of this introductory chapter.

Cox J. P., 1976, Ann. Rev. As. Ap., 14, 247

Cox A. N., Cox J. P., 1967, Sky & Telescope, 5, 278

Cox J. P., Giuli R. T., 1968, *Principle of Stellar Structure*, (New York: Gordon and Breach)

Gautschy A., Saio H., 1996, Ann. Rev. As. & Ap, 551

Ledoux P., Walraven Th., 1958, *Handbuch der Physic*, eds. S. Flügge (Berlin: Springer-Verlag), 51, 353

McGraw J. T., 1980, Space Science Review, 27, 601

Percy J. R., 1975, Scientific American, 232, 66

Robinson E. L., 1979, *White Dwarfs and Variable Degenarate Stars*, eds H. M. Van Horn and V. Weideman (Rochester, N.Y., University of Rochester Press), 343

Rosseland S., 1949, *The Pulsation Theory of Variable Stars*, Oxford University Press, London

Strohmeier W., 1972, Variable Stars, Pergamon Press Ltd., Oxford

Unno W., *et al.*, 1989, *Nonradial Oscillations of Stars*, 2nd ed., University of Tokyo Press, Tokyo

Warner B., 1988, *High-Speed Astronomical Photometry*, Cambridge University Press

Winget D. E., Fontaine G., 1982, *Pulsations in Classical and Cataclysmic*

Variable Stars, eds. J. P. Cox, and C. J. Hansen (Boulder Joint Institute for Astrophysics), 46

Winget D. E., 1988, Advances in Helio- and Asteroseismology, eds J. Christensen-Dalsgaard & S. Frandsen (Dodrecht: Reidel), 305

Chapter 2

Pulsating Stars

Abstract

The phenomenon of stellar pulsation, where a star is seen to expand and contract as a consequence of a mechanical wave traveling through it, is reviewed. The equation of radial pulsations is obtained, in the linear case, from the basic equations governing the structure of the stellar fluid. In order for the pulsations to overcome the natural damping, driving must occur. A general discussion on pulsational stability is first given, which leads to the definition of a stability coefficient. Two major driving mechanisms are then discussed, both of them taking place in the partial ionization zones of abundant atmospheric elements. The general case of nonradial pulsations, where the mass motion does not need to be along the stellar radius, is then addressed, with emphasis on the qualitative features of these pulsations. Finally, a few examples showing what physics can be learnt from the study of pulsations are briefly discussed. A second paper in this issue describes, in a less theoretical and more applied way, the prospects and limitations of the study of a very important class of pulsating stars: the pulsating white dwarfs.

2.1 Introduction

A star is in hydrostatic equilibrium if the gravity, which seeks to compress the star, is balanced everywhere by the pressure, which seeks to expand it. If a star is perturbed from this equilibrium, it will tend to oscillate, giving rise to large scale dynamical motion, usually including the entire star. These oscillations can be regarded as acoustic waves traveling across the stellar medium. In response to the cyclic changes in the physical conditions in the atmosphere, the brightness of the star will also show periodic variations: the star is then said to be pulsating (see Figure 2.1). The relative luminosity variations, in visible light, range from 0.01% (which is an observational limit) in small amplitude variables like the rapidly oscillating Ap stars, up to more than 10000% in the large amplitude Mira variable stars. This means that the latter may become 100 times brighter during a pulsation cycle. The corresponding radius changes remain tiny for nonradial pulsators (see below), but can be over 20% in radial pulsators like Cepheid variable stars. The radial velocities at maximum rate of expansion or contraction can be as high as 40-50 km/s.

The time scale Π on which these pulsations take place (at least for the fundamental modes) ought to be of the order of the time required by a sound wave to propagate through the diameter of the star (Ledoux & Walraven 1958). It ranges from a few seconds for small, dense white dwarf stars ($\bar{\rho} \sim 10^6\,\mathrm{g/cm^3}$) to a few years for tenuous supergiant stars ($\bar{\rho} \sim 10^{-9}\,\mathrm{g/cm^3}$) (see Figure 2.1). This is well described by the famous period-mean density relation, which is satisfied by most pulsating stars (Cox 1980):

$$\Pi\sqrt{\frac{\bar{\rho}}{\bar{\rho}_\odot}} = Q = \text{const} \tag{2.1}$$

where the normalization factor $\bar{\rho}_\odot = 1.4$ is the mean density of the sun, while Q is the pulsation constant. In fact, Q is not a genuine constant, as it depends, though generally weakly, on the thermal and chemical stellar structure. Observations show that Q lies in the range 0.02 - 0.11 days (Cox 1980).

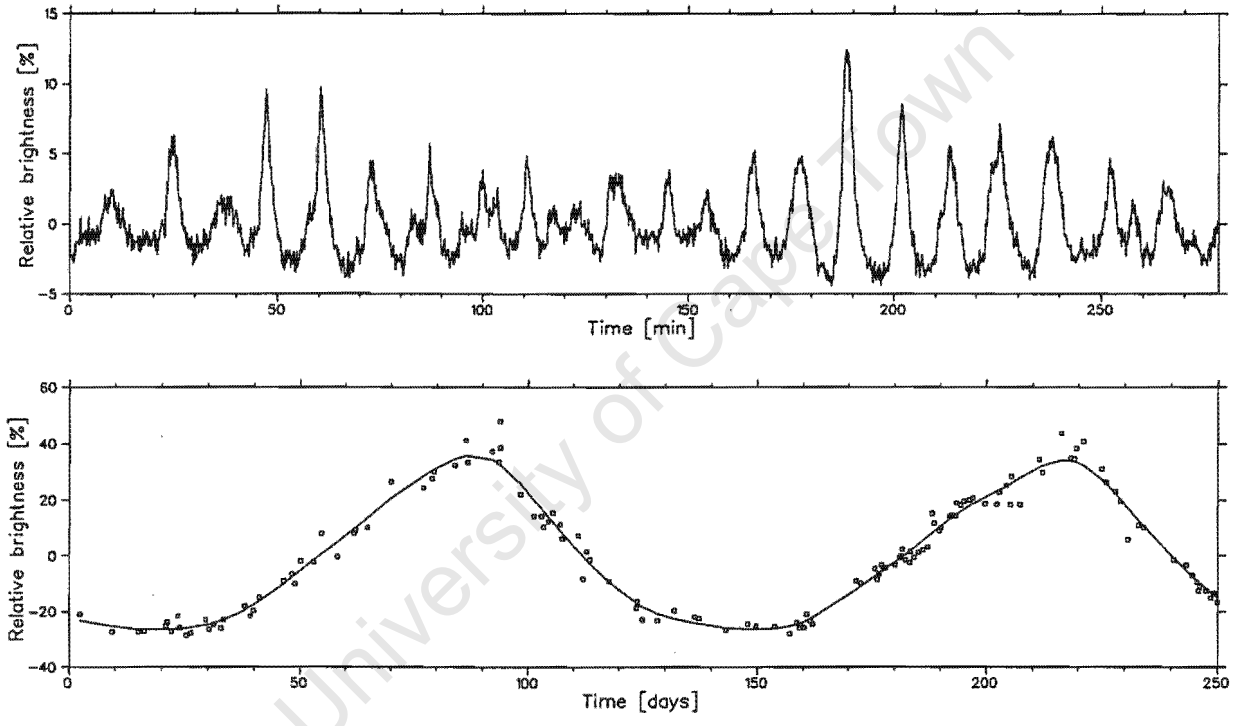

Figure 2.1: Light curves of the pulsating White Dwarf star GD358 (*upper panel*) and the Cepheid HV821 (*lower panel*). Note the difference between the scales of the two time axes.

2.2 Radial pulsations

The simplest kind of pulsation is given by the case of a pure radial compression wave traveling back and forth between the center and the stellar surface. The star, which remains spherically symmetric at all times, is thus seen to expand and contract, as if it were breathing.

In the Eulerian description, and with the assumption of spherical symmetry, the set of equations governing the dynamics of the stellar fluid is:

- The conservation of mass equation (or continuity equation):

$$\frac{dm_r}{dr} = 4\pi r^2 \rho \tag{2.2}$$

where ρ denotes the mass density, and $m_r = \int_0^r \rho dV$ is the mass within radius r.

- The momentum equation (or equation of motion):

$$\frac{d^2 r}{dt^2} = -\frac{1}{\rho}\frac{dp}{dr} - \frac{G m_r}{r^2} \tag{2.3}$$

where p is the pressure and G is the constant of gravitation.

- The conservation of energy equation

$$\frac{\partial \ln p}{\partial t} = \Gamma_1 \frac{\partial \ln \rho}{\partial t} + \frac{\rho(\Gamma_3 - 1)}{p}\frac{dE}{dt} \tag{2.4}$$

where Γ_1 and Γ_3 are the usual adiabatic exponents:

$$\Gamma_1 = \left(\frac{d\ln p}{d\ln \rho}\right)_{\rm ad} \quad , \quad \Gamma_3 = \left(\frac{d\ln T}{d\ln \rho}\right)_{\rm ad} \tag{2.5}$$

while the term dE/dt is the rate of change of energy per unit mass. It is given by the difference between energy generated by thermonuclear reactions in the core $\varepsilon(\rho, T)$, and energy dissipated mainly through radiation and convection:

$$\frac{dE}{dt} = \varepsilon - \frac{dL_r}{dm_r} \tag{2.6}$$

where L_r is the interior luminosity, or the net outwards rate of flow of energy through a sphere of radius r. This energy equation is nothing else but the first law of thermodynamic, rearranged for astronomical purposes. It is valid under the assumption that no composition changes occur as a result of the thermonuclear reactions in the core.

• An equation of energy transport which relates L_r to other physical quantities is also required. Conduction processes are normally neglected (except in white dwarfs), while the treatment of radiation is relatively straightforward. The convective contribution to L_r poses, however, serious problems, due to the lack of a proper time-dependent convection theory. In many cases time independent theory is used, where the convection efficiency remains constant along a pulsation cycle.

This set of 4 equations, together with the supplementary constitutive relations like $p = p(\rho, T)$, $\Gamma_1 = \Gamma_1(\rho, T)$, $\Gamma_3 = \Gamma_3(\rho, T)$, $\varepsilon = \varepsilon(\rho, T)$, which depend on the physical structure of the star, and certain suitable boundary conditions, constitute a system of nonlinear equations which are sufficient to determine completely the future evolution of the stellar fluid. The solution of this system comprises the real case of nonlinear, nonadiabatic radial pulsation problem, which cannot be solved analytically. If small perturbations to the static equilibrium state are assumed,

$$f = f_0\,(1 + \delta f/f_0) \tag{2.7}$$

where f represents either of the physical stellar quantities r, p, ρ, T or L_r, the above set of equations can be linearized. If adiabaticity ($dE/dt = 0$) is further assumed (no heat gains or losses by the oscillating mass elements), these linearized equations can be combined into a single linear adiabatic wave equation (LAWE) which, in the Lagrangian

description, takes the form (Cox 1980):

$$r_0\ddot{\zeta} = \zeta \cdot 4\pi r_0^2 \frac{d}{dm_r}\left[(3\Gamma_{1,0} - 4)\, p_0\right] + \frac{1}{r_0}\frac{\partial}{\partial m_r}\left[16\pi^2\, \Gamma_{1,0}\, p_0 \rho_0 r_0^6 \frac{\partial \zeta}{\partial m_r}\right] \tag{2.8}$$

where the variables with a zero subscript are the equilibrium values, while ζ is the relative displacement $\delta r/r_0$.

If the wave-length of the perturbation can be considered short compared to the length associated with spatial changes in p_0 and ρ_0, so that ∇p_0 and $\nabla \rho_0$ can be neglected, the LAWE would take the much simpler form of a pure wave equation (Landau & Lifshitz 1959):

$$\frac{\partial^2 \rho}{\partial t^2} = v_s^2 \nabla^2 \rho \tag{2.9}$$

where v_s is the adiabatic sound speed given by

$$v_s = \sqrt{\Gamma_{1,0}\frac{p_0}{\rho_0}} \tag{2.10}$$

The general solution of the LAWE (equation 2.8) may be obtained by separation of variables. Assuming a sinusoidal temporal dependence of the form $e^{i\sigma t}$, the LAWE takes the form of an eigenvalue problem, due to the boundary conditions that must be fulfilled at both the center and the surface:

$$\mathcal{L}\xi_k = \sigma_k^2 \xi_k \tag{2.11}$$

where, from (2.8), the linear operator $\mathcal{L}$ is defined by the relation

$$\mathcal{L} = -\frac{1}{\rho r^4}\frac{d}{dr}\left(\Gamma_1 p r^4 \frac{d}{dr}\right) - \frac{1}{\rho r}\left(\frac{d}{dr}[(3\Gamma_1 - 4)p]\right) \tag{2.12}$$

where σ_k^2 and ξ_k are respectively the eigenfrequencies and radial eigenfunctions of the problem, both indexed by the radial number k which represents the number of nodes between the center and the stellar surface. Any normal mode of oscillation can then be written in the form

$$\zeta_k(r,t) = \xi_k(r)\, \mathrm{e}^{i\sigma t} \tag{2.13}$$

In the linear theory, there is no interaction between different normal modes simultaneously excited. Therefore, a superposition principle can be applied, and the most general radial pulsation can be decomposed into normal modes:

$$\zeta(r,t) = \sum_k \zeta_k(r,t) \tag{2.14}$$

The homogeneity of equation (2.11) implies that the absolute amplitude of the oscillations remains undetermined, in agreement with the adiabatic approximation which assumes a perfectly conservative system. It is clear, moreover, that the adiabatic theory cannot yield any direct information regarding the existence of the pulsations, that is, the pulsational stability of the star. However, as the pulsations are nearly adiabatic throughout almost the entire star, except for the outermost layers, this theory gives quite accurate values for the pulsation periods and for the relative amplitudes of the different pulsation modes; for instance, the period-mean density relation (equation 2.1) follows directly from the LAWE. The assumption of adiabatic pulsations in stars is often a much better approximation than the assumption of adiabatic sound waves in terrestrial applications.

2.3 Pulsational stability

Nonadiabatic effects, though very minute throughout most of a pulsating star, are responsible for the driving or the damping of the oscillations. The criterion for a region in the stellar interior to be driving pulsations is the following: it must be gaining heat at maximum temperature, i.e. at maximum contraction, or losing heat at minimum temperature, i.e. at maximum expansion. Conversely, a region losing heat at maximum compression,

or gaining heat at maximum expansion, will be a damping region. An analogy is someone pushing a child on a swing: driving is provided if the swing is pushed further up when reaching maximum height, whereas damping would occur if the child receives a backward push, against the swinging motion, before he gets to the highest position.

The nonadiabatic effects yield a phase shift between pressure and density variations. It can be seen from the energy equation (2.4) that a driving region ($dE/dt > 0$ when $d\rho/dt = 0$) will see the pressure still increasing at maximum compression, and thus δp will lag behind $\delta\rho$, whereas maximum pressure would precede maximum density for a damping region. Assuming a sinusoidal motion, then it is clear that p will be larger during the expansion of the shell than during the contraction. Hence, the representation of the motion of a shell in a $p - V$ diagram will be clockwise if driving, resulting in a positive work integral done by the restoring forces on the shell over a complete cycle, $W = \oint pdV > 0$, and anticlockwise if damping, yielding a negative work integral, $W < 0$ (see Figure 2.2). This leads to a simplified picture of the pulsational stability question: each mass shell of mass dm in the star can be treated as an independent heat engine on which the work integral W can be computed. If the total driving exceeds the damping, the star will pulsate (see Figure 2.3).

A stability coefficient κ can be defined by (Cox & Guili 1968)

$$\kappa = -\frac{1}{2}\frac{<dW/dt>}{\Psi} \tag{2.15}$$

where $<dW/dt>$ is the average rate at which restoring forces work, and Ψ is the total pulsational energy. κ is nothing else but the imaginary part of the oscillation frequency w, yielding a time dependence $e^{iwt} = e^{i\sigma t} \cdot e^{-\kappa t}$ of the displacement; $\kappa < 0$ results in excited oscillations, hence instability, whereas $\kappa > 0$ means damped oscillations, hence stability.

The phase shift between restoring force (i.e. pressure) and displacement excludes a solution comprising pure standing waves; a running wave component, possibly small, will always be present, resulting in the system never passing through its equilibrium state.

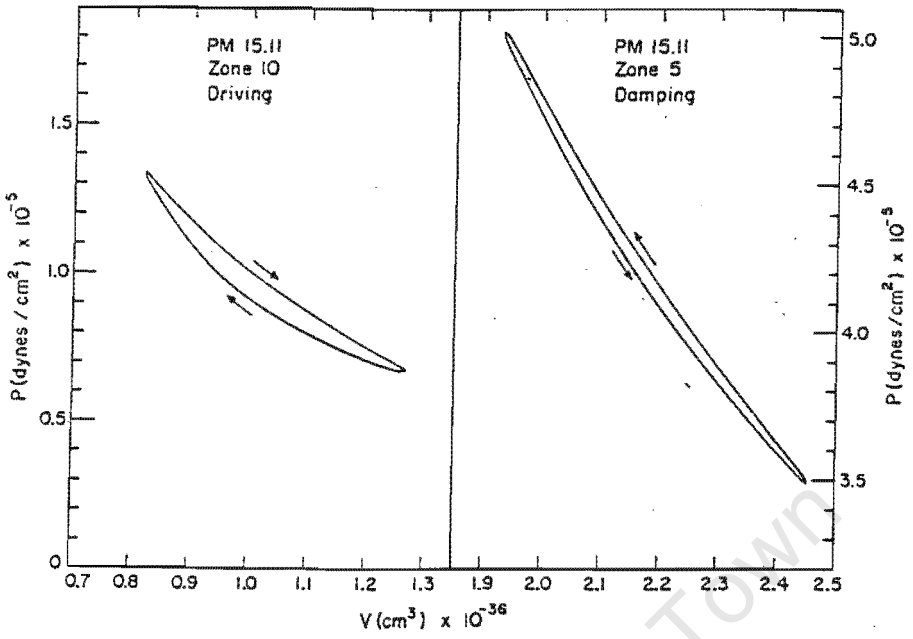

Figure 2.2: $p-V$ plot for 2 different regions in the star, obtained from a 20-zone model. Zone 5 is a damping region in the deep interior, whereas zone 10 is a driving region in the He^+ ionization zone. Reproduced from Cox *et al.* (1966).

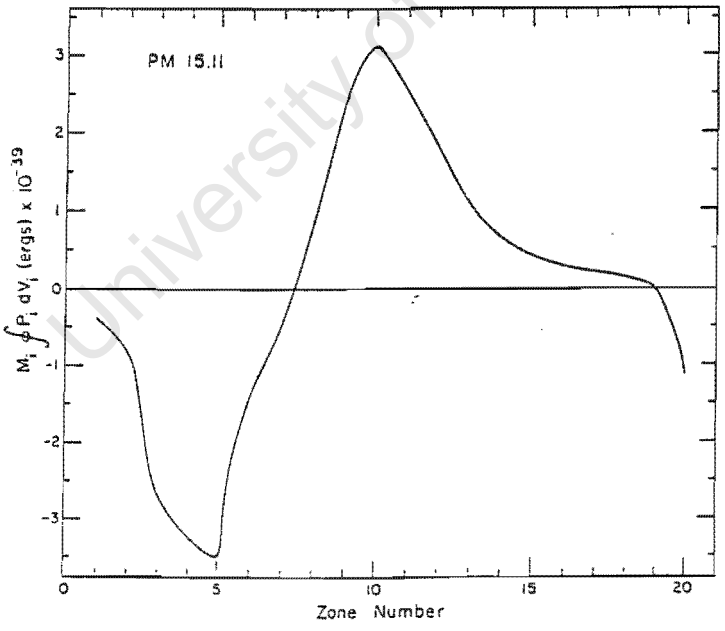

Figure 2.3: The work $M_i \oint pdV$ done on its surroundings around a complete cycle by the ith mass zone versus i for the model represented in Figure 2.2. Zone 1 corresponds to the inner core and zone 20 to the outer stellar atmosphere. Reproduced from Cox *et al.* (1966).

2.4 The driving mechanism

For a star to overcome natural damping, some process must continuously drive the pulsations. What is the actual physical mechanism responsible for the pulsational instability discussed in the previous section? As stars are nearly adiabatic throughout most of their body, driving must come from some envelope mechanism, where the adiabatic approximation does not hold. Therefore, nuclear reactions play a negligible role in the excitation of stellar pulsations, as the oscillations are of low amplitude in the deeper regions where nuclear burning occurs as already pointed out by Eddington (1917).

The mechanisms responsible for the driving of pulsations are generally ionization processes which involve zones of abundant elements in a state of partial ionization. If such a zone happens to be at a specific critical depth below the surface, it can trigger modulations of the luminosity flux. What happens is that most of the work of adiabatic compression goes into ionization energy rather than into kinetic energy of thermal motion, so that the temperature does not increase very much upon compression. This small temperature variation results in a marked dip in the luminosity variation ($\delta L_r/L_r$), the reason being that, approximately, $L_r \sim T^4$. This strong outwards decrease of the luminosity variations clearly represents absorption of energy in this region at the time of maximum compression. This region is therefore a driving zone. This direct effect of the temperature variations on the luminosity variations is referred to as the γ-mechanism (Cox *et al.* 1966).

Another possible driving effect is given by the increase of the opacity κ during compression. As $\kappa = \rho^n T^{-s}$ $(n, s > 0)$, the small variation of T in the inner ionization zone might result in an increase in the opacity, which further enhances the damming up of the radiation in this region, increasing even more the driving effect. This mechanism is known as the κ-mechanism (Baker & Kippenhahn 1962).

Brickhill (1991) showed that the convection zone of a star could also, under certain conditions, operate as a driving mechanism. When in hydrostatic and thermal equilibrium, the entropy in an efficient convection zone has an almost flat profile due to the action of the turbulent eddies (Schwarzschild 1966). If the flux entering the convection zone from below is varying on a time scale much longer than the typical turn-over time of the eddies, the convection zone will correspondingly adjust its entropy in a uniform way, and thus maintain its isentropic profile. To do so, the convective eddies alternatively

absorbs heat from the incoming flux and releases heat into the latter, thus producing periodic flux variations at the top of the zone, which may then propagate to the stellar surface (Wu 1997). This driving mechanism is referred to as *convective driving.*

2.5 Nonradial pulsations

Radial oscillations are merely a subset of a more general class of pulsations, where the displacement of a mass element from its unperturbed position may be in any direction at all, and need not to be parallel to the radius vector. The theory of these so-called nonradial pulsations is much more intricate than the corresponding radial case, for the star does not remain spherically symmetric. The basic equations of stellar structure (section 2.2) must be rewritten in this general case. If the problem is restricted to small perturbations of all the physical quantities, a general solution of the linearised system can be obtained by separation of variables. Any mode of oscillation can then be written in the form (e.g. Unno *et al.* 1989).

$$\zeta_k^{\ell,m}(r,\theta,\varphi,t) = \xi_k(r)\, Y_\ell^m(\theta,\varphi)\, \mathrm{e}^{i\sigma t} \tag{2.16}$$

where $\zeta(r,\theta,\varphi,t)$ describes the relative displacement from its equilibrium position of any mass element in the star with spherical coordinates (r,θ,φ). $\xi_k(r)$ is again the radial eigenfunction, with k nodes between the center and the surface. The angular dependence, which is the same for all the perturbed physical quantities, is given by the spherical harmonics $Y_\ell^m(\theta,\varphi)$, where $(\ell = 0,1,2,...)$ and $(m = 0,\pm1,...,\pm\ell)$. The labelling of the solutions in terms of the indices (k,ℓ,m) is very similar to the quantum mechanical description of the hydrogen atom. The ℓ and m indices describe the angular behaviour of the oscillations, which can be visualised, on the surface of the star, as alternate bright and dark areas. The image commonly given is one of a beach ball, as shown by (Figure 2.4). The special case $\ell = m = 0$, which implies $Y = 0$, corresponds to pure radial pulsations, as no angular displacement is involved.

Two classes of nonradial modes may be distinguished. These are the short period p-modes and the long period g-modes. The p-modes are characterised by a predominantly radial fluid motion, where pressure supplies most of the restoring force, whereas g-modes

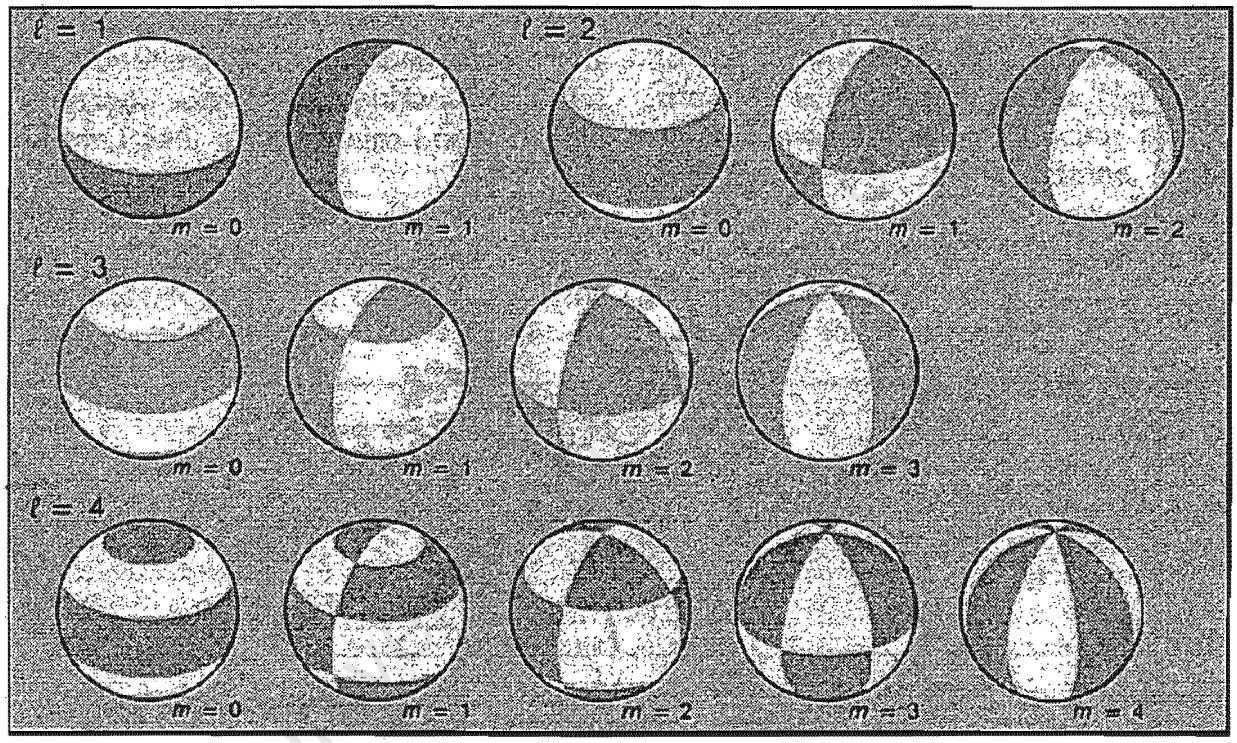

Figure 2.4: Visualisation of some simple nonradial modes. The bright and dark areas behave in the opposite manner. For instance, the mode $\ell = 2$, $m = 0$ corresponds to an oscillation where the two pole caps are alternatively both brighter or both darker than the equatorial belt that separates them. Reproduced from Winget & Van Horn (1982).

are characterised by a mainly horizontal mass displacement, where gravity acts as the main restoring force (Cox & Giuli 1968). A crude but illuminating analogy is to compare p-modes to acoustic waves, and g-modes to ocean waves, where gravity seeks to smooth out the density difference on any sphere concentric with the star.

The spectrum of eigenfrequencies, together with the distribution of nodes along the stellar radius for a typical young star with a mass 10 times that of the sun is given in Figure 2.5. The Lamb frequency, L_l, and the Brunt-Väisälä frequency, N, are two structure dependent characteristic frequencies which have the property to constrain the period range in which p and g-modes may oscillate. It is shown (e.g. Unno *et al.* 1989) that, in order for the pressure (resp. gravity) to work as a restoring force, the frequency of the oscillation should be higher (resp. lower) than the critical frequency L_l. On the other hand, the limit frequency N, with which a bubble of gas may oscillate adiabatically, must be lower (resp. higher) than the actual pulsation frequency for acoustic p-modes (resp. for gravity modes). Therefore, the region where $\sigma > L_l, N$ is called the acoustic wave propagation zone, while the region $\sigma < L_l, N$ is called the gravity wave propagation zone. The intermediate region where $L_l < \sigma < N$, or $N < \sigma < L_l$ is a non-oscillatory region representing nonpropagating (evanescent) waves. Diagrams such as Figure 2.5 are called propagation diagrams and are widely used in geophysics to study waves propagation in the earth's oceans and atmosphere (Tolstoy 1963).

Generally speaking, the g-mode eigenfunctions can show large relative amplitude ξ_r/r in the deep stellar interiors, whereas p-modes are mainly envelope modes, with significant amplitudes only in the stellar atmospheres, as seen in Figure 2.6.

In the linear nonradial theory, there is again no interaction between the different modes which can be simultaneously excited without interfering with each other. Therefore the superposition principle is valid here, and the most general stellar pulsation takes a form very similar to the one obtained for pure radial oscillations (equation 2.14):

$$\zeta(r,\theta,\varphi,t) = \sum_{k,\ell,m} \zeta_k^{\ell,m}(r,\theta,\varphi,t) \tag{2.17}$$

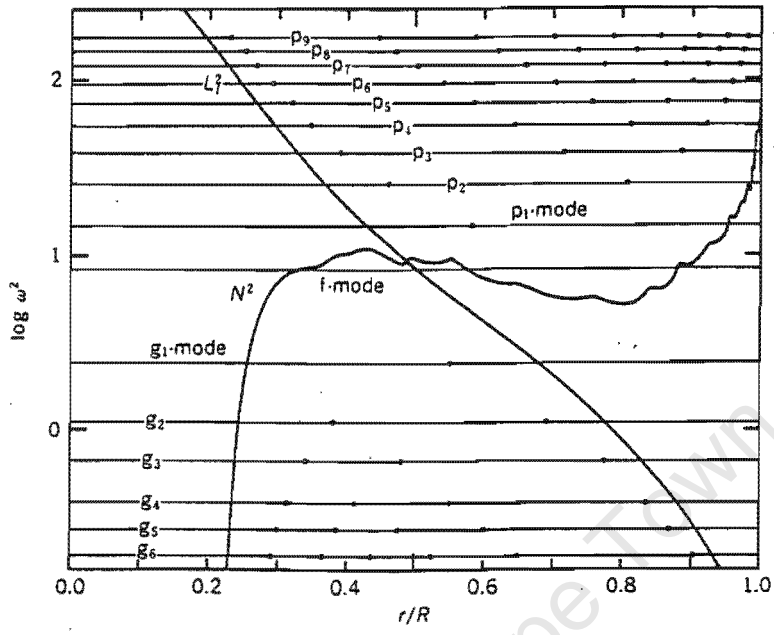

Figure 2.5: The distribution of eigenfrequencies and that of nodes of the eigenfunctions ξ_r for a young 10 $M_\odot$ in the case $\ell = 2$. The critical frequencies L_l and N delimit the region of existence of the p and g-modes. R is the stellar radius. Reproduced from Unno *et al.* (1989).

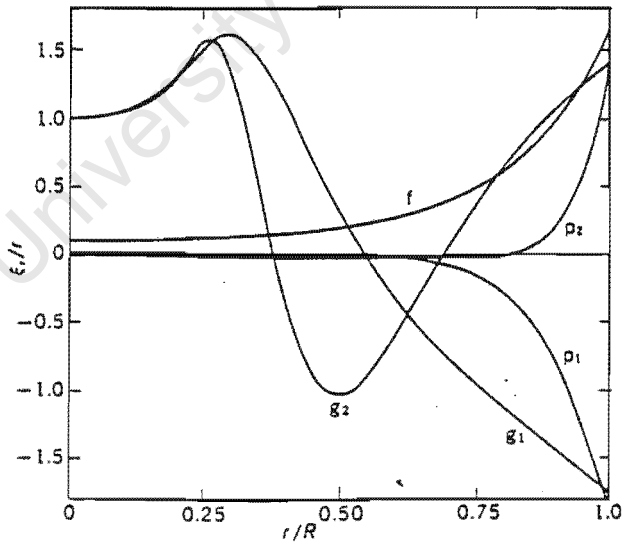

Figure 2.6: Eigenfunction of relative displacement in the radial direction, ξ/r, for the same stellar model as in Figure 2.5. Different normalizations are used at the center. R is the stellar radius. Reproduced from Unno *et al.* (1989).

2.6 Stellar pulsations: a wonderful tool for astronomers

Although stellar pulsation is a fascinating phenomenon, scientific interest in it would have rapidly faded away if it only involved studying a few odd stars, with no relation with the large non-pulsating stellar population. Although stellar pulsation is a rare phenomenon among stars, it has, however, proved of primary importance in astronomy for various reasons.

First, spectroscopic observations of stars cannot a priori tell us anything about the chemical composition and structure of their interiors as the light we receive in the telescopes has been emitted in the stellar atmospheric layers. Stellar pulsations can, however, be used as probes of the interiors of stars in order to obtain some information about their inner structures, in the same way that seismology is done on earth: this is the aim of *asteroseismology*. Quantities like rotation period, magnetic field, mass, and interior structure of a pulsating star may be derived from the analysis of the period spectrum (e.g. Bradley 1993, and references therein).

As the period spectrum in which a star is pulsating is entirely determined by its inner structure and composition, the oscillating frequencies will change over the years as a result of stellar evolution. The actual measurement of the rate of period change is a direct indication of the rate of evolution. Theoretical evolutionary models can thus be calibrated, providing fundamental information about the history and destiny of these stars. Among others, it yields constrains on their age. When applied to the oldest known pulsating stars, namely the variable white dwarfs, this provides an estimate of the age of our galaxy, the Milky Way (Winget 1988).

Our Sun is a pulsating star as well, with millions of modes excited, though all of very small amplitudes (the relative brightness changes are of the order of 10^{-7}). When observing distant stars, the light we receive from them is inevitably integrated over the stellar surface. Therefore, the beach-ball pattern shown by Figure 2.4 cannot be directly seen. In the case of the sun, its surface is resolved which enables measurement of local brightness variations. In turn, this allows the identifications of high ℓ-degree modes, which cannot be distinguished otherwise, providing us with an enormous number of probes to the interior, as each mode penetrates to a different depth and thus samples a different region of the stellar interior. Clues about the solar neutrino problem have been obtained,

as well as better understanding of the solar sunspot cycle, which is of direct interest for the terrestrial weather programs (Gough *et al.* 1996).

Among the most important pulsating stars in astronomy are the Cepheid variables. They are important because a linear relation has been found between the period of their light variations, ranging from one to a few hundreds days, and their absolute brightness. The measurement of the oscillation period of a Cepheid variable, which is easy to obtain, thus yields a determination of its absolute brightness through the period-luminosity relation. In turn, comparison of this absolute brightness with the apparent brightness gives the distance of the star. Cepheids have been widely used to establish the size and structure of our own Galaxy, as well as of distant galaxies. As they are extremely luminous stars (on average 100 times more than the sun), they can be seen at large distances, and therefore are one of the most fundamental tools for large distance scale measurements.

2.7 Conclusion

Although stellar pulsations have been intensively studied since the late 19th century, theoretically as well as observationally, our understanding of this phenomenon is far from comprehensive. In particular, when oscillations of finite amplitude are driven, various nonlinear processes occur which are not yet fully explained. Developments of nonlinear models are slow due to the complexity of the physics, but progressing. With the advent of increasingly powerful telescopes, photometric observations with higher and higher signal to noise ratio are obtained and, consequently, more and more stars are discovered to be pulsators. Astronomers are now wondering whether or not all stars are, to a certain extent, pulsating. With all that can be revealed about stellar structure and evolution from the study of these pulsations, this would surely lead to new prospects for our understanding of the Universe.

Acknowledgments

I am grateful to Darragh O'Donoghue for useful discussions as well as for his linguistic corrections.

References

Baker N., Kippenheim R., 1962, *Zeitschrift für Astrophysic*, 54, 114

Böhm-Vitense E., 1958, *Zeitschrift für Astrophysic*, 46, 108

Brickhill A. J., 1991, MNRAS, 251, 673

Cox J. P., *et al.*, 1966, ApJ, 144, 1038

Cox J. P., Guili R. T., 1968, *Principle of Stellar Structure*, eds. Gordon & Breach, New York

Cox J. P., 1980, *Theory of Stellar Pulsation*, Princeton University Press, Princeton

Eddington A. S. 1917, The Observatory, 40, 290

Gough D. O., 1996, *et al.*, *Science*, 272, 1233

Landau L. D., Lifshitz E. M., 1959, *Fluid Mechanics*, London: Pergamon Press, 4, 5.5

Ledoux P., Walraven Th., 1958, *Handbuch der Physic*, edit. S.Flugge (Springer-Verlag), Berlin, 51, 353

O'Donoghue D., 1988, *South African Journal of Science*, 84, 503

Tolstoy I., 1963, *Revue of Modern Physics*, 35, 207

Unno W., *et al.*, 1989, *Nonradial oscillations of stars*, University of Tokyo press, Tokyo

Winget D.E., Van Horn H.M., 1982, *Sky & Telescope*, 216

Wu Y., 1997, *White Dwarfs*, eds. I. Isern *et al.* (Kluwer Academic Publisher), 467

Chapter 3

Asteroseismology of pulsating white dwarf stars

Abstract

Prospects and results of the use of stellar pulsations as seismic probes of the interior of white dwarf stars are reviewed. Fundamental notions about stellar pulsation in general and about stellar evolution to the white dwarf stage are summarised, before describing in more detail the different types of pulsating white dwarfs. It is then shown how stellar parameters like mass, rotation period, magnetic field, and inner structure of white dwarfs can be obtained from the analysis of the period spectrum of their light curves. The study of the rate of period change of the oscillation modes provides a determination of the age of these stars which in turn yields a measurement of the age of the universe itself.

A discussion on the presence of nonlinearities in the period spectrum of pulsating white dwarfs is also given, which emphasises the potential of the nonlinear models, whose development is still in its infancy.

3.1 Introduction

The most common final stage of stellar evolution is represented by white dwarf stars. The most evolved white dwarfs (i.e. the coolest ones) are known to be among the oldest stars in the Galaxy. Thus, their study can potentially reveal information about the history of the Galaxy (stellar formation and evolution), in the same way that fossils can tell us about the evolution of life on earth.

The light we receive from a star is emitted in its outermost atmospheric layers, and thus, spectroscopic observations cannot reveal anything about the structure and composition of the stellar interior. The discovery of white dwarfs with variable brightness provided us with a powerful seismological tool as these so-called stellar pulsations can be used as probes of the interior of these stars.

3.2 Pulsating stars

A star is said to be pulsating if its brightness undergoes intrinsic periodic fluctuations. These variations are the consequence of a local oscillatory perturbation of the stellar equilibrium which then propagates through the stellar medium, reaches the surface and affects the outgoing luminosity flux.

The natural modes of oscillation (called normal modes) are the solutions of the system of differential equations describing stellar pulsations. In the linear theory (i.e. in the limit of very small oscillations), they are of the form (Unno *et al.* 1989)

$$\zeta(r,\theta,\varphi,t) = \xi_k(r)\ Y_\ell^m(\theta,\varphi)\,\mathrm{e}^{i\sigma t} \tag{3.1}$$

where $\zeta(r,\theta,\varphi,t)$ describes the displacement of any point in the star with coordinates (r,θ,φ). The radial and angular components of ζ are respectively given by $\xi_k(r)$ and by the spherical harmonic $Y_\ell^m(\theta,\varphi)$ ($\ell = 0,1,2,...;\ m = -\ell,...,\ell$), where the radial number k represents the number of nodes between the center and the surface of the star. The temporal behaviour is sinusoidal with angular frequency σ. Thus any normal mode is fully

described by the three indices (k, ℓ, m), in very much the same way than the labelling of the solutions of the quantum mechanical hydrogen atom.

The solutions with $\ell = 0$ (i.e. $Y(\theta, \varphi) = 0$) correspond to pure radial oscillations, which are true sound waves. In the more general case of nonradial oscillations, one distinguishes between the short period p-modes, where pressure acts as the dominant restoring force, and the long period g-modes, where buoyancy is the main restoring force (as in ocean waves) (Cox 1980).

3.3 White dwarf stars

A young star with a mass between about one and eight times that of the sun will burn its hydrogen into helium by nuclear fusion, and, when its core temperature increases above a certain value, helium burning reactions will be triggered, leaving carbon as ash. This latter phase of evolution is accompanied by significant loss of mass. Carbon might itself be ignited in the core and burn to oxygen, and possibly heavier elements, but a star of initially 1-8 solar masses will not get hot enough for these reactions to last long, if they are, in fact, ever ignited. There comes a time when nuclear reactions are no longer generating the energy needed to maintain the internal pressure that balances the force of gravity, and the star will start shrinking. If, at this stage of evolution, the mass of the star is less than 1.4 solar masses (Chandrasekhar limit), this contraction will continue until the pressure provided by the electron degeneracy prevents a further collapse (e.g. Pasachoff 1989). The star has now reached its final stage of evolution, and is then called a *white dwarf*. As the degenerate electron pressure does not depend on temperature (e.g. Böhm-Vitense 1992), the white dwarf is stable and will just cool down by radiating away its thermal energy. It will thus become fainter and fainter.

White dwarfs represent the most common end point of stellar evolution. A typical white dwarf has a mass $0.6\,M_\odot$ ($M_\odot = 2 \cdot 10^{30}$ kg = 1 solar mass), for a radius about 4 times that of the earth; this corresponds to an extreme density of about 10^6 gm/cm^3. Its surface temperature when reaching the white dwarf stage is about 10^5 K. It will then take it approximately 10 billion years to cool down completely into what is called a *black dwarf*, much longer than the total evolution of the star until then.

Table 3.1: Updated chart from O'Donoghue (1988).

Pulsator	T_{surf} [K]	Age [years]	Number discovered
PNNV	$> 10^5$	10^4	10
DOV	$> 10^5$	10^5	4
DBV	$2.5 \cdot 10^4$	10^7	8
DAV	$1.2 \cdot 10^4$	10^9	24

Stellar evolution theories predict that white dwarf stars have a degenerate carbon-oxygen core containing 99% of the stellar mass, whereas their atmosphere is made of a thin layer of residual helium (DB white dwarfs) with possibly a layer of residual hydrogen on top (DA white dwarfs). The thicknesses of the different chemical layers, rendered pure by the strong gravitational settling, remain however weakly constrained by stellar evolution models.

3.4 Pulsating white dwarfs

Four classes of pulsating white dwarfs are known, which can be distinguished by their stage of evolution (i.e. by their age). The first two classes are actually only pre-white dwarfs stars: these are the pulsating planetary nebula nuclei (PNNV), in which nuclear helium burning still takes place (although this is still controversial), and the hot DO variables (DOV stars), where cooling is dominated by plasmon neutrino emission from the deep interior (Winget 1988). Plasmon neutrinos are neutrinos emitted by electrons accelerated in a plasma, similarly to bremsstrahlung or thermal radiation of photons (Inman & Ruderman 1964). The last two known classes of compact pulsators are genuine white dwarfs in the sense that their evolution takes place at constant radius and is dominated by photon radiation; they are the DA and the DB variable white dwarfs respectively (see section 3.3). An estimate of the average age and temperature of typical stars belonging to these 4 classes can be seen in Table 3.1. Hereafter, we will abandon the white dwarf progenitors DOV and PNNV, to concentrate our discussion on the DAV and DBV only (where the 'V' always stands for variable). From now onwards, the terms pulsating or variable white dwarf will only include the two latter classes, unless otherwise mentioned.

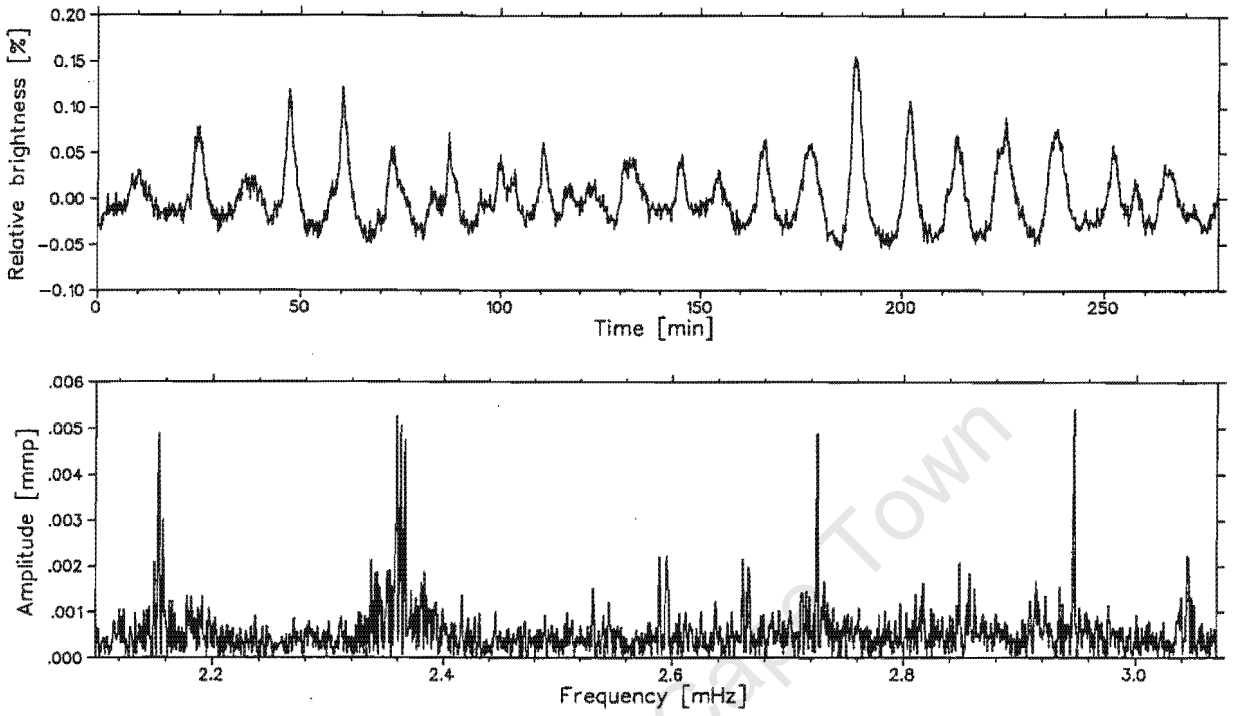

Figure 3.1: Portion of the light curve of the DBV white dwarf GD 358 obtained in 1990 (Winget *et al.* 1994) (*upper panel*); corresponding Fourier spectrum in the region of highest amplitude (*lower panel*).

No known pulsating white dwarf oscillate in just one mode. All of them are multi-periodic pulsators (Figure 3.1, bottom panel), having up to a few tens of modes simultaneously excited (Winget & Fontaine 1982). The large amplitude variables are also known for having a typical nonsinusoidal light curve (Figure 3.1, top panel), which reveals the presence of nonlinear processes.

All the observed periods of oscillation are found in the range 100 s to 1200 s. This range is in good agreement with what is expected theoretically for nonradial g-modes (Dolez & Vauclair 1981, Dziembowski & Koester 1981), whereas p-modes have much shorter periods. Therefore, it is strongly believed that the identification of the observed frequencies with g-modes is correct (Winget & Fontaine 1982). This is also consistent with the fact that radial velocity curves of pulsating white dwarfs indicate little changes in the stellar radius (McGraw 1979), which would not be the case for p-modes, which have predominantly radial mass motion.

The brightness changes, ranging from 0.1% (observational limit) up to about 20%, are due to the response of the outgoing luminosity flux to surface temperature variations (Robinson, Kepler, & Nather 1982).

3.5 Instability strip

Besides their actual brightness variation, it is almost impossible to differentiate between a pulsating white dwarf and a non-pulsating one: they fall in the same range of surface gravities and sizes, and show no specific magnetic field or peculiar rotation rate. The only difference between the variables and the non-variables is their effective equilibrium temperature. There is indeed a narrow range of temperature, called the *instability strip*, in which these stars are found to be pulsating (McGraw 1979). As a DA (respectively DB) white dwarf cools, it eventually enters this instability region, 11200 K – 12500 K (respectively 23000 K – 27000 K), in which variability occurs. The current belief is that the pulsation phenomenon is a natural phase of the white dwarf's evolution and that most, if not all, of them will become variable when passing through the instability strip (Fontaine *et al.* 1982). This is so far well supported by observations, since only few known white dwarfs with surface temperature falling in the instability range do not seem to pulsate within the observational limits (Silvotti *et al.* 1997).

The very important consequence of this discussion is that what we manage to learn about these pulsators should apply to white dwarfs in general. In other words, we are not studying a few pathological stars on their own, but really the most populous stellar class (about 8% of all stars are believed to be white dwarfs, and about 1% of the latter are pulsating).

3.6 Driving mechanism

For a variable star to be able to maintain its oscillations, some stellar mechanism must be continuously driving the pulsations in order to overcome the natural damping. Detailed models show that a stellar layer where the gas is in a partially ionized state is able to store and release radiation during the compression and expansion part of the pulsation cycle,

and thus drive the oscillations, in the same way that a child can increase the motion of a swing.

However, for this energy storage and release process to be driving effectively, its time scale must be of the order of the pulsation period of the star, which itself depends principally on the mean stellar density (Cox 1980). Crude models (Winget & Fontaine 1982) show that this partial ionization zone storage time-scale can be expressed as $\int c_v T L^{-1} dM_{ext}$, where c_v, T and M_{ext} are respectively the specific heat, the characteristic temperature, and the mass exterior to r, while L is the stellar luminosity. Generally speaking, partial ionization zones of abundant elements move deeper in the stellar interior when the stars cool. Pulsation may occur only when these zones reach a particular depth in the stellar interior where the above storage criteria is satisfied. This explain why stellar pulsations occur only in specific temperature ranges.

Theoretical models of DA variables predict instabilities for g-modes in the observed ranges of both periods and temperatures only if excited by the hydrogen partial ionization zone (Dolez & Vauclair 1981, Dziembowski & Koester 1981, Winget 1981). Two related physical processes are responsible for the actual driving of pulsations. They are referred to as the κ- and γ-mechanisms (see section 2.4)

These models also anticipated the discovery of the DB variables by predicting that the helium partial ionization zone of DBs should be pulsationally unstable for surface temperatures in the range 20000 K – 30000 K (Winget 1981).

The origin of the driving mechanism is however still controversial, since the above calculations have all been carried out in the *frozen in* approximation which assumes that the convective flux is not perturbed during the pulsational cycle (Baker & Kippenhahn 1965). As a proper time-dependent treatment of convection is not yet possible, approximations have to be made. However, not only is the convective turn-over time about a second in white dwarfs, i.e. much lower than the pulsation periods, but also most of the flux is expected to be carried by convection in the convective layers. The frozen-in approximation, on which models have relied since the early 1980s, is therefore not appropriate for white dwarfs. Furthermore, Pesnell (1987) showed that, when the frozen-in approximation is adopted, the bottom of the convection zone systematically contributes to the driving, process called *convective blocking*.

An alternative, and much more physical, treatment of convection has been proposed by Brickhill (1983), who assumed that the convective flux responds instantaneously to the pulsations. He demonstrated that, in this approximation, convection may drive g-modes via a process he called *convective driving* (Brickhill 1991). Arguing that the partial ionization zone is very thin due to the high gravity, and has a thermal time-scale much shorter than the observed pulsation periods, Brickhill claimed that the driving from the opacity mechanism ought to be overwhelmed by the radiative damping. Therefore, convective driving should be the dominant form of driving in pulsating white dwarfs. His conclusions were recently supported by Gautschy *et al.* (1996) and Goldreich & Wu (1999a).

3.7 Mode Selection mechanism

Although the pulsating white dwarfs are relatively rich in periods, the number of excited modes is far less than the actual g-mode spectrum. This implies the existence of some sort of selection mechanism which causes modes with particular values of k to be preferentially excited over other modes, perhaps even with adjacent radial overtones k. The well stratified structure of the white dwarf interiors is held responsible for this phenomenon through a process of resonance between the wave-length of certain excited modes and the thicknesses of the surface composition layers (Winget, Van Horn, & Hansen 1981). These specific waves will tend to be reflected at the transition zone between two different compositional layers, and will consequently show significant amplitude only in the atmosphere of the star. This effect, referred to as *mode trapping*, decreases the kinetic energy of these particular modes, which makes them preferentially easier to excite (Figure 3.2a). The amplitude of a trapped mode below the atmosphere is very sensitive to the thickness of the transition region between the two composition layers where reflection occurs. The thinner the transition zone, the more efficient the trapping process, and the larger the kinetic energy difference between trapped and non-trapped modes (Brassard *et al.* 1992) (Figure 3.2b).

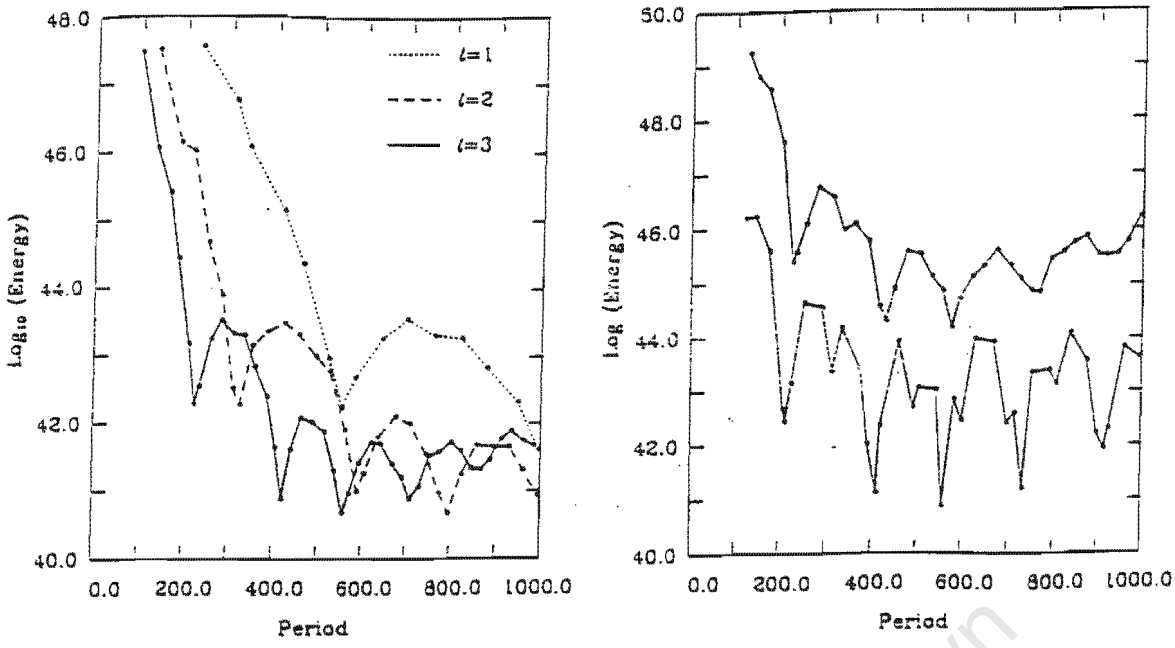

Figure 3.2: Kinetic energy required to excite a pulsation mode versus the period of the mode *(a)* for various ℓ-overtones *(left panel)* *(b)* for models with different transition zone thicknesses *(right panel)*, where the upper (resp. lower) curve refers to a model with a standard medium (resp. thin) transition zone. Reproduced from Brassard *et al.* (1992).

3.8 Asteroseismology

Spectroscopic observation of stars cannot reveal anything about the structure or composition of their interior, as the light we receive from them has been emitted in the stellar outermost layers. Stellar pulsation, on the other hand, is a phenomenon which include the participation of the whole star, not only of the photosphere. Therefore, their study can potentially be used to obtain information about the inner part of the star. This is the aim of asteroseismology, whose name comes from the fact that the pulsations are used as probes of the white dwarf interiors, in very much the same way that seismology tells us about the inner structure of the earth.

The link between the photometric observations and the asteroseismological models is given by the mode identification. The latter consists in assigning, to each different period found in the observed spectrum, the corresponding normal mode indices (k, ℓ, m). This labelling process is of vital importance as it then allows detailed comparison between theoretical models and observations.

Although this identification might seem to be a fairly straightforward exercise, it is a very tricky task for various reasons which will be discussed in section 6.2.1. Once a

correct identification has been carried out, the analysis of the period spectrum might provide various physical information about the star, as shown in the rest of this section.

3.8.1 Mean Period Spacing

The periods of high overtone g-modes of indices (k, ℓ, m) are approximately given by (Tassoul 1980):

$$\Pi_k^\ell = \frac{k}{\sqrt{\ell(\ell+1)}}\Pi_0 \quad , \quad k \gg 1 \tag{3.2}$$

where Π_0 is the characteristic g-mode spacing, which is a function of the stellar structure: it depends only weakly on the temperature and chemical composition, but is very sensitive to the level of degeneracy in the core, which itself is a direct function of the stellar mass M_*.

If ℓ is now kept fixed, the period spacing between consecutive high-overtones g-modes is given, from (3.2), by

$$\Delta\Pi = \frac{\Pi_0}{\sqrt{\ell(\ell+1)}} \tag{3.3}$$

Theoretical models having M_* and ℓ as the only free parameters can be adjusted in order to produce a characteristic period spacing matching the value of Π_0 obtained from the measurement of $\Delta\Pi$. This is the most accurate mass determination method for white dwarfs to date. For instance, the mass of the DOV star PG1159-035 has been found to be $0.60 \pm 0.01\, M_\odot$ (Kawaler 1987); the same technique yields a mass of $0.61 \pm 0.03\, M_\odot$ for the DB variable GD 358 (Bradley & Winget 1994).

Various other physical stellar parameters can be derived, once the mass of the star has been determined. The radius can be obtained from a white dwarf mass-radius relation. Combining the radius with the spectroscopically determined temperature yields the absolute stellar luminosity. In turn, comparison of the absolute and apparent (visible) luminosities gives a measurement of the distance of the star. For GD 358, the latter

seismological distance has been found to be 42 ± 3 pc (Bradley & Winget 1994), in good agreement with the stellar parallax (*trigonometrical* distance) of 36 ± 4 pc (Harrington *et al.* 1985).

3.8.2 Deviation from mean period spacing

The period spacing $\Delta\Pi$ of high overtone g-modes (equation 3.3) is truly constant only for stars of uniform composition. The stratified structure of white dwarfs makes the value of $\Delta\Pi$ depend on the mode radial order k, although the mean remains a good measure of the total stellar mass.

This deviation from uniform spacing is a consequence of the mode trapping process: modes with nodes near the transition zone between two different chemical layers will have their period shifted slightly, so that the nodes fall even closer to the transition discontinuites, thus reducing their corresponding kinetic energy (Winget, Van Horn, & Hansen 1981). This results in a much shorter period spacing between those modes which get pulled towards these trapping wells. The amount of deviation from the mean spacing depends on the quality of the trapping, which itself is sensitive to both the depth and thickness of the transition zones. The analysis of the period spacing is thus a potentially powerful seismological probe of the stellar structure.

Theoretical models can be fitted to reproduce as closely as possible the observed behaviour of the period spacing, thus providing us with a value for the thicknesses of the trapping layers (which are the free parameters of the models). This method works well for DA and DB variables. For instance, the mass of the hydrogen layer of DAV G226-29 obtained in this way is $10^{-4}\,M_*$ (Kepler *et al.* 1995), a factor of about 10,000 higher than what was though in the 1980's, while the same method applied to DBV GD 358 indicates a helium layer of about $2 \cdot 10^{-6}\ M_*$ (Bradley & Winget 1994) (see Figure 3.3), a value 10,000 times smaller than previous inaccurate predictions given by stellar evolution models.

As g-modes are envelope modes, showing large amplitude in the atmosphere only, trapping proves to be significant only in the atmospheric layers. Therefore, the analysis

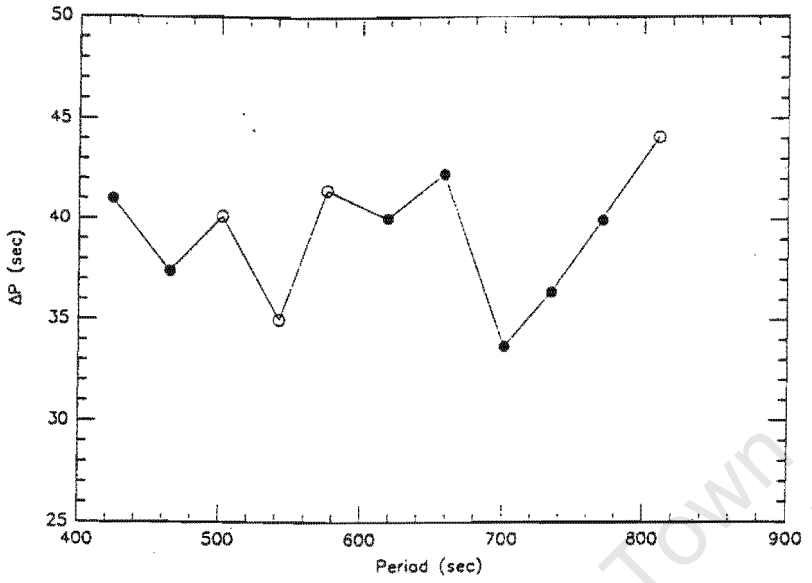

Figure 3.3: Deviation from the 39.2 sec mean period spacing observed in GD 358. The less certain periods are denoted by open dots. Each data point represents a consecutive k-overtone, ranging from $k = 18$ to $k = 8$. Reproduced from Bradley & Winget (1994).

of the deviation from mean period spacing can provide no information about the deep stellar interior.

3.8.3 Fine structure splitting

In the absence of stellar rotation or magnetic field, the normal modes have periods which are functions of k and ℓ, but not of the azimuthal number m (see section 3.2). Therefore, each mode is $(2\ell + 1)$-fold degenerate. If the star is rotating, this degeneracy is lifted, due to the break down of the spherical symmetry. Each mode then splits into a $(2\ell + 1)$ period multiplet with frequencies now a function of m. For slow rotation ($\Pi_{\rm rot} \gg \Pi_{\rm modes}$), the frequency spacing between each component of a given multiplet is uniform within a multiplet. To first order, it is given by (Unno *et al.* 1989)

$$\Delta\sigma = m\,\Omega\,(1 - C_{k,\ell}) \tag{3.4}$$

where m is the azimuthal number of the mode, Ω is the rotation frequency, and $C_{k,\ell}$ is a

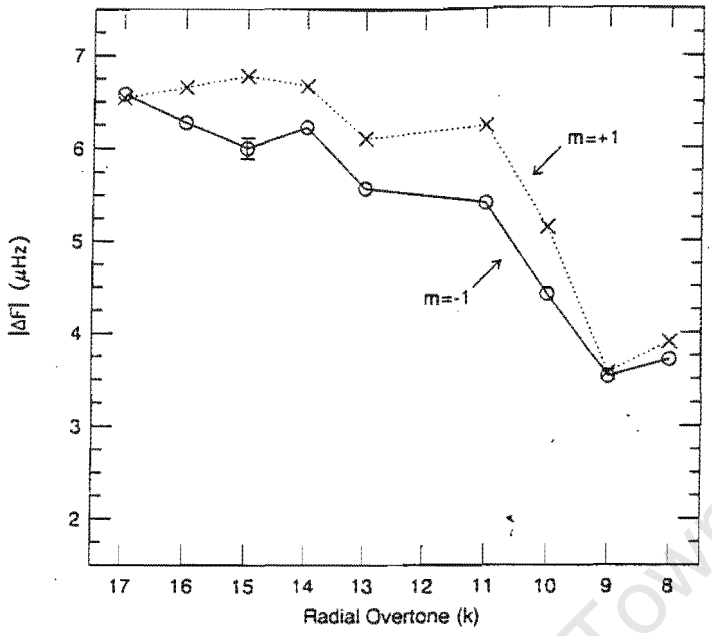

Figure 3.4: Frequency splitting within multiplets, as a function of radial overtone k. The greater splittings for larger k-values show the presence of differential rotation, while the systematically larger splittings for the $m = +1$ modes than for the $m = -1$ modes reveals the presence of a weak magnetic field. Reproduced from Winget *et al.* (1994).

complicated structural constant that depends on the model, but which can be asymptotically ($k \gg 1$) approximated by

$$C_{k,\ell} = \frac{1}{\ell(\ell+1)} \tag{3.5}$$

Evidence for rotationally split modes can be seen in many white dwarfs (see for instance the triplet at 2.37 mHz in Figure 3.1). In each case, the frequency splitting is of the order of 3 - 7 μHz, indicating a rotation period, Ω^{-1}, of about 1 - 2 days. For example the DOV star PG1159-035 is found to have a rotation period of 1.38±0.01 days (Winget *et al.* 1994). In the case of differential rotation, the splitting becomes a function of the radial order k. In the DB variable GD358, the frequency splitting increases with increasing k (Figure 3.4).

As modes of low radial order k penetrate much deeper into the stellar interior than the high k-overtones which tend to rather sample the outer part of the star, it was concluded (Winget *et al.* 1994) that GD358 is rotating differentially. The mean splitting of 6.51 μHz

for $k = 16, 17$ corresponds to a rotation period of 0.89 days, whereas the mean splitting of 3.7 μHz for $k = 8, 9$ indicates a period of 1.6 days. Consequently, Winget *et al.* (1994) claimed that the outer envelope is rotating about 1.8 times faster than the region of the outer core sampled by the low-order modes identified. This result is, however, still controversial (Fontaine, private discussion).

3.8.4 Deviation from uniform splitting

The presence of a weak magnetic field (one which perturbs but doesn't dominate the motion of the stellar plasma) breaks down the uniform fine structure splitting laid down by rotation (Figure 3.4). The intensity of the magnetic field can be derived from the amount of asymmetry, although detailed calculations are highly complicated (Jones *et al.* 1989), and the results give only an estimate of the order of magnitude rather than an accurate measurement. For the DB variable GD 358, the value of the magnetic field obtained in this way is 1300 ± 300 Gauss (Winget *et al.* 1994), a measurement about a 1000 times smaller than the limit derived from the Zeeman splitting of spectral lines.

3.8.5 Rate of period change

One of the most exciting prospects of asteroseismology is its use as an age indicator. Since the periods of the normal g-modes depend on the global properties of the star (see, for instance, equation 3.2), they will change as a result of stellar evolution, according to the relation (Winget, Van Horn, & Hansen 1983)

$$\frac{\dot{\Pi}}{\Pi} = a_1 \frac{\dot{R}}{R} - a_2 \frac{\dot{T}_{\rm m}}{T_{\rm m}} \tag{3.6}$$

where $\dot{\Pi}$ is the rate of period change, R is the stellar radius, and $T_{\rm m}$ is the maximum temperature reached during the pulsation cycle, while a_1 and a_2 are model dependent constants both of order unity. As for white dwarfs stars, the contraction rate $\dot{R}$ is about zero (this is, however, not true for pre-white dwarfs), the rate of period change depends only on the cooling rate $\dot{T}_{\rm m}$. As $\dot{T}_{\rm m} < 0$, this corresponds to an increase in the pulsation periods, or equivalently to a decrease in the frequencies.

As timings of the pulsations can be measured to an accuracy of a few seconds, observations of a pulsating white dwarf over about 10 years can detect any change that exceeds roughly $10^{-13} - 10^{-14}$ sec/sec. This yields very stringent constraints on the cooling rate $\dot{T}_{\rm m}$, which in turn allows a global calibration of the evolutionary rate at which a white dwarf moves down the cooling sequence. This calibration can then be used to determine the age of the coolest white dwarfs known. As these objects are among the oldest in the Galaxy, this provides both an estimate of the age of the Galaxy itself and, using evolutionary Big Bang models to determine the time needed for the Galaxy to form, the age of the universe. The latest estimate of the age of the universe determined in this way is 10 billion years (Winget *et al.* 1987).

3.9 Nonlinearities in the temporal spectrum

The observed light curves of most known pulsating white dwarfs show nonlinear (i.e. non sinusoidal) behaviour. Analyses of their period spectra reveal the presence of harmonics and combination frequencies of the normal modes excited (a combination mode has a frequency which is the sum or difference of frequencies of normal modes). The corresponding light curves are therefore non-sinusoidal and show characteristic features: peaks with sharp ascents, slower descents, and flat bottoms in between (see Figure 3.1).

The exact origin of these combination frequencies is at present unknown. Various phenomena could be responsible for their presence. Amongst others are harmonic distortion processes, and resonant mode coupling. Harmonic distortion occurs when the star is not able to respond linearly to the pulsations. The oscillatory wave then gets distorted in very much the same way as a sound wave behaves in a dense medium. Mode coupling is a resonant process between three[1] normal modes that happen to be in a frequency relationship of the kind $f_3 = f_1 \pm f_2$, and where not all three modes are naturally driven. The resonance can be either *parametric* (Moskalik 1985), or *direct* (Dziembowski 1979), depending on which modes in the combination are naturally unstable, and which ones are naturally damped, but excited by the nonlinear coupling. Although evidence for resonant mode coupling seems to have been seen in certain cases (O'Donoghue, Warner, & Cropper 1992), this process must be discounted in others (Winget *et al.* 1994).

[1] to keep the discussion simple

Table 3.2: Successes and prospects of asteroseismology

Observational quantity	Stellar parameter
Mean period spacing	Stellar mass
Deviation from mean period spacing	Outer layer thickness
Mode trapping	Transition zone thickness
Fine structure splitting	Rotation period
Deviation from uniform splitting	Magnetic field
Rate of period change	Cooling rate, age
Amplitude of the normal modes	?
Amplitude of the cross-frequencies	?
Amplitude changes	?

Although these nonlinear processes are conceptually well understood, they are extremely difficult to analyse phenomenologically as their lack of specific signatures render them impossible to disentangle. From a theoretical point of view, the problem is extremely difficult to address due to the highly nonlinear nature of the pulsation equations (Cox 1980). At present, no information about the star has been extracted from the study of these nonlinear features, i.e. nonlinear asteroseismology does not yet exist.

3.10 Conclusion

Asteroseismology has proved to be a powerful tool when applied to white dwarfs stars. Indeed, their rich period spectrum can reveal a lot about their internal structure, as each pulsation mode probes a slightly different depth in the stellar interior. Table 3.2 summarises what can be learnt from spectral analysis of the normal modes. However, having too many modes excited at the same time can also be a disadvantage because longer data sets are necessary in order to resolve closely-spaced frequencies (multiplets or independent overlapping modes).

All the stellar parameters given in Table 3.2 are derived from linear models. The fact that nonlinear frequencies are, generally speaking, much more numerous than normal modes shows that asteroseismology still has enormous untapped potential, due to the lack

of proper nonlinear models.

Not only is stellar pulsation a fascinating phenomenon in itself, but its study has already resulted in enormous progress in our understanding of stellar structure and evolution. This makes variable white dwarfs a rich and exciting field of research.

Acknowledgments

I am grateful to Darragh O'Donoghue, whose useful comments about the physics and vital help with the English made this publication possible.

References

Baker N, Kippenhahn R., 1965, ApJ, 142, 869 Bradley P. A., 1993, Baltic Astronomy, 2, 545

Bradley P. A., Winget D.E., 1994, ApJ, 430, 850

Brassard P., Fontaine G., Wesemael F., Tassoul M., 1992, ApJS, 81, 747

Böhm-Vitense E., 1992, *Stellar Astrophysics*, Vol.3, Cambridge University Press, Cambridge

Cox J. P., 1980, *Theory of Stellar Pulsation*, Princeton University Press, Princeton

Dolez N., Vauclair G., 1981, A&A, 102, 375

Dziembowski W. A., 1979, *White Dwarfs and Variable Degenerate Stars*, eds H. M. Van Horn & V. Weidemann, University of Rochester, Rochester, 359

Dziembowski W. A., Koester D., 1981, A&A, 97, 16

Fontaine G., *et al.*, 1982, ApJ, 258, 651

Goupil M.-J., Buchler R. B., 1994, A&A, 291, 481

Harrington R. S. *et al.*, 1985, ApJ, 90, 123

Inman C. I., Ruderman M. A., 1964, ApJ, 140, 1025

Jones P. W. *et al.*, 1989, ApJ, 336, 403

Kawaler S. D., 1987, *Advances in Helio- and Asteroseismology*, (Reidel: Dodrecht), 329

Kepler S. O. *et al.*, 1995, ApJ, 447, 874

McGraw J. T., 1979, ApJ, 229, 203

Moskalik P., 1985, Acta Astron., 35, 229

O'Donoghue D., 1988, South African Journal of Science, 84, 503

O'Donogue D., Warner B., Cropper M., 1992, MNRAS, 258, 415, 1992.

Pasachoff J. M., 1989, *Contemporary Astronomy*, Saunders College Publishing

Pesnell W. D., 1987, ApJ, 314, 598

Robinson E. L., Kepler S. O., Nather R. E., 1982, ApJ, 259, 219

Silvotti R., *et al.*, 1997, *White Dwarfs*, eds. J. Isern, M. Hernanz, and E. García-Berro (Kluwer: Dodrecht), 489

Tassoul M., 1980, ApJS, 43, 469

Unno W., Osaki Y., Ando H., Saio H., Shibahashi H., 1989, *Nonradial oscillation of stars* (2nd ed.), Univ. Tokyo Press, Tokyo

Vuille F., 1998, 11th *European White Dwarf Workshop*, eds. J.-E. Solheim & E. Meištas (San Francisco: ASP), 109

Winget D.E., 1981, PhD Thesis, University of Rochester, New York

Winget D. E, Van Horn, H. M., Hansen C. J., 1981, ApJ, 245, L33

Winget D.E., *et al.*, 1982, ApJ, 253, L29

Winget D. E., Fontaine G., 1982, *Pulsations in Classical and Cataclysmic Variable Stars*, eds. J. P. Cox & C. J. Hansen (Boulder Joint Institute for Laboratory Astrophysics), 46

Winget D. E, Hansen C. J, Van Horn H. M, 1983, Nature, 303, 781

Winget D.E et al, 1987, ApJ, 315, L77

Winget D. E., 1988, *Advance in Helio- and Asteroseismology*, eds. J. Christensen-Dalsgaard & S. Frandsen (Dordrecht: Reidel), 305

Winget D. E. *et al.*, 1994, ApJ, 430, 839

Chapter 4

Analysis techniques

4.1 Temporal spectroscopy

The advantage of the short periods of pulsating white dwarfs is that many cycles can be observed per night, therefore yielding good frequency resolution. The disadvantage is that short integration times, typically of the order of 10 s, are required to resolve the variations. In order to increase the photon counting rate, and thus the signal-to-noise ratio, these stars are usually observed in white-light. By analogy to the traditional wavelength spectroscopy, which gives maximum frequency resolution but no temporal resolution, this technique, which conversely gives maximum temporal resolution but no frequency resolution, has been called *temporal spectroscopy*.

Most analyses throughout this thesis will be conducted in the frequency domain, rather than in the time domain. This means that, instead of working directly on the light curve, I will analyse its Fourier transform. In a sense, this approach implicitly assumes that the pulsations are well represented by a superposition of sinusoids, where each of them represents an individual excited frequency. It therefore precludes addressing impartially the fundamental question as to whether the pulsations are intrinsically linear or not, as it basically presupposes that they are. The star does not know what a sinusoid is, and there is a priori no reason for it to drive the normal modes in such way. Therefore, the plain Fourier approach to the problem might distort our perception and understanding of the

pulsation mechanism. For instance, the seasonal spectral changes that have been observed in large amplitude variables cannot be well described with only the Fourier transform, for it does not provide any information on the temporal dependence of the pulsations. Time-Frequency techniques, such as wavelet analysis (Daubechies 1992, Jawerth & Sweldens 1994) might be better suited to deal with data that show definite temporal variations. Such techniques have been applied to the sun (Baudin, Gabriel, & Gibert 1994, Baudin *et al.* 1996), and to white dwarfs (Goupil, Auvergne, & Baglin 1991), yielding interesting qualitative information. The interpretation and quantification of the results were, however, difficult. Alternatively, nonlinear dynamic techniques can be used in extreme cases, as, for instance, in the search for chaos (Kolláth 1990)

Whether working in the time-domain, in the frequency domain, or in the intermediate time-frequency domain, the overall resolution is the same, and is entirely determined by the data set. No more information can be extracted using one approach rather than another, although the information obtained may be phenomenologically different, and more adapted to the actual physical discussion. The higher the resolution in frequency, the lower the resolution in time, and vice versa. It is therefore not possible to have simultaneously a maximum temporal and spectral resolution, reminiscent of the uncertainty principle of quantum physics. Maximum temporal resolution is obtained when analysing directly the light curve, and is then limited by the integration time. Conversely, maximum spectral resolution is obtained when working on the amplitude spectrum, and it is limited by the length of the data set.

Although nonlinear processes will be the main concern of this research project, several factors suggested the frequency domain as opposed to the time-frequency domain as the preferred analysis domain. First and most important, light curves are available that are long enough for their respective period structure to be resolved. It is therefore a unique opportunity to analyse the data this way. Second, a Fourier spectrum is physically easier to interpret than its time-frequency counterparts, not only because it deals with much simpler functions (sinusoids) than the typical distorted wavelet pulses, but also because the theory of pulsation itself uses plain trigonometrical solutions as ansatz (Unno *et al.* 1989). Third, if using a time-frequency type of approach, one has to make sure that the spectral resolution always remains sufficient for the beating processes not to generate misleading amplitude modulations.

If nonlinear processes are too severe, Fourier analysis is certainly not the most suited approach to the problem. However, if they are mild enough, i.e. occur on time-scales longer than the beat periods, there is a good chance to extract meaningful information on these phenomena using Fourier analysis, as it is still possible to obtain some temporal resolution by independently Fourier transforming contiguous segments of the light curve, and comparing the spectra obtained. Before using this quasi time-frequency technique, it must be ensured that no spurious beating modulation could be mistaken for nonlinear variations. The temporal resolution is therefore limited to the length of the longest beat period, which can typically be up to several days in white dwarfs. This limitation is nevertheless neither worse, nor better, than what would be obtained using any genuine time-frequency analysis technique. In particular, a true nonlinear amplitude modulation occurring on a time-scale shorter than the beatings cannot be disentangled from the latter, whatever the approach used.

The Fourier transform is a complex function. It is commonly separated into its modulus part, the amplitude spectrum, and its imaginary part, i.e. the phase spectrum. Terms such as "period spectrum", "temporal spectrum", or even "Fourier spectrum" are improperly used in the literature to refer to the amplitude spectrum. However, as long as no risk of confusion exists, these various expressions will also be used interchangeably throughout the thesis to ease the reading. The term 'power spectrum', however, refers specifically to the square of the amplitude spectrum.

The overall quality of a given amplitude spectrum is determined by its spectral window, which is the Fourier spectrum that would be obtained if the star was pulsating in just one stable noise-free frequency (Deeming 1975). Ideally, the spectral window would be composed of just the one peak corresponding to the frequency of this single oscillation mode. However, due to the finite length of any observing session, and to the daytime gaps in the data, many other peaks, that are not of genuine astrophysical origin, will appear as side lobes of this frequency, to account for these natural limitations of the data acquisition techniques.

The success of asteroseismology relies directly on our ability to perform mode identification correctly (see section 6.2), which itself depends crucially on the quality of the observed amplitude spectrum. The two factors that directly determine the quality of a temporal spectrum are its spectral resolution, and its contamination by the presence

of artifact aliases. Well-resolved alias-free amplitude spectra are therefore the necessary condition for the success of asteroseismology. These determining factors are controlled as follows:

- The length T of a data set determines entirely its spectral resolution $\Delta f = 1/T$, that is the ability to separate two closely spaced frequencies into two distinct individual peaks. To avoid spurious results in the period-finding methods, a safer value of Δf is generally considered to be $1.5/T$ (Loumos & Deeming 1977).

- To minimize aliases in the amplitude spectrum, the gaps in the data should be reduced, which relies on our ability to increase as much as possible the observing coverage.

4.2 Networks of telescopes

Any given telescope can only observe a star continuously from the time it rises until the time it sets. This duration might even be further restricted according to the time of the twilights and by cloud. The astronomer has then to wait until the following night to observe the star again. For white dwarfs, that present a rich g-mode spectrum, a single night of data is not sufficient to resolve their period structures. In order to increase the spectral resolution, these stars have to be observed for many nights in a row, leaving inherent daytime gaps in the data.

As discussed above, these daytime gaps in the light curve have an extremely harmful effect on the subsequent analysis of its Fourier spectrum, because aliases are generated which perturb the mode identification. In order to reduce these daytime gaps, i.e. increase the observing coverage, networks of telescopes have been developed whereby, when the targeted star sets for one observer, it rises for another one situated westwards of the first. A network of three telescopes, if evenly spread around the globe, in principle allows a star to be observed continuously (Schwarzschild 1995). Given that the observations can only be conducted in photometric conditions, many more observatories are in practice needed, and even then, complete coverage is difficult to attain. To date, the best multi-site campaign ever organised was the 1994 Whole Earth Telescope (Nather 1990) run on

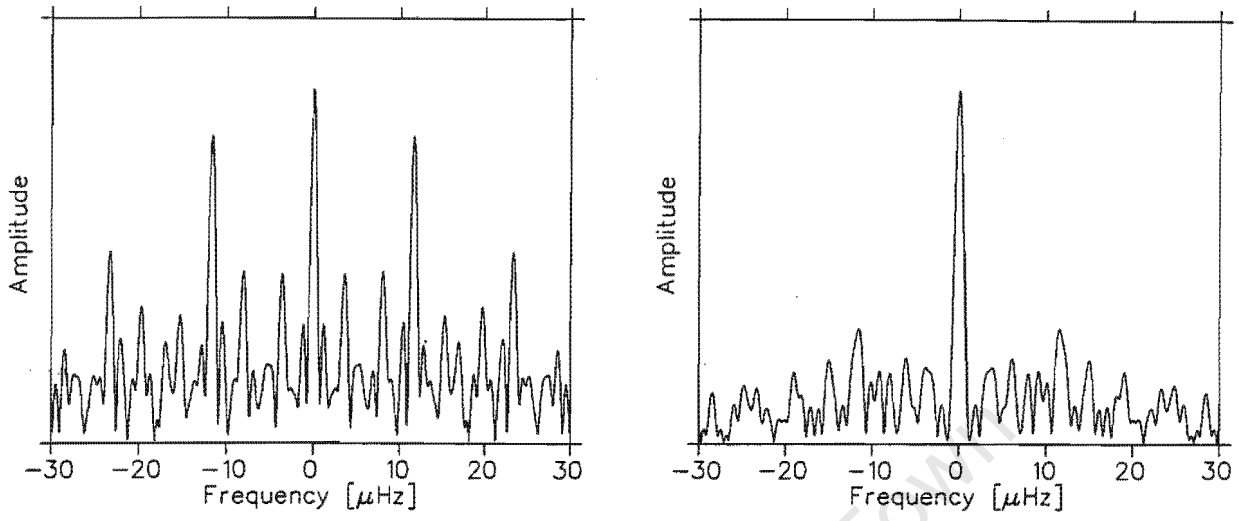

Figure 4.1: Spectral windows using all the data from the 1988 WET campaign on G29-38 (*left panel*), and using only the McDonald Observatory data (*right panel*).

the DBV GD358 (see section 6.2). A network of twelve observatories enabled this star to be followed for 80% of the time over a two week period.

The temporal spectra obtained by such multi-site campaigns benefit in two ways from the increased coverage. The presence of aliases is greatly reduced, and the frequency resolution is increased. In other words, the spectral window is greatly improved, as illustrated in Figure 4.1, where the left panel represents the window of the 1988 WET run on DBV G29-38, while the right panel is the window corresponding to the concatenated single night runs obtained at McDonald Observatory during the very same campaign.

The raw light curves gathered in each telescope during a multi-site campaign must first be individually corrected for sky background and atmospheric extinction, before being combined together with the data obtained from the other telescopes (Nather 1990). This results in a single light curve which can then be analysed as a whole, as if it had been obtained by a single telescope.

4.3 Time series analysis

I have been fortunate enough to be provided with a ready-to-use time series analysis program[1]. All the typical numerical computations, such as Fourier transforms, least-squares fits, and pre-whitening procedures, have been carried out using this code. Adaptations and extensions have nevertheless been made to the existing program, in order to match some specific needs. I describe briefly below the computing techniques used in the code.

4.3.1 Fourier transform

The Fourier transform is the fundamental tool of any frequency analysis. In the discrete case, it should however not be used as a period-finding procedure, but rather as an overall qualitative approach to the problem.

The discrete Fourier transform of the light curve is computed numerically using the algorithm by Deeming (1975). In the case where the number of required output frequencies is small enough (typically less then 2000), the numerical recursive technique proposed by Kurtz (1985) has been used to save computing time. Wherever large Fourier transforms were needed, the latter shortcut was not used, as it yields results that depart from the exact calculation method, because the inherent computation errors get accumulated from frequency to frequency.

4.3.2 Least-squares fits

Least-squares fitting methods are widely used in science because of their numerous computational and theoretical advantages (Bloomfield 1976). In the case of variable stars, these methods are mainly used to fit sinusoids to the observed light curves. Analytically, the principle consists in determining the fit parameters H, A, ω and φ of the function $y(t) = H + A\cos(\omega t + \varphi)$ by minimising the residual function

[1] c.f. acknowledgment section

$$S(H, A, \omega, \varphi) = \sum_i \{x(t_i) - [H + A\cos(\omega t_i + \varphi)]\}^2 = \sum_i [x(t_i) - y(t_i)]^2 \qquad (4.1)$$

where $x(t_i)$ is the measured time series ordinate at time t_i, i.e. the observed light curve. The computational approach depends on whether the oscillation frequency ω is a known parameter of the fit (linear least-squares fit) or not (nonlinear least-squares fit). If ω is known, then the minimising of the function $S(H, A, \varphi)$ is fairly straightforward (Bloomfield 1976). If ω is not known, the iterative approach is more complicated (Deeming 1968), and requires fairly precise input parameters, which can be obtained from a Fourier transform, or from a linear least-squares fit.

Note that the linear least-squares method is identical to the modified Fourier transform (Scargle 1982).

The errors given by linear least-squares fits are known to be statistically underestimated, whereas those given by the nonlinear counterpart are generally overestimated (except for the frequencies, but there is no sound statistical estimate of the latter). I will be very conservative, and always consider these errors obtained from the nonlinear method.

4.3.3 Pre-whitening

When carrying out the mode identification on a given temporal spectrum, one is frequently confronted with two major difficulties. Firstly, it is often problematic to determine whether a given peak, found in the vicinity of a larger frequency, corresponds to a genuine oscillation period of the star, or whether it is a window artifact. Secondly, real frequencies might be, to the limit of resolution, blended with larger peaks, and thus not detectable. In order both to differentiate between genuine pulsation frequencies and artifacts, and to reveal possible hidden low amplitude oscillation frequencies, the technique known as pre-whitening is often used. The idea is to remove from the temporal spectrum those large peaks that are suspected to hide frequencies with smaller amplitude. The procedure is the following. First the frequency, amplitude, and phase of the peak to be removed are obtained by nonlinear least-squares fitting. Then a discrete sinusoidal

light curve is built on these parameters, temporally sampled in the very same way that the observations are, so that it carries the exact signature of the spectral window. This synthetic light curve is then subtracted from the observed one, and the Fourier transform of the resulting difference is then re-computed. This procedure, illustrated in Figure 4.2, can be repeated with the next highest peak if necessary, i.e. if additional significant peaks are present.

The advantage of this cleansing technique is that it removes the synthesized frequency with its corresponding spectral leakage. The disadvantage is that neither the noise-component of this frequency, nor the spectral leakage of peaks close to this frequency, are taken into account (Clemens 1994). However, the interference of closely separated frequencies can never be completely avoided. The sole way of reducing the overlapping of spectral (leakage) features is to increase the quality of the window. As an alternative to pre-whitening, the CLEAN algorithm can also be used (Roberts *et al.* 1987), but this technique gives less control over the results, and more precautions are necessary (Michel 1993).

4.3.4 Period-finding procedure

When few peaks, widely separated in frequency, are present in the amplitude spectrum, the determining of their respective characteristics is straightforward. Individual nonlinear least-squares fitting procedures are conducted for each identified peak, where the respective input parameters are simply obtained from the Fourier transform of the light curve, as discussed above.

However, when closely separated frequencies are simultaneously present, the situation is more delicate because of possible spectral leakage interference between these peaks. Let me consider a star having just a triplet of frequencies excited. The period-finding procedure in such a situation is the following. The fit parameters of the highest peak of the multiplet are first obtained by traditional nonlinear least-squares method. This peak is then removed from the spectrum by pre-whitening, which also removes its window features that might interfere with the two other peaks. This exact procedure is then repeated for the second highest frequency, and finally for the third one. The characteristics of these three peaks are then used as inputs for a multi-variate nonlinear least-squares procedure

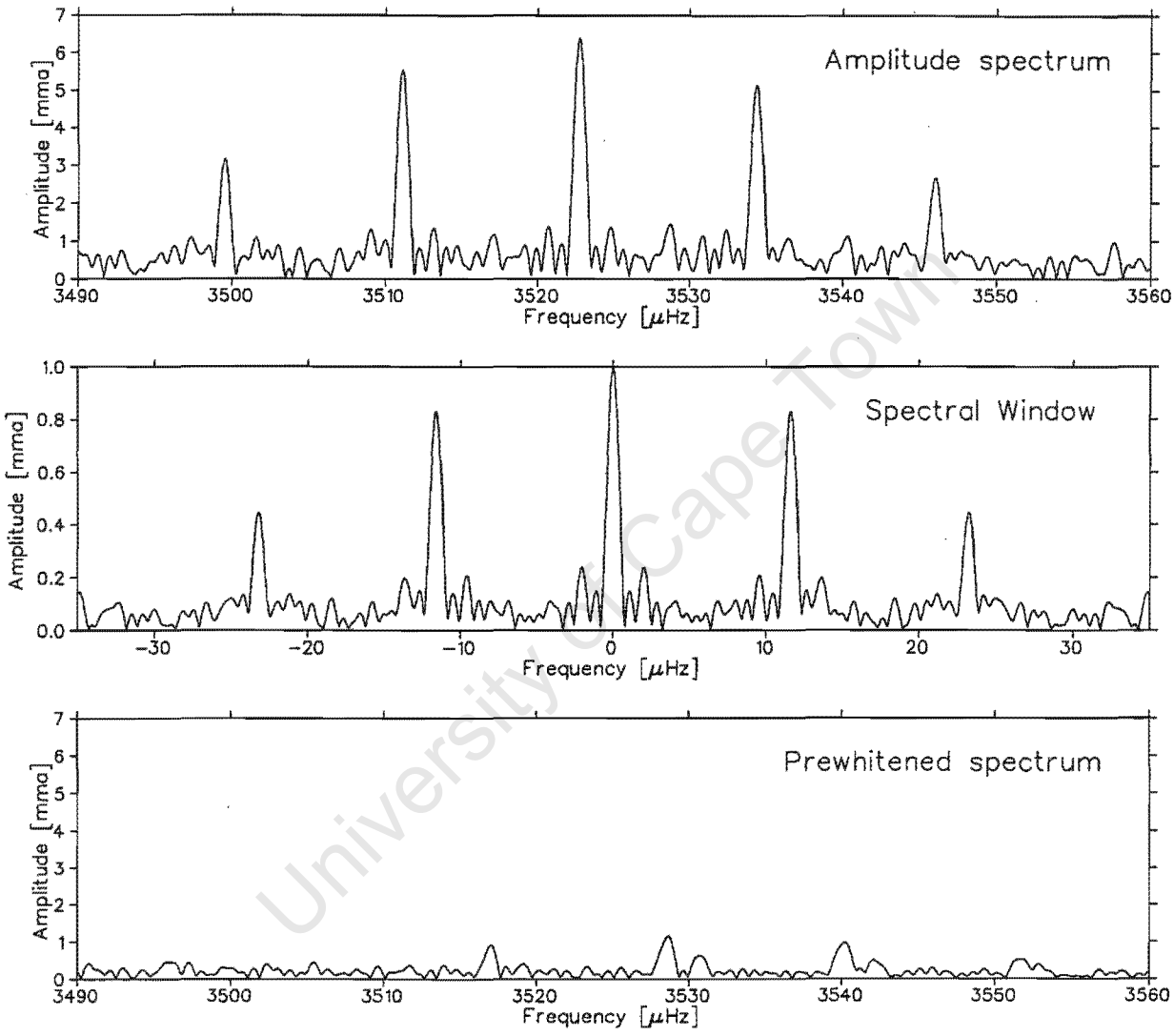

Figure 4.2: Pre-whitening technique. The top panel shows a portion of the amplitude spectrum of G29-38 as obtained during a single-site campaign conducted at McDonald in September 1989. The middle panel shows the corresponding spectral window. The bottom panel shows the same portion of the amplitude spectrum after the highest frequency has been removed by pre-whitening. A new frequency has clearly been uncovered by the procedure.

which fits all three peaks simultaneously.

This last step is very important and does not yield, a priori, the same results as the sequential application of the individual least-squares fits, because the spectral leakage interference of the smallest peaks on the largest ones is not taken into account in the latter procedure.

4.4 Beats

Beating is a well known physical phenomenon that occurs when two closely separated frequencies ν_1 and ν_2 are simultaneously vibrating. The resultant wave turns out to be a sinusoidal oscillating at the frequency $(\nu_1 + \nu_2)/2$, and modulated in amplitude by the *beat frequency* $|\nu_1 - \nu_2|/2$:

$$A\cos(\omega_1 t) + A\cos\omega_2 t = 2A\left[\cos\frac{\omega_1 - \omega_2}{2}t\right]\cos\frac{\omega_1 + \omega_2}{2}t \tag{4.2}$$

where I have assumed, for simplicity, that the waves have the same amplitude A, and where $\omega_{1,2} = 2\pi\nu_{1,2}$. The quantity $|\nu_1 - \nu_2|^{-1}$ is the beat period, that is the time necessary for the pulsation to cover an entire modulation cycle.

This beat phenomenon is easily visible in the light curve of variable white dwarfs where stellar rotation splits the eigenmodes into closely spaced frequencies. The components of these multiplets will beat against each other with amplitude modulation periods typically of a few days. If a star with such a multiplet structure is observed over just one night, the data will thus cover only a part of the beat cycle, and there is a good chance that the amplitudes measured in the temporal spectrum will be incorrect. Suppose, for instance, that the data sample only the part of the beat cycle where the superposition of the two waves is destructive. The average amplitude of the light curve gathered is then lower than if the data were to sample the constructive region of the beat cycle. This will be reflected in the temporal spectrum where the amplitude of the two modes will depend on what part of the beat cycle has been sampled. If the average yearly temperature in a given region on earth is evaluated using only the data corresponding to the summer season, will not reflect the true average. In the same way, Fourier analysis cannot extrapolate the

behaviour of nonexistent data.

From one night to the next, different sections of the beat cycle might be observed, thus yielding different amplitude spectra, even though the stellar pulsations have remained the same. If two modes have the same true amplitude A, the corresponding amplitudes measured in the Fourier spectrum of the light curve can range from 0 to $2A$, depending on both the length of the data set and the phase of the beat cycle. Many astronomers have reported, in the 1970s and 1980s, nonlinear behaviour of variable white dwarfs, whereas they were just seeing unresolved beatings.

The systematic errors made on the amplitudes of beating modes decrease rapidly, although asymptotically, with the increasing length of the data set. If the observed light curve covers an entire beat cycle, or more, the relative errors on the amplitude are small. The beatings are then said to be resolved. If Π_b is the beat period, it should not be a surprise that $1/\Pi_b$, i.e. the beat frequency, corresponds to what has been defined as the spectral resolution in section 4.1. A point has, however, to be made. A non-continuous data set of total length larger than the beat period, does not necessary sample completely the beat cycle, and might therefore not resolve it. For instance, consider a star that has two modes excited, separated by a 11.6 μHz frequency, which corresponds exactly to a one-day beat period. If the star is observed from only one observatory, no matter how many consecutive nights of data are gathered on this star, the beats will never be resolved, because the same portion of the cycle is sampled again and again. Assuming a conservative 7 hours of observation per night, Table 4.1 indicates, for various beat frequencies in the range of interest, how many nights are necessary for the beat cycle to be completely sampled. Considering that the typical frequency splitting due to stellar rotation is found to lie in the range 4-7 μHz, this clearly shows that it is extremely difficult, if not impossible, to resolve fully the amplitude spectrum of such a star with single-site campaigns, even in the case where the pulsations are absolutely stable, i.e. perfectly linear.

Table 4.1: Number of observing nights (of 7 hours each) necessary to entirely sample the beat cycle. 'n-r' mean the cycle cannot be resolved, whatever the number of nights.

Frequency separation [μHZ]	Beat period [hours]	Nights required
11.6	24	n-r
9.3	30	5
8.4	33	7
7.7	36	n-r
5.9	47	33
5.8	48	n-r
5.1	55	9
4.6	60	n-r

4.5 Combination frequencies

Several discussions in this thesis will revolve around harmonics and combination frequencies, as these are the sole definite nonlinear features that have been identified in variable white dwarf spectra. It is therefore important to clearly define what these features are. Consider a pulsating star which oscillates in just two eigenmodes at frequencies f_1 and f_2. If a peak appears at a frequency $f_c = n_1 f_1 \pm n_2 f_2$, where n_1 and n_2 are integers, then it is a combination frequency. In the particular case where $n_2 = 0$ (resp. $n_1 = 0$), the combination frequency is a pure harmonic of the fundamental f_1 (resp. f_2).

A given combination frequency may have one of two physical origins. Firstly, it can be an eigenmode that accidentally happens to fall precisely at this frequency, in which case it is a resonant mode (e.g. Dziembowski 1982). The g-mode spectrum being so densely populated, such accident is, in principle, not exceptional. Resonant coupling is even thought to be responsible for the saturation phenomenon that prevents the modes to grow over a certain limit amplitude in white dwarfs (Dziembowski 1980). Secondly, a combination frequency can be a nonlinear peak, whose possible origins will be discussed in section 5.3. In this case, the terms "nonlinear frequency", "cross-frequency", "harmonic distortion", or "combination mode" are all used interchangeably in the literature, although the appellation "mode" can be misleading as it suggests "eigenmode". I will also be using

these different expressions synonymously, except for "combination mode" from which I will deliberately keep away.

4.6 Units

The light curves I have kindly be provided with were normalized to have a zero mean luminosity. The amplitude of the oscillations around this zero light level were then measured in the unit of milli-modulation intensity (mmi), which is a linear representation of the fractional intensity of modulation in the light curves $\delta I/I$. A value of 1000 mmi thus means 100% peak to peak modulation.

The amplitudes in the frequency domain will correspondingly be measured in the milli-modulation amplitude unit (mma). The micro-modulation power unit (μmp) is also used in the literature to measure squares of amplitudes. Unless a physical reason necessitates powers to be used, I will tend to rather analyse amplitude spectra than power spectra, because they reflect better how the star actually pulsates.

Chapter 5

Nonlinear behaviour of the DAV G29-38

5.1 Introduction

G29-38 is the most observed DAV, mostly thanks to the work of Scot Kleinman (Kleinman *et al.* 1998), who studied this star extensively for his PhD thesis (Kleinman 1995). Altogether, 40 observing campaigns have been conducted on this star over a 10 year period (1985-1994), amounting to over 1100 hours of data. The analyses presented in this chapter are based entirely on this data set, which has been kindly made available to me[1]. The principal aim of Kleinman's project was to uncover the pulsation eigen-structure of this star. This was not a trivial task, because G29-38's amplitude spectrum appeared drastically different from one observing season to the next. He nevertheless managed to uncover an underlying structure of recurrent modes, on which most of the work presented in this chapter will be based.

Although Kleinman attempted a mode identification, i.e. assigned indices (k, ℓ, m) to the frequencies he believed to be eigenmodes, he did not claim that this labelling was indisputable. I will still use the same identification throughout the thesis, but purely for the purpose of discussion. My approach being mainly phenomenological, most of the

[1] c.f. acknowledgments section

analyses conducted here do not rely on the mode identification. In section 5.4, however, the mode identification will be specifically discussed, in particular the important issue of the spherical degree ℓ. The validity of Kleinman's labelling will then be addressed.

As will be explained in the next section, I have concentrated on the five best data sets out of the vast amount of data available on G29-38 (see Table 5.2 in section 5.2). Although Kleinman has precisely identified each peak in the period spectrum, I have nevertheless recomputed each frequency, according to the procedure described in section 4.3.4, for my own purposes. Not that I did not trust the excellent job he performed, but I needed information he did not include in his frequency tables, such as the phases of the identified modes, as well as the errors on the amplitude and phases as obtained from the least-square methods. Where direct comparison is possible, our respective results show to be virtually identical. Frequencies are identical to within (0.06 μHz). The differences could be explained by possible different sequential approaches in the pre-whitening procedures.

My complete frequency table is shown in Table 5.1. The peaks thought to be normal modes, according to Kleinman's analysis, are indicated by their radial order k. The harmonics and combination frequencies are indicated by the k-order of the eigenmodes that combine to form them. Once again, these k-orders are mentioned for the sole purpose of indicating what modes combine together, as well as to facilitate the discussion. They should not thus be considered as correct.

The third column in Table 5.1 indicates in which year the peak was observed. If a peak, such as $k = 4$ for instance, is found in several of the five data sets considered, its identification is given in each case.

Section 5.2, 5.3, and 5.4 each represent individual papers that I have written and submitted to the Monthly Notices of the Royal Astronomical Society[2]. I am sole author of these first two papers, which report on the evolution of the amplitude and phase spectra of G29-38. The third paper, reproduced in section 5.4, was co-authored with Pierre Brassard, who helped me understand and use his second order model (Brassard *et al.* 1995), and made several physical comments on the observed results. I suggested this study, carried out the analyses, and wrote the paper.

[2]see "Important note" at the beginning of the thesis for explanations

Table 5.1: Complete frequency table for G29-38. The normal modes are indicated by their probable k-order. The combinations are labelled by the k-orders of the modes that combine to form them. The lower indices "+" and "–" indicate the probable azimuthal degree $m = \pm 1$, while the modes with an $m = 0$ index are indicated without any subscript.

Frequency ν [μHz]	Combination $k_1 \pm k_2$	Year	Amplitude A [mma]	Phase φ [rad]	Error δA [mma]	Error $\delta\varphi$ [rad]
372.646	8-10	1988	5.39	-2.10	0.31	0.06
553.347	10-18	1988	2.62	-1.61	0.31	0.12
806.537	24?	1993	1.75	0.85	0.37	0.21
843.388	8-16	1985	3.34	-0.63	0.38	0.11
866.181	6-10	1988	3.59	-1.67	0.31	0.09
871.830	22?	1993	3.63	1.48	0.36	0.10
888.150	8-17	1993	7.31	-3.07	0.36	0.05
1092.368	18	1988	4.38	1.42	0.31	0.07
1118.556	17	1993	14.03	-0.40	0.35	0.03
1163.325	16	1985	24.58	-0.54	0.35	0.01
1235.410	15	1992	29.94	-2.17	0.23	0.01
1297.222	14	1993	8.58	-0.55	0.36	0.04
1297.560	14	1989	1.47	0.90	0.17	0.11
1334.379	6-16	1985	6.16	-3.11	0.38	0.06
1367.238	13	1993	2.53	-2.11	0.37	0.14
1369.620	13	1988	6.30	1.40	0.31	0.05
1383.290	?	1993	3.96	-2.76	0.36	0.09
1464.399	?	1985	5.15	2.56	0.38	0.07
1473.989	12	1993	9.73	1.90	0.36	0.04
1525.759	?	1989	2.41	-2.19	0.17	0.07
1541.499	11	1985	7.51	2.71	0.38	0.05
1625.729	10_-	1988	56.01	-0.83	0.22	0.00
1627.877	10_-	1985	30.33	-2.06	0.34	0.01
1632.764	10_-	1993	31.43	1.88	0.28	0.01
1637.602	10	1993	8.09	1.57	0.36	0.04
1638.675	10	1992	10.60	2.87	0.28	0.03
1642.135	10_+	1993	9.27	1.26	0.36	0.04

Table 5.1: – *continued*

Frequency ν [μHz]	Combination $k_1 \pm k_2$	Year	Amplitude A [mma]	Phase φ [rad]	Error δA [mma]	Error $\delta\varphi$ [rad]
1811.749	9	1993	4.28	1.83	0.36	0.09
1986.231	8?	1989	8.58	-0.46	0.16	0.02
1998.366	8_-	1988	7.55	2.98	0.31	0.04
2006.583	8	1993	6.05	1.51	0.36	0.06
2006.793	8	1985	5.14	-2.62	0.38	0.07
2020.040	8_+?	1989	11.76	2.86	0.16	0.01
2025.657	8_+?	1992	2.71	2.16	0.29	0.11
2105.486	7[1]	1988	3.57	2.88	0.31	0.09
2326.708	2x16	1985	4.31	-1.61	0.38	0.09
2491.886	6_-	1988	6.07	-2.44	0.31	0.09
2492.218	6_-	1989	9.06	-0.96	0.16	0.02
2492.445	6_-	1985	3.44	3.05	0.37	0.30
2492.461	6_-	1993	6.11	0.05	0.36	0.06
2492.817	6_-	1992	11.11	0.91	0.28	0.03
2497.188	6	1993	1.57	-2.15	0.36	0.48
2497.261	6	1988	4.63	2.27	0.31	0.01
2497.303	6	1989	0.91	0.58	0.17	0.18
2497.478	6	1985	6.82	-2.11	0.37	0.15
2501.622	6_+	1992	4.50	1.56	0.29	0.06
2501.755	6_+	1993	5.74	2.91	0.36	0.06
2502.279	6_+	1989	4.06	0.55	0.17	0.04
2502.446	6_+	1985	8.00	-0.82	0.37	0.13
2502.834	6_+	1988	10.90	0.95	0.31	0.03
2627.700	?	1985	2.37	1.91	0.38	0.16
2747.526	?	1989	1.95	-2.47	0.17	0.09
2751.439	$17 + 10_-$	1993	7.23	1.63	0.36	0.05
2791.239	16+10	1985	4.34	-2.57	0.38	0.09

[1]This mode has not been labelled as such by Kleinman (1995)

Table 5.1: – *continued*

Frequency ν [μHz]	Combination $k_1 \pm k_2$	Year	Amplitude A [mma]	Phase φ [rad]	Error δA [mma]	Error $\delta\varphi$ [rad]
2817.442	5	1988	2.06	2.25	0.31	0.15
2929.994	14+10_	1993	5.00	1.78	0.36	0.07
2962.093	6-16+10	1985	2.22	2.56	0.38	0.17
2995.284	?	1988	2.64	1.22	0.31	0.12
3106.633	12+10_	1993	4.37	-2.00	0.36	0.08
3169.856	11+10	1985	3.52	-1.58	0.38	0.11
3251.439	2x10	1988	12.10	-1.26	0.31	0.03
3255.837	2x10	1985	2.73	2.08	0.38	0.14
3265.328	2x10_	1993	4.22	-1.45	0.36	0.09
3270.068	10_+10	1993	2.08	-1.44	0.37	0.18
3274.981	2x10	1993	4.65	3.08	0.36	0.08
3444.492	9+10_	1993	2.72	-2.18	0.37	0.13
3522.754	4	1989	6.40	1.39	0.16	0.03
3522.758	4	1992	6.87	-1.62	0.29	0.04
3522.768	4	1988	3.64	-1.62	0.31	0.09
3522.873	4	1993	3.64	-1.50	0.36	0.10
3522.926	4	1985	3.01	1.51	0.38	0.13
3539.773	?	1993	1.62	-1.29	0.37	0.23
3639.214	8+10_	1993	3.64	-2.87	0.36	0.10
3660.415	6+16	1985	2.80	0.69	0.38	0.13
3731.749	7+10	1988	5.19	-0.23	0.31	0.06
3972.542	2x8	1989	0.83	-0.64	0.17	0.20
4006.829	$8_- + 8_+$	1989	1.34	2.06	0.17	0.13
4128.579	6_++10	1988	7.48	0.02	0.31	0.04
4130.226	6+10	1985	3.32	-2.04	0.38	0.11
4134.553	$6_+ + 10_-$	1993	3.02	-0.97	0.37	0.12
4219.312	3?	1993	1.73	2.08	0.37	0.21

Table 5.1: – *continued*

Frequency ν [μHz]	Combination $k_1 \pm k_2$	Year	Amplitude A [mma]	Phase φ [rad]	Error δA [mma]	Error $\delta\varphi$ [rad]
4230.804	?	1993	1.78	0.89	0.37	0.20
4384.568	2x10_+17	1993	2.28	-2.64	0.37	0.16
4393.275	2x10+17	1993	1.96	-2.30	0.37	0.19
4439.416	?	1993	1.19	2.15	0.37	0.31
4478.468	$6_- + 8$	1989	1.38	-0.81	0.17	0.12
4522.233	$6_+ + 8$	1989	1.34	-2.48	0.17	0.13
4562.700	2x10_+14	1993	2.25	-1.66	0.37	0.16
4733.835	?	1989	0.58	-2.37	0.17	0.29
4907.446	2x10_+10	1993	1.50	0.13	0.37	0.24
4984.358	2x6_	1989	0.26	-1.67	0.17	0.64
4989.363	6_+6	1989	0.33	1.17	0.17	0.51
4994.444	$6_- + 6_+$	1989	0.60	0.21	0.17	0.28
5148.471	4+10	1988	1.37	-1.84	0.31	0.23
5357.482	7+2x10	1988	3.78	-0.86	0.31	0.08
5497.284	?	1989	0.65	2.63	0.17	0.26
5647.723	2	1989	0.82	-2.44	0.17	0.20
5754.295	6+2x10	1988	3.52	-0.49	0.31	0.09
5758.558	6+2x10	1985	0.81	0.58	0.38	0.46
6983.198	7+3x10	1988	1.58	-1.29	0.31	0.20
9086.780	1	1988	0.70	-0.41	0.31	0.44

5.2 Evolution of the temporal spectrum of G29-38

Abstract

An analysis of the evolution of the amplitude spectrum over many seasons of the DA pulsating white dwarf G29-38 has been performed. Neither beating nor resonant mode coupling can account for the observed appearance and disappearance of modes, although some of them clearly grow while others get damped. Some unknown nonlinear, and possibly nonadiabatic, process has therefore to be invoked, which affects both the mode selection mechanism and the driving efficiency on a time-scale as short as a day.

5.2.1 Introduction

The analysis of the period spectra, also called temporal spectra, of pulsating white dwarfs can reveal a lot about the internal structure of these stars. This is the aim of asteroseismology: using the pulsations in order to probe stellar interiors and extract various stellar parameters (e.g. Kawaler & Hansen 1989). Tens of pulsation frequencies are often simultaneously excited in variable white dwarfs, but generally few of them are normal modes, i.e. natural eigenperiods of oscillation. The others are harmonics and combination frequencies (a combination frequency is a linear combination of frequencies of normal modes). The asteroseismological models to date incorporate only the normal modes. The study of the nonlinear frequencies is therefore important, not only to understand better the physics of stellar pulsations, but also to gain further asteroseismological insights into white dwarf interiors.

The nonlinear processes undergone by the large amplitude pulsating white dwarfs are to date very poorly understood. This is not only because the nonlinear domain is itself difficult to probe, but also because a variety of nonlinear phenomena may affect the pulsations simultaneously and are almost impossible to disentangle.

From a theoretical point of view, the problem is extremely difficult to tackle due to the

highly nonlinear nature of the equations governing the pulsations (Cox 1980). Various nonlinear phenomena, such as harmonic distortion (Brassard *et al.* 1995, Brickhill 1992, Wu 1997) or mode coupling (Goupil and Buchler 1994, Dziembowski 1982, Moskalik 1985), may take place simultaneously in large amplitude pulsators. However, each of the models available to date treats only one of these processes at a time, therefore providing limited comparison with the observations.

From an observational point of view, the study of nonlinear phenomena via the analysis of light curves is rendered difficult by the presence of beating which may be mistaken for nonlinear processes. The stellar rotation engenders multiplet splitting, in the amplitude spectra, of the order of a few μHz, which generates beating processes in the range 1 to 4 days. In order for any changes observed in the amplitude spectrum to be considered real, i.e. of genuine astrophysical origin and not due to the data acquisition and analysis techniques, it is of prime importance to have all the beating processes resolved. This requires *uninterrupted* data sets of several days at least. Only with the advent of multi-site campaigns, like the Whole Earth Telescope (WET; Nather *et al.* 1990), could data sets of such length and quality be gathered.

All this explains why so much remains to be done in the field of nonlinear pulsations in white dwarfs.

The work presented here is based on the use of both single and multi-site data to determine the nature and functioning of the nonlinear processes undergone by the DA variable white dwarf G29-38. Section 5.2.2 presents G29-38 and the available data; the results of an analysis of the evolution of the period spectrum are given in section 5.2.3; section 5.2.4 shows what information can be obtained from the evolution of the variance of the light curve; in section 5.2.5 we examine in more detail the dramatic amplitude changes in the pulsations recorded in 1985; section 5.2.6 summarises the work and draws conclusions.

5.2.2 The DA variable G29-38

G29-38 is the most intensively observed pulsating white dwarf: over 1100 hours of data have been gathered over a 10 year period. Full details of the data set are given in

Table 5.2: Description of the 5 data sets suitable for the nonlinear analysis.

Year	Month	Observatory	Number of runs	Length (hours)
1985	August	SAAO, McDonald	17	86
1988	November	WET campaign	52	175
1989	September	McDonald	17	102
1992	September	WET campaign	27	42
1993	September	McDonald	11	52

Kleinman *et al.* (1994, 1998) to which the reader is referred for details. Like all large amplitude DAV stars, the pulsations of G29-38 show distinct nonlinear behaviour, seen in the amplitude spectrum by the presence of many harmonics and combination frequencies. Drastic amplitude changes are also seen which may also be due to nonlinear effects such as mode coupling. In this sense, G29-38 seems to be an ideal star to study the evolution of its pulsations. However, in order for an amplitude analysis to be carried out, it is vital to work with data sets long enough for the beating of the numerous frequencies to be, if not completely resolved, at least under control. This means that in order to attribute the possible amplitude changes observed in the temporal spectrum to nonlinear processes, such changes should be significantly larger than the error caused by unresolved beating. With this restriction, the data from only 5 campaigns of those listed by Kleinman *et al.* (1998) were found suitable for this purpose. This subset is listed in Table 5.2.

5.2.3 Evolution of the temporal spectrum

Altogether, 70 individual modes and combinations frequencies have been identified in the temporal spectra (another name for amplitude spectra) corresponding to the 5 data sets listed in Table 5.2 (Kleinman *et al.* 1998). The photometric variability of pulsating white dwarfs is widely accepted to be due to nonradial g-mode oscillations (Dziembowski & Koester 1981, Dolez & Vauclair 1981, Winget 1981). Probable radial, spherical, and azimuthal indices (k, ℓ, m) were assigned to each mode by Kleinman (1995). Whilst this identification is not as yet secure, we have nevertheless adopted it in the present paper for the purposes of discussion (Table 5.1)

Among these 70 identified frequencies, only 4 modes are present in 3 or more of the spectra of the 5 data sets; of these 4 modes, 3 show multiplet structure. The vast majority of the other frequencies identified are present in one data set only, so that the spectra of these 5 data sets look very different from each other (Figure 5.1). In this sense, G29-38 is not ideal for our purposes because, when modes are merely present or absent, instead of undergoing variations slow enough to be sampled by the data, little can be done other than record the changes.

The evolution of the amplitudes of these recurrent modes, as measured in the Fourier transforms of these 5 light curves, is shown in Figure 5.2. In order to compare the relative changes of each mode, the amplitudes have been normalised. The normalising factor for each mode is the mean value of its amplitude over the 5 data sets, that is $\bar{A} = (\sum_i^5 A_i)/5$. This quantity, $\bar{A}$, is given in Figure 5.2 for each mode.

Before drawing any conclusion, two points have to be made. First, although these recurrent modes are among the highest peaks observed in the period spectrum, they are nevertheless very few compared with the numerous modes excited in each season. Secondly, nothing is known about the behaviour in between the data points in Figure 5.2; the different data points should therefore be considered on their own, without their connecting lines.

With these qualifications, Figure 5.2 clearly shows that some modes experience significant growth while other get damped. As the amplitude spectra used for the analysis have their eigenperiod structure resolved, the changes are thus intrinsic. This conclusion is not new, but serves as confirmation both of the work of Kleinman *et al.* (1998) and of the general belief that intrinsic variation is ubiquitous among large amplitude variable white dwarfs. However, spectral changes have been regularly reported in pulsating white dwarfs since the 1970s that were ulteriorly found not to be intrinsic but merely due to unresolved beating processes. It is therefore important, once and for all, to settle the controversy: intrinsic spectral changes do exist in variable white dwarfs.

The evolution reported in Figure 5.2 also suggests correlation in the amplitude changes. Indeed, the modes labelled ($k = 4$, $\ell = 1$, $m = 0$), and ($k = 6$, $\ell = 1$, $m = -1$) experienced a relative increase between 1988 and 1989, and a similar decrease between 1992 and 1993, while the other recurrent modes underwent opposite behaviour. This suggests that dynamical coupling exists between these modes. Mode coupling is a resonant phenomenon

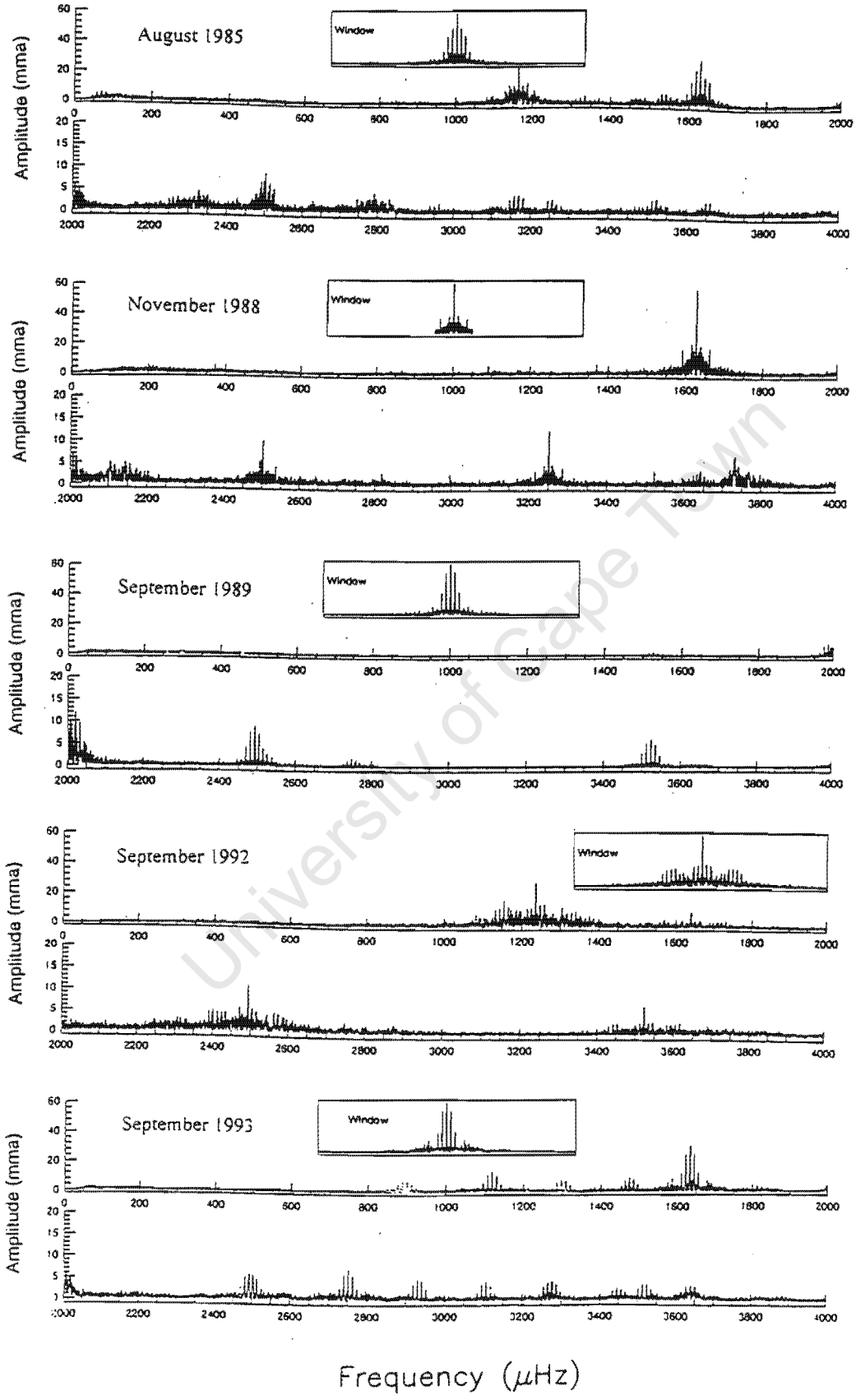

Figure 5.1: Period spectra of the 5 best data set on G29-38. Reproduced from Kleinman (1995).

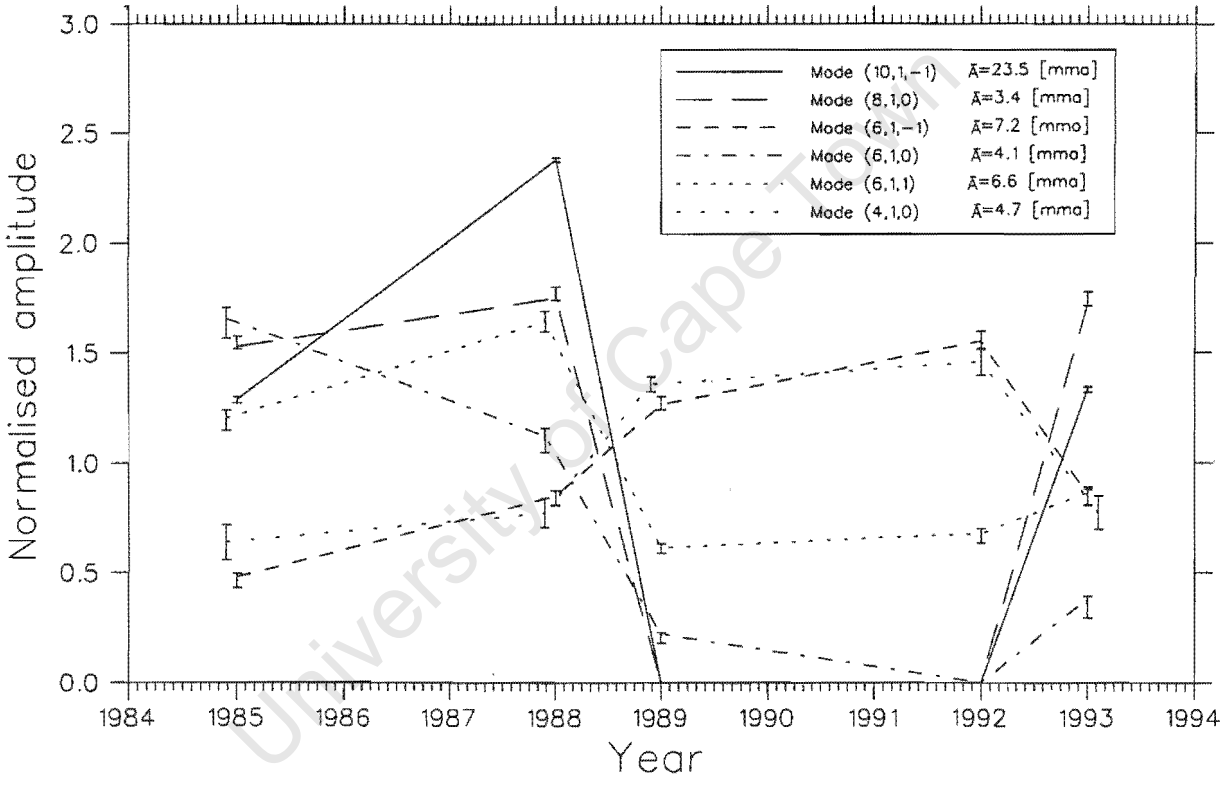

Figure 5.2: Evolution of the 6 persistent modes identified in G29-38, together with their probable (k, l, m) indices. Each mode has been normalized by its time average N.

between normal modes which happen to have a linear relation between their frequencies, and where not each of them are naturally driven. In a 3-mode coupling, for instance, this frequency relation is $f_3 = f_1 \pm f_2 + \delta f$, where δf is small and shows that the coupling may occur within a certain bandwidth. The resonance can be either *parametric* (Moskalik 1985), or *direct* (Dziembowski 1979), depending on which modes in the combination are naturally unstable, and which ones are naturally damped, but excited by the nonlinear coupling.

Various such coupling scenarios can be suggested for the frequencies shown in Figure 5.2, but unfortunately no other evidence can be found which identifies or excludes a particular scheme. A few points can nevertheless be made which suggest that resonant mode coupling is actually not the prime cause of the observed changes:

- No direct coupling is possible between the modes in Figure 5.2, because no linear relation exist between their frequencies. Furthermore, their combination frequencies, which could play the role of the naturally stable modes excited by direct resonance, are not systematically observed in each season, and, when they are, their relative phases are all consistent with harmonic distortion rather than mode coupling (see section 5.3 & 5.4). Mode coupling between these observed modes is therefore not likely to be responsible for the amplitude changes observed.

- Normal modes with spherical degree $\ell > 3$ are not expected to be visible photometrically (Dziembowski 1977). Mode coupling between such frequencies and the visible modes identified could also potentially account for the seasonal spectral changes observed in Figure 5.2. We believe, however, that this is not the case. If each of the identified modes were to be individually coupled to an invisible high ℓ degree mode, each such resonance would form an independent dynamical system. Therefore, there would be, a priori, no reason for the observed modes to behave in the apparently correlated way shown in Figure 5.2. Although no argument can rule out simultaneous coupling with invisible modes, these considerations nevertheless suggest that it is not responsible.

- The analysis shown in Figure 5.2 is concerned with only 6 frequencies out of the 70 identified, none of the latter having a stable amplitude. Of these 70 frequencies, only 23 are thought to be normal modes, 40 have been identified as combination frequencies, and the rest are unidentified (Kleinman 1995; Table 5.1). The numerous

combination frequencies cannot all be naturally damped modes excited by resonances. Indeed, using an argument by Winget *et al.* (1994), the density of g-modes decreases with increasing frequency, and becomes too sparse to account for all the combinations identified. We therefore believe that the majority of these combination frequencies probably arise from harmonic distortion. This belief is given sound quantitative support in section 5.3 & 5.4.

Although these considerations do not strictly exclude resonant mode coupling as the mechanism responsible for the changes recorded, we nevertheless suggest that some other nonlinear process occurs which globally affect the pulsational driving and the mode selection mechanism of the star. This contention will be developed in more detail at the end of the next subsection.

Very important clues could be extracted from Figure 5.2 if the latter contained many more data points, with closer temporal spacing. This would not only provide a better limit for the time-scale of the amplitude variations, but also indicate whether the correlations observed are real or just a misleading consequence of the lack of data points. Unfortunately, major difficulties appear at this stage. First, no other data set can be used without facing the problem of badly unresolved beating (especially with those modes showing multiplet structure). Second, if the star is rotating, the modes corresponding to running waves (i.e. those having $m \neq 0$) will show cyclic variations due to the periodic drift of the pulsation's nodal lines. Only if the observation of the star covers the entire rotation period, is this effect resolved. As the rotation period of G29-38 is not known, apparent seasonal variations of this nature could also be misinterpreted as nonlinear effects.

5.2.4 Evolution of the variance of the light curve

Further progress can be made, however, using the variance of the light curve defined as $\mu = \sum_i^N (y_i - \bar{y})^2/(N-1)$, where the y_i are the measured time series ordinates, $\bar{y}$ is the average over the y_i, and N is the number of data points in the run considered. It shows only very weak dependence on unresolved beating provided that more than 2 or 3 modes are simultaneously excited to comparable amplitude (Vuille, in preparation). This quantity may therefore be used as an excellent indicator of the time-scale on which spectral changes occur in the pulsations, as most of the data sets available can be used,

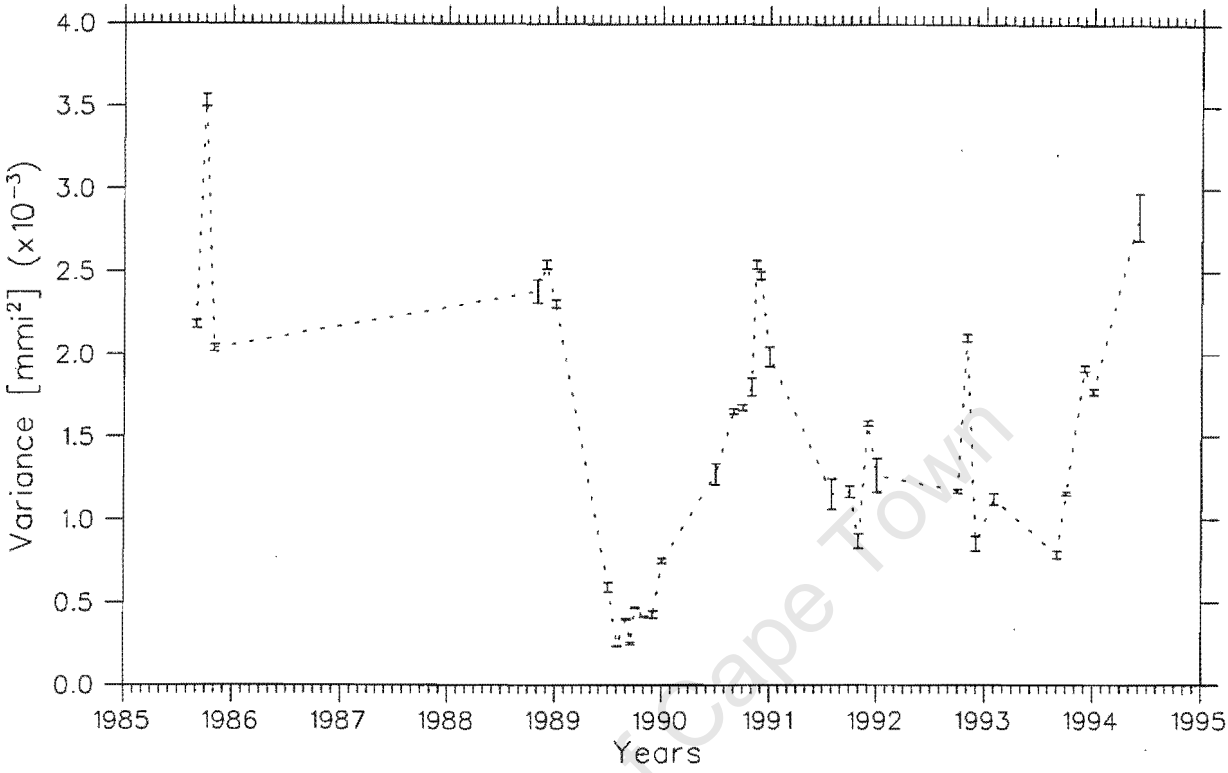

Figure 5.3: Evolution of the variance of G29-38's light curve.

almost regardless of their length. The evolution of the variance of G29-38 light curve is shown in Figure 5.3, where the various data sets used for the analysis are described in Kleinman *et al.* (1994, 1998). In order to reduce the effect of the typical low frequency noise, the data sets first had their long period variations removed using polynomial fitting.

Figure 5.3 suggests that changes on a wide range of time scales are taking place: at one extreme, long term variations on a yearly time-scale are visible, as shown by the steady increase of the variance from late-1989 to early-1991. At the other extreme, rapid changes on a monthly time-scale are taking place, as seen for instance in 1985, or in late-1992. Could these extremes arise from the same physical origin, or must different nonlinear processes be invoked? As the variance is a quantity that has no direct physical interpretation, its use as an indicator of the physical process in action is very limited. This is due to the fact that all modes are treated on an equal basis according to their amplitude in the period spectrum, and that their inertia, or energy content, is not taken into account at all in the variance.

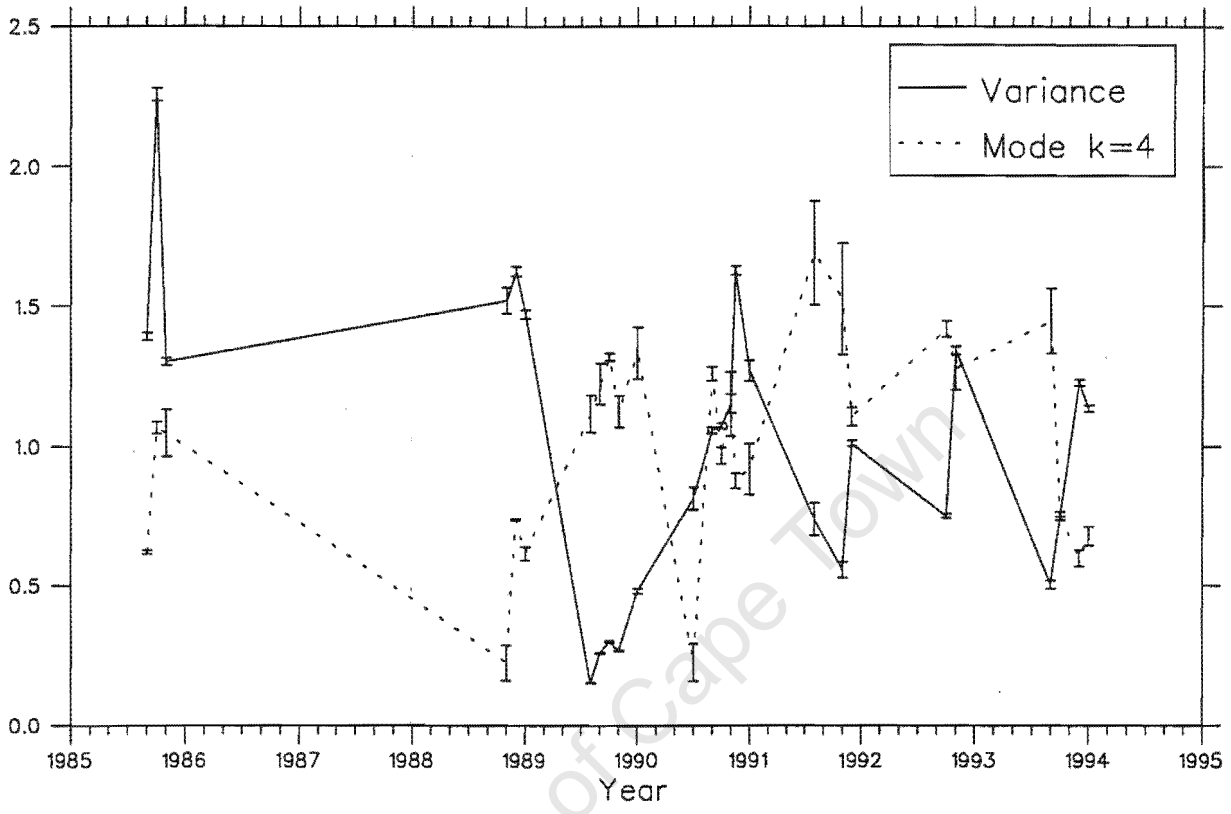

Figure 5.4: Plot of the variance of the G29-38 light curve and of the amplitude of mode $k = 4$. Both curves have been normalised by their mean value. Only the runs where $k = 4$ is sufficiently well resolved have been used.

The variance measures the evolutionary time scale of the modes dominating the period spectrum, but does not provide any information about the actual energy distribution in the pulsations at any time. Other than deducing the time-scales of the processes taking place, it is not possible to interpret physically the changes seen in the variance curve in Figure 5.3. It is of interest, however, to compare the behaviour of the amplitude of the mode $k = 4$ with that of the variance of the light curve (Figure 5.4). As the $k = 4$ mode does not show any multiplet structure, its amplitude is not affected by long period beating. Its peak is therefore resolved even in single night runs, which enables much better time resolution to be obtained than that shown in Figure 5.2.

Apart from the behaviour in 1985, which will be considered in the next section, the two curves plotted in Figure 5.4 show a clear tendency to be anti-correlated, i.e. the amplitude of the $k = 4$ mode increases whenever the variance is seen to drop, and vice

versa. Before drawing any conclusion, an important point has to be made. Generally speaking, the higher the frequency of a normal mode (i.e. the lower its k-order), the deeper its penetration in the stellar interior, and thus, the higher its mechanical energy content (at comparable surface amplitude). The process of mode trapping (Winget and Fontaine 1982) may alter this picture somewhat, but the global tendency remains the same (Brassard *et al.* 1992). Various models fitted by Bradley and Kleinman (1996) show that the $k = 4$ mode is always roughly one order of magnitude more energetic than $k = 6$, and nearly two orders of magnitude more energetic than $k = 10$, at normalised surface amplitude. Therefore, even though the measured amplitude of the $k = 4$ mode is about one order of magnitude lower than that of the dominant modes $k = 6$, 8, and 10 (Table 5.1), it still contains comparable energy. Therefore, bearing in mind that the evolution of the variance reflects the global behaviour of those modes showing the largest amplitudes, the anti-correlation seen in Figure 5.4 implies that a substantial amount of the pulsational energy gets transferred back and forth between those large amplitude high k-order modes and the recurrent $k = 4$ mode.

In other words, Figure 5.4 tends to indicate that a global correlation exists between the evolution of the visible modes, which was a conclusion already suggested from the analysis of Figure 5.2. If this correlation is real, then resonant processes cannot be held responsible for such a global evolution as the different mode coupling systems would be dynamically independent of each other. This implies that some nonlinear phenomenon, other than mode coupling, has to be invoked that affects the pulsation modes globally rather than individually. Because the mode selection mechanism and the pulsational driving determine entirely which modes are excited and to what amplitudes, we suggest that the efficiency and functioning of these mechanisms might not remain stable, but vary in time, so that different modes are driven at different times, thus inducing spectral changes. Three physical processes could possibly account for such behaviour.

• At present, the mode selection mechanism is very poorly understood. Even though the structure of the stellar envelope determines entirely the linear growth rates of the normal modes, it is not clear which of the numerous modes with positive growth rates actually benefit from the driving. This area is as yet completely unstudied, and a priori, the competition between the modes susceptible to be excited can even lead to time-dependent solutions (Moskalik, private communication).

• The pulsations themselves could be the physical process that triggers nonlinear evolution. When a mode is driven, the growing amplitude of its mechanical oscillation creates periodic changes that perturb more and more the physical structure of the stellar atmosphere. This might both affect the linear growth rates of the modes, and the selection mechanism, which, in turns, could generate significant amplitude changes. This could also explain the stability of the small amplitude pulsators, whose oscillations would not become large enough to perturb the atmospheric structure sufficiently for the mode selection mechanism to be affected.

• Because time-dependent treatment of convection is not yet possible, the effect of the turbulent convective flux on the pulsations is not at all understood. Since convective driving is believed to be the dominant driving process in DAV type stars (Brickhill 1991, Gautschy *et al.* 1996, Wu 1997, Goldreich & Wu 1999a), the dynamical interaction between the pulsations and turbulent convection certainly plays a role in the mode selection process, as suggested by Kawaler & Hansen (1989) and by Winget (1988). The highly nonlinear and time-dependent nature of the convection/pulsations interaction could a priori generate complex nonlinear behaviour (Cox 1976). Goldreich & Wu (1999b) have started to investigate this interaction and showed how turbulent viscosity can act as a mode damping process.

These suggestions are fruitful avenues for further research, although investigations are extremely difficult due to the highly nonlinear nature of these phenomena.

5.2.5 The 1985 event

The evolution of the variance of the light curve (Figure 5.3) revealed a peculiar behaviour of the pulsations during the 1985 season. The first 3 data points in Figure 5.3 correspond to observing runs done in respectively August, September and October 1985. From August to September, the variance of the light curve has increased by more than 60%, before falling back to its August level by October. It is of interest to determine whether this outburst is due to a sudden increase of one specific mode, or whether it is a behaviour shared by many modes. The September light curve is fortunately nearly long enough (30

hours) for the 20 modes identified by Kleinman (1995) in the August run to be resolved in the September amplitude spectrum, although some unresolved beating problem might complicate the picture. The quality and length of the October light curve is, on the other hand, not suitable for this purpose. We have therefore monitored the amplitude of the 20 identified mode during the August-September period only. The results are shown in Figure 5.5.

A net increase in power is recorded in every mode identified in the August data set. The few possible exceptions are the low amplitude combination frequencies where the increase is comparable to the statistical error, and is therefore not significant. The mode identified as $k = 11$ is the only peak that experienced a slight drop in amplitude, although this decrease is not significant either.

Beating cannot account for the observed variations as both the August and the September data sets are long enough for their respective eigenperiod structure to be resolved, except for the $k = 6$ triplet in the September light curve. The amplitude changes recorded in this triplet cannot be due to beating only, because its lowest component in the August spectrum, namely $m = -1$, becomes by far the largest in September, which is impossible to explain solely by beating. Therefore, nonlinear and/or nonadiabatic processes must be responsible for the observed changes. Mode coupling can, in this case, be ruled out for the following reasons.

First, the latter is a transfer process by which energy gets exchanged between the modes coupled to each other. Some modes should experience energy loss, while others should see their power increase. In 1985 all modes increased, thus ruling out any possible energy exchange in between them. Note that the energy loss recorded in mode $k = 11$ cannot on its own balance the increase in all the other modes, first because it is a very low amplitude mode, secondly because it has much smaller inertia than lower order modes like $k = 4$ or $k = 6$, and third because it does not show any combination frequencies (except for $k = 10 + 11$) that might indicate a coupling with all the other visible modes present. Although mode coupling is not a hamiltonian process that strictly conserves energy, it can securely be concluded that mode coupling between the visible modes is not the main mechanism responsible for the observed changes.

Second, Mode coupling between the identified modes and some invisible modes (such as modes with high spherical ℓ-index, or interfacial modes (Rosenthal & Gough 1994))

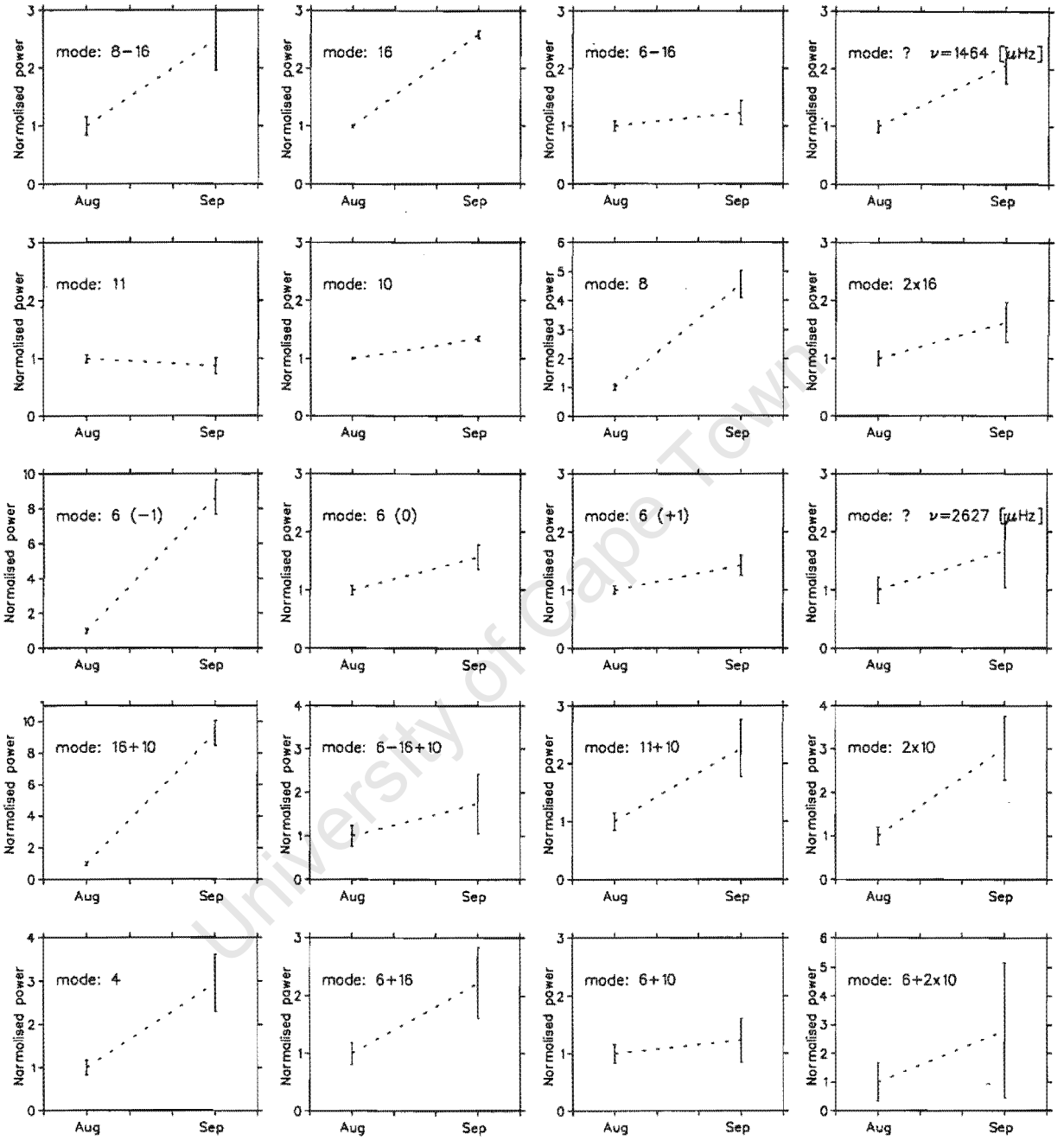

Figure 5.5: Relative evolution of the 20 modes identified in August 1985 over a one month period, together with their probable k radial order. The combination frequencies are labelled by the k-value of the modes that combine to form them. The "?" refers to uncertain or unknown identification for the frequency indicated. The different ordinate scales in each panel allows for the large range of relative variation recorded.

can also quite securely be discarded on the following grounds; the participation of every single mode in a resonant process is unlikely, because mode coupling is supposedly a rare phenomenon that requires specific resonant conditions. Furthermore, even if all the observed modes were actually coupled to invisible modes, each such resonant process would form an independent dynamical system, and there would be no reason for them to behave in a correlated way as seen in Figure 5.5. This is an argument already given out earlier, in a different context, when analysing the seasonal amplitude modulations (Figure 5.2).

This 1985 event strongly suggests that something is globally changing in the star, whereby all the modes are simultaneously affected. Contrary to the conclusion drawn after the analysis of Figure 5.2, the process that has to be invoked here does not seem to perturb the selection mechanism, as all the modes identified in August are still present in September. It strongly affects, however, the efficiency of the driving mechanism, in a complex frequency dependent manner, as not all the modes experience the same relative growth (Figure 5.5). The energy available in the pulsations increases steeply on a very short time-scale and gets distributed among the excited modes, without affecting the stellar structure and thus the selection mechanism. Note that there is no unmistakable signature of nonlinear behaviour, so that the process in action might in fact be purely nonadiabatic, which was definitely not the case for the phenomena discussed under section 5.2.3 and 5.2.4.

In order to refine the measurement of the time-scale over which these 1985 changes occur, we monitored the variance of the light curve during the August data set by dividing the latter into 6 consecutive segments of 14 hours each. The result is shown in Figure 5.6, where significant variations are seen to occur on a daily time-scale. This is a very interesting result as the linear growth rates are thought to be of the order of a month for white dwarfs (Moskalik 1985, Dziembowski and Koester 1981, Lee and Bradley 1993). This indicates that this 1985 "outburst" is most probably not due to a pure nonadiabatic growth, as suggested above, but that some nonlinear process has also to be invoked, which affects the light curve on a daily time-scale.

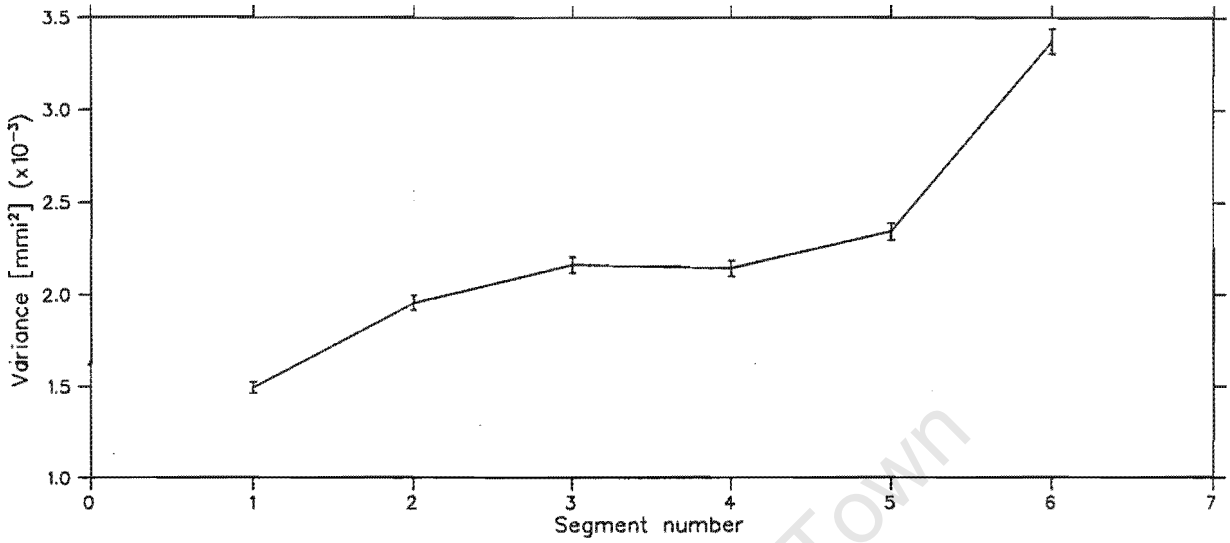

Figure 5.6: Evolution of the variance of the light curve during the August 1985 observing campaign. The data set has been split into 6 consecutive segments of 14 hours each.

5.2.6 Conclusion

We have studied the evolution of the period spectrum of the pulsating white dwarf G29-38. This investigation has been limited by the non-recurrence of most modes, by the long period beating generated by the eigentriplets, and simply by the complexity of the temporal spectrum having tens of modes simultaneously excited. Therefore, this analysis is mostly qualitative, and is aimed at showing evolutionary trends, identifying the possible cause of the nonlinear behaviour, and estimating the time-scales over which the amplitude variations occur. We drew the following conclusions:

- The numerous harmonics and combination frequencies identified in the amplitude spectrum suggest these are mainly harmonic distortions rather than individual normal modes. This excludes resonant mode coupling between the visible modes as the dominant cause of the spectral changes recorded.

- Mode coupling processes between visible and invisible modes cannot be ruled out as being primarily responsible for the amplitude variations. However, different globally-correlated changes in the observed modes strongly suggest that some other non-linear processes occur, that affect both the driving and the selection mechanism.

- Various time-scales, ranging from daily to seasonal, have been shown to dominate the variations in the amplitude spectrum at different times, suggesting that different nonlinear processes are competing in G29-38.

We also speculated over the nature of these nonlinear phenomena, and determined various possible origins for the nonlinear behaviour of G29-38. The theory available to date is, however, not sufficiently developed to identify or exclude any of the mechanisms proposed.

Finally, we showed how the variance can be used as a global time-scale indicator for amplitude variations. As suggested by Moskalik (private communication), it would be interesting to follow the evolution of the variance in different frequency bands, by applying Fourier filters to the light curve. This would indicate how the pulsational power gets transferred between these different bands, on a time scale that is shorter than that of the beating processes.

Evidently, there is still a lot to be learnt from the phenomenology of the nonlinear pulsations. However, theoretical efforts are mostly needed, in order for any comparison with the observations to be possible.

Acknowledgments

I am indebted to S. Kleinman who has generously provided me with the data on G29-38, and to P. Moskalik who has made numerous valuable comments on this manuscript. I am also grateful to D. O'Donoghue for his general supervision, for lending me his time series analysis program, and for his precious linguistic corrections. My thanks also go to D.E. Winget, R.E. Nather, M-J. Goupil, S.J. Kleinman, M.H. Montgomery and S.D. Kawaler for helpful discussions. Finaly I would like to acknowledge all the WET observers without whom none of the above nonlinear analysis would have been possible.

References

Bradley P. E., Kleinman S. J., 1996, *White Dwarfs*, ed. J. Isern, M. Hernanz, & E. Garcia-Berro (Dodrecht: Kluwer), 445

Brassard P., Fontaine G., Wesemael F., 1992, ApJ, 81, 747

Brassard P., Fontaine G., Wesemael F., 1995, ApJS, 96, 545

Brickhill A. J., 1983, MNRAS, 204, 537

Brickhill A. J., 1991, MNRAS, 251, 673

Brickhill A. J., 1992, MNRAS, 259, 529

Buchler J. R., Goupil M-J, 1984, ApJ, 279, 394

Cox J. P., 1980, *Theory of Stellar Pulsation*, Princeton University Press, Princeton.

Dolez N., Vauclair g., 1981, A&A, 102, 375

Dziembowski W., 1977, Acta Aston., 27, 203

Dziembowski W., 1979, IAU Colloquium No 53, *White Dwarfs and Variable Degenerate Stars*, ed. H. M. Van Horn and V. Weidemann, (Rochester, N.Y.: University of Rochester), p. 359

Dziembowski W., Koester D., 1981, A&A, 97, 16

Dziembowski W., 1982, Acta. Astro., 32, 148

Goldreich P., Wu Y., 1999a, ApJ, 511, 904

Goldreich P., Wu Y., 1999b, submitted

Kawaler S. D., Hansen C. J., 1989, *White Dwarfs*, ed. G. Wegner (Springer-Verlag: Berlin), 97

Kleinman S. J., *et al.*, 1994, ApJ, 436, 875

Kleinman S. J., 1995, Ph.D. thesis, Univ. Texas, Austin

Kleinman S. J., *et al.*, 1998, ApJ, 495, 424

Lee U., Bradley P. A., 1993, ApJ, 418, 855

Moskalik P., 1985, Acta Astra, 35, 229

Nather R. E., *et al.*, 1990, ApJ, 361, 309

Rosenthal C. S., Gough D. O., 1994, ApJ, 423, 488

Winget D. E., 1981, Ph.D. thesis, University of Rochester, New York

Winget D. E., Fontaine, G., 1982, in *Pulsations in Classical and Cataclysmic Variable Stars*, ed. J. P. Cox and C. J. Hansen (Boulder Joint Institute for Laboratory Astrophysics), 46.

Winget D. E., 1988, *Advance in Helio- and Asteroseismology*, ed. J. Christensen-Dalsgaard and S. Fransen, 304

Winget D. E., *et al.* 1994, ApJ, 430, 839

Wu Y., 1997, Ph.D. thesis, California Institute of Technology, Passadena

5.3 Evolution of the phase spectrum of G29-38

Abstract

An analysis of the phase spectrum of the DA pulsating white dwarf G29-38 over many seasons has been performed. This complements a companion paper that analysed the evolution of the temporal spectrum of G29-38.

We show that, with one exception, the relative phases of the harmonics and combination frequencies are all oscillating in phase with their parent modes. This not only suggests that these non-linear frequencies owe their presence to harmonic distortion and not to resonant mode coupling, but it also explains the typical pulse shapes observed in the light curves of large amplitude variable white dwarfs.

The one exceptional cross-frequency that does not show a phasing with its parent modes is thought to be a resonance.

5.3.1 Introduction

Spectroscopic observation of stars cannot reveal anything about the structure or composition of their interior, as the light we receive from them has been emitted in the outermost stellar layers (e.g. Böhm-Vitense 1992). Stellar pulsation, on the other hand, involves the whole star, not only the photosphere (e.g. Cox 1980). Therefore, stellar pulsation analysis can potentially be used to obtain information about the inner part of the star. This is the aim of asteroseismology, whose name comes from the fact that the pulsations are used as probes of the variable stars' interiors, in much the same way that seismology tells us about the inner structure of the earth.

At present, all the asteroseismological information on variable white dwarfs is obtained from the study of their period spectra (e.g. Kawaler & Hansen 1989, O'Donoghue 1995), which reflect only part of the information contained in the original light-curves. Indeed, the complex Fourier transform is usually separated into its modulus part (the amplitude,

or temporal spectrum, also incorrectly called the Fourier spectrum), and its corresponding argument part (the phase spectrum). Although the study of the phase spectrum is potentially fruitful, there has been, to date, no analysis of this kind done on pulsating white dwarfs.

As the most observed DAV type star, G29-38 is, a priori, an ideal star with which to initiate phase spectrum analysis. Data from about 40 observing sessions distributed over 10 almost consecutive years are available. Among them are two Whole Earth Telescope campaigns (WET; Nather *et al.* 1990) carried out in 1988 and 1992 respectively. A primary comparative analysis of the comprehensive data set has been carried out by Kleinman *et al.* (1998), which enabled the underlying structure of eigenmodes to be uncovered.

The results of the first analysis of the phase spectrum of G29-38 are reported here. A study of the evolution of the phases of the normal modes is presented in section 5.3.2. Section 5.3.3 deals with the relative phases of the combination frequencies observed. Section 5.3.4 concludes the analysis.

5.3.2 Phases of the recurrent modes

Kleinman *et al.* (1998) showed that tens of modes are simultaneously excited in G29-38, but very few of them are recurrent over the years. Only 4 eigenmodes are present in almost every season, 3 of which show multiplet structure. In order for multiplets to be resolved, data sets longer than the corresponding beat periods are required. Among all the observing campaigns conducted, only 5 data sets are long enough to satisfy this condition. They are described in both Kleinman *et al.* (1998) and in Table 5.1 and 5.2.

To each identified peak in the temporal spectrum corresponds a phase which is the imaginary part of the Fourier transform of the light curve at the corresponding frequency. Using nonlinear least-squares fitting, we computed, individually in each of the 5 data sets, the phases of the recurrent modes. We chose the reference time $t = 0$ to be at the start of the 1988 WET campaign. The results are plotted in Figure 5.7.

No obvious trend or correlated evolution can be seen in the phases over the years. This is, in a sense, expected as the peaks are not found at exactly the same frequency in each

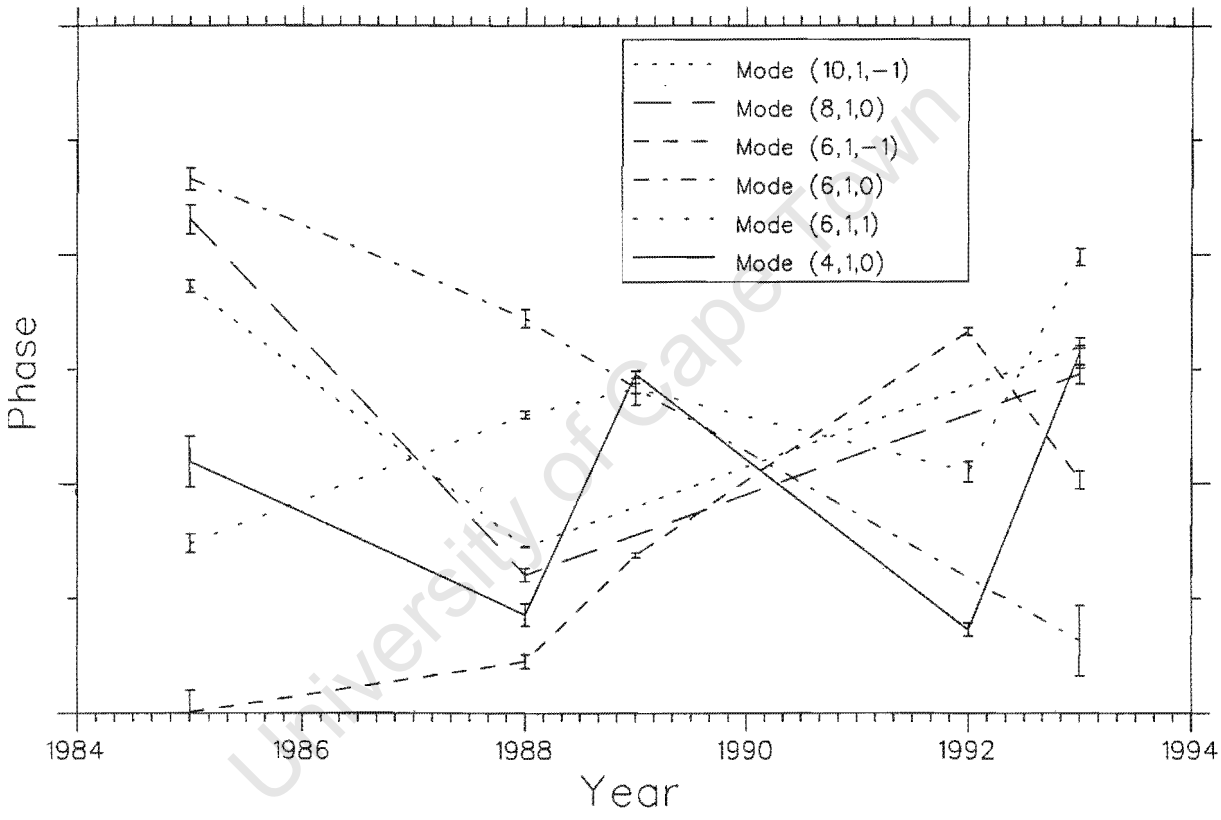

Figure 5.7: Evolution of the phase of the recurrent modes, together with their probable sets of indices (k, ℓ, m).

season, but experience slight frequency shifts up to about 2 μHz (Table 5.1). This may easily induce large phase shifts as, from one season to the next, each oscillation mode goes through a few tens of thousands of cycles.

Only if a mode is stable enough in frequency and well resolved in each season can the gaps between the data sets be bridged, and its phase possibly monitored. Even though the $k = 4$ mode, that corresponds to a 283 s period, seems to satisfy these criteria (its seasonal shift does not exceed 0.18 μHz (Table 5.1)), the evolution of its phase still appears erratic (Figure 5.7). Kleinman *et al.* (1994), however, conducted a very similar analysis on this 283 s mode, using the same data sets, and concluded that its phase was constant (with possibly a slow secular change). The discrepancy between their results and ours arises from the way the frequencies have been measured. We determined, in each season, the phase of the $k = 4$ mode as that corresponding to the frequency of the maximum of its peak, as given by nonlinear least-squares fitting, whereas they ran a linear least-squares routine on each data set using a fixed frequency corresponding to the average of the $k = 4$ frequencies observed over the seasons. The difference between our results and those from Kleinman *et al.* illustrates to what extent tiny frequency shifts may induce large phase changes, which also shows the limitation of measuring absolute phases in isolated data sets.

We then reproduced, for the 283 s mode, the results of Kleinman *et al.* using their approach, before applying this technique to the $k = 6$, $k = 8$, and $k = 10$ modes. The latter analysis did not yield more meaningful results than the approach we first used (Figure 5.7). This is simply because these modes are not sufficiently stable in frequency, and probably not isolated enough in the temporal spectrum, for them to be resolved to the required accuracy.

5.3.3 Relative phases of the combination frequencies

If a peak in the temporal spectrum has a frequency ν_c which is the sum or the difference of frequencies of two normal modes, $\nu_c = \nu_1 \pm \nu_2$, then it is a (first order) combination frequency, or nonlinear frequency. Correspondingly, the relative phase of a combination frequency is normally defined by $\varphi_r = \varphi_c - (\varphi_1 \pm \varphi_2)$, which physically represents the phasing of this nonlinear frequency compared to that of its parent modes. Relative phases

have the property (which absolute phases do not have) of being independent of any reference point in time, i.e. they are invariant under translations of the origin of the time-axis $t \longrightarrow t - t_0$. Indeed, a shift of the time origin induces the following changes in the individual phases:

$$\cos(\omega_i t + \varphi_i) \longrightarrow \cos\left[\omega_i(t - t_0) + \varphi_i\right] = \cos(\omega_i t + \varphi_i')$$

where $\omega_i = 2\pi\nu_i$, and $\varphi_i' = \varphi_i - \omega_i t_0$. The new relative phase φ_r' therefore writes

$$\varphi_r \longrightarrow \varphi_r' = \varphi_r - \left[\omega_c - (\omega_1 \pm \omega_2)\right] t_0 = \varphi_r$$

In each data set, we can therefore chose the reference time $t_0 = 0$ at the start of the first observing run, thus avoiding the cycle count problems discussed above when measuring absolute phases. The measurement of the relative phases remains nevertheless very sensitive to the frequency resolution. It is also sensitive to the integration time used for the data acquisition which should be, as a rule of thumb, at least 20 times shorter than the pulsation periods. Since the data were gathered in 10 s integrations, while the shortest observed periods are about 400 s for normal modes and about 200 s for cross-frequencies, the above criteria is satisfied.

The relative phase of a harmonic or a combination frequency is a potentially very fruitful measurement, possibly carrying a distinctive signature of the non-linear process in action. Indeed, if a given combination frequency owes its presence to harmonic distortion, also called the "pulse shape effect", it is expected to be in phase with its parent modes, or possibly slightly preceding them.

Two different pulse shape effects have to be distinguished. First is the nonlinear response of the emergent flux to the surface temperature variations ($L \propto \sigma T^4$). It is the most fundamental harmonic distortion because it is the first deviation from linearity appearing in the period spectrum. This is especially the case for DA variables whose visible part of the spectrum falls in the highly non-linear portion of their energy distribution, and to a lesser extent for pulsating DB white dwarfs whose optical spectrum lies on the rather linear Rayleigh-Jeans tail due to their higher effective temperature. The luminosity variations respond instantaneously and naturally in phase to the surface temperature

variations, and thus the harmonics of a given oscillation mode will all be generated in phase with each other (Brassard *et al.* 1995).

The second pulse shape effect is due to the non-linear response of the stellar medium to the perturbation travelling through it; similar to the way an acoustic wave gets distorted along its path in a dense fluid (Rudenko & Soluyan 1977), a finite amplitude wave generated at the base of the ionization zone will get distorted on its way to the stellar surface, and part of the energy contained in the initial frequency will get naturally distributed into harmonics and combination frequencies.

More specifically, a sinusoidal flux perturbation at the base of the convection zone generates cyclic variations of the thickness of the convective layer. When the flux increases, it heats up the bottom of the convective zone which consequently reduces its size, until the flux reaches its maximum. The opposite behaviour occurs when the flux decreases. The heating of the convection zone takes time, so that the radiative emergent flux at the stellar surface is delayed in phase compared to the flux perturbation at the base of the convective layer (unless the oscillation period is much longer than the turn over-time of the eddies, but such modes are not expected to be visible (Wu 1997, Goldreich & Wu 1999). This delay depends on the state of the convective layer: when it is thick, it needs much energy to heat up, and the response time is accordingly low; when it is thin, i.e. when the flux is close to its maximum, the response time is almost instantaneous and the flux perturbation at the bottom and at the top of the convection zone are almost in phase for a little while. This non-constant delay, i.e. the nonlinear response of the convection zone to the flux perturbation, is directly responsible for distorting the originally sinusoidal flux, and thus for generating harmonics and combination frequencies.

If a combination frequency is not due to harmonic distortion, it could be a resonant mode. A resonant mode is a normal mode, naturally damped, but driven by a coupling with the naturally unstable parent modes (Dziembowski 1982, Moskalik 1985). Modes generated in such a way have, a priori, no reason to be in phase with their parent modes because resonant processes are only dependent on the relative amplitudes of the coupled modes during the different stages of the corresponding limit cycles (Goupil and Moskalik, private communications). A phase relationship between the coupled modes may, however, exist in certain cases of resonance, but it is not necessarily an "in phase" one (Kowács & Buchler 1989).

Therefore, depending on the nonlinear process in action, we might or not observe a phasing of the nonlinear frequencies, which might lead to the possible identification or exclusion of a specific scheme. The relative phases of all the combination frequencies identified in the 5 spectra discussed in section 5.3.2 are shown in Figure 5.8.

The first four panels represent the relative phases identified in each individual data set, while the bottom panel, labelled "Sum", contains all the relative phases put together. A clear tendency for the relative phases to be grouped around $\varphi_r = 0$ can be seen, meaning that the majority of the combination frequencies tend to be in phase with their parent modes. According to the above discussion, this strongly suggests that most combination frequencies owe their presence to harmonic distortion rather than to mode coupling, although nothing can be argued for any individual case.

Only 2 non-linear frequencies are recurrent, i.e. present in more than one of the 5 data sets. They are the harmonic $k = 2\text{x}10$ at 3255 μHz, and the sum frequency combining mode $k = 6$ and mode $k = 10$ at 4129 μHz, both present in 1985, 1988, and 1993. The relative phases of these recurrent non-linear frequencies have remained fairly constant over the years, while the phase of the individual eigenmodes involved in the combination experienced significant changes (Figure 5.7). This fact strengthens our contention that these frequencies are likely to be harmonic distortions rather than resonances.

The measurement of phases being very frequency sensitive, high signal-to-noise ratio and accurately resolved peaks are required. It is therefore not surprising to see quite a few data points off the $\varphi_r = 0$ line in Figure 5.8. Precise frequency identification is especially difficult for multiplet components of small amplitude due to spectral leakage from the larger components. Figure 5.9 is a replot of the last panel of Figure 5.8 with all the data points corresponding to combinations involving a minor component of a multiplet removed. Three combination frequencies are left that show a definite non-zero relative phase. They are indexed $k = 8 - 17$, $k = 11 + 10$ and $k = 7 + 10$ in Figure 5.9 according to the probable k-radial order of their parent modes[3]. An interesting test has been further conducted on these 3 non-linear frequencies. Instead of taking the phases φ_c corresponding to the frequencies given by the maximum of each of these peaks in the amplitude spectrum, we measured these combination phases by fixing the fitting

[3]The peak identified at 2105.473 μHz in the September 1988 temporal spectrum is thought to be $k = 7$ although it has not been identified as such by Kleinman *et al.* (1998).

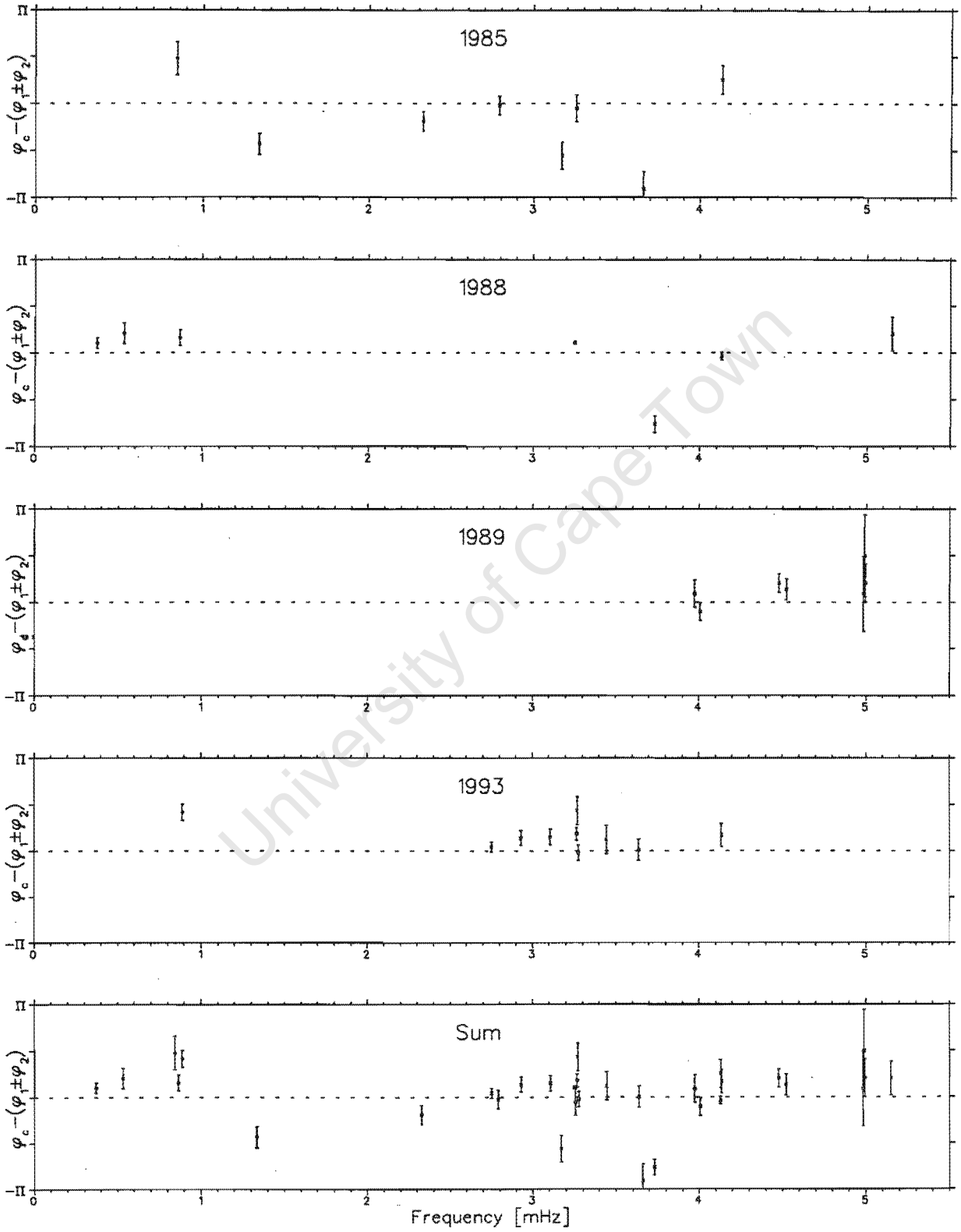

Figure 5.8: Relative phases of the nonlinear frequencies identified in the 5 spectra described in paper 1. The circles represent difference frequencies, the crosses the sum frequencies, and the squares the pure harmonics.

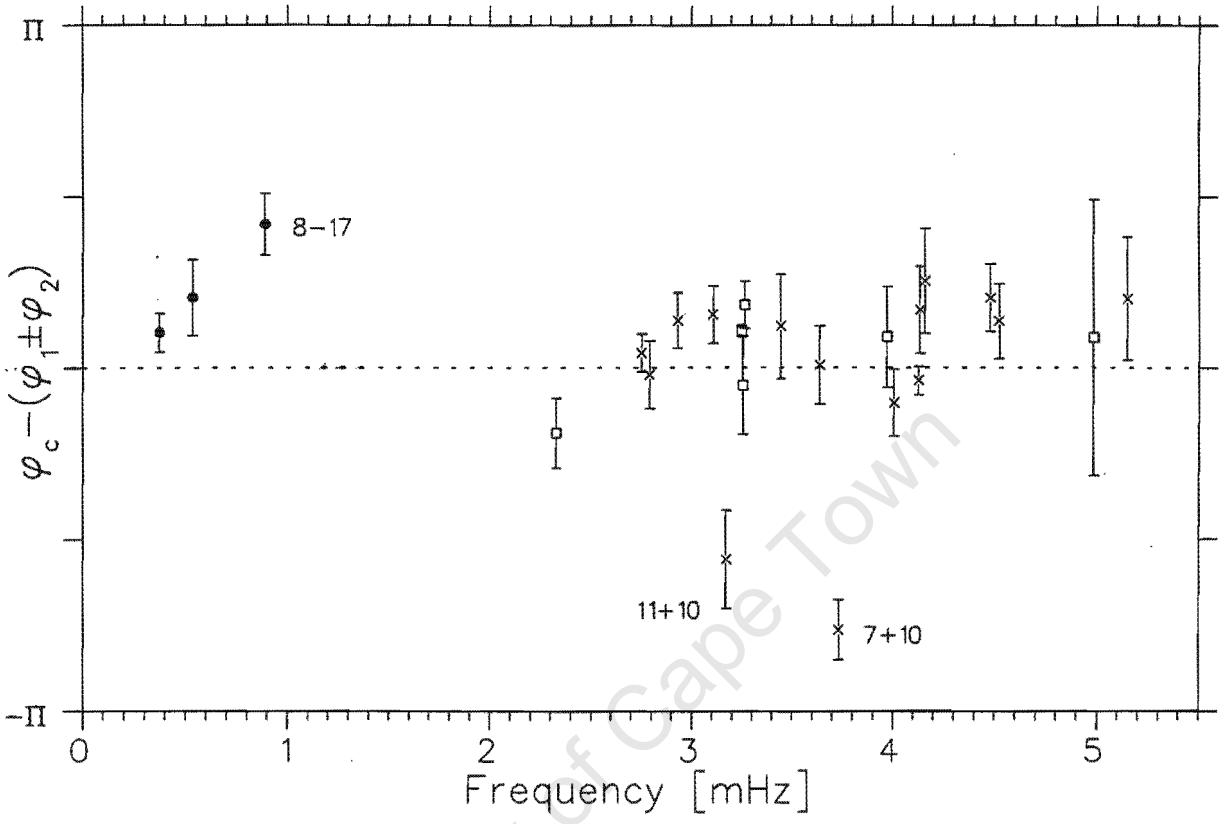

Figure 5.9: Replot of the last panel of Figure 5.8 with the combinations involving a minor component of a multiplet removed.

frequencies at the exact frequencies given when combining the parent modes. For instance, for the combination frequency $7+10$, instead of the phase $\varphi_c = -2.7$ that corresponds to the maximum of the peak at 3731.757 μHz, we measured φ_c at $f_7 + f_{10} = 3731.201$ μHz, where f_7 and f_{10} are the frequencies of the parent modes. This gave the value $\varphi_c = 2.1$.

The corresponding relative phases obtained with these new φ_c values are respectively $\varphi_r^{8-17} = 1.35$, $\varphi_r^{11+10} = 0.26$ and $\varphi_r^{7+10} = 0.03$. This exercise did not change anything for the combination $8-17$, but did shift the relative phases of both $10+11$ and $7+11$ very close to zero. This strongly suggests that the two latter sum frequencies were blended with noise and possible spectral leakage which made their frequency identification, and thus their phases, not very accurate. This illustrates a point made previously, that tiny errors in the frequency identifications may generate significant phase shifts. While $k = 11+10$ and $k = 7+10$ are thus thought to be harmonic distortion effects, the definite non-zero

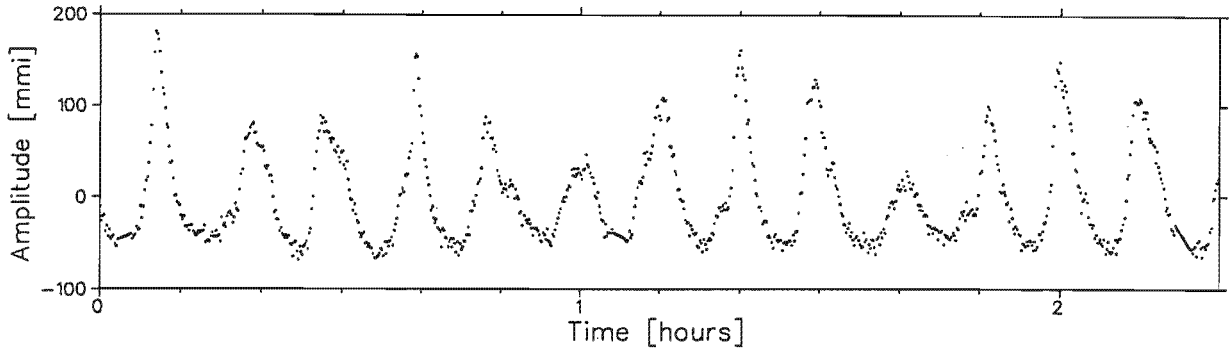

Figure 5.10: Portion of the G29-38 light curve, as observed during the 1988 WET campaign. The typical features, pulse shapes with sharp rises, slightly milder decays, and flat bottoms in between (see the amplitude scale), can clearly be seen.

value of the $k = 8 - 17$ relative phase strongly suggests it is not.

The latter eigenmode is a good candidate to be a coupled mode, not only because its relative phase stands out, but also because its relative amplitude does as well (see section 5.4). The measured amplitude of $k = 8 - 17$ is indeed larger than that of $k = 8$. This could be explained by harmonic distortion only if $k = 17$ was at least one order of magnitude larger than $k = 8$, which it is not. Unfortunately, with the actual data set, no further analysis can be carried out to investigate this possibility.

The global phasing of the frequencies produces, as a consequence, a light curve showing definite sharp pulse shapes with flat bottoms in between (Figure 5.10). If these nonlinear features are considered to arise from the nonlinear response of the medium to the flux perturbation, they can be physically comprehended; the flat bottoms reflect the large delay of the emergent flux compared to that at the bottom of the convection zone when the flux is minimum, while the sharp pulses express the quasi-instantaneous response when the flux is maximum.

If the nonlinear frequencies are not perfectly in phase with their fundamental modes, but slightly preceding them, that is $0 < \varphi_r \ll \pi$, then the light curve ought to show peaks with steep ascents and milder descents. Therefore, if the slight advances that can, globally speaking, be observed in Figure 5.9 are real and not a consequence of the statistical techniques used for the analysis, then asymmetrical pulse shapes should be visible in the light curve; and they are indeed. Figure 5.10 displays a typical portion of

G29-38 light curve which shows nicely these specific features.

If, on the other hand, the nonlinear frequencies have their phases preceding that of their fundamental modes, then the pulse shapes in the light curve would show opposite behaviour, that is slow ascents and steeper descents, which is definitely not what is observed. Figure 5.11 illustrates these different phase-dependent characteristics with a synthetic light curve constructed from only one frequency and its first harmonic. It is important to note that the ratio $R = A_0/A_1$ of the amplitude of the fundamental to the amplitude of its harmonic determines the importance of the pulse shape distortion. In particular, the flattest bottoms in between the peaks (i.e. the ones with a zero-curvature at their minimum) are obtained for $R = 4$, while the typical observed values for R fall in the range 3.9-5.2. The bottom panel of Figure 5.11 shows the sharpening effect of the second harmonic on the light curve.

An advance in phase is expected from the nonlinear response of the medium to the "mechanical" wave travelling through it (Brickhill 1992, Wu 1997), but not from the nonlinear response of the radiative transfer (Brassard *et al.* 1995). This therefore suggests that the former phenomenon is the one dominating in the pulsations. This issue will be addressed in full detail in section 5.4. The model of Wu actually give a quantitative prediction for the phase advance. For harmonics, it takes the form[4]:

$$\varphi_r = \frac{\pi}{2} - \arctan(2\omega\tau_c)$$

where ω is the pulsation frequency, and τ_c is roughly the thermal time-scale of the convection zone. Since this model predicts modes to be visible only if $1 < \omega\tau_c <\simeq 10$, this implies that φ_r falls in the range 0.05-0.46. A very similar range is predicted for sum frequencies, while that for difference frequencies is slightly shifted away from zero. The average value of the relative phases measured (Figure 5.9) is 0.15 ± 0.12, which thus agrees well with the predictions.

The point has to be made that the characteristic features observed in the G29-38 light curve happen to be shared by all known large amplitude pulsating white dwarfs. It has never been clear what the physical origin of these typical non-sinusoidal pulse shapes was,

[4]Note that in equation 8.12, 8.14 and 8.15 of Wu (1997), the "$-\pi/2$" should actually be "$+\pi/2$" (Wu, private communication)

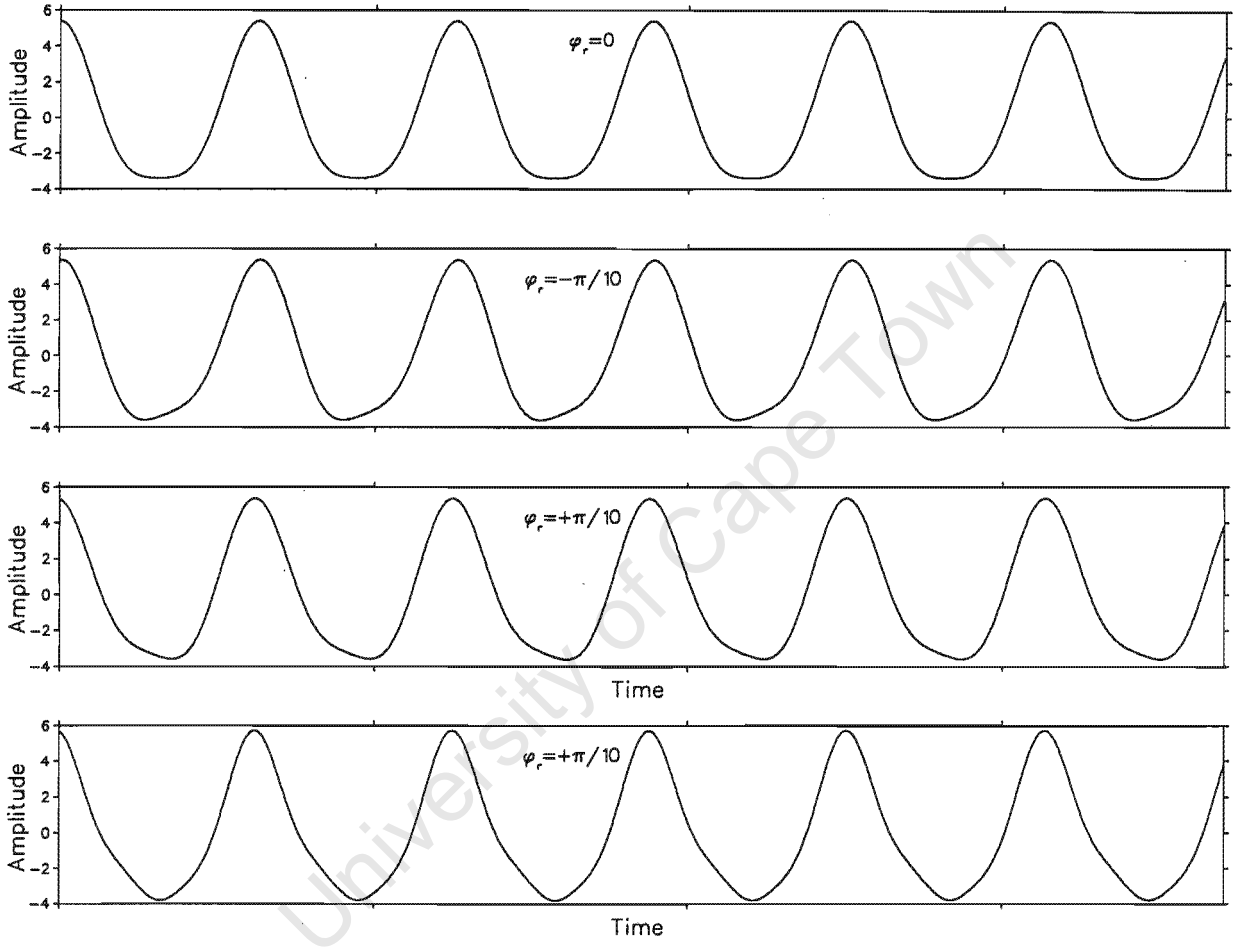

Figure 5.11: Synthetic light curves constructed on one frequency and its first harmonic, i.e. $A = A_0 \cos(wt) + A_1 \cos(2wt + \varphi_r)$, when the harmonic is respectively in phase with its fundamental (*top panel*), lagging behind the fundamental (*second panel*), and preceding the fundamental (*third panel*). The ratio $R = A_0/A_1$ has been chosen to be 4.4, which corresponds to the measured value for the dominant mode in the 1988 WET campaign. In the bottom panel, the second harmonic has been added to the synthetic light curve, with an amplitude $A_2 = 0.33A_1$, and a phase advance similar to that of the first harmonic.

but it can now be asserted that harmonic distortion is the prime cause. In support of this affirmation is the fact that these characteristic features are not intermittent, but remain constant in time. This is indeed what is expected from harmonic distortion, in the sense that, if it is a strong enough phenomenon to affect visibly the light curve, then it ought to be a permanent effect, irrespective of any other nonlinear processes possibly undergone by the pulsations, such as intrinsic amplitude variations.

5.3.4 Conclusion

The analysis of the phase spectrum, still in its infancy, has proved to be fruitful as it has ruled out the identification of combination frequencies in the amplitude spectrum as due to mode coupling; instead, harmonic distortion effects are responsible. However, one of the difference frequencies identified, the combination of modes with probable indices $k = 8$ and $k = 17$ at 888 μHz, is thought to be a resonance, as its phase does not fit the harmonic distortion picture.

The analysis of the relative phases of combination frequencies could not strictly differentiate between the two most important harmonic distortion effects, because they have too similar signature. The slight phase advance of the cross-frequencies nevertheless suggests that the nonlinear response of the stellar medium to the oscillatory flux perturbation is dominating the nonlinear radiative transfer effects. It has also been shown that the specific phasing of the nonlinear frequencies is entirely responsible for the characteristic pulse shape features observed in the light curve of G29-38. As these features are typical for all large amplitude variable white dwarfs, it is tempting to generalize our conclusion to this whole class of stars.

Acknowledgments

I am extremely grateful to Scot Kleinman for having provided me with the G29-38 data sets, and to Pawel Moskalik, whose helpful criticism made this publication possible. I am also grateful to Darragh O'Donoghue for his precious scientific feed-back and for the time he spent correcting my English. My thanks also go Y. Wu, S. Kleinman, and P. Bradley for helpful discussions. I would like also to acknowledge all the WET observers without

whom the above phase analysis would not have been possible.

References

Böhm-Vitense E., 1992, *Stellar Astrophysics*, Vol.3, Cambridge University Press, Cambridge.

Brassard P., Fontaine G., Wesemael F., 1995, ApJS, 96, 545

Brickhill A. J., 1992, MNRAS, 259, 529

Cox J. P., 1980, *Theory of Stellar Pulsation*, Princeton University Press, Princeton.

Dziembowski W., 1982, Acta Astr., 32, 147

Kawaler S. D., Hansen C. J., 1989, *White Dwarfs*, ed. G. Wegner (Springer-Verlag: Berlin), 97

Kleinman S. J., 1995, Ph.D. thesis, University of Texas, Austin

Kleinman S. J., *et al.*, 1998, ApJ, 495, 424

Kowács G., Buchler J. R., 1989, ApJ, 346, 898

Kurtz D. W., 1990, A&AR, 28, 607

Moskalik P., 1985, Acta Astr., 35, 229

Nather R. E., *et al.*, 1990, ApJ, 361, 309

O'Donoghue D., 1995, Ap&SS, 230, 63

Rudenko O. V., Soluyan S. I., 1977, *Theoretical Foundations of Nonlinear Acoustics*, Plenum Publishing Corp., New-York

Unno W., *et al.*, 1989, *Nonradial Oscillations of Stars*, 2nd edition, University of Tokyo Press, Tokyo

5.4 Relative amplitudes of the cross-frequencies

Abstract

In each season where the DA pulsating white dwarf G29-38 has been observed, its period spectrum appeared very different, but it always contained a forest of harmonics and cross-frequencies. The ratios A_c/A_1A_2 of the amplitudes A_c of these non-linear frequencies to the product A_1A_2 of the amplitudes of their corresponding parent modes have been measured. The results have been compared to the prediction given by two existing theoretical models. The conclusion of this analysis is that the non-linear frequencies present in the period spectrum of G29-38 owe their presence mostly to the inelastic response of the stellar medium to the perturbation travelling through it, rather than to the non-linear response of the emergent luminous flux to the surface temperature variation. This analysis also confirmed that most identified modes are $\ell = 1$, as previously asserted.

5.4.1 Introduction

Pulsating white dwarfs experience periodic luminosity variations that can be observed in, for instance, white light high-speed photometry. The light curve obtained in this way can then be Fourier transformed. The resulting amplitude spectrum will show numerous peaks that indicate the different periods at which the star is pulsating simultaneously. Some of these peaks correspond to normal modes, i.e. to oscillation eigen-frequencies of the star, while others do not, and are called non-linear frequencies. The latter are either harmonics or combination frequencies (another term for cross-frequencies) in the sense that their frequencies are either the sum, or the difference, of frequencies of excited normal modes.

These non-linear frequencies cannot exist on their own, nor can they be described by a set of indices (k, l, m), in the same way that normal modes are (Unno *et al.* 1989), as they are not related in any way to the actual pulsation mechanism. Instead, they owe their presence to the non-linear response of the star to the pulsations. Part of the power

originally contained in the eigenmodes, or parent modes, gets naturally distributed into these combination frequencies. This phenomenon is called harmonic distortion, or "the pulse shape effect", and may have two main physical origins.

First is the inelastic response of the stellar medium to the perturbation travelling through it; a normal mode driven to a finite amplitude at the base of the convection zone will see its corresponding sinusoidal wave being distorted on its way to the surface, similar to the way an acoustic wave behaves in, for instance, water (Rudenko & Soluyan 1977). Second is the non-linear response of the outgoing Eddington flux to the surface temperature variations, which is directly related to the relation $L \sim \sigma T_{\rm eff}^4$. Whatever the origin of the harmonic distortion is, its effect is to spread part the energy contained in the original frequency amongst harmonics and, in the case where more than one normal mode is excited simultaneously, combination frequencies.

As the cross-frequencies bear no relation to the pulsation mechanism, they cannot reveal anything about the selection and driving mechanisms of the star. However, their amplitudes directly depend on the amount of non-linear response experienced by the star, which itself depends on the physical conditions in the stellar interior. Therefore, the study of these pulse shape effects can potentially lead to constraints on some atmospheric parameters, as done, for instance, in the case of the DAV G117-B15A (Brassard *et al.* 1993, Fontaine & Brassard 1994).

The DAV G29-38 has been extensively observed over the period 1985-1994, during which about 40 photometric campaigns targetted this star, including two Whole Earth Telescope runs (Nather 1990) in 1988 and 1992 (Kleinman *et al.* 1998). Although the period spectrum of this star has shown tremendous qualitative changes from season to season, numerous combination frequencies could always be identified. The various analyses of sections 5.2 and 5.3 led to the conclusion that most of the latter were due to harmonic distortion and not to resonant mode coupling. However, as none of the different harmonic distortion processes bear a distinctive signature, it is difficult to disentangle them to try and determine which one, if any, is dominating in G29-38. The purpose of the present paper is precisely to address this question. The comparison of the measured amplitudes of the cross-frequencies with those predicted by the theoretical models should yield clues as to what process can mostly be held responsible for the presence of these nonlinear features.

Section 5.4.2 describes and compares the theoretical models available to date. Section 5.4.3 presents the observational results and compares them with the theoretical predictions. Section 5.4.4 concludes the analysis.

5.4.2 Theoretical models

Three different models exist that treat harmonic distortion effects: Brickhill (1991a, 1991b, 1992a, 1992b); by Brassard *et al.* (1995); and Wu (1997). Each of these models treats only one of the harmonic distortion process. This is precisely why the present confrontation of the theoretical predictions with the observations should tell us which of those processes is dominating in G29-38. The model from Wu has already been tested, precisely in the case of G29-38, where good agreement was obtained (Wu 1997). We will therefore concentrate our comparative analysis on the models of Brickhill and Brassard.

Because these two models are built on the linear adiabatic theory, they cannot yield any information as to the stability of the modes. No rules concerning either the selection mechanism, that preferentially excite some normal modes over others, or the driving mechanism, that determines the amplitudes of the excited modes (Winget & Fontaine 1982) are therefore included. The models of Brickhill and BFW are thus not able to determine whether a particular mode should appear or not in the period spectrum, nor what its amplitude should be. However, what these models can do is to predict the frequencies, amplitudes and phases of the combination modes, given the characteristics of the excited eigenmodes.

Both these models consider only the case of small amplitude pulsators, where the perturbation can be expressed as a Taylor series around the equilibrium position. To second order of perturbation, first harmonics and cross-frequencies will naturally appear in the synthetic spectrum with amplitudes A_c proportional to the product $A_1 A_2$ of their parent modes (or $\propto A^2$ in the case of pure harmonics). This provides a direct way of comparing theory and observation, as the ratio $A_c/A_1 A_2$ is then free of any absolute amplitude dependence and can be readily measured in the observed period spectra.

As these models are designed for small amplitude pulsators, where a development to second order of perturbation describes correctly the nonlinear pulsations, it is not clear

to what extend they can successfully be applied to a large amplitude variable like G29-38, where higher order effects might be significant. In particular, if modes with the same geometry are compared (i.e. same ℓ and m indices), their cross-frequencies are expected to have the same relative amplitudes, i.e. the same ratios A_c/A_1A_2. This is not the case any more if third (or higher) order effects are present, as the latter would directly affect the amplitudes of the normal modes (see section 6.2 & 6.3).

5.4.2.1 The model of Brickhill

The theoretical model proposed by Brickhill treats the non-linear response of the medium, more specifically of the convection zone, to the oscillatory perturbation, but neglects the non-linear relation between the emergent flux and the surface temperature. His discussion is based on a numerical model of the outer layer of the DAV stars extending down to the base of the driving zone, that is below the convection zone (Brickhill 1991a). Assuming that the linear theory provides an adequate representation of the spatial and temporal behaviour of both the horizontal displacement and the pressure changes (Brickhill 1992a), this model follows numerically the evolution of the temperature wave along its way up to the surface of the star.

From the non-linear (i.e. non-sinusoidal) behaviour of the temperature variations at the stellar surface, the emergent flux is obtained (Brickhill 1992b) following the prescription given by Robinson, Kepler, & Nather (1982, RKN hereafter). This very important work showed that the luminosity variations can be accounted for exclusively by surface temperature changes, and that other factors such as geometric distortions, or gravity variations are negligible. To second order of perturbation, the local emergent flux in Brickhill's model is given by (Brickhill 1992b):

$$\begin{aligned}\frac{\delta F}{F} \;=\; Real\Bigg\{ & \sum_i A_i\, Y_i\, \mathrm{e}^{\sigma_i t+\psi_i} \\ & + \sum_i a\, A_i^2\, Y_i^2\, \mathrm{e}^{2\sigma_i t+\psi_{ii}} \\ & + \sum_i \sum_k b\, A_i A_k\, Y_i Y_k\, \mathrm{e}^{(\sigma_i+\sigma_k)t+\psi_{i+k}} \\ & + \sum_i \sum_k c\, A_i A_k\, Y_i Y_k\, \mathrm{e}^{(\sigma_i-\sigma_k)t+\psi_{i-k}} \Bigg\}\end{aligned} \tag{5.1}$$

where the Y_i are the spherical harmonics of degree ℓ_i and azimuthal degree m_i, while a, b and c are model dependent constants. For models corresponding to $\log g = 8$, their respective values are $a \approx 4.5$, $b \approx 9$, and $c \approx 8$ (Brickhill 1992b). The four lines in the above equation describe the flux perturbation at each point on the stellar surface generated respectively by the normal modes of amplitude A_i, frequency σ_i, and phase ψ_i (1st line), by their first harmonics (2nd line), by their sum frequencies (3rd line), and by their difference frequencies (4th line). a, b, and c thus represent the factors of proportionality, or coupling constants, between these various non-linear components and the original normal modes, as far as the local flux is concerned.

The integration of the local emergent luminosity flux over the visible disc of the star is also done following the RKN prescriptions. This assumes a linear relationship between flux and surface temperature variations, which therefore neglects the effects of radiative transfer, but allows an analytical approach. Furthermore, other approximations have been made by RKN for the treatment of the atmosphere, such as use of a linear limb darkening law (RKN equation 14), omission of the temperature dependence of the latter limb darkening (RKN equation 11), and use of a gray atmosphere, i.e. with the continuous opacity being wavelength independent (Böhm-Vitense 1989).

The amplitudes of the harmonics and cross-frequencies, as measured in the Fourier spectrum of the light curve, are then given analytically by functions of the form $A_c = A_1 A_2 f(\Theta)$. A_1 and A_2 are the amplitudes of the respective parent modes, while $f(\Theta)$ is a trigonometric function of the viewing angle Θ, which is the angle between the line of sight and the axis of symmetry of the surface perturbations. The amplitude ratio $A_c/A_1A_2 = f(\Theta)$ can then be calculated and is a function of just the viewing angle Θ. Unfortunately, the viewing angle is generally not known, so that direct comparison between the predicted and measured amplitude ratios is possible only when the function $f(\Theta)$ is a constant (see section 5.4.3).

The range of values taken by the amplitude ratio A_c/A_1A_2 for all possible $(\ell_1, m_1; \ell_2, m_2)$ combinations of normal modes, with ℓ_1, $\ell_2 \leq 2$, are given in Tables 5.3 and 5.4. Most ratios have a minimum value (corresponding normally to either $\Theta = 0$ or $\Theta = \pi/2$), but no upper limit. This is explained by the fact that the normal modes change their phase

Table 5.3: Minima and maxima of the ratio A_h/A^2 for harmonics given by the two models of Brickhill and BFW respectively.

		Brickhill's model		BFW's model	
ℓ_1	m_1	$\min(A_h/A^2)$	$\max(A_h/A^2)$	$\min(A_h/A^2)$	$\max(A_h/A^2)$
1	0	6.22	∞	0.19	∞
1	±1	3.64	3.64	0.08	0.08
2	0	13.66	∞	0.51	∞
2	±1	0.03	∞	< 0.01	∞
2	±2	5.78	5.78	0.46	0.46

over the visible disc, and thus there is always a viewing angle for which they are invisible. For instance, if $\Theta = 90°$, the mode $\ell = 1, m = 0$ has a zero visible amplitude A_1, as the opposite brightness of the two hemispheres will exactly cancel each other when integrating the light over the stellar disc. However, the corresponding harmonic does not change its phase at all over the visible disc (true for all harmonics of standing waves), and will thus have a finite amplitude A_c whatever the viewing angle is. The corresponding ratio A_c/A_1A_2 can thus become infinite.

5.4.2.2 The model of Brassard *et al.*

The BFW model (Brassard *et al.* 1995) supposes that the first nonlinearities appearing in the period spectrum are due to the highly non-linear relation between the emergent flux and the surface temperature. This is expected to be particularly true for DAVs, because the visible part of their continuous spectrum lies in the highly non-linear region of their energy distribution, and to a lesser extent for DB variables as their higher effective temperature shifts their visible light into the Rayleigh-Jeans tail. Assuming a sinusoidal surface temperature wave, an approximation referred to as the *first linearization*, this model integrates numerically the appropriate exact radiative transfer equations to obtain the emergent Eddington flux.

Analytically, the model is based on the linear, adiabatic theory of stellar pulsation, with the emergent specific intensity being expanded in a Taylor series around the equilibrium temperature T_0. By keeping terms up to second order in ΔT, first order harmonics and

Table 5.4: Minima and maxima of the ratio A_c/A_1A_2 for combination frequencies given by the two models of Brickhill and BFW respectively.

				Brickhill's model		BFW's model	
ℓ_1	m_1	ℓ_2	m_2	min $\left(\frac{A_c}{A_1A_2}\right)$	max $\left(\frac{A_c}{A_1A_2}\right)$	min $\left(\frac{A_c}{A_1A_2}\right)$	max $\left(\frac{A_c}{A_1A_2}\right)$
1	0	1	0	12.44	∞	0.38	∞
1	0	1	±1	7.14	7.14	0.17	0.17
1	±1	1	±1	7.28	7.28	0.17	0.17
1	±1	1	∓1	17.85	∞	0.60	∞
2	0	1	0	15.91	∞	0.44	∞
2	0	1	±1	10.21	∞	0.38	∞
2	±1	1	0	7.28	7.28	0.17	0.17
2	±1	1	∓1	2.59	2.59	0.11	0.11
2	±1	1	∓1	16.05	∞	0.44	∞
2	±2	1	0	2.58	2.58	0.11	0.11
2	±2	1	±1	2.58	2.58	0.11	0.11
2	±2	1	∓1	29.29	∞	0.98	∞
2	0	2	0	27.31	∞	1.01	∞
2	±1	2	0	10.67	∞	< 0.01	∞
2	±1	2	±1	0.05	∞	< 0.01	∞
2	±1	2	∓1	62.92	∞	2.43	∞
2	±2	2	0	15.68	∞	0.38	∞
2	±2	2	±1	5.82	5.82	0.36	0.36
2	±2	2	∓1	16.80	∞	0.39	∞
2	±2	2	±2	11.57	11.57	0.91	0.91
2	±2	2	∓2	74.24	∞	2.80	∞

combination frequencies will appear naturally in the synthetic period spectrum. These non-linear peaks will also have amplitudes proportional to the product of the amplitudes of their parent modes, that is again $A_c \propto A_1 A_2$ ($A_h \propto A^2$ in the case of harmonics). The corresponding constants of proportionality are both temperature and surface gravity dependent. The most recent values for G29-38's effective temperature and surface gravity are respectively $T_{\rm eff} \approx 11820°$ K, and $\log g \approx 8.14$ (Bergeron *et al.* 1995). We have calculated, for each $\ell = 1$ and $\ell = 2$ combinations, the ratios A_c/A_1A_2 corresponding to this model. They are listed in the last two columns of Tables 5.3 and 5.4. It can be seen that, for any ℓ and m combinations, these ratios are between one and two order of magnitude lower than the predictions from Brickhill's model.

5.4.3 Comparison with observations

Out of the 40 observing campaigns conducted on G29-38, only 5 of them are long enough for the beating due to multiplet splitting to be resolved. They are described in Table 5.1 and their respective amplitude spectra are displayed in Figure 5.1. Altogether, 40 non-linear frequencies have been identified in the period spectra corresponding to these 5 campaigns (Kleinman *et al.* 1995), 31 of them being first order combination, while 9 of them being second order combinations, i.e. combination of 3 modes. We have measured the amplitude ratio A_c/A_1A_2 in each of these 31 first order cases according to the rule that the smallest of the 3 peaks forming each combination is the non-linear frequency, while the other two are the parent normal modes. The results are plotted in Figure 5.12 as a function of the frequencies of the non-linear modes.

Clearly, most ratios are of the same order of magnitude, although they could, according to Tables 5.3 and 5.4, have a priori any values depending on both the viewing angle Θ and their set of indices (ℓ, m). The viewing angle being a stellar parameter, it is of course the same for each mode, which therefore suggests that the non-linear frequencies observed in G29-38 are combinations of normal modes having mostly the same ℓ and m degrees.

The viewing angle Θ being unknown, a direct comparison between the measured ratios A_c/A_1A_2 and the ones predicted by the models is a priori not possible. However, in certain specific cases, the above ratio happens not to be dependent on the viewing angle, but is simply a constant (see Tables 5.3 and 5.4). This is the case only for those cross-

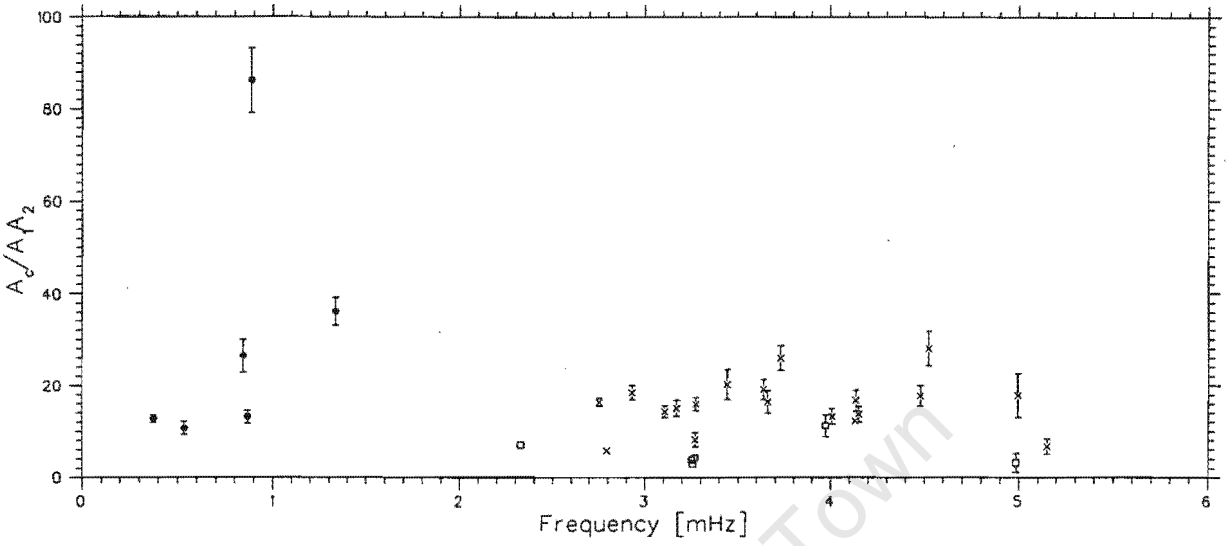

Figure 5.12: Ratio A_c/A_1A_2 for the 31 first-order combination frequencies. The abscissa indicate the frequencies f_c of the latter combinations. The circles, crosses and squares represent respectively difference frequencies, sum frequencies, and harmonics.

frequencies that are changing phase over the visible disc, like their parent modes do. Indeed, whatever the normal mode considered, a value of the viewing angle Θ always exists, for which the bright and dark areas cancel each other geometrically, so that its visible amplitude is actually zero. This is a direct consequence of the fact that the light received in the telescopes is unavoidably integrated over the visible disc, as the stellar surface cannot be resolved. Mathematically, only the combination frequencies that can be described in terms of just one spherical harmonic function Y_m^ℓ, rather than in terms of a linear combination of them, do change their phase over the visible disc. This is, for instance, always true for harmonics of running waves with equal spherical and azimuthal degrees, $\ell = m$, whereas it is never the case for combinations of pure standing waves, i.e. with azimuthal degree $m = 0$ (see Tables 5.3 and 5.4).

In order to determine which of the observed amplitude ratios, $A_c?A_1A_2$, are independent of the viewing angle Θ, and could thus be used for comparison with the theoretical predictions, secure mode identification is therefore required. This strengthens the importance of the mode identification without which hardly any asteroseismology can be performed. According to the work of Kleinman *et al.* (1998), the majority of the modes observed in G29-38 are thought to be $\ell = 1$. Assuming, for now, that they are all $\ell = 1$,

the various measured ratios of Figure 5.12 have been sorted out, in Figure 5.13, according to whether they are dependent of the viewing angle Θ (bottom panel), or independent of Θ (top panel). This sorting out depends therefore exclusively on the identification of the m index of each mode as the degree ℓ has been provisionally imposed to be 1. The data points in Figure 5.13 have been labelled by the k-orders of the respective parent modes that combines to form them, together with the year in which they have been observed. These k-values, taken from Kleinman (1995), do not represent a secure identification. Their values should therefore be considered as purely indicative of which frequencies are combined together.

The various levels corresponding to the predictions by Brickhill are also plotted in Figure 5.13 for the different ℓ and m combinations. Harmonic levels are indicated by the one set of indices $[\ell, m]$, while the combination frequencies are indicated by two sets $[\ell_1, m_1; \ell_2, m_2]$. In the top panel these levels are fixed, whereas in the bottom panel they are given for the Θ values corresponding to best fits of the different categories of combinations. The corresponding BFW values are too small to appear in the graph.

Provided the above $\ell = 1$ assumption is correct for most modes, it is clear, from the top panel of Figure 5.13, and according to Tables 5.3 and 5.4, that Brickhill's results are of the right order of magnitude, while BFW's ones are not. Prior to drawing any conclusions, a more detailed comparison between the observations and Brickhill's predictions is required. Although most harmonics and two sum frequencies are well fitted by Brickhill's model, most combination frequencies identified in 1988 and 1993 are about 3 times larger than the actual predictions. A detailed step by step analysis will possibly help clarifying this issue.

1. Because the modes $k = 7, 8, 9, 11, 12, 14, 17$, individually combined to $k = 10$ in 1993, all show very similar amplitude ratios (Figure 5.13, top panel), this strongly suggests that these modes all have the same ℓ and m indices. Their period spacing is in good agreement with that expected for $\ell = 1$ (Kleinman *et al.* 1998), while the fact that these modes never show any multiplet structure suggests they are $m = 0$. Note that $k = 14$, observed in 1988 at 1297 μHz, has been observed in 1997 at 1288.6 μHz (Van Kerkwijk *et al.* 1999). If these are really two observations of the same mode, the above conclusion is in contradiction with the one by Clemens *et al.* (1999), who identified this mode as $\ell = 2$.

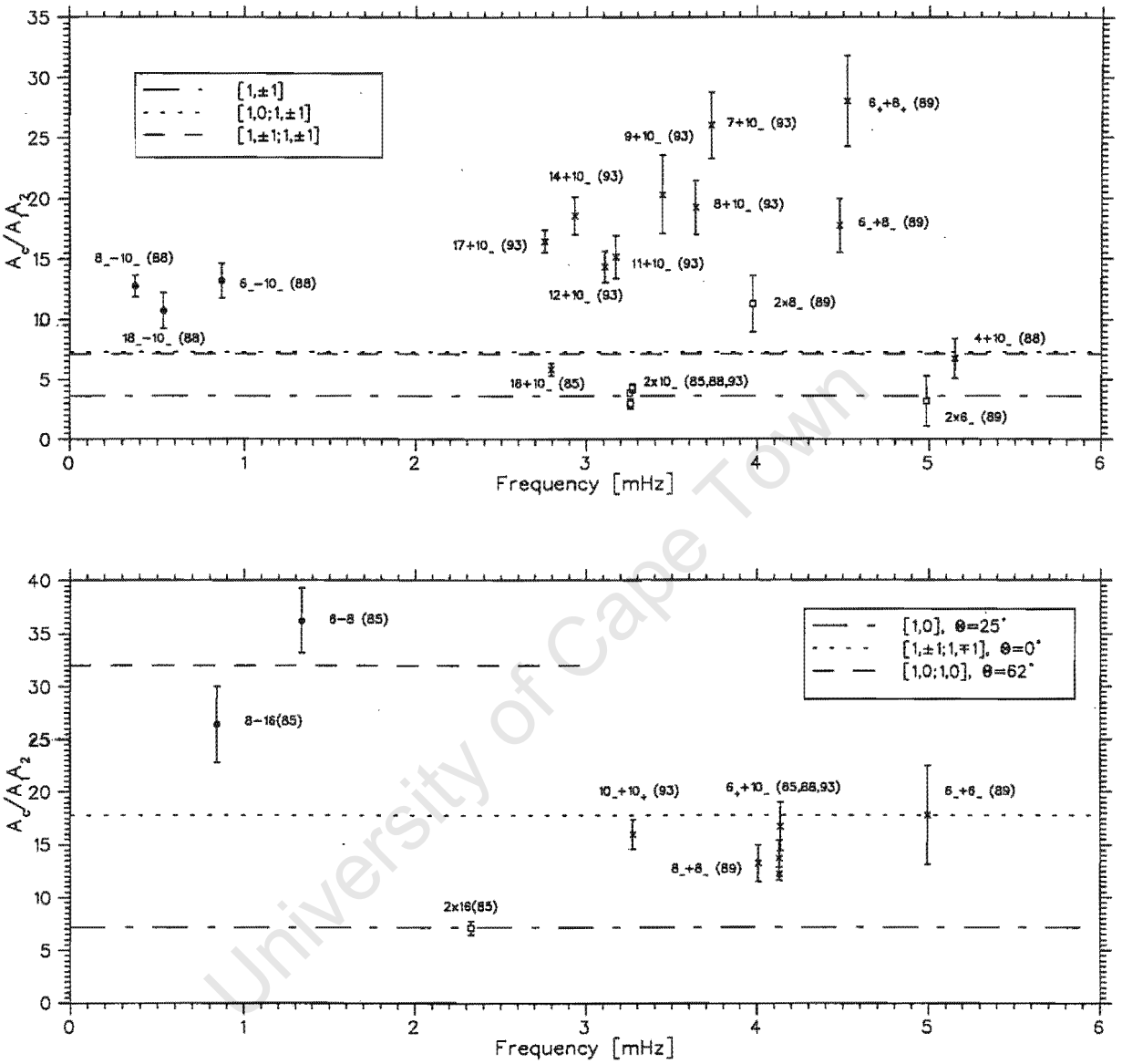

Figure 5.13: Ratios A_c/A_1A_2 for the combination frequencies that are respectively independent of the viewing angle Θ (*top panel*), and Θ-dependent (*bottom panel*). The data points have been labelled by the k-orders of the respective parent modes, together with the year in which they have been observed; the "+" and "–" lower indices indicate azimuthal degrees $m = \pm 1$, while the modes with $m = 0$ are given without subscripts. The abscissa indicates the frequencies f_c of the combination frequencies. The circles, crosses and squares represent respectively difference frequencies, sum frequencies, and harmonics. Brickhill's predictions of interest for harmonics $[\ell, m]$ and combination frequencies $[\ell_1, m_1; \ell_2, m_2]$ are indicated by fixed levels *(top panel)* and with a corresponding Θ value *(bottom panel)*.

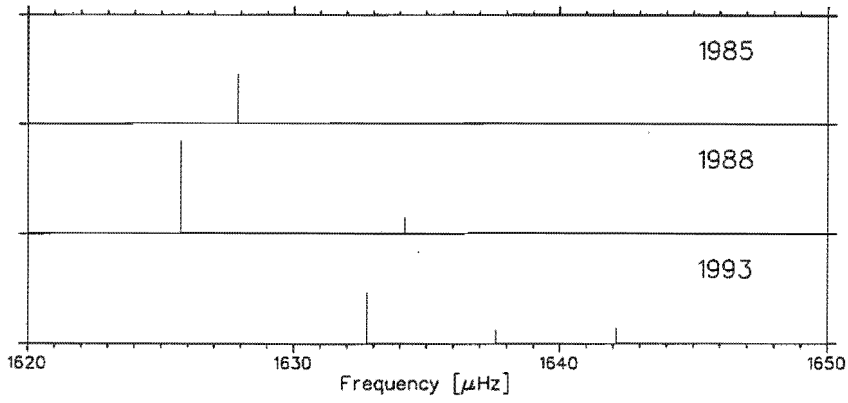

Figure 5.14: A schematic plot of the multiplet $k = 10$ in 3 different years.

2. The same remark applies to the modes $k = 6$, $k = 8$, and $k = 18$, also combined to $k = 10$, that all show extremely similar difference frequencies ratios in 1988 (Figure 5.13, top panel). Their frequencies complements well the $\ell = 1$ period spacing discussed in point (1) above, which strengthens our contention that this identification is correct.

3. The top panel of Figure 5.13 also shows that the difference frequencies have, globally speaking, slightly smaller ratios than the sum frequencies. This is a prediction of Brickhill's model, provided modes of same ℓ and m are compared (see equation 5.1 in section 5.4.2.1). This is again in good agreement with the assertions previously made in point (1) and (2) above.

4. The $k = 10$ multiplet shows a very different structure from seasons to season, experiencing both amplitude and frequency variations (up to 7 μHz), as seen in Figure 5.14. Only in the 1993 spectrum does it show a clear multiplet feature. Two possibilities have to be discussed here, although none of them give full satisfactory results.

   - if this $k = 10$ peak is an $\ell = 1$ mode, then the largest component in the 1993 triplet is definitely $m = -1$ (Figure 5.14). In turn, this is likely to be also true for the 1985 and 1988 largest peaks as the 3 corresponding harmonics ($2 \times 10\_$) not only show the same relative amplitudes, but are well fitted by Brickhill's model (Figure 5.13, top panel). Furthermore, an $\ell = 1$ identification would be consistent with the above described period spacing (Kleinman *et al.* 1998), and with the conclusion by Clemens *et al.* (1999). However, this would imply

that this multiplet has experienced an enormous seasonal frequency shift. The latter could hardly be explained by mode trapping as this would require G29-38 to have a thin H-layer (Brassard *et al.* 1992), which is in contradiction with the current belief (Bradley 1996, Clemens 1993, 1994, Kleinman *et al.* 1998). Furthermore, this $\ell = 1$ identification also implies that all the 1993 corresponding sum frequencies ratios are, as assumed, independent of the viewing angle Θ, with an average value at around 18, which is 3 times larger than the value predicted by Brickhill's model. The same remark is true for the difference frequencies ratios observed in 1988 (Figure 5.13, top panel). This mismatch could possibly be explained by the non-applicability of the model to large amplitude DAVs, but the frequency shift of the triplet remains a mystery. Third order interactions could perhaps be the cause (see section 6.2 & 6.3), but this is not obvious at all.

- if this $k = 10$ mode is an $\ell = 2$, then the large peak in the 1993 multiplet is likely to be the $m = 0$ component, to be consistent with the 1985 and 1988 observations, whose respective largest peak would then correspond to the $m = -2$ component (Figure 5.14). Although the 1993 sum frequencies ratios could be fitted with a value of the viewing angle at around $\Theta = 14°$, the minimum possible value for the harmonic ratio is 13.6, for $\Theta = 0$ (Table 5.3), which is about 3 times larger than the observations. Furthermore, the 1988 difference ratios should be found at 2.6 according to the model (Table 5.4), whereas their values are observed to be about 13.

To try and understand the observations with $k = 10$ being an $\ell = 2$ mode thus leads to a complete mismatch. We therefore believe the $\ell = 1$ identification is correct, because the unexplained features are at least consistent with each other.

5. The mode labelled $k = 8$ shows a peculiar behaviour in 1989. Not only is its harmonic relatively 3 times larger than all the other ones observed (Figure 5.13, top panel), but its frequency experienced an enormous 12 μHz shift from 1988 to 1989 (Table 5.1). This suggests that we might not be seeing the same mode. This 1989 harmonic ratio at 11.4 ± 2.4 (Figure 5.13) is consistent with an $\ell = 2$, $m = 0$ mode, whereas the predicted value is 13.7 (Table 5.3).

6. If the mode $k = 16$ observed in 1985 is $\ell = 1$, $m = 0$, then its first harmonic ratio of

7.1 (Figure 5.13, bottom panel) corresponds, in Brickill's model, to a viewing angle $\Theta = 25° \pm 8°$.

7. If the sum frequencies in the bottom panel of Figure 5.13 are indeed combinations of respectively $(\ell = 1, m = 1)$ and $(\ell = 1, m = -1)$ modes, then these observed ratios are all too low to fit into Brickhill's model. Indeed, the latter predicts a minimum value of 17.8 corresponding to a viewing angle $\Theta = 0°$. However, it has to be stressed that the identification of harmonics of modes belonging to a multiplet is very difficult because they are often blended. For instance, a peak has been observed in 1989 with frequency corresponding to the combination $6_- + 6_+$, which is impossible to disentangle from the harmonic $2 \times 6_0$ of the central peak.

8. Although the two difference frequencies (8-16) and (6-8) (Figure 5.13, bottom panel) have very different values, they are not far apart in terms of viewing angle. Provided the identification $\ell = 1$, $m = 0$ for the normal mode under concern is correct, then $\Theta = 60° \pm 3°$ indeed encompasses both of them. This is explained by the fact that, when Θ is large, the normal modes corresponding to standing waves, that is with $m = 0$, are very small, and actually vanish at $\Theta = 90°$. Therefore, a small error in the viewing angle may induce a large change in the corresponding amplitude ratio A_c/A_1A_2.

9. In Figure 5.12, the ratio at 888 μHz was, with a value at around 85, much larger than any others (it has not been plotted in Figure 5.13). This difference frequency, which corresponds to the combination 8-17, was already anomalous when the phase analysis was performed (section 5.3), which led to the suspicion that this frequency might be a resonant mode rather than a harmonic distortion peak. The fact that it is also discrepant in the present analysis strengthens this suspicion. A possible mis-identification is discarded as not only is power definitely present, but the frequency match is one of the best observed with $f_c - (f_8 - f_{17}) = 888.150 - (2006.587 - 1118.553) = 0.116$ μHz.

5.4.4 Conclusion

The lack of a secure mode identification for G29-38 made this whole analysis very intricate. In particular, it had to be assumed that the eigenmodes identified were all $\ell = 1$. In most

cases, this assumption proved to be consistent with the analyses conducted subsequently, and was eventually adopted as correct. The stronger argument in favour of this $\ell = 1$ contention arose from the clear clustering of most amplitude ratios A_c/A_1A_2, which suggested that the majority of the normal modes identified were of the same spherical degree, most probably $\ell = 1$, in keeping with the period spacing analysis by Kleinman *et al.* (1998). However, the mode identified as $k = 8$ in 1989 might be an $\ell = 2$, although no clear evidence could be put forward. The analysis also confirmed the probable discovery of a resonant mode at 888 μHz, corresponding to the combination 8-17.

As far as the comparison with the theoretical models is concerned, it was first shown that the model of Brickhill fits the amplitudes of the non-linear frequencies much better than the BFW model, whose predictions are about one order of magnitude too low. This directly suggests that the non-linear response of the convection zone to the oscillatory perturbation travelling through it is a much stronger effect than the non-linear response of the emergent flux to the surface temperature variations. However, as both these models are built on the same degree of approximation, their analytical predictions are essentially identical, although their physical approach is different. It is therefore surprising that their numerical predictions are so different. It was determined that the discrepancy lies in the value of the coupling constants a, b and c (equation 5.1). For instance, $a \approx 4.5$ in Brickhill's model (see section 5.4.2), but is only about 0.2 in BFW's model for an 11500°K star.

While the present work represents the first test of Brickhill's model, BWF's model has been successfully tested in the case of the DAV G117-B15A (Brassard *et al.* 1993). Built on 3 eigenmodes only, the latter model reproduced well the 10 frequencies observed in the amplitude spectrum of this star. The discrepancy between the excellent agreement in the case of G117-B15A, and the poor match for G29-38 is surprising. However, G117-B15A being a much lower amplitude pulsator than G29-38, this suggests that third (and higher) order effects may be too significant in G29-38 for perturbation theory to be applied. The comparison of the ratios A_c/A_1A_2 of the combination frequencies with that, A_h/A^2, of the first harmonics supports this contention. It can be shown, using plain trigonometric arguments, that, to second order of perturbation, these two quantities should satisfy $A_c/A_1A_2 = 2\,A_h/A^2$ (compare Table 5.3 and 5.4, see also Brickhill 1992a). This is, however, not what is observed in G29-38 (Figure 5.13), suggesting the presence of higher order perturbations.

Despite these considerations, Brickhill's second order model gives satisfactory results. The latter could unfortunately not be compared to BFW's predictions in the case of G117-B15A, for the coupling parameters a, b and c (equation 5.1), that are not true constants, but temperature and surface gravity dependent functions, are provided only in the one case that, by chance, corresponds quite well to G29-38. This truly limits the applicability and testing of Brickhill's model.

Although the exact origin of the discrepancy between the two models could not be uncovered, it seems nevertheless that the radiative transfer is really not the dominating nonlinear process in G29-38. The model of Wu (1999), which is built on the same assumptions as Brickhill's model, fully supports this conclusion. This is quite surprising as the visible part of the emission spectrum of the DA white dwarfs lies precisely in the highly nonlinear part of their energy distribution, where a relation of the type $L \propto T^4$ applies. The effects of the radiative transfer are thus expected to be the first significant deviation from linearity. As mentioned earlier, this is, however, not necessarily the case for DB variables, whose visible part of the spectrum lies in the fairly linear Rayleigh-Jeans tail of the energy distribution, where the white light luminosity L is more or less proportional to the temperature T.

Although Brickhill's predictions are of the right order of magnitude, it has not been possible, even by trying to attribute different indices ℓ and m to the identified modes, to fit properly the various amplitude ratios observed. This could merely be due to the fact that this model is not designed for a large amplitude pulsator like G29-38. For this reason, the viewing angle Θ could not be determined as the different measurements were not consistent with each other. On the other hand, the mismatch could also come from the fact that it is not clear whether the model accounts for normal modes involved simultaneously in many combinations. For instance, only one combination frequency involves the mode $k = 10$ in 1985, whereas the same mode generated 8 cross-frequencies in 1993 (Figure 5.13). Therefore much more of this normal mode's initial energy has been spread into combination frequencies in 1993 than in 1985, which correspondingly lowers its amplitude and increases thus the amplitude ratio A_c/A_1A_2.

Proper comparison between theory and observation will be possible only once a model that encompasses all different non-linear processes is constructed. A first step in this direction would be to combine Brickhill's and BFW's models. This could be achieved by

using Brickhill's non-sinusoidal surface temperature distribution as the input for BFW's model. A DA variable with a secure mode identification is also crucially needed.

References

Bergeron F., *et al.*, 1995, ApJ, 449, 258

Böhm-Vitense E., 1989, *Introduction to Stellar Astrophysics*, Vol. 2, Cambridge University Press, Cambridge

Bradley P. A., 1996, ApJ, 468, 350

Brassard P., *et al.*, 1993, in White Dwarfs: Advance in Observation and Theory, ed. M.A. Barstow, NATO ASI Series, 403, 485

Brassard P., Fontaine G., Wesemael F., 1992, ApJS, 80, 369

Brassard P., Fontaine G., Wesemael F., 1995, ApJS, 96, 545

Brickhill A.J., 1991a, MNRAS, 251, 673

Brickhill A.J., 1991b, MNRAS, 252, 334

Brickhill A.J., 1992a, MNRAS, 259, 519

Brickhill A.J., 1992b, MNRAS, 259, 529

Clemens J. C., 1993, Baltic Astron., 2, 407

Clemens J. C., 1994, PhD thesis, Univ. Texas, Austin

Clemens J. C., Van Kerkwijk M. H., Wu Y., 1999, in press

Fontaine G., Brassard P., 1994, *Stellar and Circumstellar Astrophysics*, eds. G. Wallerstein and A. Noriega-Crespo, 57, 195

Jones P. W., 1989, ApJ, 336, 403

Kleinman S. J., 1995, PhD thesis, Univ. of Texas, Austin

Kleinman S. J., *et al.* 1998, ApJ, 495, 424

Nather E. D., 1990, ApJ, 361, 309

Robinson E. L., Kepler S. O., Nather R. E., 1982, ApJ, 259, 219 (RKN)

Rudenko O. V., Soluyan S. I., 1977, *Theoretical Fundations of Nonlinear Acoustics*, Plenum Publishing Corp., New-York

Unno W., *et al.*, 1989, *Nonradial Oscillations of Stars*, 2nd edition, University of Tokyo Press, Tokyo

Van Kerkwijk M. H., 1999, in press

Chapter 6

Nonlinear behaviour of the DB variable GD358

6.1 Introduction

The prospects for nonlinear analysis are better for the DBV GD358 than for the DAV G29-38, because its temporal spectrum undergoes milder changes. In G29-38, frequencies were appearing and disappearing which precluded any analysis other than record the changes. Besides a few recurrent modes whose evolution could be followed, no real cyclic pattern in the behaviour of this star could be uncovered. There are three main reasons why GD358 ought to be a more fruitful candidate for the study of nonlinearities:

- Its pulsations seem to be fairly stable, with "come-and-go" modal behaviour occurring to a much lesser extent, although the 1996 observing campaign yielded some surprises (see section 6.3.4).
- It has been twice the target of the Whole Earth Telescope, and both campaigns gathered light curves of excellent quality, much better than those from the WET runs conducted on G29-38. In particular, these two data sets are so long that they can even be segmented into contiguous subsets that each have their period structure resolved; the comparative analysis of these subsets might enable short term amplitude variations to be detected.

- Since a fairly secure mode identification has been carried out on this star, specific quantitative analyses could possibly be performed. In particular, it was possible to analyse the evolution of the pulsational energy in the visible modes, i.e. the mechanical energy contained in the pulsations, which might yield interesting clues as to the nature of the nonlinear processes in action.

This chapter is built around two publications that were both submitted to the Monthly Notices of the Royal Astronomical Society in early June 1999. The first one, which makes up section 6.2, comprises the following 40 authors, listed in the order they appear in the publication.

F. Vuille,[1] D. O'Donoghue,[2] D. A. H. Buckley,[2] C.-M. Massacand,[3,26] J. E. Solheim,[3] S. Bard,[4] G. Vauclair,[5] O. Giovannini,[6] S. O. Kepler,[6] A. Kanaan,[7] J. L. Provencal,[8] M. A. Wood,[9] J. C. Clemens,[10] S. J. Kleinman,[11,25] M. S. O'Brien,[12] R. E. Nather,[13] D. E. Winget,[13] A. Nitta,[13] E. W. Klumpe,[13] M. H. Montgomery,[13,14] T. K. Watson,[15] P. A. Bradley,[16] D. J. Sullivan,[17] K. Wu,[18] T. M. K. Marar,[19] S. Seetha,[19] B.N. Ashoka,[19] H. S. Mahra,[19] B. C. Bhat,[19] V. C. Babu,[19] E. M. Leibowitz,[20] S. Hemar,[20] P. Ibbetson,[20] E. Mashals,[20] E. Meištas,[21,26] P. Moskalik,[22] S. Zoła,[23,24] J. Krzesiński,[24] G. Pajdosz[24]

[1]Department of Astronomy, University of Cape Town, Rondebosch 7700, South Africa

[2]South African Astronomical Observatory, P.O. Box 9, Observatory 7935, South Africa

[3]MR, Nordlysobservatoriet, Universitetet i Tromso, N-9037 Tromso, Norway

[4]University of Oslo, Institute of Theoretical Astrophysics, Blindern, N–0315, Oslo, Norway

[5]Observatoire Midi-Pyrenees, 14 Avenue E. Belin, 31400 Toulouse, France

[6]Instituto de Fisica, Universidade Federal do Rio Grande do Sul, 91500-970 Porto Alegre - RS, Brazil

[7]Dep. de Fisica - UFSC, Campus Universitario - Trindade, CEP 88040-900 – Florianopolis – SC, Brazil

[8]Sharp Laboratory, Dept. of Physics and Astronomy, University of Delaware, Newark, DE 19716, USA

[9]Dept. of Physics and Space Sciences, Florida Institute of Technology, 150 W. University Blvd., Melbourne, FL. 32901-6975, USA

[10]Campus Box: 3255, 264 Phillips Hall, Chapel Hill, NC 27599, USA

[11]Iowa State University, Department of Physics and Astronomy, Ames, IA 50011, USA

[12]Department of Physics, Grinnell College, P.O. Box 805, Grinnell, IA 50112-0806

[13]Astronomy Dept., University of Texas at Austin, Austin, TX 78712, USA

[14]Institute for Astronomy, Türkenschanzstraße 17, A-1180 Vienna, Austria
[15]Information Technology Services, Southwestern University, Georgetown, TX 78626, USA
[16]XTA, MS B220, Los Alamos National Laboratory, Los Alamos, NM 874545, USA
[17]Department of Physics, Victoria University of Wellington, P.O. Box 600 Wellington, New Zealand
[18]Research Centre for Theoretical Astrophysics, University of Sydney, NSW 2006, Australia
[19]Technical Physics Divison, ISRO Satellite Centre, Airport Road, Bangalore, 560 017, India
[20]University of Tel Aviv, Department of Physics and Astronomy, Ramat Aviv, Tel Aviv 69978, Israel
[21]Institute of Theoretical Physics and Astronomy, Goštauto 12, Vilnius 2600, Lithuania
[22]Copernicus Astronomical Center, Polish Academy of Sciences, ul. Bartycka 18, 00-716 Warsaw, Poland
[23]Astronomical Observatory, Jagiellonian University, ul. Orla 171, 30-244 Cracow, Poland
[24]Mt. Suhora Observatory, Cracow Pedagogical University, ul. Podchorazych 2, 30-084 Cracow, Poland
[25]Guest observer at Siding Spring Observatory, Australia
[26]Guest observer at Assey-Turgen Observatory, Kazakhstan

The reason for this lengthy list of co-authors is that it is the first major publication which uses the data gathered during the 1994 Whole Earth Telescope campaign on GD358, involving the participation of 12 observatories and 39 observers. All these collaborators are therefore naturally co-authors of this paper.

I did not take part in the observations, nor did I perform the data reduction, a task that fell to the Principal Investigator (PI) of the campaign, Ed Nather (1995). However, I carried out the whole analysis, and wrote the paper, whose content can thus be considered as my own unaided work, besides a scientific suggestion by Pierre Brassard (see below) and natural feed-back from some of the co-authors.

This paper chiefly presents the mode identification carried out on the 1994 WET data set. This task was a necessary and important first step to any subsequent analysis, both for my own purposes and for that of anyone wanting to perform seismological investigation of this star. This analysis is not a trivial repetition of the mode identification performed on the 1990 WET data set, because the main purpose of this second campaign was precisely to compare the temporal spectrum of GD358 four years apart. Although the work was certainly facilitated by directly comparing this 1994 data set with the 1990 mode identification, new difficulties appeared, despite the better resolution and S/N ratio, which did not make the analysis straightforward.

Section 6.3 is made up of a publication that has Pierre Brassard and myself as authors. Pierre Brassard suggested the origin of the odd peaks that perturb the eigentriplet structures, and provided some numerical data (see Table 6.7), obtained with his as yet unpublished numerical model. I suggested this study, carried out all the analyses presented, and wrote the paper.

6.2 Mode identification in the 1994 WET run on GD358

Abstract

We present a detailed mode identification performed on the 1994 Whole Earth Telescope (WET) run on GD358. The results are compared to that obtained on the same star from the 1990 WET data. The two respective temporal spectra show very few qualitative differences, although amplitude changes are seen in most modes, including the disappearance of the mode identified as $k = 14$ in the 1990 data. The excellent coverage and signal-to-noise ratio obtained during the 1994 run leads to the secure identification of combination frequencies up to fourth order, i.e. peaks that are sums or differences of up to four parent frequencies, including a virtually complete set of second order frequencies, as expected from harmonic distortion. We show how the third order frequencies are expected to affect the triplet structure of the normal modes by back–interacting with them. Finally, a search for $\ell = 2$ modes was unsuccessful, not verifying the suspicion that such modes had been uncovered in the 1990 data set.

6.2.1 Introduction

Variable white dwarfs are believed to pulsate in nonradial gravity modes, or g-modes (Dolez & Vauclair 1981, Winget & Fontaine 1982). Their multi-periodicity requires very long continuous data in order for their period structure to be resolved, for which purpose the Whole Earth Telescope (WET; Nather 1990) has been designed. Any pulsation mode can be represented by a solution of the differential equations describing stellar pulsations, of the form (e.g. Unno *et al.* 1989)

$$\zeta(r, \theta, \varphi, t) = \xi_k(r)\ Y_\ell^m(\theta, \varphi)\, \mathrm{e}^{-i\sigma t}$$

where $\zeta(r, \theta, \varphi, t)$ describes the displacement from equilibrium of any point in the star with

spherical coordinates (r, θ, φ). $\xi_k(r)$ is the radial eigenfunction, with k nodes between the centre and the surface, which describes the radial behaviour of the star. $Y_\ell^m(\theta, \varphi)$ is the spherical harmonic function of index ℓ and m ($\ell = 0, 1, 2, ...$; $m = 0, \pm 1, ..., \pm \ell$), while $\sigma = \sigma_{klm}$ is the oscillation frequency. The ℓ and m indices describe the angular behaviour of the oscillations, which can be visualised, on the surface of the star, as alternate bright and dim areas. For a given stellar model, a normal mode is entirely determined by the three indices (k, ℓ, m).

Mode identification, that is the labelling of each frequency present in the temporal spectrum with its corresponding set of indices (k, ℓ, m), is the essential link between theory and observation. Asteroseismology uses the pulsations in order to extract physical information about the star, by providing the input parameters to the theoretical models (Kawaler & Hansen 1989, Winget 1988), and can only be performed once correct mode identification has been carried out. Unfortunately, mode identification is not at all a straightforward exercise for various reasons:

- To the limit of a typical frequency resolution, various (k, ℓ, m) combinations can often match a given observed period.
- Only the modes having an amplitude significantly above the noise level can be detected and possibly identified.
- Modes with spherical degree $\ell \geq 4$ are not expected to be visible photometrically because the light received in the telescopes is unavoidably integrated over the stellar disc, and the numerous bright and dim areas on the stellar surface geometrically tend to cancel each other out (Dziembowski 1977).
- The frequencies of the normal modes depend on various structural parameters of the star, which are a priori not accurately known.
- The observed periods do not necessarily correspond to normal modes. Harmonics and combination frequencies due to pulse shape effects are often present (Brickhill 1992, Brassard *et al.* 1995.
- Artifact frequencies, called aliases, may appear in the period spectrum due to gaps in the data set (Scargle 1981, 1982, Nather *et al.* 1990).

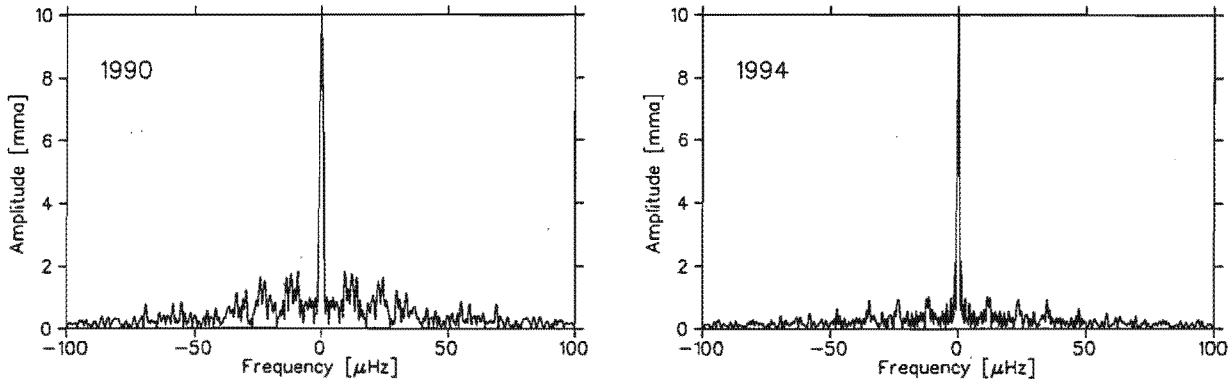

Figure 6.1: Comparison of the spectral windows as observed in 1990 *(left panel)* and 1994 *(right panel)*

- Not all successive overtones are excited. For reasons not clearly understood the mode selection mechanism tends to excite a few frequencies among all the possible ones (Winget & Fontaine 1982).

- The process of mode trapping may slightly shift the natural frequencies of the normal modes, causing the periods to deviate from their asymptotic equal spacing (e.g. Brassard *et al.* 1992).

GD358 was the first DB pulsator to be discovered (Winget *et al.* 1982). It has since been observed twice with the WET, in 1990 and 1994. The very good coverage and signal-to-noise ratio obtained during the 1990 WET run led to quite a secure mode identification that labelled all the normal modes with a spherical index of $\ell = 1$ (Winget *et al.* 1994). Mode identification performed on the 1994 WET data is reported here, and a detailed comparison with the 1990 results is carried out. A comparison of the seismological model which best fits the new data with the models of Bradley & Winget (1994) which fitted the 1990 period spectrum will be reported elsewhere (Bradley, in preparation).

The rest of our paper is organised as follows. Section 6.2.2 presents the 1994 WET data; section 6.2.3 reports the complete mode identification, and discusses the differences with the 1990 results; section 6.2.4 concludes the analysis.

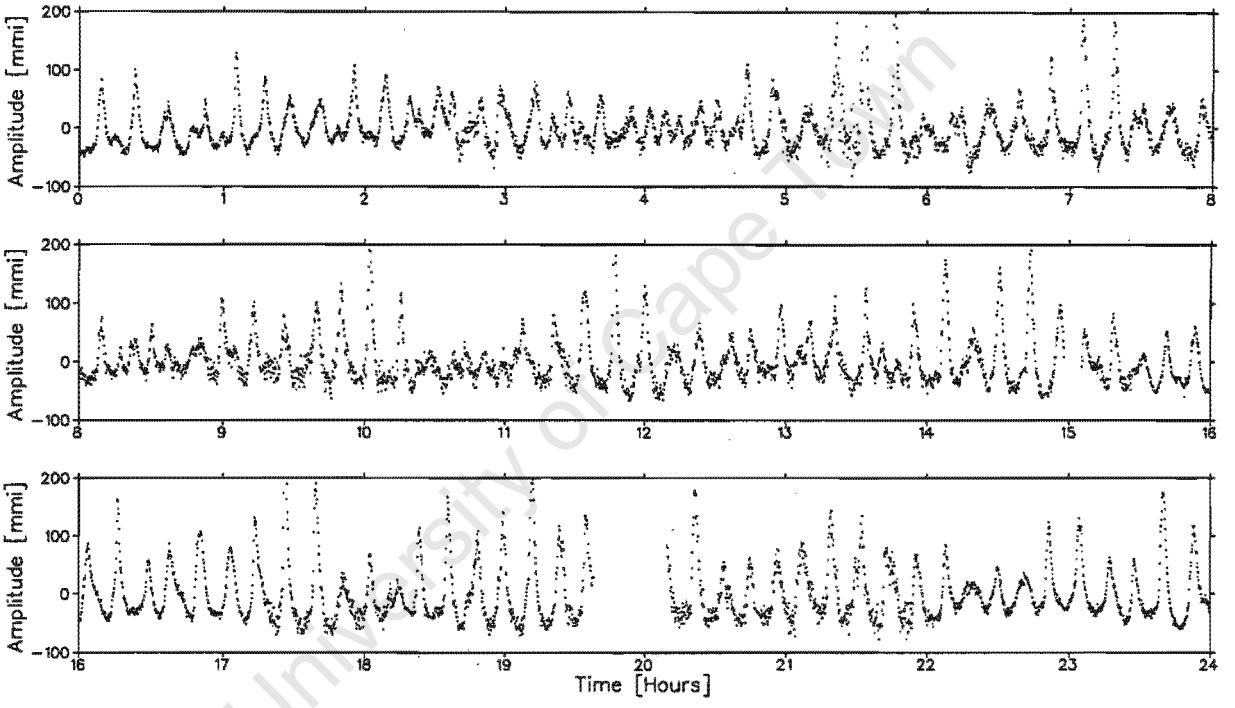

Figure 6.2: A 24 hour portion of GD358's light curve as obtained during the 1994 WET campaign, after the individual runs from the different telescopes have been combined together. Only two small gaps are apparent.

6.2.2 The 1994 WET data

Although the quality of the 1990 WET campaign on GD358 was excellent (~65% coverage), the 1994 one was even better, as seen for example by comparing the two corresponding spectral windows (Figure 6.1); the largest side-lobes are only about 10% in amplitude compared to nearly 20% in the 1990 data set. 342 hours of high-speed photometric observations were gathered over 2 weeks with a network of 10 telescopes well distributed around the world (South Africa (SAAO), La Palma (NOT), France (OHP), Brazil (Itajuba), Texas (McDonald), Hawaii (Mauna Kea), Australia (Siding Spring), India (Nainital), Israel (Wise), Poland (Mt. Suhora)). About 69 hours of data were actually overlapping, i.e. two telescopes were simultaneously observing the star. Therefore the campaign in effect yielded 273 hours of independent observations, corresponding to an unprecedented 80% coverage. Observations were done under photometric conditions using two or three channel photometers equipped with photomultiplier detectors with bi-alkali photocathodes. Photons have been gathered in consecutive 10 s integrations, and no filter was used in order to increase the signal-to-noise ratio.

The 93 runs (Table 6.1) were reduced individually by subtracting the sky background and correcting for atmospheric extinction, before being combined together into a single light curve; details can be found in Nather (1995). Figure 6.2 shows a 24 hour portion of the concatenated light curve, where the coverage is the best. It can be seen that the signal-to-noise ratio is extremely high, which should allow us to identify even more peaks than in 1990.

6.2.3 Mode identification

6.2.3.1 Comparison with the 1990 spectrum

The present mode identification is based on the analysis carried out on the 1990 WET data (Winget *et al.* 1994), as well as on the progress report by Nather (1995), which pointed out the qualitative resemblance between the 1990 and 1994 period spectra. Based on the above analyses, most 1994 multiplets found in the range 1200-2500 μHz can readily be identified as the ones observed in 1990 (Figure 6.3).

Table 6.1: Journal of Observations

Telescope	Run Name	Date [UT]	Start Time [UTC]	Run Length [s]
Mauna Kea 0.6m	jcc-0225	1994 May 2	11:56:00	10500
Sid. Spring 0.6m	sjk-0322	1994 May 2	14:29:30	18890
OHP 1.9m	gv-0404	1994 May 2	22:35:10	15430
NOT[1] 2.5m	jesb01	1994 May 3	1:08:10	15950
McDonald 0.75m	ra321	1994 May 3	4:33:50	23830
Mauna Kea 0.6m	jcc-0226	1994 May 3	7:54:00	1470
Mauna Kea 0.6m	jcc-0227	1994 May 3	8:20:00	22920
Sid. Spring 0.6m	sjk-0323	1994 May 3	16:07:30	12860
OHP 1.9m	gv-0406	1994 May 3	21:06:00	20680
NOT 2.5m	jesb03	1994 May 3	21:46:40	2610
SAAO 0.75m	sa-b004	1994 May 3	22:13:10	11610
McDonald 0.9m	ra322	1994 May 4	3:20:20	450
McDonald 0.9m	ra323	1994 May 4	3:38:30	20860
Mauna Kea 0.6m	jcc-0229	1994 May 4	7:40:00	25300
Sid. Spring 0.6m	sjk-0327	1994 May 4	13:26:00	12530
Sid. Spring 0.6m	sjk-0328	1994 May 4	16:55:30	9710
SAAO 0.75m	sa-b009	1994 May 4	21:27:00	13060
NOT 2.5m	jesb08	1994 May 4	21:46:00	27920
Mt. Suhora 0.6m	suh-0007	1994 May 4	22:00:00	10530
SAAO 0.75m	sa-b010	1994 May 5	2:34:30	5260
McDonald 0.9m	ra325	1994 May 5	3:09:50	27010
Mauna Kea 0.6m	jcc-0231	1994 May 5	7:36:00	25040
Sid. Spring 0.6m	sjk-0332	1994 May 5	13:02:00	14770
Sid. Spring 0.6m	sjk-0333	1994 May 5	17:15:00	1940
Nainital 1m	n44-0254	1994 May 5	17:27:10	12620
OHP 1.9m	gv-0408	1994 May 5	21:10:20	20460
NOT 2.5m	jesb09	1994 May 5	21:20:40	29450
SAAO 0.75m	sa-b013	1994 May 5	21:53:20	12320

[1]Based on observations made with the Nordic Optical Telescope (NOT), operated on the island of La Palma jointly by Denmark, Finland, Iceland, Norway, and Sweden, in the Spanish Observatorio del Roque de los Muchachos of the Instituto de Astrofisica de Canarias.

Table 6.1: – *continued*

Telescope	Run Name	Date [UT]	Start Time [UTC]	Run Length [s]
McDonald 2.1m	ra326	1994 May 6	6:09:00	13690
Mauna Kea 0.6m	jcc-0233	1994 May 6	8:54:00	20200
McDonald 0.9m	ra328	1994 May 6	10:57:00	970
Sid. Spring 0.6m	sjk-0337	1994 May 6	12:54:00	22580
OHP 1.9m	gv-0410	1994 May 6	20:36:30	22370
SAAO 0.75m	sa-b015	1994 May 6	21:31:40	9570
Itajuba 1.6m	ro050	1994 May 7	4:38:50	13450
Mauna Kea 0.6m	jcc-0235	1994 May 7	7:32:00	24780
Sid. Spring 0.6m	sjk-0341	1994 May 7	12:48:30	22600
Nainital 1m	n44-0255	1994 May 7	15:47:10	25430
OHP 1.9m	gv-0412	1994 May 7	20:54:20	10180
SAAO 0.75m	sa-b017	1994 May 7	21:54:20	22070
Itajuba 1.6m	ro051	1994 May 8	2:59:20	10100
Mauna Kea 0.6m	jcc-0237	1994 May 8	7:26:00	25420
Sid. Spring 0.6m	sjk-0345	1994 May 8	12:46:00	22620
Mt. Suhora 0.6m	suh-0008	1994 May 8	20:13:30	19860
Wise 1m	el-005	1994 May 8	20:15:41	240
Wise 1m	el-006	1994 May 8	20:19:44	560
Wise 1m	el-007	1994 May 8	20:54:01	9230
SAAO 0.75m	sa-b020	1994 May 8	22:06:50	20270
Wise 1m	el-008	1994 May 8	23:41:51	7500
Mauna Kea 0.6m	jcc-0238	1994 May 9	10:23:00	14680
Sid. Spring 0.6m	sjk-0349	1994 May 9	12:47:00	22590
Wise 1m	el-010	1994 May 9	14:59:58	3206
OHP 1.9m	gv-0414	1994 May 9	21:16:50	19390
SAAO 0.75m	sa-b022	1994 May 9	21:23:40	21870
Itajuba 1.6 m	ro056	1994 May 10	6:46:50	3880
Mauna Kea 0.6m	jcc-0240	1994 May 10	7:15:00	11550
Mauna Kea 0.6m	jcc-0241	1994 May 10	10:33:40	14800
Sid. Spring 0.6m	sjk-0350	1994 May 10	12:38:30	19240
Nainital 1m	n44-0256	1994 May 10	15:21:10	26750
Sid. Spring 0.6m	sjk-0351	1994 May 10	18:02:00	3340

Table 6.1: – *continued*

Telescope	Run Name	Date [UT]	Start Time [UTC]	Run Length [s]
Wise 1m	el-011	1994 May 10	18:35:22	230
Wise 1m	el-012	1994 May 10	19:15:51	200
Wise 1m	el-013	1994 May 10	19:27:50	2340
Wise 1m	el-014	1994 May 10	20:17:21	19520
Mt. Suhora 0.6m	suh-0009	1994 May 10	21:32:20	14760
SAAO 0.75m	sa-5726	1994 May 10	21:42:00	20270
Itajuba 1.6 m	ro059	1994 May 11	2:24:40	1780
Itajuba 1.6 m	ro060	1994 May 11	4:01:50	1880
McDonald 2.1m	ra332	1994 May 11	5:02:00	8750
Mauna Kea 0.6m	maw-0132	1994 May 11	7:17:20	26050
Sid. Spring 0.6m	sjk-0352	1994 May 11	12:34:00	22580
SAAO 0.75m	sa-5728	1994 May 11	20:53:00	23490
Mt. Suhora 0.6m	suh-0010	1994 May 11	21:58:30	11970
McDonald 2.1m	ra333	1994 May 12	3:19:50	2640
Mauna Kea 0.6m	maw-0134	1994 May 12	7:15:00	26200
Mt. Suhora 0.6m	suh-0011	1994 May 12	20:29:30	17020
SAAO 0.75m	sa-5730	1994 May 12	20:42:00	24100
Mauna Kea 0.6m	maw-0136	1994 May 13	7:02:10	3590
McDonald 2.1m	tkw-0045	1994 May 13	9:00:30	7310
Mauna Kea 0.6m	maw-0137	1994 May 13	9:19:10	4460
Mauna Kea 0.6m	maw-0138	1994 May 13	11:30:50	10690
Sid. Spring 0.6m	sjk-0358	1994 May 13	12:42:30	21520
Mt. Suhora 0.6m	suh-0012	1994 May 13	19:50:20	21120
McDonald 2.1m	tkw-0046	1994 May 14	4:14:00	13840
Mauna Kea 0.6m	maw-0140	1994 May 14	7:00:00	26900
Sid. Spring 0.6m	sjk-0362	1994 May 14	12:47:00	21010
McDonald 2.1m	tkw-0047	1994 May 15	5:29:30	19890
Mauna Kea 0.6m	maw-0142	1994 May 15	6:56:20	27040
Sid. Spring 0.6m	sjk-0367	1994 May 15	12:31:30	21660
Mt. Suhora 0.6m	suh-0013	1994 May 15	20:49:10	16880
McDonald 2.1m	tkw-0049	1994 May 16	4:23:00	19640
Mauna Kea 0.6m	maw-0144	1994 May 16	6:49:00	6540
Sid. Spring 0.6m	sjk-0372	1994 May 16	12:40:00	21060

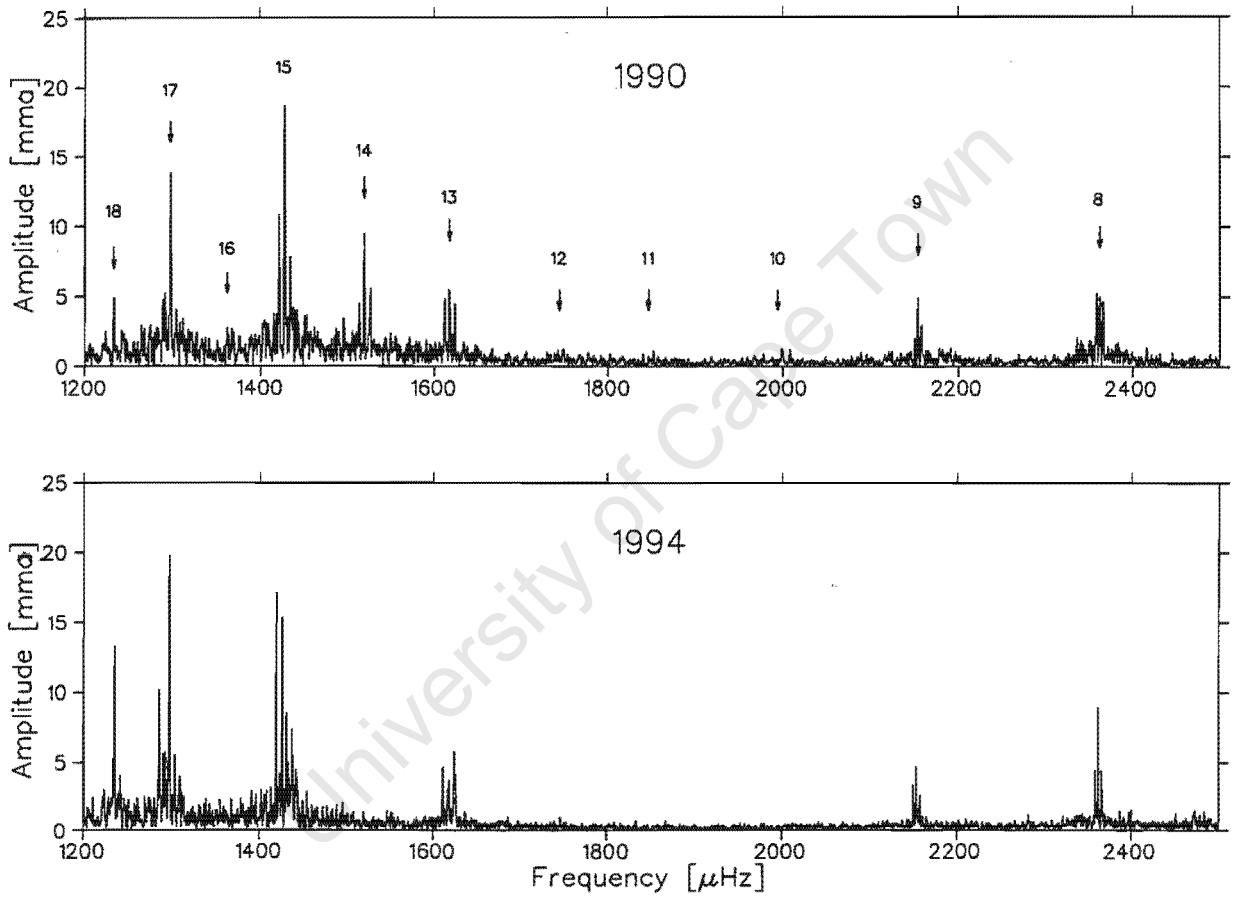

Figure 6.3: Comparison of the temporal spectra, in the frequency interval with largest amplitude, from the 1990 *(upper panel)* and 1994 *(lower panel)* WET campaigns. The radial orders k identified in the 1990 spectrum are indicated in the top panel.

While the two spectra look quite similar at first glance, there are significant quantitative differences between them. Most importantly, nearly all the modes experienced significant amplitude changes. The mode $k = 14$, third largest mode in 1990, almost disappeared in our data set. A closer look shows that the central peak of this triplet can still be found, although it is barely above the noise level, making its identification somewhat less certain. The $k = 18$, $k = 17$, and $k = 8$ modes experienced significant growth, while the $k = 11$ and $k = 10$ became undetectable. These last two modes were only marginally detectable in the 1990 data set.

6.2.3.2 The "odd" multiplet structures

Although the labelling of each multiplet in this data set with its k-order was a straightforward exercise, thanks to the work of Winget *et al.* (1994), the identification of each of their individual m-components requires a closer analysis. This is because the regular triplet structures recorded in 1990 do not repeat as obviously in 1994 (Figure 6.3). In particular, this is the case for the four dominant modes, namely $k = 18$, $k = 17$, $k = 15$, and $k = 13$, each of which displays a complicated pattern of peaks. The left panel of Figure 6.4 is a close-up of these four multiplets, where the frequencies that are probably part of the triplet identified in the 1990 data are marked with long arrows, while the extra significant "odd peaks" are indicated by arrowheads. The modes $k = 8$ and $k = 9$ do not exhibit this structure, as they both form a distinctive triplet, whose components can be readily identified (Figure 6.3).

In his progress report, Nather (1995) has shown that all the little peaks (referred to as the 'grass') surrounding the $k = 8$ triplet are due to spectral leakage from the data gaps (Nather *et al.* 1990). When an artificial light curve is synthesized from only the three frequencies of the triplet, and is then sampled as the original data were and subtracted from the observed light curve, all the small surrounding peaks are eliminated. This is, a priori, surprising as the spectral window (Figure 6.1) looks impressively good. This exercise, however, shows that the combined window effect of closely separated frequencies can have a complementary effect that becomes much more significant than the spectral window might suggest.

We applied a pre-whitening procedure to try and clarify the situation for the $k = 18$, 17,

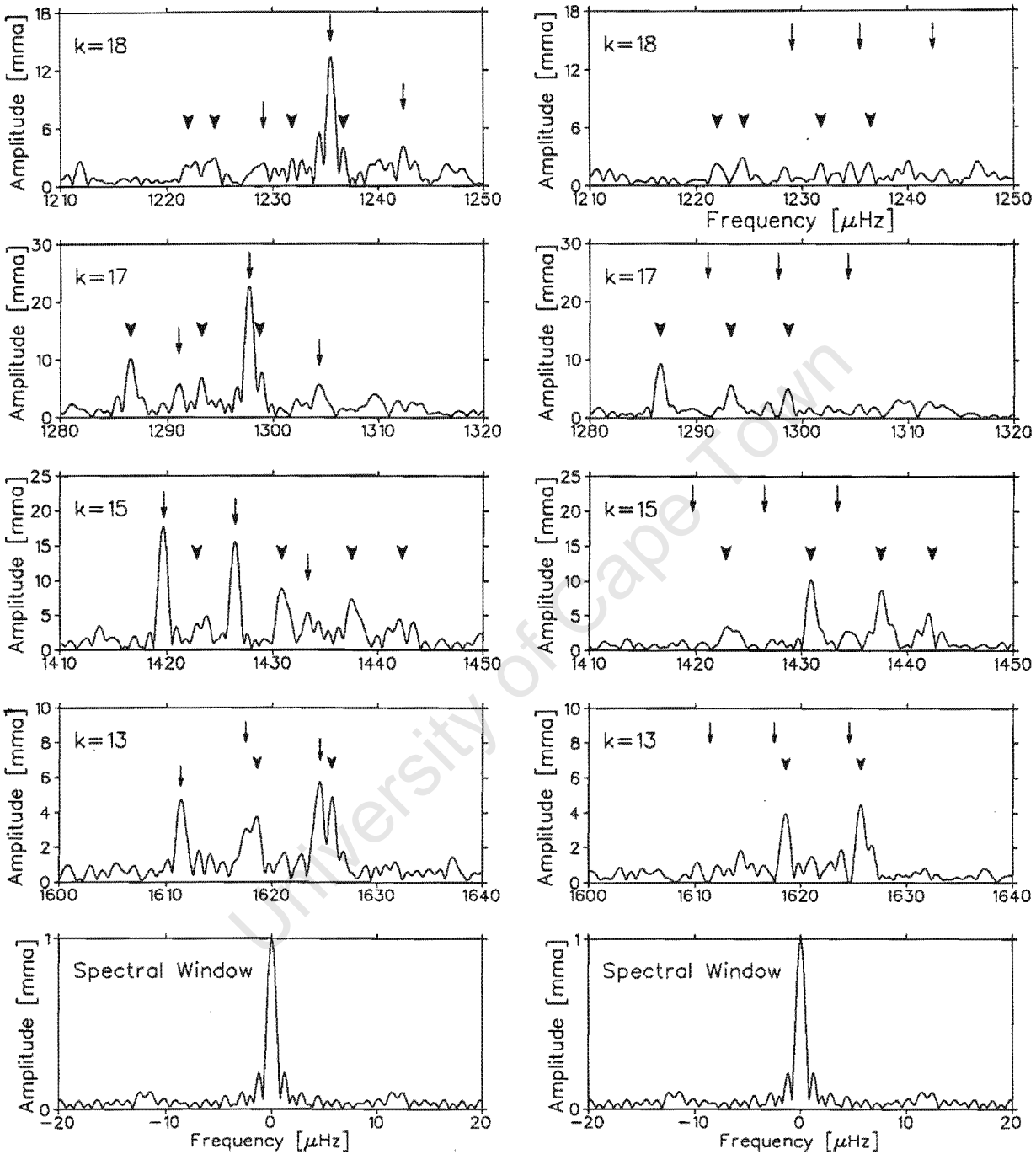

Figure 6.4: Close-up on the four multiplets that dominate the period spectrum *(left panel)*, and after these peaks have been simultaneously fitted by nonlinear least-squares and removed *(right panel)*. In each case, the frequencies that are thought to form the original triplets are marked with arrows, while the extra significant "odd" peaks, those not removed by the pre-whitening procedure, are indicated by arrowheads. The bottom panels show the corresponding spectral window.

15 and 13 multiplets. In order to differentiate between real modes and possible window artifacts, the larger peaks were successively removed, in each of the above multiplets, by the traditional pre-whitening technique. This means that a synthetic light curve constructed using the frequency, amplitude and phase obtained by nonlinear least squares fitting the highest peak of a given multiplet. This synthetic sinusoid was then subtracted from the original light curve, and the resulting Fourier spectrum was then re-computed. This whole procedure was then repeated with the next highest peak, until no significant power was left. Very simply stated, the peaks that had to be removed by this pre-whitening technique, i.e. all the ones marked with arrows and arrowheads in the left panel of Figure 6.4, are probably real, while the ones that disappeared naturally during the process are probable window artifacts. This procedure does assume the absence of amplitude modulation on time-scales significantly shorter than the WET run; any amplitude variation present would also leave behind some small peaks that are spurious.

This procedure did indeed "mow the lawn", as noticed by Nather (1995) for the $k = 8$ multiplet, in the sense that all the small peaks around each of the multiplets considered were satisfactorily removed. This however did not affect any of the "odd" large amplitude peaks, the ones indicated by arrowheads in the left panel of Figure 6.4, and no simple triplet structure could thus be uncovered. A simultaneous removal of the peaks marked with arrows in the left panel of Figure 6.4, which is the technique actually used by Nather (1995), did not remove any of the peaks marked by arrowheads either, as seen in the right panel of Figure 6.4.

We then realized that all these "odd" frequencies are situated at between 11 and 12 μHz from the peaks of the triplets identified in 1990. This suggests that they could be aliases generated diurnally, repeating with a frequency of 11.6 μHz (which corresponds to a 24 hour period). We first considered a possible timing error, where the clock of one of the observing sites might not be properly synchronised with the others. A synthetic light curve of the length of the entire campaign was built from the 33 largest frequencies securely identified in the temporal spectrum. We then computed cross-correlation functions between each individual run and the corresponding portion of this synthetic light curve. The purpose of this procedure was to determine whether one of the observing sites might show a shift in all of its runs compared to the mean of all the timings, as represented in the synthetic light curve. No timing error was, however, uncovered to the $\sim$ 10 s resolution given by this method.

Various other attempts to try and uncover the origin of these "odd" side peaks (Figure 6.4) were unsuccessful. For instance, we investigated the possibility of frequency, amplitude, or phase variations of the normal modes during the course of the observing campaign. Such changes, even large, would introduce potentially asymmetrical side lobes, but hardly big enough to account for the observed ones.

We were led to the conclusion that all the peaks marked with arrows and arrowheads in the left panel of Figure 6.4 are real, in the sense that they are of genuine pulsational origin, rather than being artifacts of the observing and/or time series analysis techniques. Also, these cannot be a superposition of $\ell = 1$ and $\ell = 2$, or 3, multiplets, because the period spacing between successive modes (multiplets) is not the same for different ℓ (Kawaler 1986; see also section 6.2.3.5).

6.2.3.3 A probable origin of the "odd" multiplet structures

Consider the simple case of a star pulsating in two eigenmodes with frequencies ν and μ respectively. If the star is a low amplitude pulsator, only two (first order) peaks will appear in the period spectrum, at frequencies ν and μ. If the two modes have a high enough amplitude, nonlinear pulse shape distortion might become important enough that higher order peaks will become visible in the spectrum, in the form of harmonics and combination frequencies. To the second order of perturbation, peaks will be found at frequencies 2ν, 2μ, $\nu + \mu$ and $|\nu - \mu|$. To the third order, 10 new peaks can appear, at frequencies 3ν, 3μ, $2\nu + \mu$, $\nu + 2\mu$, $|2\nu - \mu|$, $|\nu - 2\mu|$, $2\nu - \nu$, $2\mu - \mu$, $\nu + \mu - \mu$ and $\nu + \mu - \nu$, that will naturally start to back-interact with the normal modes. Indeed, the original eigenmode at ν (resp. μ) has extra power added to it in the form of the third order components $2\nu - \nu$ and $\nu + \mu - \mu$ (resp. $2\mu - \mu$ and $\nu + \mu - \nu$).

From the third order of perturbation upwards, the notion of simple modes does not exist any more, as the non-linear frequencies generated by the finite amplitude eigenmodes back-interact with the latter, resulting in each peak in the spectrum becoming a complex set of components. The story becomes even more intricate in the case where ν and μ are both split by stellar rotation (Unno *et al.* 1989) into a triplet with components (ν_-, ν_0, ν_+) and (μ_-, μ_0, μ_+). For instance, the resulting central peak at frequency ν_0 will be a superposition of 12 components generated as follows:

$$\nu_0 \ ,$$
$$2\nu_0 - \nu_0 \ , \quad \nu_0 + \nu_- - \nu_- \ , \quad \nu_0 + \nu_+ - \nu_+ \ ,$$
$$\nu_0 + \mu_- - \mu_- \ , \quad \nu_0 + \mu_0 - \mu_0 \ , \quad \nu_0 + \mu_+ - \mu_+ \ ,$$
$$\nu_- + \nu_+ - \nu_0 \ , \quad \nu_- + \mu_+ - \mu_0 \ , \quad \nu_- + \mu_0 - \mu_+ \ ,$$
$$\nu_+ + \mu_- - \mu_0 \ , \quad \nu_+ + \mu_0 - \mu_+$$

In the presence of a magnetic field or differential rotation, as may be the case for GD358 (Winget *et al.* 1994), the frequency splitting is not constant any more, but becomes dependent on both k and m (Jones *et al.* 1989). In this case, the above 5 last components would not fall exactly at the original eigenfrequency ν_0. This clearly indicates how a simple triplet structure can potentially be altered by third order combination peaks when harmonic distortion is strong enough. This principle, proposed by Brassard (private communication), has been conceptually illustrated here with two triplets only. It is nevertheless not difficult to extrapolate what can be expected in the case of a real star with several more modes excited.

The multitude of third order combination frequencies identified in the temporal spectrum of GD358 (see section 6.2.3.4) provides ample evidence that such harmonic distortion is present. We can thus try and apply this principal to its 6 large amplitude normal modes, each of which displays a triplet structure. It is easy to show that each triplet generates, on its own, 18 back-interacting third order frequencies, while the combination with any other triplet creates 27 third order components in each triplet. This implies that each triplet in GD358 is, to third order of perturbation, made of 18 + (6-1)×27 = 153 components. Even tiny as individuals, these components are so numerous that they can have large enough combined amplitudes to transform a simple triplet into a rich complex multiplet. All that is needed is a significant third order effect, which is precisely the case for GD358 (see section 6.2.3.4).

The multiplets $k = 16$, $k = 15$, and $k = 13$ are expected to be more affected by these third order processes than the other eigenmultiplets; indeed, in addition to the 153 above components, they are also blended with other nonlinear frequencies, combinations of 3 different modes, that accidentally happen to fall within these multiplets, as shown in Table 6.2.

Table 6.2: Blending of the triplets $k = 16$, $k = 15$, and $k = 13$ by accidental third order matches. The first and second columns indicate the k-order of the eigentriplets and the frequency of their central peak. The third column indicates which nonlinear frequencies, described by the k-order of the modes that combine to form them, accidentally blend the eigentriplets listed in the first column. The last column shows where these nonlinear frequencies fall, and should be compared to column 2.

k	ν_k [μHz]	$k_1 + k_2 - k_3$	$\nu_1 + \nu_2 - \nu_3$ [μHz]
16	1362.468	2x17-18	1364.206
16	1362.468	18+15-17	1359.923
15	1426.402	18+13-15	1433.687
13	1617.502	2x15-18	1617.273

These accidental third order components are expected to be of much greater importance than the ones discussed earlier, as a combination of different modes is always stronger than a combination involving twice the same mode (Brickhill 1992). This can be clearly observed to the first order of perturbation where harmonics are systematically smaller than the corresponding cross-frequencies (Winget *et al.* 1994). It is therefore not surprising to see these three triplets being very strongly affected. The most obvious case is that of $k = 13$, whose amplitude is comparable to that expected for the nonlinear peak (2x15-18) that affects it. It is not surprising either that the $k = 16$ eigenmode cannot be identified. The lack of power at this latter frequency might be due to destructive beating between the probable $k = 16$ and the numerous third order peaks expected.

Although the definite presence of third order harmonic distortion strongly suggests that this effect is responsible for the alteration of the dominant triplets (Figure 6.4, left panel), no theoretical model exists to date for DB variables that could provide quantitative support to this qualitative assertion. Furthermore, we cannot find a satisfactory explanation why the triplets are not similarly altered in 1990. We have applied the same pre-whitening procedure to each of the 1990 triplets, which nearly, but not quite, removed all significant power. The peaks left were, however, not sufficiently above the noise level to be claimed real.

This difference in behaviour between 1990 and 1994 could possibly be explained by

the increase in amplitude of most modes. Because this harmonic process is perturbative, it might be that a small increase in the first order amplitudes may generate significant increase in the third order effects. Alternatively, the 1994 triplets might be perturbed by some photometrically invisible modes with high ℓ-index, that were not present in 1990. This remains, however, speculative, until numerical calculations will be able to settle the issue.

6.2.3.4 Complete $\ell = 1$ frequency table

The full amplitude spectrum is given in Figure 6.5, where each panel has a different vertical scale to accommodate the wide range of amplitudes observed. The complete list of identified $\ell = 1$ modes and combination frequencies, together with their physical parameters, is given in Tables 6.3 to 6.6. All the phases, φ, listed have been measured with the starting time of the run being the point of reference $t_0 = 0$, which corresponds to the Julian Date JD=2449474.503834. The columns labelled $\delta\nu$ represent the error on the frequency identification, as given by the nonlinear least-squares fits.

Table 6.3 describes the normal modes. As discussed in section 6.2.3.3, the multiplets labelled $k = 13$, 15, 17, and 18 are probable blends with peaks of third order origin. Only the frequencies that are thought to be part of the original triplet have been listed.

The last column of Table 6.3 indicates the frequency difference between the same modes identified in the 1990 and 1994 campaigns. Globally speaking, no significant frequency shifts are recorded, although slight variations occurred in all the multiplets, with the exception of the $k = 8$ and $k = 9$ modes. The stability and relatively low amplitudes of these two modes, reinforces our conclusion that the other dominant modes are perturbed by third order effects. In particular, no third order combination involving only $k = 9$ and $k = 8$, such as (2x9+8), or (2x8+9), could be identified.

Our eigenmode identification also supports some of the asteroseismological results of Winget *et al.* (1994). In particular, the slightly larger splittings of the prograde ($m = +1$) modes compared to these of the retrograde modes ($m = -1$) (Table 6.3, penultimate column) suggest the presence of a weak magnetic field.

Tables 6.4 and 6.5 list the second order frequencies, i.e. the first harmonics and combi-

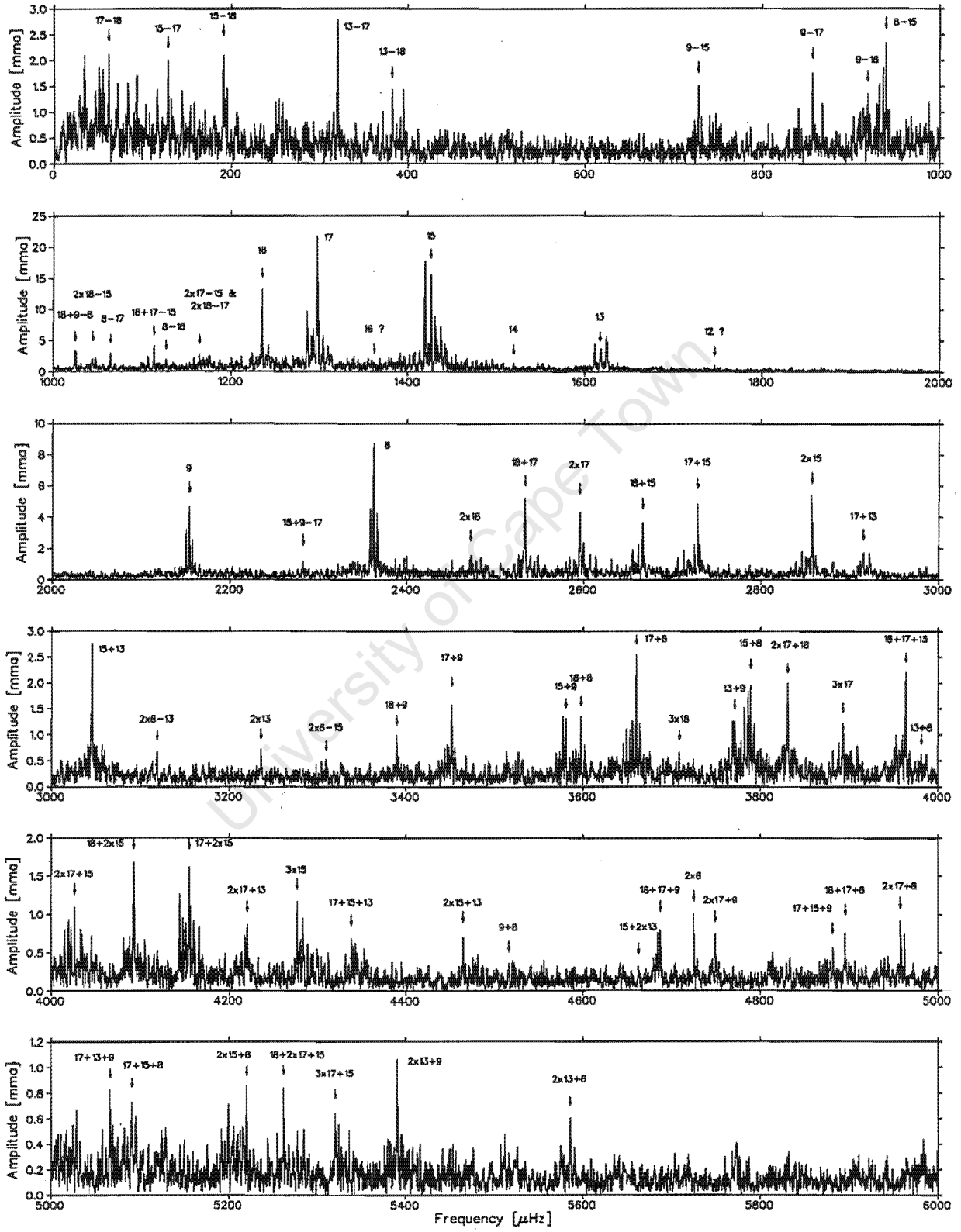

Figure 6.5: Complete 1994 temporal spectrum. The eigenmodes are indicated by their radial order k, while the cross-frequencies are labelled by the k-orders of the normal modes that combine to form them. The amplitude scale is given in mma units and is different for each panel.

nation frequencies, that are respectively differences and sums of two frequencies of $\ell = 1$ modes. Although the sums show definite multiplet structures, as expected when combining two triplets together, only the largest component has, deliberately, been identified in each case. Surprisingly enough, it is not always the expected peak corresponding to the combination of the largest components of the parent triplets. For instance, the frequency identified at 1430.837 μHz and labelled $\hat{15}$ (see Table 6.3), one of the "odd" peaks of the $k = 15$ multiplet (Figure 6.4, left panel), shows many sum frequencies, while the larger $m = 0$ component at 1426.402 μHz does not.

As 6 eigentriplets have been securely identified in GD358, $6^2 = 36$ combination multiplets could possibly be found to second order of perturbation, of which 15 correspond to difference frequencies, 6 to harmonics, and 15 to sum frequencies. Virtually all of them have been found, as 31 cross-frequencies, each corresponding to the largest peak in these combination multiplets, out of 36 possible have been securely identified. The ones missing may either be blended with other peaks, or not sufficiently above the noise level for a secure identification to be permitted. This very strongly suggests that these nonlinearities are mostly harmonic distortions, in good agreement with our claim that this process is responsible, at higher order of perturbation, for the "odd" muddled structure of the eigenmultiplets.

The limitation of our extinction removal technique produces low signal-to-noise ratio below $\sim$ 200 μHz. The identification of difference frequencies in this spectral region remains therefore uncertain, and should be considered with caution.

Table 6.6 lists the third and fourth order frequencies. Although numerous third order combinations were found in the 1990 spectrum, the very high signal-to-noise ratio of this 1994 run allowed, for the first time, the identification of fourth order combination modes (2 of them), i.e. frequencies that are the sum of four frequencies of normal modes.

The last column of Table 6.4, 6.5 and 6.6 shows how precise the matches are between the measured frequencies of the combination modes, and the calculated sums of the frequencies of the corresponding normal modes. It is quite remarkable to see that, besides a few exceptions probably due to blending, these matches are accurate to within a few tenths of micro-Herz or less, i.e. barely above the frequency errors given by the nonlinear least-squares fits.

Table 6.3: The identified $\ell = 1$ normal modes. The "?!" indicates modes whose identification is secure but that are strongly affected by the presence of peaks of probable third order origin. The "?" indicates a less secure identification. The "odd" peak, at 1430.837 μHz, in the $k = 15$ multiplet has been indicated because it shows many combination frequencies. It has been labelled $\hat{15}$ solely to allow reference in the discussion.

k	m	Frequency ν [μHz]	$\delta\nu$ [μHz]	Period [s]	Amplitude A [mma]	Phase φ [radian]	Splitting [μHz]	$\nu_{94} - \nu_{90}$ [μHz]
18	-1	1229.009	0.034	813.67	2.46	-1.03	6.52	-
18	0	1235.531	0.006	809.37	13.56	1.05	-	2.078
18	+1	1242.383	0.020	804.90	4.11	2.01	6.85	-
17	-1	1291.072	0.012	774.55	6.38	0.62	6.66	0.072
17	0	1297.727	0.004	770.58	22.15	2.23	-	0.147
17	+1	1304.443	0.013	766.61	6.09	-2.60	6.72	0.323
16	-1	1355.505	0.038	737.73	2.22	0.49	6.96	-0.075
16?!	0	1362.468	0.060	733.96	1.42	2.71	-	0.618
16	+1	1368.611	0.038	730.67	2.25	-0.34	6.14	0.111
15	-1	1419.626	0.004	704.41	18.63	1.93	6.78	1.644
15	0	1426.402	0.005	701.06	16.64	0.11	-	0.868
$\hat{15}$	?	1430.837	0.007	698.89	10.57	0.70	4.44	-
15	+1	1433.342	0.013	697.67	5.72	2.43	6.94	0.698
14	0	1519.960	0.064	657.91	1.32	-2.433	-	1.010
13	-1	1611.346	0.017	620.60	5.00	-2.76	6.16	-0.454
13?!	0	1617.502	0.025	618.24	3.33	-0.08	-	0.122
13	+1	1624.558	0.014	615.55	5.93	0.87	7.01	-1.062
12?	0?	1746.714	0.081	572.50	1.05	-2.70	-	2.834
9	-1	2150.490	0.027	465.01	3.14	2.61	3.64	-0.080
9	0	2154.127	0.018	464.23	4.76	0.78	-	0.027
9	+1	2157.838	0.031	463.43	2.73	-1.00	3.71	0.168
8	-1	2358.881	0.018	423.93	4.54	0.99	3.75	0.031
8	0	2362.634	0.009	423.26	9.23	2.81	-	0.074
8	+1	2366.506	0.020	422.56	4.22	-1.94	3.87	0.046

Table 6.4: The identified second order difference frequencies. All are combinations of standing waves, i.e. of the $m = 0$ component of the parent modes.

Combination $k_1 - k_2$	Frequency ν_c [μHz]	$\delta\nu_c$ [μHz]	Amplitude A [mma]	Phase φ [radian]	$\nu_c - (\nu_1 \pm \nu_2)$ [μHz]
17-18	62.082	0.040	2.15	2.50	0.114
15-17	128.795	0.042	2.01	-1.62	0.120
15-18	191.012	0.038	2.24	-0.27	0.141
13-17	320.278	0.029	2.86	-2.89	0.503
13-18	382.416	0.059	1.44	-1.27	0.445
9-15	727.677	0.055	1.54	1.01	0.048
9-17	856.473	0.047	1.80	-1.53	0.073
9-18	918.772	0.062	1.36	-1.28	0.176
8-15	939.295	0.035	2.39	-0.67	3.063
8-17	1064.866	0.029	2.97	0.87	0.041
8-18	1127.118	0.043	1.98	1.64	0.015

6.2.3.5 Search for $\ell = 2$ modes

Winget *et al.* (1994) suggested the presence of $\ell = 2$ modes, although none could specifically be identified. This possibility encouraged them to search for a period spacing corresponding to the $\ell = 2$ range, which they found. This led them to conclude that $\ell = 2$ modes were probably present, but with amplitudes too low above noise level for them to be identified. With the better signal-to-noise ratio of the 1994 data, we hoped that these modes could possibly be uncovered, so we repeated the search procedure. We searched for a period spacing $\Delta\Pi_\ell$ that could correspond to an $\ell = 2$ pattern in the 1994 amplitude spectrum. To do so, the period spacing for the $\ell = 1$ modes must first be determined, which then provides the typical $\ell = 2$ spacing according to the asteroseismological relation (Tassoul 1980)

$$\Delta\Pi_\ell = \frac{\Pi_0}{\sqrt{\ell(\ell+1)}} \quad \Rightarrow \quad \Delta\Pi_1 = \sqrt{3}\,\Delta\Pi_2$$

where Π_0 is the characteristic g-mode spacing, which is a function of the stellar structure. The asymptotic period spacing $\Delta\Pi_1$ could be obtained by averaging the measured period

Table 6.5: The identified second order sum frequencies. The "?!" indicates a combination with a secure k-order identification, but which is a composite blend of various m-degree components of the parent multiplets. The subscripts "+" and "–" refer to the azimuthal degree $m = \pm 1$, whereas no subscript means $m = 0$. The mode referred to as $1\hat{5}$ represents the "odd" frequency at 1430.837 μHz in the $k = 15$ multiplet.

Combination $k_1 + k_2$	Frequency ν_c [μHz]	$\delta\nu_c$ [μHz]	Amplitude A [mma]	Phase φ [radian]	$\nu_c - (\nu_1 \pm \nu_2)$ [μHz]
2x18	2472.259	0.050	1.69	0.66	1.197
18+17	2533.201	0.016	5.23	2.96	0.057
2x17	2595.413	0.018	4.68	-1.83	0.041
18+$1\hat{5}$	2666.308	0.023	3.72	1.96	0.060
17+$1\hat{5}$	2728.535	0.017	5.04	3.11	0.029
$15_0 + 1\hat{5}$	2857.246	0.016	5.39	0.67	0.007
$17+13_+$	2922.260	0.048	1.78	-2.92	0.025
$16+13_+$	2986.384	0.096	0.89	-0.40	0.642
$15_- + 13_+$?!	3045.225	0.031	2.76	2.81	1.041
$13_- + 13_+$	3235.984	0.120	0.73	-2.06	0.980
18+9	3389.657	0.085	0.99	1.90	0.001
17+9	3451.812	0.049	1.74	3.05	0.042
15+9	3580.477	0.064	1.32	1.10	0.052
18+8	3598.068	0.062	1.36	-2.17	0.097
17+8	3660.366	0.033	2.55	-1.25	0.005
3x18	3708.923	0.120	0.70	0.69	2.330
13+9	3771.076	0.065	1.30	2.91	0.553
15+8	3788.998	0.041	2.09	-3.11	0.038
13+8	3981.578	0.140	0.63	-1.09	1.442
9+8	4516.654	0.230	0.37	-2.00	0.107
2x8	4725.263	0.084	1.01	-0.26	0.005

Table 6.6: The identified second and third order cross-frequencies. The "?!" indicates combinations with secure k-order identification, but which are intricate blends of various m-degree components from the parent multiplets. The subscripts "+" and "−" indicate the azimuthal degree $m = \pm 1$, whereas no subscript means $m = 0$. The mode referred to as $\hat{15}$ represents the "odd" frequency at 1430.837 μHz in the $k = 15$ multiplet.

Combination $k_1 + k_2 \pm k_3$	Frequency ν_c [μHz]	$\delta\nu_c$ [μHz]	Amplitude A [mma]	Phase φ [radian]	$\nu_c - (\nu_1 \pm \nu_2)$ [μHz]
18+9-8	1024.836	0.025	3.42	-2.28	2.188
$18_0 + 18_+ - 15_+$	1047.691	0.038	2.24	-0.95	0.614
$18 + 17 - 15_-$	1113.524	0.020	4.18	+1.71	0.108
2x17-15_+	1164.531	0.030	2.86	1.63	0.086
15+9-17	2282.419	0.073	1.17	-1.10	0.383
$8_0 + 8_+ - 13_-$	3118.864	0.130	0.68	-0.50	1.07
$8_0 + 8_+ - 15_-$	3309.679	0.162	0.53	-0.64	0.165
2x17+18	3830.844	0.042	2.00	-0.14	0.141
3x17	3893.098	0.069	1.23	1.01	0.083
18+17+$\hat{15}$	3964.011	0.038	2.21	-1.96	0.084
2x17+$\hat{15}$	4026.340	0.077	1.11	-1.05	0.049
18+15_0 + $\hat{15}$	4092.716	0.050	1.70	2.37	0.054
17+15_- + 15_0	4144.509	0.065	1.30	0.17	0.754
17+15_0 + $\hat{15}$	4155.027	0.050	1.69	2.86	0.061
2x17+13_+	4220.868	0.097	0.88	0.43	0.856
15_- + 15_0 + $\hat{15}$	4276.815	0.073	1.17	-3.09	0.005
17+15+13 ?!	4338.428	0.120	0.70	1.93	3.203
2x15+13_-?!	4464.925	0.110	0.74	-1.55	0.775
15+13_- + 13_+	4662.922	0.260	0.32	1.18	0.616
18+17+9	4687.374	0.097	0.88	-2.31	0.011
2x17+9	4749.606	0.110	0.74	-0.57	0.025
17+$\hat{15}$+9 ?!	4881.714	0.140	0.59	-0.58	0.977
18+17+8	4895.777	0.100	0.84	0.30	0.115
2x17+8	4958.048	0.092	0.92	1.20	0.040
17+13+9 ?!	5066.454	0.100	0.84	0.89	2.902
17+$\hat{15}$+8	5090.980	0.110	0.77	0.63	0.218
15_- + $\hat{15}$+8	5220.021	0.099	0.86	-2.81	0.148
18+2x17+$\hat{15}$	5261.705	0.098	0.87	0.54	0.117
3x17+15	5320.162	0.130	0.68	-2.24	0.579
13_- + 13_+ + 9	5390.458	0.079	1.07	-2.18	0.423
2x13_-+8	5585.843	0.140	0.62	-1.78	0.517

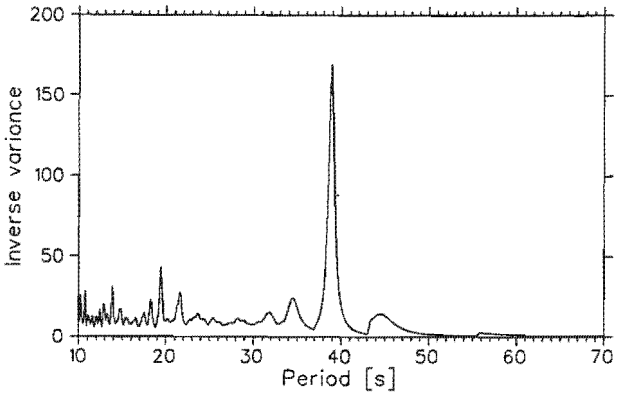

Figure 6.6: Inverse variance versus period spacing.

spacings (Table 6.3), but the inverse variance method (O'Donoghue 1994) is a more sound statistical method for this purpose. We fitted a set of equally spaced periods to the identified $\ell = 1$ modes, and calculated the inverse variance of the residuals for each fit. The inverse variance is maximised for a period spacing of 38.9 s (Figure 6.6), which we thus consider to be the $\ell = 1$ period spacing. According to the above equation, the corresponding $\ell = 2$ spacing should then be 22.5 s.

The inverse variance technique cannot be used to search for a possible $\ell = 2$ underlying structure, because it is a check procedure rather than a search procedure; we do not have a set of peaks that we suspect to be $\ell = 2$ modes, and we therefore have no input frequencies with which to feed the inverse variance method. A completely objective search method consists in computing the Fourier transform of the period transform (FTPT hereafter), where the latter is simply the amplitude spectrum of Figure 6.5 with the frequency scale transformed into a period scale. The FTPT, computed in the range $1000 - 4000\,\mu$Hz, is shown in the left panel of Figure 6.7.

The peak at 39.3 s correspond to the $\ell = 1$ period spacing, and is 0.4 s different from the value determined by the inverse variance method. A period spacing is found at 22.2 s, but definitely not significant enough to claim an $\ell = 2$ discovery, as it is closely flanked by two larger peaks at 21.2 s and 23.6 s. An inherent difficulty is that the numerous $\ell = 1$ modes and cross-frequencies generate many period spacings, thus perturbing the search for an $\ell = 2$ spacing. Furthermore, harmonics of genuine period spacings appear naturally in the FTPT as an obvious consequence of the computing technique.

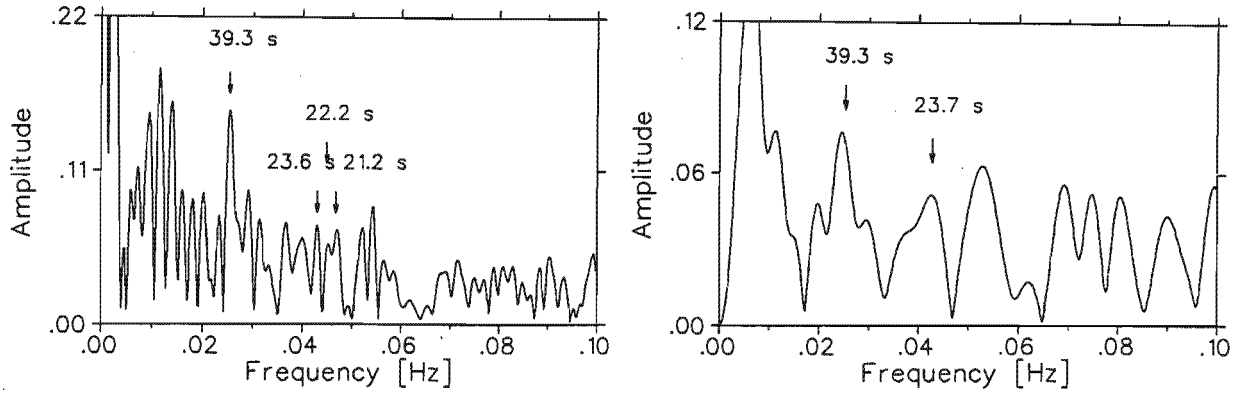

Figure 6.7: FTPT of the regions 1000-4000 μHz *(left panel)* and 2000-4000 μHz *(right panel).*

In order to possibly get rid of all those peaks directly generated by the $\ell = 1$ multiplets, the FTPT has been recomputed in the frequency range $2000-4000\,\mu$Hz, which is the range where $\ell = 2$ modes with radial order $k = 8$ to $k = 18$ should be found, according to the model of Bradley & Winget (1994). The result is shown in the right panel of Figure 6.7. Not only has the peak at 21.2 s completely disappeared, but the 22.2 s is now blended with the 23.7 s (previously 23.6 s) which has substantially decreased in amplitude. We would have expected the opposite behaviour, i.e. an increase in resolution and possibly amplitude, if one of these peaks were to correspond to an $\ell = 2$ period spacing.

Furthermore, it is a fairly straightforward exercise to produce a 22 s spacing using the identified cross-frequencies. For instance the sequence of modes identified as (17+15), (17+13), (2x8-13), (18+8), (18+17+15) and (17+15+13) have the respective spacings 23.4 s, 22.5 s, 21.4 s, 24.3 s, 21.7 s, and 22.7 s, averaging precisely at 22.7, which we believe contributes significantly to the peak observed in the FTPT.

We conclude that, despite the better quality of the 1994 WET data, we have found no evidence for the presence of $\ell = 2$ modes in GD358.

6.2.4 Conclusion

The excellent coverage and signal-to-noise ratio obtained during the 1994 WET run on GD358 allowed us not only to confirm the mode identification carried out on the 1990 data set (Winget *et al.* 1994), which was the main purpose of this second campaign (Nather

1995), but also to uncover many more excited cross-frequencies. No significant peak remains in the period spectrum that has not been identified as an $\ell = 1$ eigenmode of the star or an associated cross-frequency. Although GD358 presents a complicated spectrum, with over 70 significant peaks (Figure 6.5), its underlying pulsation structure can be entirely explained in terms of just 6 excited eigentriplets, and the forest of distinctive combination frequencies identified.

The nearly complete set of second and third order frequencies (those missing may well be blended with other identified peaks) strongly suggests that the majority of these nonlinear modes are due to harmonic distortion, and not to other nonlinear processes such as resonant mode coupling. We have conceptually shown how the third order cross-frequencies are thought to affect the regular structure of the eigenmode triplets. However, due to the lack of a detailed theoretical model that could predict the importance of this effect for DB variables, this idea remains qualitative, although third order frequencies are definitely present with significant amplitudes. A more detailed analysis of this nonlinear phenomenon, together with an analysis of the evolution of GD358's temporal spectrum will be presented in the next section.

The search for possible $\ell = 2$ modes remained unsuccessful, both because virtually no peaks are left unidentified in the period spectrum, and because no significant period spacing at around 22.7 s could be detected in the FTPT.

The present work, together with the corresponding paper on the 1990 WET campaign (Winget *et al.* 1994) provides the framework for further asteroseismological study of GD358, and other DB variables.

Acknowledgments

We are indebted to Pierre Brassard for valuable physical discussions.

References

Bradley P. A., Winget D. E., 1994, ApJ, 430, 850

Brassard P., *et al.*, 1992, ApJS, 81, 747

Brassard P., Fontaine G., Wesemael F., 1995, ApJS, 96, 545

Brickhill A. J., 1992, MNRAS, 259, 529

Dolez N., Vauclair G., 1981, A&A, 102, 375

Dziembowski W., 1977, Acta Aston., 27, 203

Jones P. W., 1989, ApJ, 336, 403

Kawaler S. D., Hansen C. J., Winget D. E., 1985, ApJ, 295, 547

Kawaler S. D., Hansen C. J., 1989, *White Dwarfs*, eds. G. Wegner (Springer-Verlag: Berlin), 97

Nather R. E., *et al.*, 1990, ApJ, 361, 309

Nather R. E., 1995, Baltic Astro., 4, 321

O'Donoghue D., 1994, MNRAS, 270, 222

Scargle J. D., 1981, ApJS, 45, 1

Scargle J. D., 1982, ApJ, 263, 835

Winget D. E., *et al.*, 1982, ApJ, 262, L11

Winget D. E., Fontaine G., 1982, *Pulsations in Classical and Cataclysmic Variable Stars*, eds. J. P. Cox and C. J. Hansen (Boulder Joint Institute for Laboratory Astrophysics), 46.

Winget D. E., 1988, *Advance in Helio- and Asteroseismology*, eds. J. Christensen-Dalsgaard & S. Frandsen (Reiden: Dodrecht), 305

Winget D. E., *et al.*, 1994, ApJ, 430, 839

Unno W., *et al.*, 1989, *Nonradial Oscillations of Stars*, 2nd edition, University of Tokyo Press, Tokyo

6.3 Nonlinear behaviour of GD358

Abstract

An analysis of the evolution of the pulsating behaviour of DB variable GD358 is presented, based on the data from the 1990 and 1994 WET runs and on a 1996 three-site campaign. We clearly show that harmonic distortion can be held responsible for most of the nonlinear behaviour of GD358. It accounts not only for the presence of most, if not all, cross-frequencies, but also for the small amplitude variations recorded during the WET campaigns, which are strongly suspected to be generated by beating between the normal modes and the numerous third order combination frequencies. Due to their inherent physical nature, we claim these harmonic distortion effects are certainly significant in all large amplitude pulsating white dwarfs, and could certainly explain entirely the nonlinear behaviour of most of them.

We, however, had recourse to resonant mode coupling to account for the exceptional behaviour of GD358 observed in 1996, which could be qualitatively compared to a theoretical limit cycle. Measurements of damping rates of 1.0×10^{-5} s^{-1} and 1.5×10^{-5} s^{-1} were obtained, which we believe correspond to the first measurements of linear nonadiabatic damping rates in pulsating white dwarfs.

6.3.1 Introduction

The discovery of GD358 in 1982 (Winget *et al.* 1982a) was a triumph in that a new class of pulsating stars was discovered after its existence had been predicted theoretically (Winget 1981, Winget *et al.* 1982b). This star has since been regularly observed, as its large brightness variations (up to 20%) makes it an ideal target to study nonradial stellar pulsations. In particular, two Whole Earth Telescope campaigns (WET, Nather 1990) were conducted on this star in 1990 (Winget *et al.* 1994) and 1994 (Nather 1995; also section 6.2), which made it possible to resolve completely its period structure. Even though the 1990 and 1994 temporal spectra are qualitatively very similar (section 6.2), significant

amplitude changes were recorded in each normal mode, indicating either changes in the stellar atmospheric structure, or the presence of some nonlinear process that would affect the amplitudes on a yearly time-scale.

To date, nonlinear properties of stellar pulsations are poorly understood. Yet, it is important to study these processes, not only to understand better the astrophysics of the pulsations themselves, but also to take better advantage of the insight offered by asteroseismology. Asteroseismology is a technique that uses the pulsations to probe the stellar interior, in order to extract physical information about the star (Winget 1988, Kawaler & Hansen 1989).

In order to obtain clues about the nonlinear processes possibly taking place in GD358, the evolution of both its period spectrum and its phase spectrum, which are respectively the modulus and argument parts of the Fourier transform of the light curve, have been analysed. Section 6.3.2 reports on the evolution of the period spectrum, and suggests the probable cause of the variations observed. Section 6.3.3 analyses the phase spectrum, and determines what the dominant nonlinear processes in action are. Section 6.3.4 presents and analyses the 1996 data, obtained from a 3-site campaign, during which the star was caught in a drastically different pulsating state. Section 6.3.5 reports on the evolution of the mechanical energy contained in the visible modes. Section 6.3.6 concludes the analysis.

6.3.2 The period spectrum

6.3.2.1 Spectral evolution

Because the 1990 and 1994 WET runs contain respectively 140 and 270 hours of almost continuous data, and because the beat periods generated by the identified eigentriplets range from 40 to 80 hours (Winget *et al.* 1994; section 6.2), the two corresponding amplitude spectra have their period structure resolved. These data sets are actually long enough even to be split into consecutive segments that are themselves fully resolved. The 1990 light curve can be segmented into 2 slightly overlapping subsets of 80 hours each, while the 1994 light curve can be divided into 3 contiguous 90 hour segments. The Fourier transform has been computed for each of these 5 subsets, and the results are shown in

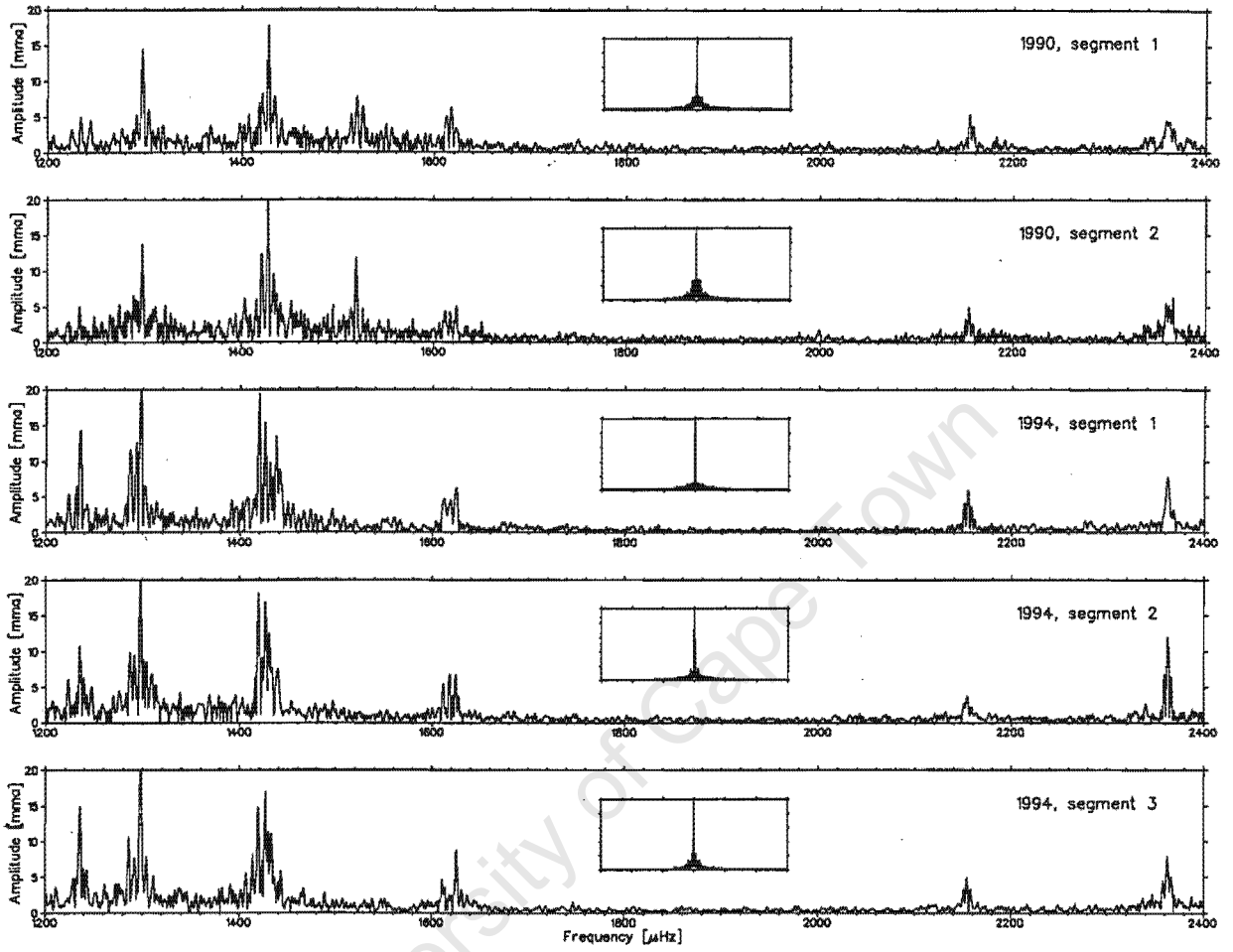

Figure 6.8: Amplitude spectra of sub-sets of the 1990 and 1994 WET runs, in the frequency range of highest modulation.

Figure 6.8.

Not only can differences be seen between the 1990 and the 1994 data sets, as already pointed out both by Nather (1995) and in section 6.2, but significant amplitude variations are also seen during the course of these two campaigns, despite the fact that all the normal mode beating is resolved. Therefore, some process, other than multiplet beating, has to be invoked to account for these amplitude variations.

Although intrinsic amplitude modulation comes to mind, there is also the possibility that some unresolved hyperfine frequency structure is hidden within the frequency resolution of each mode, which generates beating of extremely long periods. Such an hypothesis

has never been considered, as the theory of pulsation does not predict any further splitting than that due to stellar rotation (e.g. Unno *et al.* 1989). However, for large amplitude pulsators, like GD358, it is possible that some cross-frequencies appear within the excited multiplets, that could generate such beating processes and potentially perturb their regular and stable structure. This idea, already briefly discussed in section 6.2, is developed in detail in the next section.

6.3.2.2 Third order beating processes

A low amplitude pulsator, like the DAV G226-29 (Kepler *et al.* 1983), behaves linearly, in the sense that its light curve is sinusoidal, and only the frequencies corresponding to the excited eigenmodes will thus appear in its period spectrum. A large amplitude pulsator does not, however, behave linearly, because the stellar medium responds nonlinearly to the finite amplitude oscillations that perturbs its equilibrium. As a direct consequence, part of the energy initially contained in the normal modes will get naturally spread into harmonics and combination frequencies of these modes, in exactly the same way that an acoustic wave gets distorted along its path in a dense fluid like, for instance, water (Thuras *et al.* 1935). This phenomenon had already been addressed analytically by Poisson in 1808. As a result, the light curve is not sinusoidal anymore, but its pulse shapes appear distorted; this nonlinear process has thus been called harmonic distortion, or "the pulse shape effect".

Consider the simple case of a star oscillating in just two eigenfrequencies ν and μ. If their amplitudes are infinitesimal, the idealistic case of a linear pulsator, only two peaks will thus be present in the period spectrum, at frequencies ν and μ. Observationally, a variable star will still be considered a linear pulsator as long as the nonlinear features are tiny enough to be lost in the noise. If the normal modes have finite amplitudes, harmonic distortion effects will become visible. We assume hereafter that the latter effects are still small enough to allow for a perturbation theory, which is certainly a good approximation in most pulsating white dwarfs. To the first order of perturbation, only the eigenmodes are found in the power spectrum. To the second order, 2 harmonics and 2 combination frequencies will appear at frequencies 2ν, 2μ, $|\nu-\mu|$ and $\nu+\mu$. Depending on the power of the eigenmodes, on the effectiveness of the harmonic distortion effect, and on the signal-to-noise ratio of the data set, higher order frequencies may as well become visible in the

spectrum. To the third order of perturbation, 10 new peaks may appear at frequencies

$$
\begin{aligned}
&3\nu \ , \ 3\mu \\
&2\nu + \mu \ , \ \nu + 2\mu \\
&|2\nu - \mu| \ , \ |\nu - 2\mu| \\
&2\nu - \nu \ , \ 2\mu - \mu \ , \ \nu + \mu - \nu \ , \ \nu + \mu - \mu
\end{aligned}
$$

Note that the combinations in the fourth line have the same frequencies as those of the original eigenmodes, i.e. ν and μ. This means that the normal modes have lost their individual identity, and each of them is now made of three superimposed peaks. At even higher order, more and more components, of smaller and smaller amplitude, will appear at the original eigenfrequencies, resulting in peaks being intricate complex of components of order 1, 3, 5, etc. From third order, the notion of individual modes does not thus exist any more.

The situation becomes even more complicated if the normal modes are split by stellar rotation into multiplets. Assuming, for the purpose of discussion, an $\ell = 1$ spherical index, the original frequencies ν and μ then split into triplets with components (ν_-, ν_0, ν_+) and (μ_-, μ_0, μ_+). To first and second orders, these now 6 eigenmodes still retain their individual identity, whereas to third order, each of them becomes a complex superposition of numerous components. For instance, the peak at ν_0 is now made of 12 different components, 11 of which are harmonic distortion frequencies. These 12 components are

$$
\begin{aligned}
&\nu_0 \ , \\
&2\nu_0 - \nu_0 \ , \ \nu_0 + \nu_- - \nu_- \ , \ \nu_0 + \nu_+ - \nu_+ \ , \\
&\nu_0 + \mu_- - \mu_- \ , \ \nu_0 + \mu_0 - \mu_0 \ , \ \nu_0 + \mu_+ - \mu_+ \ , \\
&\nu_- + \nu_+ - \nu_0 \ , \ \nu_- + \mu_+ - \mu_0 \ , \ \nu_- + \mu_0 - \mu_- \ , \\
&\nu_+ + \mu_- - \mu_0 \ , \ \nu_+ + \mu_0 - \mu_+
\end{aligned}
$$

If the star is rotating differentially, or if a magnetic field is present, the frequency splitting is not constant any more, but becomes dependent on both the radial order k and the azimuthal number m of the mode considered (Jones *et al.* 1989). In this case, the last 5 of the above components do not fall at exactly the original frequency ν_0, but form side-lobes of this central peak. Depending on the frequency resolution of the data set, these side frequencies appear either as individual peaks, thus altering the original triplet structure and complicating the mode identification (section 6.2), or are blends with the eigenmode at ν_0. In any case, the presence of these third order peaks closely flanking the normal modes induce very long and complex beating processes which affect the apparent stability of the normal modes.

These third order combination frequencies nevertheless have amplitudes which are far too small individually, especially in the perturbation approximation, to affect significantly the normal modes. Their combined effect can, however, become large. It is easy to show that any given multiplet self-generates $n^2(n-1)$ third order combinations that fall in the frequency span of the multiplet, where $n = 2\ell + 1$ is the number of components in each multiplet. In addition to these, the interaction between any given multiplet and any other multiplet will generate an extra n^3 third order components falling in this same frequency range. In total, each multiplet will thus get affected by a set of $Nn^3 - n^2$ third order frequencies, where N is the number of identified multiplets, all assumed to be of same degree ℓ. If the latter assumption does not hold, the above relation is slightly more complicated. Nevertheless, third order frequencies are numerous. In the case of GD358, 153 third order components are thus expected to blend each of the 6 multiplets identified in the 1994 data set (Table 6.3).

The multiplets of cross-frequencies are lower in amplitude and span a larger frequency range than their corresponding parent triplets, reminiscent of the spreading of the wave packet. Furthermore, the distribution of the third order frequencies in each multiplet is of a quasi-gaussian type; it can easily be shown that two thirds of these peaks appear within $\Delta\sigma$ around the central $m = 0$ eigenmode, the remaining third falling within $3\Delta\sigma$, where $\Delta\sigma$ is the largest frequency splitting observed in the amplitude spectrum. The frequency splitting observed in GD358 ranges from 4 to 7 μHz, so the 153 frequencies expected in each triplet thus fall within 21 μHz of its central peak, while about 100 of them appear within 7 μHz. As the extremely good resolution of the 1994 campaign is "only" about 1/270 hrs $\simeq$ 1 μHz, it is evident that these 153 frequencies are not resolved

in this amplitude spectrum, and will probably never be; assuming, for the purpose of discussion, that these 153 peaks are equally spaced in frequency, the resolution necessary to separate them in the amplitude spectrum is thus 7/153=0.046 μHz, which can only be obtained with a data set spanning 9 months.

Third order harmonic distortion is definitely a significant effect in GD358, as revealed by the presence in the period spectrum of numerous third order combination frequencies (Winget *et al.* 1994; also Table 6.6). We believe that the corresponding beating processes can account for most of the amplitude variations recorded in Figure 6.8. This is strongly supported by the presence of numerous odd frequencies in the dominant multiplets (Table 6.4). Unfortunately, due to the high complexity of the phenomenon (too many frequencies involved), no specific dynamical signature of the process can possibly be found.

In order to give some quantitative support to this qualitative assertion, we have conducted some numerical tests using an as yet unpublished DA pulsation model (Brassard *et al.* in preparation). Unfortunately, no equivalent model exists to date for DB variables. This model considers that the pulse shape distortions that appear in the light curves of variable white dwarfs are entirely due to the highly nonlinear response of the emergent luminosity flux to the surface temperature variation ($L \sim \sigma T_{\rm eff}^4$). By integrating the exact radiative transfer equations, nonlinearities will naturally appear in the spectrum in the form of harmonics and combination frequencies, whose amplitudes are predicted by the model. The model is presented analytically to second order of perturbation in Brassard *et al.* (1995).

The input parameters used are $T_{\rm eff} = 12000^\circ$ K, $\log g = 8$, and convection has been treated in the ML6 approximation. We chose the relative surface temperature variation to be $\varepsilon_T = \delta T/T = 0.1$, yielding typical amplitudes of 6.26% for the $\ell = 1$, $m = 0$ eigenmodes. The effect of the third order frequencies on the amplitude of each mode has been computed as a function of the number $N_{\rm m}$ of modes present in the spectrum. The results of this analysis are shown in the first two columns of Table 6.7. The same analysis has been repeated in the presence of stellar rotation (but without magnetic field), where $N_{\rm t}$ is correspondingly the number of excited triplets. The results are presented in the last two columns of Table 6.7.

This numerical analysis clearly shows that the third (and possibly higher) orders peaks

Table 6.7: Measured amplitude A of a mode when N_m modes are excited (*first two columns*). Measured amplitude A of the central peak of a triplet when N_t triplets are excited (*last two columns*).

N_m	A	N_t	A
1	6.26	1	6.32
2	6.38	2	6.50
3	6.48	3	6.64
4	6.56	4	6.75

can significantly affect the amplitude of normal modes; when only 4 modes (respectively 4 triplets) are present in the spectrum, each mode has its original amplitude increased by respectively 5% for a non-rotating star, and by 8% if rotational splitting occurs. Caution is however necessary when extrapolating these results obtained from a DA model onto a DB variable. However, if third order cross-frequencies are present with significant amplitude in the period spectrum, they ought to affect the first order modes, regardless of the type of star considered; the beating and superposition effects depend solely on the amplitude of these third order frequencies and on the length of the data set, which is limited by the data acquisition technique. Similar tests, carried out with modes of different spherical index ℓ, showed that the corresponding interaction between third order frequencies and normal modes can affect the amplitudes of the eigenmodes in a much more significant way. Further numerical analyses are required to complement this preliminary study.

These third order effects are expected to be even more important if computed with Brickhill's model (Brickhill 1992), as the coupling constants are much larger than in the Brassard *et al.* model, thus generating combination frequencies with much larger amplitudes (section 5.4). The design of Brickhill's model does not however permit the same numerical tests to be conducted.

Table 6.7 also shows that the presence of the third order frequencies affects the normal modes in a purely constructive way, i.e. their amplitude A increases with the number of modes N_m and triplets N_t. This is a direct consequence of both the harmonic distortion frequencies being always in phase with their parent modes (section 5.3). A destructive interaction could nevertheless be obtained, with the same phasing property, if the coupling constants of the model are negative.

6.3.2.3 Amplitudes of the cross-frequencies

The mode selection mechanism, which preferentially excites certain frequencies over others in the vast g-mode spectrum, is not understood at present. Although the process of mode trapping is known to play an important role (e.g. Brassard *et al.* 1992), its exact influence on the driving is not yet fully comprehended. In particular, it is neither understood why the g-modes with positive growth rates are not all excited, nor why the trapped modes do not necessarily have larger amplitudes than the non-trapped ones, as seen for instance in the DOV PG1159-035 (Kawaler 1988), although the former are easier to excite.

As a consequence, no predictions can yet be made as to what modes should be excited, and to what amplitude. However, given the eigenstructure of the star, three theoretical models exist (Brickhill 1992, Brassard *et al.* 1995, Wu 1997), that predict the amplitudes of the harmonics and cross-frequencies resulting from harmonic distortion. The model of Wu has been tested, in the specific case of GD358, and yields satisfactory results considering the low signal-to-noise ratio of the data set used for the analysis (Wu 1997). The models of Brickhill and of Brassard *et al.* only treat the case of the DA variables, and are thus not applicable as such for DB white dwarfs.

To make a qualitative comparison with these models, the relative amplitudes of all the cross-frequencies identified in the 1990 (Winget *et al.* 1994) and 1994 (section 6.2) temporal spectra of GD358, have nevertheless been measured. We define them by the ratio, A_c/A_1A_2, of the amplitude, A_c, of the combination modes to the product, A_1A_2, of those of their parent modes (see section 5.4). The results is shown in Figure 6.9, where each relative amplitude has been plotted as a function of the frequency of the corresponding nonlinear peak.

Much information can be extracted from Figure 6.9. First, there is no difference in the relative amplitudes in 1990 and 1994, although the absolute amplitudes of the eigenmodes experienced significant changes (Figure 6.8). This indicates that the evolution of the amplitudes of the combination frequencies followed, proportionally, that of their parent modes, as expected from harmonic distortion. Only the $k = 8$ mode, at 4725 μHz, has not complied with this behaviour. Its relative amplitude has a value of 12.3 in 1994, consistent with the other harmonics, whereas its 1990 value is 43.8 (Figure 6.9). It would be surprising if this mode was a resonance, as its relative phase suggests, both in 1990

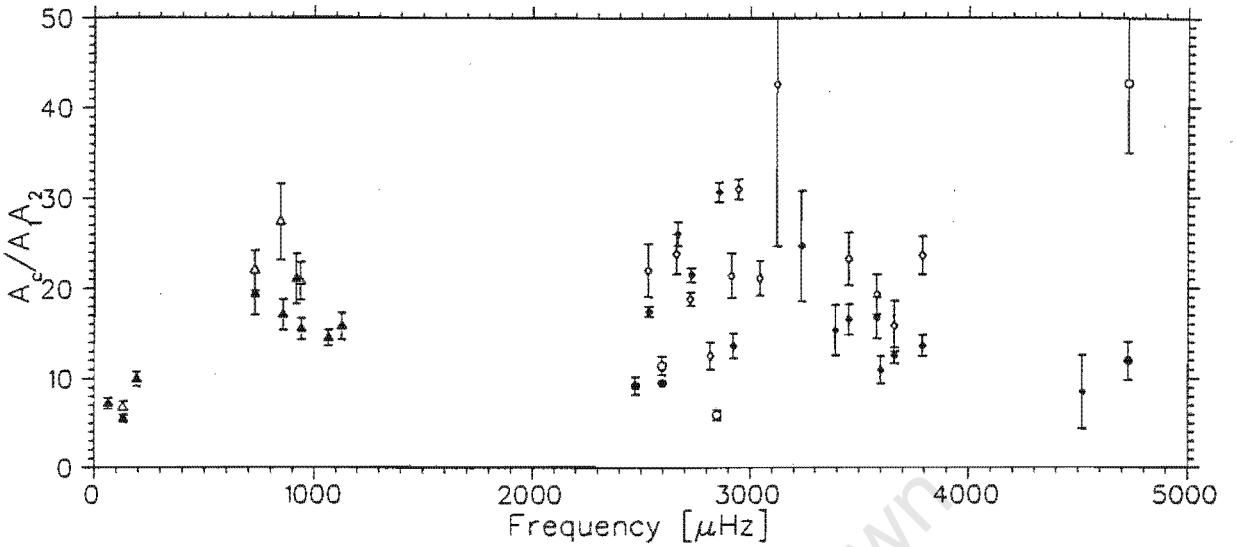

Figure 6.9: Relative amplitudes A_c/A_1A_2 of the first harmonics and cross-frequencies. The 1990 and 1994 data are represented by respectively open and filled plotting symbols. The difference modes are indicated by triangles, the harmonics by circles, and the sum modes by lozenges.

and 1994 (c.f. Figure 6.10 in section 6.3.4), it is a harmonic distortion peak. The only possible explanation why this harmonic is so large in 1990 is that it is significantly blended by noise and/or accidental third order frequencies. Its 1990 phase measurement is then probably fortuitously correlated to that of its fundamental.

The amplitude ratio A_c/A_1A_2 is dependent on the type of nonlinear frequency considered (i.e. harmonic or combination mode), on the geometric properties of the eigenmodes (i.e. on their spherical and azimuthal degree ℓ and m), and on the viewing angle of the star (i.e. the angle between the line of sight and the pulsation axis). The harmonics and cross-frequencies corresponding to modes with same ℓ and m indices are thus expected all to have identical relative amplitudes, as the viewing angle is, of course, a constant. Therefore, the very similar relative amplitudes measured (Figure 6.9) strongly suggests that the normal modes are all of the same degree ℓ, most probably $\ell = 1$ according to the analysis by Winget *et al.* (1994). The small but definite spread in amplitude observed in Figure 6.9 might then be accounted for by third and fourth order effects, that respectively affect the amplitudes, A_1 and A_2, of the normal mode, and those, A_c, of the second order peaks. Noise, of course, also plays a significant role, especially for those cross-frequencies with low amplitudes.

It can be shown, from simple geometric considerations (Brickhill 1992), that harmonics should have twice as small amplitudes as the combination frequencies. This is in effect observed in Figure 6.9, which clearly shows that the sum and difference frequencies have about the same relative amplitudes, and are definitely larger than the harmonics, although not quite twice.

No particular attention should be given to the four very low frequency (< 200 μHz) difference modes; the signal-noise-ratio is low in this spectral region due to poor extinction removal technique, and the amplitudes of these four peaks are certainly strongly affected, resulting in anomalous amplitude ratios. It is however surprising (accidental?) that all four of them have similar relative amplitudes.

Finally, the value of the relative amplitudes ratios A_c/A_1A_2 measured for GD358 (Figure 6.9) happen to be extremely similar to those for the DAV G29-38 which roughly fall in the value range 3-10 for harmonics, and 15-24 for cross-frequencies (see Figure 5.13 in section 5.4.3). As the compositional structure of DA and DB white dwarfs are not the same (the DAs have a thin H-layer, which the DBs do not have, floating on top of the He-atmosphere), this might just be a coincidence. However, various considerations makes us think this match might not be accidental, and that it could actually reflect the similar nature of the harmonic distortion mechanisms that possibly prevail in DA and DB variables.

We have shown in section 5.4 that, in G29-38, the harmonic distortions generated by the nonlinear response of the stellar medium to the oscillatory perturbation were much more important than the distortions due to the radiative transfer ($L \sim \sigma T_{\rm eff}^4$). Although the models of Brickhill and of Brassard *et al.* have not yet been adapted to the DB variables, therefore preventing a detailed comparison of the harmonic distortion effects, the nonlinearities due to the response of the flux to the temperature variations are expected to be even less in these stars, because their optical spectra lie on the Rayleigh-Jeans tail of the flux distribution curve, where an almost linear relationship between luminosity and temperature ($L \sim T$) prevails. These considerations, put together, suggest that harmonic distortion is mostly due to the response of the stellar medium rather than of the radiative transfer. The issue will only be settled once models are developed for DBs, and systematic comparison performed. A comparison between the relative amplitudes observed in various DAVs and various DBVs should also be carried out.

6.3.3 The phase spectrum

Although the frequencies of the normal modes measured in 1990 and 1994 are the same to within 1-3 μHz (Table 6.3), no such stability is recorded for their corresponding phases. This is however not surprising, because the different oscillation modes went through more than 10^6 cycles in the 4 year lapse, and the slightest frequency shift may easily result in a different cycle count, and thus in a completely different phase measurement. The relative phases, $\varphi_r = \varphi_c - (\varphi_1 \pm \varphi_2)$, of the nonlinear frequencies compared to those of their parent modes are potentially much more meaningful quantities to measure, because they are invariant under a translation of the time origin (see section 5.3). In the above definition of the relative phase φ_r, φ_c represents the phase of the combination frequencies, φ_1 and φ_2 are the phases of the parent modes, and the $\pm$ signs refers to combination frequencies being respectively sum modes ($\nu_c = \nu_1 + \nu_2$) and difference modes ($\nu_c = \nu_1 + \nu_2$).

The relative phases of all the second and third order cross-frequencies are shown in Figure 6.10, where they are plotted as a function of their corresponding frequencies. The top and bottom panels represent the 1990 and 1994 data respectively. A very clear tendency for these relative phases φ_r to be grouped around zero can be seen, which is the typical signature of harmonic distortion (see section 5.3).

This confirms, on independent grounds, the assertion made in section 6.3.2.2 that resonant mode coupling is not the dominant process responsible for the presence of cross-frequencies in the 1990 and 1994 amplitude spectra. Nothing can however be argued for any specific combination mode; a relative phase showing a definite non-zero value does not necessarily mean a resonant mode has been found, because the measurement of phases is very sensitive to blending by noise and/or nearby frequencies, especially for small amplitude peaks. Conversely, a cross-frequency being perfectly in phase with its parent modes does not prove it is a harmonic distortion, because a resonant mode could accidentally show such a phasing.

Only the global trend of relative phases should therefore be considered. However, a few individual cases still deserve specific discussion. Amongst them, the difference frequency (8-15), at 939 μHz, is of particular interest: its measured frequency ν_c is, both in 1990 and 1994, 3 μHz away from its expected ($\nu_8 - \nu_{15}$) value obtained when combining the frequencies of the mode $k = 8$ and $k = 15$ (Table 6.3 and 6.4 in section 6.2). Due to the stability and size of this mismatch, noise perturbation is therefore discarded as a possible

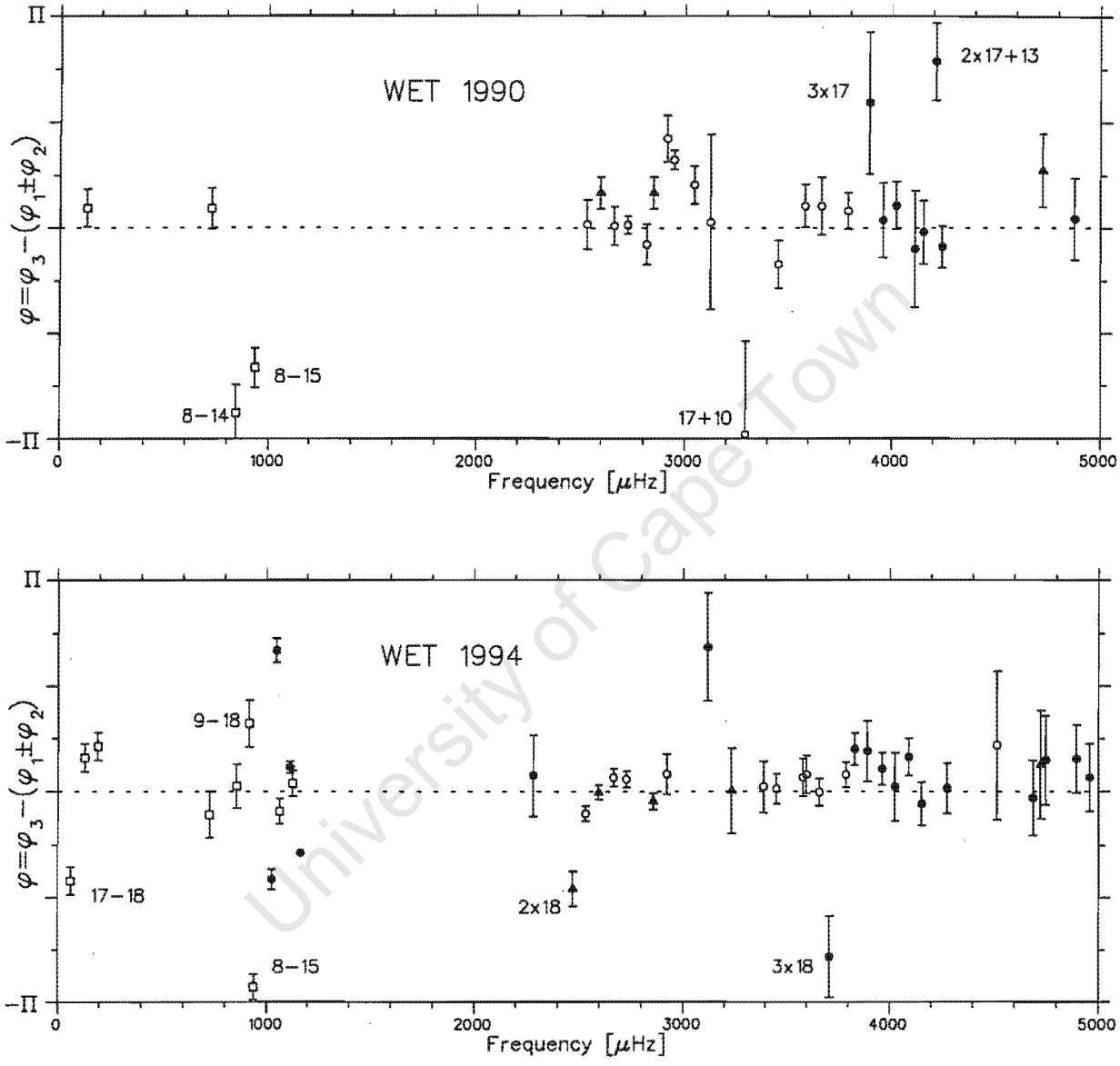

Figure 6.10: Relative phases of the combination modes as a function of their frequencies. The difference modes are indicated by open squares, the first harmonics by triangles, the first order combinations by open circles, and the second order combinations by filled circles. Some of the cross-frequencies whose relative phases shows a definite non-zero value are labelled, for the sake of discussion, by the k-order of the normal modes that combine to form them.

cause, and so is spectral leakage from a nearby mode as the closest identified frequency, (9-18), is not only smaller than (8-15), but also situated 20 μHz away. Furthermore, no third order harmonic distortions are expected at around this frequency. The frequency mismatch is then probably of astrophysical origin. As resonant processes may occur within a certain frequency band (Dziembowski 1993), this phenomenon is strongly suspected. There is unfortunately no easily recognizable signature of such a mode coupling process, and this (8-15) difference frequency thus remains not more than a good candidate to be a resonant mode.

The non-zero value of the (17+10) relative phase possibly indicate a mis-identification of the $k = 10$ eigenmode in 1990, as already suggested in section 6.2. On the other hand, the harmonic (2x18) is probably affected by the third order cross-frequencies (15+8-17) and (13+9-17) that both fall within 20 μHz.

6.3.4 The 1996 event

Although the 1990 and 1994 period spectra look very similar, a three-site campaign between China, Poland and the U.S.A conducted in August 1996 caught the star in a drastically different pulsating mood (Nitta *et al.* 1999), as seen in Figure 6.11. While the amplitude spectra of the two WET runs each display a pattern of dominant modes in the range 1200-1700 μHz, with typical amplitudes at around 10-20 mma (Figure 6.8), the August 1996 state is radically different. First, only two modes, the $k = 8$ at 2362 μHz and $k = 9$ at 2154 μHz, are present in the latter spectrum. Second, the power of the $k = 8$ mode was one order of magnitude larger, in the first few runs of the campaign, than any previously observed peak ever identified in GD358. Third, the power spectrum is clearly changing on a daily time-scale.

Not only is this behaviour evidently not accountable for by beating, but it very similar to what was observed some 19 years ago in the DAV GD385[1] (Fontaine *et al.* 1980). GD385 had been first, and for about 6 days, caught in a phase where only one frequency was present. Suddenly, from one day to the next, it showed numerous normal modes, with frequencies all much lower than the one observed the previous day and which had now disappeared. Such behaviour, as well as the one observed in Figure 6.11, can only be

[1]Not to be mistaken for DBV GD358.

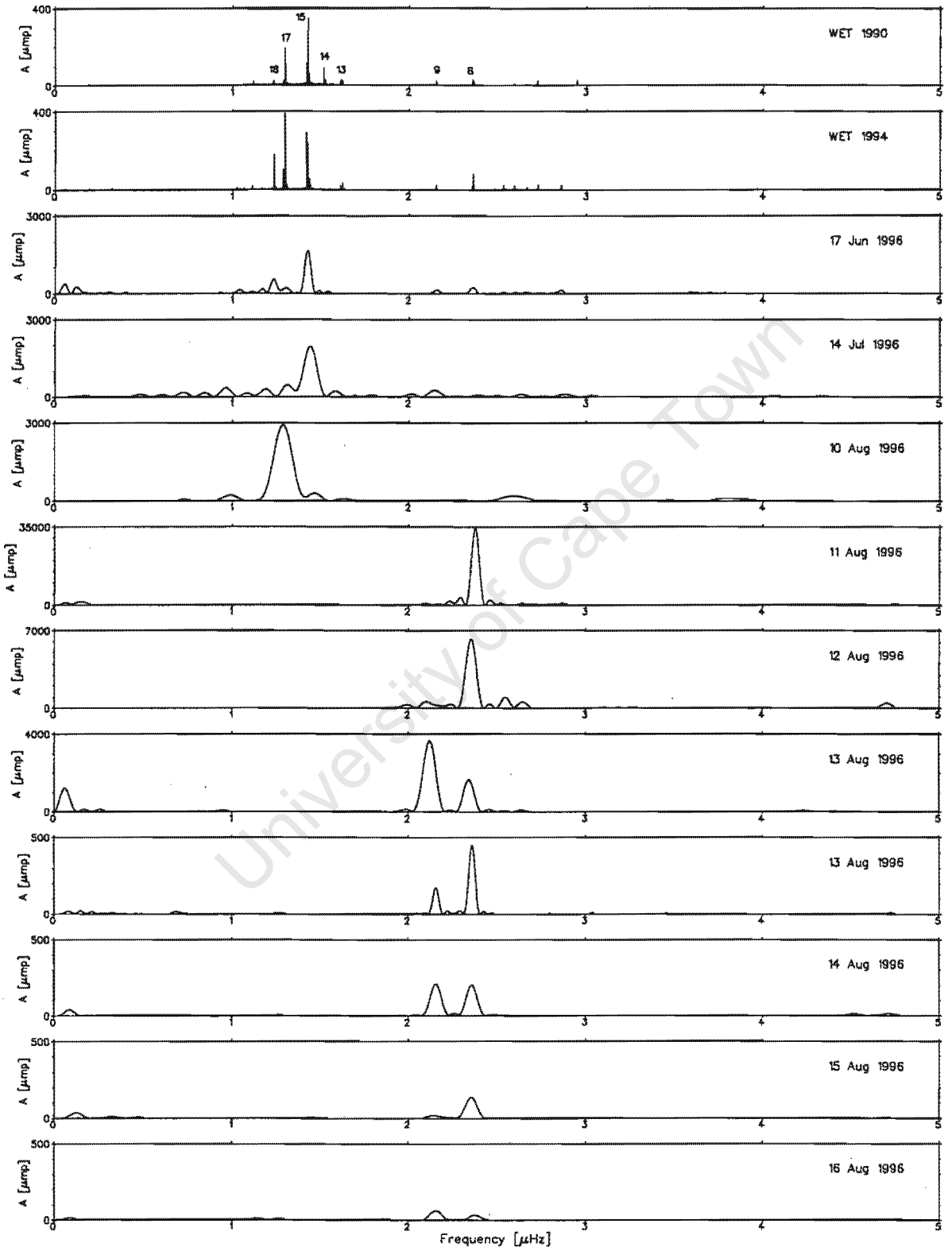

Figure 6.11: Comparison of the two WET amplitude spectra with those computed on the individual 1996 runs. The amplitude scale in given in μHz and is different in each panel to accommodate for the large variations observed. The identified modes in 1990 are indicated by their radial order k.

explained in a nonlinear context, although nonadiabaticity might play a significant role as well.

The formalism used to investigate the dynamics of nonlinear mode coupling uses amplitude equations, or AEs (Dziembowski 1982, Moskalik 1985, Buchler & Goupil 1984, 1994). Two types of terms are present in the AEs: the nonadiabatic terms and the nonlinear terms. The nonadiabatic terms are linear in the modal amplitudes, and do not conserve energy. The corresponding growth rates are predicted by linear nonadiabatic models to be in the range $10^{-7} - 10^{-3}$ s^{-1} (Bradley, private communication). Very low k-order modes would have even lower growth rates, but these modes are not expected to be excited to detectable amplitude. The nonlinear terms, on the other hand, are quadratic in the amplitudes, and therefore govern the dynamical interaction of the modes, whose time-scale depends greatly on the type of coupling considered and on the phase of the corresponding limit cycle. According to the numerical analysis carried out to date, they seem to range from much shorter (Moskalik 1985) to much longer (Goupil, Dziembowski, & Fontaine 1997) than the time scale for purely non-adiabatic growth.

If the August 1996 behaviour is considered on its own, it qualitatively resembles one of the parametric resonant limit cycle solutions of the AEs, described by Moskalik (1985). Through most of this cycle, an overstable mode f_0 grows exponentially on the "long" time-scale governed by its linear (nonadiabatic) growth rate. Once f_0 has reached a given amplitude, two coupled mode f_1 and f_2, linearly damped but driven by the resonance $f_0 = f_1 + f_2$, starts growing in amplitude at the expense of f_0, which consequently decreases in amplitude on a very short time-scale (estimated between 2 and 150 hours by Moskalik 1985). The nonlinear driving then decreases as a result of the decrease of f_0, and the natural damping of f_1 and f_2 takes over their evolution on a time-scale expected to be roughly between 10^2 and 10^5 s (i.e. damping rates of $10^{-2} - 10^{-5}$s^{-1}) (Bradley private communication), depending mostly on the k-order of the modes. The cycle then starts again.

As far as the time-scales and the qualitative aspect of this cycle are concerned, it matches well the 1996 observations, where $k = 8$ and $k = 9$, which show a similar evolution, could represent the stable modes f_1 and f_2 driven by the resonant coupling. However, no mode is found in the spectrum that could play the role of the overstable f_0 mode. Although the mode $k = 17$, observed on the 10$^{\text{th}}$ of August (Figure 6.11), could

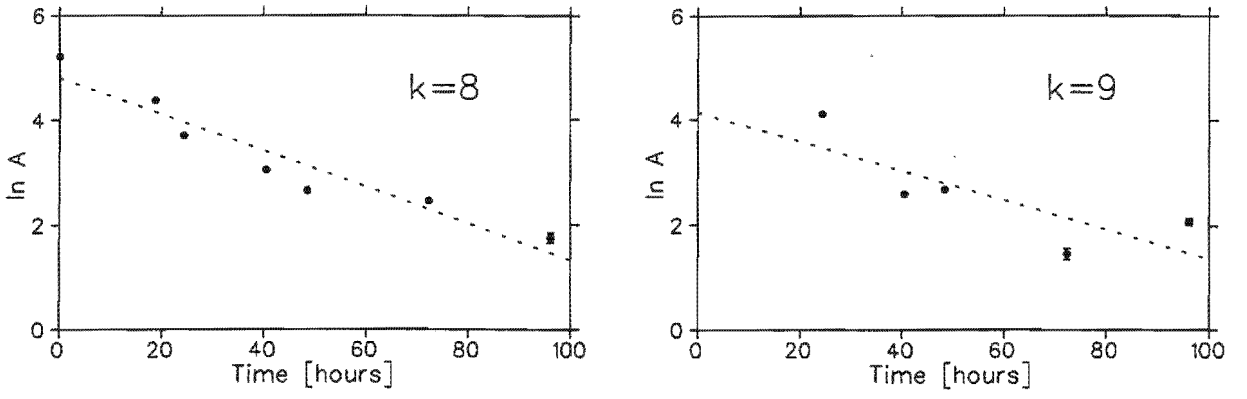

Figure 6.12: Evolution of the amplitudes, A, of the modes $k = 8$ and $k = 9$ during the 1996 observing session.

qualitatively take the role of f_0 as it disappeared when $k = 8$ grew, as expected from the limit cycle considered, the $k = 17$, $k = 9$, and $k = 8$ modes do not, however, have a linear frequency relationship, $f_0 = f_1 + f_2$, between them, and cannot therefore be directly coupled to each other. No combination modes of these three normal modes can be identified in the 1996 power spectrum; not only were all of these observed in 1994 (see Table 6.5 in section 6.2), but they were consistent with harmonic distortion rather than with mode coupling (section 6.3.3).

Another possibility is that $k = 8$ is the overstable mode, while $k = 9$ and $k = 8 \pm 9$ are the stable modes of the process, the latter being not detectable because the nonlinear driving never exceed its natural damping.

The discussion of these different mechanisms remain therefore speculative. As the AE formalism has only been developed to the second order of perturbation, and for three modes only, its applicability to real pulsators with complex spectra is obviously limited. Furthermore, the coupling coefficients of the AEs have not yet been calculated, although it can be done ab initio (Goupil & Buchler 1994), which is another limiting factor when trying to compare theory and observation. Therefore, the qualitative resemblance discussed above should thus already be considered as a support for the idea.

Even though the $k = 8$ and $k = 9$ modes are not resolved into their expected triplets in the individual August 1996 runs (Figure 6.11), we have nevertheless monitored their amplitude during the course of this campaign as seen in Figure 6.12.

The logarithmic scale used clearly indicate an exponential decay for the $k = 8$ mode, whereas such behaviour is less obvious for the $k = 9$ mode. Beating is nevertheless expected to perturb the measurements to some extent, so that only the global evolutionary trend should be considered significant in Figure 6.12. The e-folding times for the decay of these modes, obtained by least-squares fits, are respectively $\tau_8 = 28.7 \pm 3.9$ hours at a 98% confidence level, and $\tau_9 = 36.1 \pm 16.0$ hours, at a mere 70% confidence level. If $k = 8$ and $k = 9$ are indeed, at least in 1996, stable modes driven by a parametric resonant process, then these two consistent decay time-scales might well represent the first measurements of linear damping times in a pulsating white dwarf star. The corresponding linear (nonadiabatic) damping rate are $\gamma_8 = 1/\tau_8 = (0.97 \pm 0.12) \times 10^{-5}$ s^{-1} and $\gamma_9 = 1/\tau_9 = (1.45 \pm 0.24) \times 10^{-5}$ s^{-1}. They are consistent with the above discussed predictions for DB variables.

6.3.5 Evolution of the pulsational energy

Could the mechanical energy contained in the pulsation modes remain constant even though amplitude modulation, not due to beating, is observed in the period spectrum? Well it could, but there is a priori no reason why it should. Indeed, spectral changes can be either purely nonadiabatic, in which case the pulsational energy is, by definition, not conserved, or of (nonlinear) mode coupling origin, which is not a Hamiltonian process (because of the linear nonadiabatic term in the amplitude equations), and thus does not conserve energy either. Roughly speaking, during a resonant process, the energy, rather than being directly exchanged between the coupled modes, gets transferred via the thermal reservoir of the star, which does not necessarily redistribute all the energy received.

Nevertheless, the computation of the pulsational energy may yield interesting information in some cases, such as GD358, where the spectral changes are extreme. The kinetic energy $E_{\rm k}$ of the entire oscillatory motion is given by

$$E_{\rm k} = \int_M \rho v^2 d^3r \tag{6.1}$$

where v is the velocity, ρ the local density, and M the mass of the star. In the case of a linear pulsator with only one mode excited, the velocity can be written

$$v(r,t) = a\,\omega\,\zeta(r,t) = a\,\omega\,\xi\,e^{i\omega t} + \text{c.c.} \tag{6.2}$$

where ω is the angular eigenfrequency of oscillation, a is the amplitude of the pulsation, possibly slowly varying in time, and ξ is the spatial part of the eigenfunction of the radius variation ζ. Both ξ and ω can be obtained from linear theory. Assuming a time scale for any amplitude variations much longer than the oscillation period, $E_{\rm k}$ becomes, after averaging over one period

$$< E_{\rm k} >= a^2\omega^2 I \tag{6.3}$$

where I is the oscillatory moment of inertia, given by (Unno *et al.* 1989)

$$I = \int_M \rho\,\xi^2\,d^3\rho \tag{6.4}$$

The difficulty is that a, or a^2, is not directly measurable. What is in fact observed is the relative variation of the luminosity

$$\frac{\delta L}{L} = a\left[\left(\frac{\delta L_r}{L_r}\right)_{\rm sp}\right]_{r=R} e^{i\omega t} + \text{ c.c.} \tag{6.5}$$

where the term in square brackets is the spatial part of the eigenfunction of the luminosity variation, evaluated at the stellar surface R, which can also be obtained from linear analysis. For white dwarfs $\left(\frac{\delta L}{L}\right)_{\rm sp} \sim 4\left(\frac{\delta T}{T}\right)_{\rm sp}$ may be a reasonable approximation.

The amplitude A measured from the observed period spectrum is simply the relative luminosity variation averaged over one period

$$A = < \frac{\delta L}{L} > = a\left[\left(\frac{\delta L}{L}\right)_{\rm sp}\right]_{r=R} \tag{6.6}$$

Combining equations 6.3 and 6.6 yields

$$< E_{\rm k} > = A^2 \omega^2 I^2 \left[\left(\frac{\delta L}{L} \right)_{\rm sp} \right]^{-2}_{r=R} \tag{6.7}$$

where A is measured from the observed amplitude spectrum, while the other quantities are obtained from the linear theory. The result is independent of the normalisation used at the stellar surface.

The actual computation of the pulsational energy, in a real case like that of GD358, is however not straightforward at all. Four major difficulties arise that necessitate strong assumptions to be made.

First, the above analytical computation has been developed in the case where only one mode is excited. If the star does pulsate simultaneously in many modes, as all pulsating white dwarfs do, the geometrical interaction of the modes has to be taken into account by combining their respective spherical harmonic functions. However, in the special case where all the modes have the same spherical index ℓ, there is no geometrical cancellation between them, and the total pulsational energy is merely the sum over the kinetic energies of each mode. We therefore assume, in keeping with the mode identification by Winget *et al.* (1994), that all the identified modes are $\ell = 1$.

Second, any amount of pulsational energy can be hidden in photometrically invisible frequencies such as high ℓ-index modes, or interfacial modes. Only the energy contained in the visible modes can therefore be computed.

Third, the normal modes are not completely resolved due to third order beating (Figure 6.8). Their amplitude cannot thus be measured accurately, which introduces an unquantifiable error.

Fourth, it is not clear how the energy contained in the combination frequencies should be treated. In fact, it depends on the origin of these nonlinear frequencies, which is not exactly known. Assuming they are all harmonic distortion peaks, in keeping with the discussion in section 6.3.2.3, a rough estimate of the error made by neglecting these nonlinear frequencies can be made. We claim that the energy contained in any given eigenmode is larger than the energy of all its combination frequencies put together. This estimate is based on two considerations, one observational, one physical. First, the power

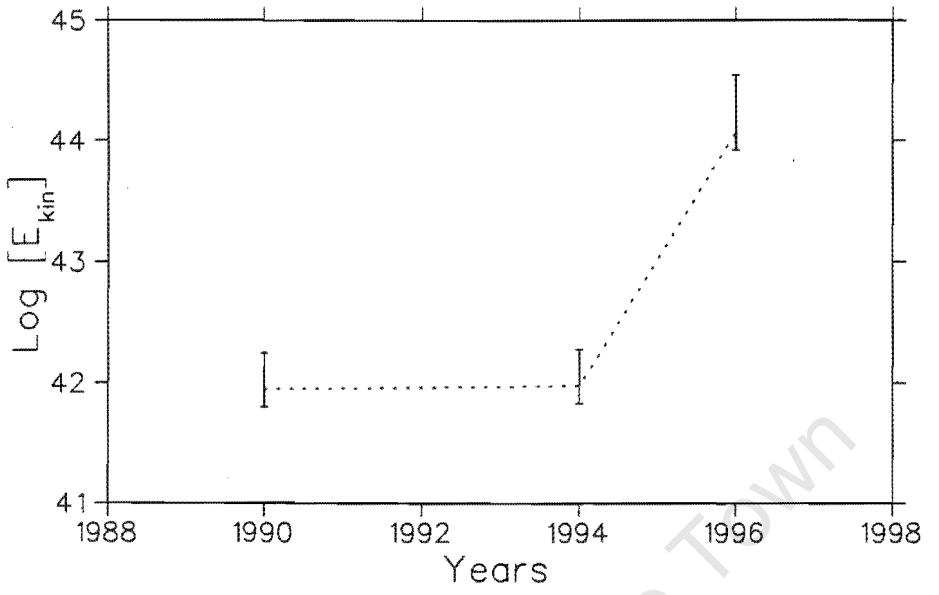

Figure 6.13: Evolution of the pulsational energy.

of any combination frequency is always observed to be at least one order of magnitude lower than that of its corresponding parent modes (see Table 6.3 to 6.6 in section 6.2). Second, the eigenfrequencies must always remain larger than their harmonics, otherwise the star would be able to change its oscillation frequency; such a frequency switch is physically inconceivable, unless the harmonic that becomes the dominant mode is itself an eigenmode, corresponding to the accidental resonant case.

In this regard, a very conservative error of a 100% on the computed pulsational energy has been assigned, which should account for these various considerations, as well as for the fact that the 1996 spectra are not resolved.

We have computed, from equation 6.7, the kinetic energy of the 1990, 1994, and (11 August) 1996 temporal spectra. The values of $\omega^2 I^2$ and $\left[\left(\frac{\delta L}{L}\right)_{\rm sp}\right]^{-2}_{r=R}$ were obtained from the nonadiabatic model proposed by Bradley & Winget (1994). The results of this analysis is shown in Figure 6.13.

Despite our very conservative error estimate, the August 1996 energy content is about two orders of magnitude larger than in 1990 and 1994. Because low k-order modes penetrate, generally speaking, much deeper into the stellar interior than large k-order modes do, their mechanical energy is correspondingly much higher at comparable amplitude A.

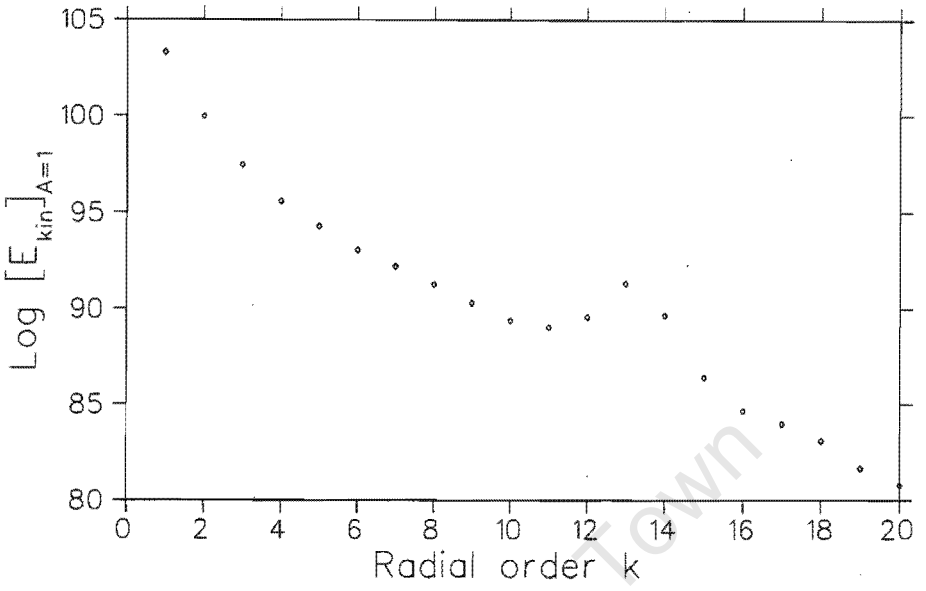

Figure 6.14: Kinetic energy normalised to a modal amplitude $A = 1$, as a function of the radial order k.

This effect can clearly be seen in Figure 6.14 which shows the energy content of each mode at normalised modal amplitude $A = 1$. The deviation from a monotonic decrease is due to mode trapping (Winget & Fontaine 1982). Figure 6.14 indicates that, although the modes $k = 15$, $k = 17$, $k = 18$ are dominating the 1990 and 1994 amplitude spectra (Winget *et al.* 1994; Table 6.3 in section 6.2), their energy content is almost negligible compared to that of the $k = 8$, $k = 9$, and $k = 13$ modes. This implies that the behaviour recorded in Figure 6.13 is only weakly dependent upon variations in the model parameters, i.e. upon changes in the mode identification.

The spectral changes from 1994 to 1996 cannot be accounted for by pure nonlinear mode coupling processes for various reasons. First, 6 triplets, i.e. 18 modes, have been identified in the 1994 spectrum, while basically only one, the $k = 8$ was found in August 1996. It is hardly conceivable to have all these modes simultaneously coupled, not only because resonances are supposedly scarce phenomena, but also because the combination frequencies, which could play the role of the stable modes driven by the resonant process, were shown to be harmonic distortion frequencies (see section 6.3.2 and 6.3.3). Furthermore, even if the modes were all resonant, they would still form independent dynamical systems, and would a priori have no reason to disappear simultaneously in 1996. It is therefore legitimate to consider that the majority of the modes identified in 1990 and

1994 are non-resonant, but simply linearly driven unstable modes, with their amplitude limited by some nonresonant saturation mechanism.

These considerations lead us to the conclusion that some process, other than mode coupling, has probably to be invoked to account for the dramatic spectral changes recorded between 1994 and 1996. The driving and the mode selection mechanisms are very suspicious candidates, because they are directly responsible for what mode is excited, and to what amplitude. The functioning and inter-relationship of these processes are very poorly understood at present. In particular, it is not clear why the modes with a positive growth rate are not all excited, which indicates that a competition for the driving exist between the unstable modes.

Clues are certainly hidden in the interaction between convection, which is expected to carry most of the flux in white dwarfs (Wu 1997), and pulsations. Proper time-dependent treatment of convection does not yet exist due to the highly nonlinear nature of the phenomenon. For decades investigations of white dwarfs pulsations have relied on the frozen-in approximation, where the convective flux is expected not to be perturbed during the pulsational cycle. Only recently have attempts been made to remove this questionable approximation and replace it by an instantaneous adjustment of the convective flux to the pulsations (Brickhill 1991, Goldreich & Wu 1999). Still in their infancy, these new developments promise to open a whole new theoretical field of research.

6.3.6 Conclusion

We have shown how high order harmonic distortion effects may not only alter the regular eigenmultiplet structure of a pulsating white dwarf, but also generate extremely long and complex beating processes that might be mistaken for intrinsic amplitude changes. In the case of GD358, we claim that such harmonic distortion effects can mostly account for the odd multiplet structures observed in 1994 (see Figure 6.4 in section 6.2) as well as for the spectral changes recorded between 1990 and 1994. The same phenomenon is likely to be important in a number of large amplitude compact pulsators, and could possibly explain most of their light curves; we believe that, besides harmonic distortion, the pulsations in white dwarfs are mostly linear. Genuine nonlinear processes, such as resonant mode coupling, need to be invoked only to explain unusual behaviours, as suggested by

Dziembowski (1993).

Such unusual behaviour has been observed in the 1996 campaign on GD358. It clearly appeared that some much stronger nonlinear phenomenon than that of harmonic distortion had to be invoked. We found a qualitative resemblance between this behaviour and a synthetic limit cycle obtained from the amplitude equation formalism. Although our understanding of the 1996 behaviour is speculative, we still measured the decay rates of two modes (respectively $1.0 \times 10^{-5}\,\mathrm{s}^{-1}$ and $1.5 \times 10^{-5}\,\mathrm{s}^{-1}$), that might correspond to linear (nonadiabatic) damping rates.

The analysis of the relative phases and relative amplitudes of the harmonics and cross-frequencies not only securely confirmed the suspicion that these nonlinear frequencies were of harmonic distortion origin, but helped identifying the spherical degree ℓ of the normal modes. In the near future, the study of these nonlinearities should yield quantities such as the viewing angle of the star, as already attempted in section 5.4 and by Wu (1997), and eventually provide specific information about the internal structure of the stellar medium. The advent of nonlinear asteroseismology might be just around the corner.

Acknowledgments

We are grateful to Atsuko Nitta and the observers of the 1996 3-site campaign (D. E. Winget, S. O. Kepler, D. Koester, J. Krzesiński, G. Pajdosz, X. Jiang, S. Zoła) for making their data available for this investigation. We are also grateful to Marie-Jo Goupil and Pawel Moskalik for helpful discussions on mode coupling. We also want to thank Paul Bradley and Mike Montgomery for making their numerical model available to us. Finally, we would like to acknowledge all the WET observers without whom none of these above nonlinear analyses would have been possible.

References

Bradley P. A., Winget D. E., 1994, ApJ, 430, 850

Brassard P., Fontaine G., Wesemael F., Tassoul M., 1992, ApJS, 81, 747

Brassard P., Fontaine G., Wesemael F., 1995, ApJ, 96, 545

Brickhill A. J., 1991, MNRAS, 251, 673

Brickhill A. J., 1992, MNRAS, 259, 529

Buchler J. R., Goupil M.-J., 1984, ApJ, 279, 394

Cox J. P., 1980, *Theory of Stellar Pulsation*, Princeton University Press, Princeton

Dziembowski W. A., 1982, Acta Asto., 32, 147

Dziembowski W. A., 1993, in I.A.U Colloq. 137, *Inside the stars*, eds. W. Weiss and A. Baglin, 521

Fontaine G., *et al.*, 1980, ApJ, 239, 898

Goldreich P., Wu Y., 1999, ApJ, 511, 904

Goupil M.-J., Buchler J. R., 1994, A&A, 291, 481

Goupil M.-J., Dziembowski W. A., Fontaine G., 1997, Baltic Astro., 7, 21

Jones P. W., *et al.*, 1989, ApJ, 336, 403

Kawaler S. D., 1988, in I.A.U. Colloq. 123, *Advances in Helio- and Asteroseismology*, eds. J. Christensen-Dalsgaard and S. Fransen, (Dodrecht: Reidel), 329

Kawaler S. D., Hansen C. J., 1989, in IAU Colloq. 114, *White Dwarfs*, eds. G. Wegner, (Springer-Verlag: Berlin), 97

Kepler S. O., Robinson E. L., Nather R. E., 1983, ApJ, 271, 744

Moskalik P., 1985, Acta Astro., 35, 229

Nather E. L., *et al.*, 1990, ApJ, 361, 309

Nather E. L., 1995, Baltic Astro., 4, 321

Nitta A., 1999, *11th European Workshop on White Dwarf Stars*, eds. J.-E. Solheim and E. Meistas, (San Francisco: ASP), 104

Thuras A. L., Jenkins R. T., O'Neil H. T., 1935, J. Acoustic Soc. Am., 6, 173

Unno W., *et al.*, 1989, *Nonradial Oscillations of Stars*, 2nd ed., University of Tokyo Press, Tokyo

Winget D. E., 1981, PhD thesis, Univ. of Rochester, New York

Winget D. E., Robinson E. L., Nather R. E., 1982a, ApJ, 262, L11

Winget D. E., *et al.*, 1982b, ApJ, 252, L65

Winget D. E., Fontaine G., 1982, *Pulsations in Classical and Cataclysmic variable stars*, ed. J. P. Cox and C. J. Hansen, 46

Winget D. E., 1988, in Advances in Helio- and Asteroseismology, ed. J. Christensen-Dalsgaard and S. Fransen, (Dodrecht: Reidel), 305

Winget D. E., 1991, *7th European Workshop on White Dwarfs*, eds. G. Vauclair and E. M. Sion, (Dodrecht: Kluwer), 129

Winget D. E., *et al.*, 1994, ApJ, 430, 839

Wu Y., 1997, Ph.D. thesis, California Institute of Technology, Passadena

Chapter 7

Discussion and conclusions

7.1 Discussion

The time has come to summarise concisely the findings of this research. In the introduction of this thesis, I expressed some of the questions that I wished to address. Let me ask each of the questions again to see which of them have received satisfactory answers.

• *Can we detect any amplitude changes in the period spectrum which can with certainty not be explained by beating*[1]*?*

The answer is clearly positive; amplitude changes have been recorded in the period spectra of both G29-38 and GD358, which could not be due to beating. Intrinsic spectral changes are nevertheless difficult to distinguish from apparent ones, and a concise summary of what led to this conclusion is necessary.

Even though the data sets selected for this research project were long enough for the beating between the excited normal g-modes to be resolved, amplitude changes in the period spectra from one observing campaign to the next were nevertheless observed. Although such spectral changes are directly suggestive of nonlinear process, I have demonstrated that this is not necessarily the explanation: higher order beating processes might

[1]Here I really mean any kind of beating.

be responsible. Third and higher order harmonic distortion peaks are difficult, if not impossible, to resolve because they can be numerous and very closely flanking normal modes, thus generating very long and complex beating processes. No matter how long the given data set, if amplitude variations are observed in a temporal spectrum, high order beating processes should be thoroughly considered before reporting intrinsic nonlinear behaviour.

The realisation of the importance of the effects of high order beating on the normal modes has both positive and negative consequences. The positive aspect is that the pulsations of large amplitude variable white dwarfs might be mostly linear, thus simplifying greatly the theoretical approach required. The negative aspect is that the prospects of nonlinear asteroseismology are worse: no observations can ever practically be long enough for all the beating processes to be fully resolved, as the frequency separation between first and third order peaks can be extremely small, depending on the importance of the symmetry breaking effects such as stellar rotation and magnetic field. If the star is non-rotating, the m-degeneracy is not lifted and the eigenmodes are not split into multiplets. In this case, high order beating does not occur, but the nonlinear peaks then exactly superpose themselves onto the normal modes. Each peak in the period spectrum then becomes an inextricable complex of components of order 1, 3, 5, etc., and the nonlinear asteroseismological prospects do not look any better.

These high order processes do not, however, impede the success of linear asteroseismology, as the latter does not extract information from the amplitudes of the normal modes, but solely from their frequencies, which are not affected.

Two types of amplitude changes could be observationally distinguished in G29-38 and GD358: mild amplitude variations and drastic spectral changes. Mild variations imply that the period spectrum remains qualitatively the same, even if amplitude changes in specific excited modes take place. Such behaviour was observed, for instance, from comparison of the 1990 and 1994 WET campaigns on GD358, and even during the course of these runs. Drastic spectral changes, on the other hand, appear rather as metamorphoses of the pulsating state of a star, where the period spectrum experiences large qualitative changes, i.e. where different sets of normal modes appear to be present at different times and/or where extremely large amplitude changes are recorded. High order beating processes can potentially account for the mild type of changes, but certainly not for the drastic ones.

The identification of genuine amplitude variations thus remains a delicate question. In conclusion, only when no combination frequencies can be identified, or when the star presents drastic spectral changes, can high order beating be securely excluded as the cause of the variations, and consequently nonlinear (and/or possibly nonadiabatic) processes invoked. Such exceptional behaviour was seen in G29-38, which presented a very different period spectrum in each season it was observed, and in GD358 during the 1996 campaign, which caught the star in an exceptional pulsating state, which had never before been seen in this star. This therefore has led me to conclude that intrinsic amplitude changes do occur in both the DAV G29-38 and the DBV GD358.

Although this point merely confirms the general belief that intrinsic amplitude variation is almost ubiquitous among large amplitude pulsators, the answer to this question was an important first step towards the analysis of nonlinear processes. Even though amplitude changes in pulsating white dwarfs has been regularly reported since the 1970s, these spectral changes were ulteriorly found not to be intrinsic but due to "overinterpretations of undersampled data" (Winget 1988). It was therefore important once and for all to settle the issue: pulsating white dwarfs do show intrinsic nonlinear behaviour.

Determining the origin of intrinsic amplitude variations is at present a very difficult task; several phenomena can be invoked, but most of them cannot be studied theoretically because of their highly nonlinear nature. Therefore, none of these processes has a known distinctive observational signature which might enable them to be identified or excluded. I have proposed five different mechanisms that could potentially affect the stability of modes, and thus generate spectral changes. These are either nonlinear, or nonadiabatic, or both:

1. Resonant mode coupling is the best known process which can generate modal amplitude variations. It is the only such process which has at present been addressed theoretically, thanks to the development of the perturbative amplitude equations formalism.

Because of the possible coupling between identified normal modes and invisible high-degree ℓ modes , resonant processes can never be strictly excluded when intrinsic amplitude changes are observed. However, in a number of cases such as the seasonal changes in G29-38, I claimed mode coupling was probably not responsible for the spectral changes, because too many modes showed correlated evolution. Mode coupling is a supposedly scarce phenomenon which requires specific resonant conditions. If three-mode coupling

is rare, resonant processes involving more modes are even rarer. Therefore, it is difficult for mode coupling to account for spectral changes involving tens of modes as observed in G29-38.

2. At present, the mode selection mechanism is a very poorly understood process. Even though the structure of the stellar envelope entirely determines the linear growth rates of the normal modes, it is not clear which of the numerous modes with positive growth rates actually benefit from the driving. This area is as yet completely unstudied, and a priori, the competition between the modes with the potential to be excited can even lead to time-dependent solutions (Moskalik, private communication).

3. The pulsations themselves could be the physical process that triggers nonlinear evolution. When a mode is driven, the growing amplitude of its mechanical oscillation creates periodic changes that perturb more and more the physical structure of the atmosphere. This might both affect the linear growth rates of the modes, and the selection mechanism, which, in turn, could generate significant amplitude changes. This could also explain the stability of the small amplitude pulsators, whose oscillations would not become large enough to perturb the atmospheric structure sufficiently for the selection mechanism to be affected. It is certainly worth investigating this possibility numerically, and it might not require too much effort.

4. Because a time-dependent treatment of convection is not yet possible, the effect of the turbulent convective flux on the pulsations is to date not at all understood. Convective driving is now believed to be the dominant driving process in DAV type stars (Brickhill 1991, Gautschy *et al.* 1996, Wu 1997, Goldreich & Wu 1999a), so the dynamical interaction between the pulsations and turbulent convection certainly plays a role in the mode selection process, as suggested by Kawaler & Hansen (1989) and by Winget (1988). The highly nonlinear and time-dependent nature of the convection/pulsations interaction could a priori generate complex nonlinear behaviour (Cox 1976). Goldreich & Wu (1999b) have started to investigate this interaction and showed how turbulent viscosity can act as a mode damping process. It would be very interesting to determine whether this damping could affect the excited mode selectively, in the same way that mode trapping does. Effort in this direction is definitely needed.

5. As mentioned above, the structure of the stellar envelope determines entirely the linear

growth rates of the normal modes, i.e. it determines which frequencies could possibly be excited. Therefore, if the atmosphere of a pulsating star experiences physical changes, its resultant pulsating eigenstructure might consequently be affected, and in turn its period spectrum as well. The effect of stellar evolution on the pulsations is expected to be observed, but we are rather invoking changes which are not linked to the natural evolution of the star. What might these changes be?

Turbulent processes, or sudden eruptive events can potentially perturb the stable atmospheric structure sufficiently to affect the pulsations of the star. Such changes, stochastic, cyclic or secular, in the stellar compositional and/or physical structure cannot be excluded because one cannot argue with certainty that any star is in a completely steady state. Phenomena such as the 22 year solar cycle, the quasi disappearance of the pulsations in the famous prototype pulsator δ Cephei (Fernie, Kamper, & Seager 1993), or the stochastic-type pulsating behaviour of certain rapidly oscillating Ap stars (e.g. Matthews *et a;.* 1987), can probably not be explained without inferring structural changes.

Amplitude variations generated in such a way are purely linear nonadiabatic, as only the growth rates, and possibly the mode selection mechanism, are affected.

These suggestions are fruitful avenues for further research, although investigations are extremely difficult due to the highly nonlinear or non-cyclic nature of these phenomena.

• *What is the origin of the numerous nonlinear frequencies identified in the amplitude spectra of pulsating white dwarfs?*

Several independent analyses have been conducted to try and address this question, and they all yield consistent results; although nothing can be said about any individual nonlinear peak, generally speaking the latter owe their presence to harmonic distortion effects, that is, to the inability of the stellar medium to respond linearly to the oscillatory perturbation. I was led to this conclusion by the observation of

1. the consistent phasing of the cross-frequencies with that of their parent modes;

2. the consistent relative amplitudes of the cross-frequencies;

3. the systematic presence of the cross-frequencies at different orders of perturbation;

4. the complex multiplet structure of the cross-frequencies.

The relative phases of the nonlinear frequencies were found, both in G29-38 and in GD358, to be slightly in advance of that of their parent modes. This suggested that the origin of harmonic distortion lies in the nonlinear response of the convection zone to the pulsations, as advocated by Brickhill (1992) and Wu (1997), rather than in the nonlinear response of the emergent flux to the surface temperature variations, as suggested by Brassard *et al.* (1995). This conclusion was well established, in the case of G29-38, by the comparison of the measured relative amplitudes with those predicted by these three models.

• *What is the origin of the typical nonlinear features observed in the light curves of all large amplitude pulsating white dwarfs?*

Pulsating white dwarfs showing light curves with distorted pulse shapes were known from the beginning of their history, since such features had been observed in the first of them, DAV HL Tau 76 (Landolt 1968). The existence of harmonics and cross-frequencies in the power spectra of these stars was first identified by McGraw & Robinson (1975). Since then it has always been implicitly understood that these combination frequencies were somehow responsible for the nonlinear features seen in the light curves. This understanding has, however, never been more than conceptual, as no one has ever analysed these nonlinearities. In particular, it has never been clear to what extent the cross-frequencies are responsible for the pulse shape distortions, and what individual visual impact each of them has on the light curve.

I have determined that the characteristic sharply peaked pulse shapes separated by flat bottoms, observed both in G29-38 and GD358, are direct consequences of the global phasing of the cross-frequencies with their parent modes, i.e. direct consequences of harmonic distortion.

Provided the origin of harmonic distortion lies in the nonlinear response of the convection zone, as suggested above, then the characteristic pulse shapes with sharp ascents and slower descents, as observed in G29-38 and GD358, can receive a physical explanation.

When the (sinusoidal) flux at the bottom of the convection zone increases, the convective layer becomes thinner and thinner and consequently its response time to the pulsations becomes shorter. Therefore, the emergent flux is strongly delayed when the flux at the bottom of the convection zone is minimum, and almost in phase when it is maximum, which explains the sharp rise. When the flux at the bottom of the convection zone starts decreasing, the convection zone reappears, but not as fast as it disappeared, so that the flux at the top and at the bottom of the convective layer remains in phase for a little while before the delay appears again. This hysteresis phenomenon explain the slower descent observed in the pulse shapes of the light curves.

Because harmonic distortion is a natural deviation from linearity, and because it automatically generates characteristic pulse shapes in the light curves, these features can be considered as a signature of harmonic distortion. This means that, whatever the white dwarf considered, if its light curve presents cycles with sharp uphills, milder downhills, and with flat bottoms in between, it is strongly suggestive of pulse shape distortion. More generally, this consideration can be extrapolated to any radial and nonradial intrinsic variable, as harmonic distortion ought to be ubiquitous among pulsating stars, even if its effect is not necessarily visible.

One practical aspect of this signature is that it is easy to recognise visually; it can fairly securely be judged whether or not harmonic distortion is a significant effect, just by looking at the light curve.

- *Can we find a cyclic pattern in the appearance and disappearance of modes?*

G29-38 is known to be a "multiple state" pulsator, because each time it is observed, its temporal spectrum is different, presenting a new set of excited modes. Kleinman *et al.* (1998) uncovered an underlying structure of modes that were recurrent, in the sense that they were observed in more than one season, although they might have disappeared for a while in between. I was hoping to uncover a possible cyclic pattern in this come-and-go type of behaviour, but the analysis was seriously constrained by the small number of these recurrent modes compared to the numerous frequencies that were observed only once and never reappeared again. Correlated evolution between those recurrent modes was nevertheless uncovered, which clearly showed that some increased in amplitude while others decreased. No substantive conclusions could be drawn from this, although resonant

mode coupling is not thought to be responsible for this behaviour, despite the correlated evolution.

• *Can a specific resonant process be uncovered?*

It is difficult to provide a definite answer. Potential resonant processes have certainly been discovered, but I could not determine whether this was the only explanation. The difficulty in addressing this question is two-fold. First, we lack theoretical models of multi-mode limit cycles that can be quantitatively compared to the observations. Second, the coupling time-scales are expected to be of the order of a day for pulsating white dwarfs, while the beat periods can be up to several days; these two processes might therefore be extremely difficult to disentangle, which seriously restricts the possibilities for analysis.

Specific amplitude changes that could not be attributed to beating have been recorded both in G29-38 and in GD358. In the latter case qualitative similarities could even be found between its 1996 behaviour and a theoretical limit cycle, but this is as far as the analysis could be taken.

The measurement of the relative phases of the combination frequencies has revealed a technique for selecting potential candidate resonances. Two such frequencies have been discovered, one in G29-38 and one in GD358, that should be watched with particular attention during future observations of these stars.

• *Can any qualitative and/or quantitative comparison be made between the observed non-linear features and those predicted by theoretical models?*

From a qualitative point of view, it was already known that the models by Brickhill (1992b) and by Brassard *et al.* (1995) were able to produce synthetic light curves that resembled the typical nonlinear features observed in pulsating white dwarfs. I therefore decided to attempt a quantitative confrontation of these models with the observations available. Unfortunately, this analysis could only be performed in the case of G29-38, because these models have not yet been adapted to DB variables. Since the outcome of these models depends on the mode identification, and since secure labelling does not exist yet for G29-38, the whole analysis was rendered very intricate. Some interesting conclu-

sions could nevertheless be obtained. First, it appears that Brickhill's predictions are of the right order of magnitude, whereas those by Brassard *et al.* are not. As these models were each treating a different nonlinear process, this led to conclude that the process considered by Brickhill dominates over that considered by Brassard *et al.*, a conclusion which is also fully supported by the recent theoretical work from Wu (1997) and Goldreich & Wu (1999a). Physically speaking, this means that the nonlinearities generated by the radiative transfer, involving a highly nonlinear relationship between the luminosity and the surface temperature, seems to be negligible compared to the nonlinear response of the stellar medium to oscillatory perturbation. This is a surprising result, especially since the Brassard *et al.* model has been successfully tested in the case of the DAV G117-B15A (Brassard *et al.* 1993). However, since G117-B15A is a low amplitude nonlinear pulsator, it might indicate that Brickhill's nonlinearities only appear at a certain amplitude level, whereas Brassard's nonlinear behaviour is inherently present. When the amplitude becomes large enough, the response of the convection zone may suddenly get highly nonlinear, and generate nonlinearities which dominates over those induced by the Brassard's scheme. The convection zone behaves similarly to a loud-speaker which gives a linear response up to a certain sound level, or at least produces nonlinearities which are not audibly affecting the music. If the sound reaches a certain critical intensity, the loud-speaker suddenly saturates and badly distorts the musical signal, as often heard if the volume button of a hi-fi system is turned to the maximum.

- *What is the saturation phenomenon that limits the amplitudes of the excited modes?*

This research did not tell me what the saturation process is, but it did tell me what it is not. Amplitudes in pulsating white dwarfs have been claimed (Dziembowski 1980) to be limited by nonlinear coupling between modes. This process, first treated numerically by Ishida (1990), was thought to become important before the opacity mechanism, which drives the pulsations, gets saturated (Christy 1966). Wu (1997) confirmed theoretically that parametric resonance can saturate the modal amplitudes in white dwarfs.

However, I have clearly shown throughout this thesis that the combination frequencies are basically all harmonic distortion peaks, rather than resonant modes. For mode coupling to function as the amplitude limiting phenomenon, all the modes should be coupled in individual resonant mechanisms. This is clearly not the case, which excludes mode

coupling as the main saturation process.

Stellingwerf (1980) showed that, if the saturation of the driving were the prime limiting mechanism in white dwarfs, then their amplitudes ought to be about two orders of magnitude larger than actually observed. This saturation mechanism was discarded for this reason. However, the numerical approach used did not include a time-dependent treatment of convection, because this was, and still is, computationally intractable. To date, most codes assume that the convective flux is not perturbed during the pulsation cycle, an assumption known as the frozen-in approximation (Baker & Kippenhahn 1965). This is certainly wrong for white dwarfs because the typical turn-over time, and thus the adjustment time, for the convective eddies is much shorter than the observed pulsation periods. Furthermore convection carries up to 90% of the flux in the driving region (Brickhill 1983).

No one knows what the outcome of the convection/pulsation interaction ought to be, but "it may reveal phenomena not even hinted at by the present theory" (Cox 1976). In particular, the flux carried by the pulsations in the driving zone could well be limited by the action of convection that could remove energy from the linearly driven modes, a process I call "convective saturation", by analogy to "convective driving". The situation is similar to that of the convective subphotospheric layers where the radiative losses prevent the temperature gradient from approaching its adiabatic value (Dziembowski 1980).

Support for this contention is found in Goldreich & Wu (1999b) who addressed theoretically the question of the convection/pulsations interaction. They found that convective saturation does exist but is only supposedly efficient in limiting the amplitudes of long period ($\pi > 1000$ s) overstable modes. Considering that their calculations rely on the inappropriate quasi-adiabatic approximation (Brickhill 1991a, 1991b), convective saturation might well be found to be the major amplitude limiting process once this approximation is removed. I hope that these considerations will bring back the natural saturation of the driving for consideration as the mechanism responsible for the amplitude limitation in white dwarfs.

The lack of a proper time-dependent treatment of the convective flux can be considered as the major failure of present pulsation theory. Efforts in this direction are badly needed, not only to try and address the question of the saturation mechanism, but also because the origin of the mode selection mechanism is thought to lie in the convection/pulsation

interaction (Kawaler & Hansen 1989, Winget 1988). Theoretical investigations by Goldreich & Wu (1999a, 1999b), and Wu & Goldreich (1999) are very promising in this respect.

• *What information about the star can potentially be obtained from the analysis of the nonlinear features, i.e. how fruitful can nonlinear asteroseismology possibly be?*

Not much nonlinear asteroseismology could be carried out during this thesis, simply because few quantitative nonlinear models exist. However, the analysis of the nonlinear features has directly helped constrain the mode identification in both G29-38 and GD358, where I could determine that that most modes ought to have the same spherical degree ℓ. This is probably the greatest help that will be obtained from nonlinearities in the near future, i.e. before the advent of nonlinear models. Analyses similar to mine have actually already been performed, to a lesser extent, by Brickhill (1992b), and Wu (1997).

It is clear that the relative amplitudes of the nonlinear modes reflect directly the physical conditions in the stellar interior. The analysis of these peaks can thus potentially reveal much about the underlying structure of the star, possibly complementing or securing the information obtained by traditional linear asteroseismology. Unfortunately, the discrepancy recorded between the predictions from the second order models by Brickhill (1992) and by Brassard *et al.* (1992) precluded the determination of any physical quantity, which shows that a lot of work remains to be done in this field. In particular, a model that encompasses the different harmonic distortion effects needs to be developed. In this respect, the full numerical approach by Brassard *et al.* (in preparation) holds promise.

• *Are the pulsations intrinsically linear or nonlinear?*

I have shown that the very similar relative amplitudes and phases of the combination frequencies are consistent with what is expected from harmonic distortion. This directly suggests that the pulsations are intrinsically linear, and that the nonlinear features observed are only due to the response of the star to the linearly driven oscillations. However, the question is more intricate than it appears. Why could intrinsic nonlinear driving not actually generate nonlinear features having the very same characteristics? Well, there is a priori no reason why it could not, and some oscillatory systems definitely do. For instance, heart beats, which are often compared in the literature to stellar pulsations,

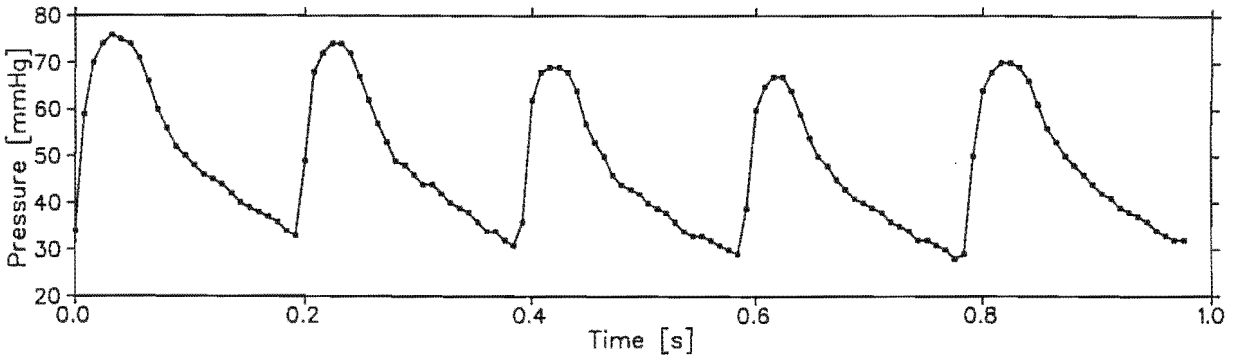

Figure 7.1: Pressure in the aorta of a rat during five cardiac cycles.

are definitely nonlinearly driven. Cardiac cycles closely resemble the light curve of large amplitude pulsating white dwarfs, as seen, for instance, in Figure 7.1, which shows the blood pressure variations in the aorta of a rat, measured just at the exit of the heart (Figure 7.1).

Although this naive analogy may give pause for reflection, I nevertheless claim that the pulsations in white dwarfs are intrinsically linear. I base my contention on the following arguments:

- Nonlinear features appear only in the light curve of large amplitude pulsators, which is exactly what is expected from harmonic distortion. Once the amplitude becomes too large, then the stellar medium cannot respond linearly anymore to the finite amplitude perturbation. Among others, this would explain the observed correlation between the size of the pulsation amplitudes and the shape of the corresponding light curves (e.g. Robinson 1979, McGraw 1980): the larger the amplitudes, the stronger the pulse shape distortions, and vice versa. If, on the other hand, the driving were itself nonlinear, harmonic and cross-frequencies should appear in the temporal spectrum regardless of the amplitude of the luminosity variations, and no correlation between the amount of distortion and the amplitudes should a priori be observed. Recalling my above analogy, an animal heart beats in an intrinsically nonlinear way, and the shape of the pressure curve seen in Figure 7.1 would be qualitatively the same in large rats and a small rats, or even in large and small animal species. Large amplitude pulsating white dwarfs should thus be compared to loud-speakers, rather than to hearts: loud-speakers behave linearly if the amplitude is small, but saturate

if the amplitude is too high, thus producing a distorted output signal.

- In GD358, the excellent resolution and S/N ratio allowed the identification of virtually all the possible second and third order cross-frequencies, which is also consistent with harmonic distortion effects. There would be, a priori, no reason for a nonlinear driving to systematically excite all the combination frequencies at all orders of perturbation.

- A systematic phase & amplitude correlation has been shown to exist between the normal modes and their related combination frequencies, which strongly suggests that these frequencies are physically related to each other. Such a global correlation of all the harmonics and cross-frequencies with their parent modes would be hard to explain were they generated by nonlinear driving. In particular, they would be no particular reasons why the harmonics should be systematically smaller than the combination frequencies, and why the nonlinear peaks should always be in phase with their fundamentals.

Indeed, the amount of "a prioris" is important. However, this clearly indicates that too many coincident circumstances are required for the driving to be able to produce the characteristic nonlinear features observed. That the Fourier analysis approach, which is nothing but a data analysis technique, yields a good description of the pulsations is not fortuitous, but must have some underlying physical meaning. In respect of these considerations, I assert that the pulsations in G29-38 and GD358 are intrinsically linear, in the sense that they are linearly driven, and that the nonlinear features in their amplitude spectra are mostly due to harmonic distortion. It is very tempting to extrapolate this conclusion to the entire pulsating white dwarf class, but more work is probably still required before this contention is secure.

7.2 Conclusions

For the reader's convenience, I list here below the conclusions reached by this thesis.

- Even though a given data set obtained by temporal spectroscopy is long enough for the beating between the normal modes to be resolved, beating processes between the

normal modes and third (and higher) order combination frequencies may generate amplitude modulations in the period spectrum. I called this process *high order beating.*

- High order beating may probably explain most apparent changes seen in the period spectrum of large amplitude pulsating white dwarfs, provided harmonic distortion is strong enough to produce significant third order combination frequencies.

- Spectral changes have been observed in both the DAV G29-38 and the DBV GD358 which were too drastic to possibly be accounted for by high order beating. Intrinsic amplitude changes do therefore occur in pulsating white dwarfs.

- Most, if not all, combination frequencies identified in the DAV G29-38 and in the DBV GD358 are due to harmonic distortion. Resonant mode coupling, if present, occurs only marginally.

- The nonlinear response of the convection zone to the pulsations is the dominant harmonic distortion effect in the DAV G29-38. The nonlinear response of the emergent flux to the surface temperature variations is negligible in comparison. The same conclusion probably holds for the DBV GD358.

- Virtually all the combination frequencies identified in the DAV G29-38 and the DBV GD358 oscillate in phase with (or slighly in advance of) their parent modes. This property is directly responsible for the characteristic pulse shapes observed in the light curve of large amplitude pulsating white dwarfs, i.e. peaks with sharp ascents, slower descents, and flat bottoms in between. These typical features can be considered as a signature of harmonic distortion for the whole class of pulsating white dwarfs, and possibly for any class of pulsating star.

- The analysis of the relative amplitude of the combination frequencies helped constrain the mode identification in both the DAV G29-38 and the DBV GD358. With the advent of nonlinear asteroseismology, many clues about the underlying structure of pulsating white dwarfs should be obtained from these nonlinear frequencies.

- No cyclic pattern in the appearance and disappearance of modes has been uncovered in the DAV G29-38, despite a certain correlation between the recurrent modes.

Resonant mode coupling is nevertheless thought not to be responsible for the observed spectral changes. Other nonlinear and/or nonadiabatic processes have been suggested which affect directly the driving and the mode selection mechanisms.

- A qualitative resemblance was found between the behaviour of the DBV GD358 as observed in 1996 and that of a theoretical limit cycle. The rapidly evoluting period spectrum observed may thus be caused by resonant mode coupling.
- Measurements of decay rates of $1.0 \times 10^{-5}\,\mathrm{s}^{-1}$ and $1.5 \times 10^{-5}\,\mathrm{s}^{-1}$ were obtained for two modes identified in the 1996 run on DBV GD358. They are believed to correspond to linear nonadiabatic damping rates.
- Parametric resonance is not the dominant amplitude limiting process in pulsating white dwarfs. Instead, the natural saturation of the driving mechanism, i.e. the saturation of the convective driving, might be responsible.
- The pulsations of the DAV G29-38 and DBV GD358 are believed to be intrinsically linear, in the sense that they are linearly driven. This contention might be true for all pulsating white dwarfs.

Bibliography

Ando H., Osaki Y, 1975, Publ. As. Soc. Japan, 27, 581

Baglin A., Schatzman E., 1969, *Low Luminosity Stars*, eds S. S. Kumar (Gordon and Breach: new York), 385

Baker N., 1966, *Stellar Evolution*, eds. R. F. Stein and A. G. W. Cameron (New York Plenum Press), 333

Baker N. H., Kippenhahn R., 1962, Zeitung für Astrophysic, 54, 114

Baker N. E., Kippenhahn R., 1965, ApJ, 142, 868

Baudin F., Gabriel A., & Gibert D., 1994, A&A, 285, 29

Baudin F., *et al.*, 1996, A&A, 311, 1024

Bergeron F., *et al.*, 1995, ApJ, 449, 258

Bloomfield P., 1976, *Fourier Analysis of Time Series: An Introduction*, eds. J. Willey & Sons, New York

Böhm-Vitense E., 1958, *Zeitschrift für Astrophysic*, 46, 108

Bradley P. A., 1993, Baltic Astro., 2, 545

Bradley P. A., Winget D.E., 1994, ApJ, 430, 850

Bradley P. A., 1996, ApJ, 468, 350

Bradley P. E., Kleinman S. J., 1996, *10$^{\text{th}}$ European White Dwarf Workshop*, eds. J. Isern, M. Hernanz, & E. Garcia-Berro (Dodrecht: Kluwer), 445

Brassard P., Fontaine G., Wesemael F., Tassoul M., 1992, ApJS, 81, 747

Brassard P., *et al.* 1993, *White Dwarfs: Advance in Observation and Theory*, eds. M. A. Barstow (Kluwer Academic Publisher), 485

Brassard P., Fontaine G., & Wesemael F., 1995, ApJS, 96, 545

Breger M., 1980, ApJ, 237, 169

Breger M., *et al.*, 1995, A&A, 297, 473

Brickhill, A. J., 1975, MNRAS, 170, 404

Brickhill A. J., 1983, MNRAS, 204, 537

Brickhill A.J., 1991a, MNRAS, 251, 673

Brickhill A.J., 1991b, MNRAS, 252, 334

Brickhill, A. J., 1992a, MNRAS, 259, 519

Brickhill, A. J., 1992b, MNRAS, 259, 529

Buchler J. R., Kowács G., 1986, ApJ, 303, 749

Buchler J. R., Goupil M.-J., 1984, ApJ, 279, 394

Buchler J. R., Goupil M.-J., Hansen C. J., 1997, A&A, 321, 159

Castor J. I., 1971, ApJ, 166, 109

Chanmugam G., 1972, Nature, 236, 83

Christensen-Dalsgaard J., Gough D. O., 1975, *Mem. Soc. Roy. Sci. Liège*, 8, 309

Christy R. F., 1964, Rev. Mod. Phys., 36, 555

Christy R. F., 1966, ApJ, 144, 108

Clemens J. C., 1993, Baltic Astron., 2, 407

Clemens J. C., 1994, PhD thesis, Univ. Texas, Austin

Clemens J. C., Van Kerkwijk M. H., Wu Y., 1999, in press

Cox A. N., & Cox J. P., 1967, Sky and Telescope, 5, 279

Cox J. P., 1955, PhD Thesis, University of Indiana.

Cox J. P., *et al.*, 1966, ApJ, 144, 1038

Cox J. P., 1966, ARA&A, 14, 247

Cox J. P., 1976, Ann. Rev. As. Ap., 14, 247

Cox J. P., Giuli R. T., 1968, *Principle of Stellar Structure*, (New York: Gordon and Breach)

Cox J. P., 1980, *Theory of Stellar Pulsation*, Princeton University Press, Princeton

Daubechies I., 1992, *Ten Lectures on Wavelets*, Eds SIAM

Deeming T. J., 1968, Vistas in As., 10, 125

Deeming T. J., 1975, Ap&SS, 36, 137

Deupree R. G., 1974, ApJ, 190, 631

Deupree R. G., 1975, ApJ, 198, 419

Dolez N., Vauclair G., 1981, A&A, 102, 375

Dziembowski W. A., 1975, *Mem. Soc. Roy. Sci. Liège*, 8, 287

Dziembowski W., 1977, Acta Aston., 27, 203

Dziembowski W. A., 1979, *White Dwarfs and Variable Degenerate Stars*, eds. H. M. Van Horn and V. Weideman (Rochester, N.Y.: University of Rochester Press), 359

Dziembowski W. A., 1980, *Nonradial and Nonlinear Stellar Pulsations*, eds. H.A. Hill H. A. & W. A. Dziembowski, (Springer-Verlag), 22

Dziembowski W. A., Koester D., 1981, A&A, 97, 16

Dziembowski W. A., 1982, Acta Astron., 32, 148

Dziembowski W., 1982, A&A, 32, 147

Dziembowski W. A., 1993, *Inside the Stars*, eds. W. W. Weiss and A. Baglin, 521

Eddington A. S., 1917, The Observatory, 40, 290

Eddington A. S., 1918a, MNRAS, 79, 2

Eddington A. S., 1918b, MNRAS, 79, 177

Faulkner J., Gribbin J. R., 1968, Nature, 218, 734

Fernie J. D., Kamper K. W., Seager S., 1993, ApJ, 416, 820

Fontaine G., *et al.*, 1980, ApJ, 239, 898

Fontaine G., *et al.*, 1982, ApJ, 258, 651

Fontaine G., Brassard P., 1994, *Stellar and Circumstellar Astrophysics*, eds. G. Wallerstein and A. Noriega-Crespo, 57, 195

Gautschy A., Saio H., 1996, Ann. Rev. As. & Ap, 551

Goldreich P., Wu Y., 1999a, ApJ, 511, 904

Goldreich P., Wu Y., 1999b, submitted

Gough D. O., 1996, *et al.*, *Science*, 272, 1233

Goupil M.-J., Auvergne M., Baglin A., 1991, A&A, 250, 89

Goupil M.-J., Buchler J. R., 1994, A&A, 291, 481

Goupil M.-J., Dziembowski W. A., Fontaine G., 1997, Baltic Astro., 7, 21

Hansen C. J., 1980, *Nonradial and Nonlinear Stellar Pulsation*, eds. H. A. Hill and W. A. Dziembowski (Springer-Verlag: Berlin), 445

Harper R. V. R., Rose W. K., 1970, ApJ, 162, 963

Harrington R. S. *et al.*, 1985, ApJ, 90, 123

Hesser J. E., Ostriker J. P., & Lawrence G. M., 1969, ApJ, 155, 919

Hill H. A.., 1980, *Nonradial and Nonlinear Stellar Pulsation*, eds. H. A. Hill and W. A. Dziembowski (Springer-Verlag: Berlin), 174

Iben I., 1971, ApJ, 166, 131

Inman C. I., Ruderman M. A., 1964, ApJ, 140, 1025

Jawerth B., Sweldens W., 1994, *Society for Industrial & Applied Mathematics*, 36, 377

Jerzykiewicz M., 1980, *Nonradial and Nonlinear Stellar Pulsation*, eds. H. A. Hill and W. A. Dziembowski (Springer-Verlag: Berlin), 96

Jones P. W. *et al.*, 1989, ApJ, 336, 403

Kawaler S. D., Hansen C. J., Winget D. E., 1985, ApJ, 295, 547

Kawaler S. D., 1988, *Advances in Helio- and Asteroseismology*, eds. J. Christensen-Dalsgaard and S. Frandsen, (Reidel: Dodrecht), 329

Kawaler S. D., & Hansen C. J., 1989, *White Dwarfs*, eds. G. Wegner (Springer- Verlag: Berlin), 97

Keely D. A., 1979, *White Dwarfs and Variable Degenerate Stars*, eds. H. M. Van

Horn and V. Weideman (Rochester, N.Y.: University of Rochester Press), 388

Kepler S. O., *et al.*, 1982, ApJ, 254, 676

Kepler S. O., Robinson E. L., Nather R. E., 1983, ApJ, 271, 744

Kepler S. O., 1984a, ApJ, 278, 754

Kepler S. O., 1984b, PhD Thesis, University of Texas, Austin

Kepler S. O. *et al.*, 1995, ApJ, 447, 874

King D. S., *et al.*, 1973, ApJ, 182, 859

Klapp J., Goupil M.-J., Buchler J. R., 1985, ApJ, 296, 514

Kolláth Z., 1990, MNRAS, 247, 377

Kleinman S. J., *et al.*, 1994, ApJ, 436, 875

Kleinman S. J., 1995, Ph.D. thesis, Univ. Texas, Austin

Kleinman S. J., *et al.*, 1998, ApJ, 495, 424

Kowács G., Buchler J. R., 1989, ApJ, 346, 898

Kurtz D. W., 1985, MNRAS, 213, 773

Kurtz D. W., 1990, Ann. Rev. Ast. Ap., 28, 607

Landau L. D., Lifshitz E. M., 1959, *Fluid Mechanics*, London: Pergamon Press, 4, 5.5

Landolt A. U., 1968, ApJ, 153, 151

Lasker B., Hesser J., 1969, ApJ, 158, L171

Lasker B., Hesser J., 1971, ApJ, 163, L89

Lawrence G. M., Ostriker J. P., Hesser J. E., 1967, ApJ, 148, L161

Ledoux P., Walraven Th., 1958, *Handbuch der Physic*, eds. S. Flügge (Berlin: Springer-Verlag), 51, 353

Lee U., Bradley P. A., 1993, ApJ, 418, 855

Lindblom L., 1999, submitted

Loumos G. L., Deeming T. J., 1977, Ap&SS, 56, 285

Matthews J. M., *et al.*, 1987, ApJ, 313, 782

McGraw J. T., Robinson E. L., 1975, ApJ, 200, L89

McGraw J. T., 1977, PhD Thesis, University of Texas, Austin

McGraw J. T., 1979, ApJ, 229, 203

McGraw J. T., Robinson E. L., 1976, ApJ, 205, L155

McLaren R., 1989, Ap&SS, 160, 255

Michel E., *et al.*, 1992, A&A, 255, 139

Michel E., 1993, *Delta Scuti Stars Newsletter*, eds. M. Breger, 6, 19

Moskalik P., 1985, Acta Astron., 35, 229

Moulton C., 1909, ApJ, 29, 257

Nather R. E., 1973, Vistas of As., 15, 91

Nather R. E., *et al.*, 1990, ApJ, 361, 309

Nather R. E., 1995, Baltic Astro., 4, 321

Nitta A., 1999, *11th European Workshop on White Dwarf Stars*, eds. J.-E. Solheim and E. Meistas, (San Francisco: ASP), 104

O'Donoghue D., 1986, *Seismology of the Sun ans Distant Stars*, eds D. Gough (Cambridge University Press: Cambridge), 467

O'Donoghue D., 1988, *South African Journal of Science*, 84, 503

O'Donoghue D., Warner B., Cropper M., 1992, MNRAS, 258, 415, 1992.

O'Donoghue D., 1994, MNRAS, 270, 222

O'Donoghue D., 1995, Ap&SS, 230, 63

Osaki Y., Hansen C. J., 1973, ApJ, 185, 277

Ostriker J. P., Tassoul J. L., 1968, Nature, 219, 577

Pasachoff J. M., 1989, *Contemporary Astronomy*, Saunders College Publishing

Ritter A, 1879, Wiedemanns Ann, 8, 179

Ritter A, 1881, Wiedemanns Ann, 13, 366

Roberts D. H., *et al.*, 1987, AJ, 93(4), 968

Robinson E. L., Nather R. E., McGraw J. T., 1976, ApJ, 210, 211

Robinson E. L., 1979, *White Dwarfs and Variable Degenarate Stars*, eds H. M. Van Horn and V. Weideman (Rochester, N.Y., University of Rochester Press), 343

Robinson E. L., Kepler S. O., Nather R. E., 1982, ApJ, 259, 219

Rosenthal C. S., Gough D. O., 1994, ApJ, 423, 488

Rudenko O. V., Soluyan S. I., 1977, *Theoretical Foundations of Nonlinear Acoustics*, Plenum Publishing Corp., New-York

Sauvenier-Goffin E., 1949, Ann. D.Ap, 12 39

Scargle J. D., 1981, ApJS, 45, 1

Scargle J. D., 1982, ApJ, 263, 835

Schatzman E., 1958, *White Dwarfs*, (Amsterdam: North Holland)

Schwarzschild B., 1995, Physics Today, 48, 5, 19

Silvotti R., *et al.*, 1997, *White Dwarfs*, eds. J. Isern, M. Hernanz, and E. García-Berro (Kluwer: Dodrecht), 489

Simon N. R., Cox A. N., Hodson S. W., 1980, ApJ, 237, 550

Smith M. A., 1980, *Nonradial and Nonlinear Stellar Pulsation*, eds. H. A. Hill and W. A. Dziembowski (Springer-Verlag: Berlin), 60

Stellingwerf R. F., 1974, ApJ, 192, 139

Stellingwerf R. F., 1975, ApJ, 195, 441

Stover R. J., *et al.*, 1980, ApJ, 240, 865

Strohmeier W., 1972, *Variable Stars*, Pergamon Press Ltd., Oxford

Tassoul M., 1980, ApJS, 43, 469

Thuras A. L., Jenkins R. T., O'Neil H. T., 1935, J. Acoustic Soc. Am., 6, 173

Tolstoy I., 1963, *Revue of Modern Physics*, 35, 207

Tuggle R. S., Iben I., 1972 ApJ, 178, 455

Unno W., *et al.*, 1989, *Nonradial Oscillations of Stars*, 2nd ed., University of Tokyo Press, Tokyo

Van Kerkwijk M. H., 1999, in press

Von Sengbusch K., 1970, Mitt. Astro. Ges., 32, 228

Vuille F., 1998, 11th *European White Dwarf Workshop*, eds. J.-E. Solheim & E. Meištas (San Francisco: ASP), 109

Warner B., Nather R. E., 1970, MNRAS, 147, 21

Warner B., Nather R. E., 1972, MNRAS, 156, 1

Warner B., Robinson E. L., 1972, Nature, 239, 2

Willstrop R. V., 1969, Nature, 221, 1023

Winget D. E., 1981, PhD Thesis, University of Rochester, New York

Winget D. E., Van Horn H. M., Hansen C. J., 1981, ApJ, 245, L33

Winget D. E., Fontaine G., 1982, *Pulsations in Classical and Cataclysmic Variable Stars*, eds. J. P. Cox, and C. J. Hansen (Boulder Joint Institute for Astrophysics), 46

Winget D. E., Robinson E. L., Nather R. E., 1982, ApJ, 262, L11

Winget D.E., Van Horn H.M., 1982, *Sky & Telescope*, 216

Winget D.E., *et al.*, 1982, ApJ, 253, L29

Winget D. E., *et al.*, 1982b, ApJ, 252, L65

Winget D. E, Hansen C. J, Van Horn H. M, 1983, Nature, 303, 781

Winget D.E et al, 1987, ApJ, 315, L77

Winget D. E., 1988, *Advances in Helio- and Asteroseismology*, eds. J. Christensen-Dalsgaard & S. Frandsen (Dordrecht: Reidel), 305

Winget D. E., 1991, *White Dwarfs*, eds. G. Vauclair and E. Sion (Kluwer Academic Publisher), 129

Winget D. E., *et al.*, 1994, ApJ, 430, 839

Wu Y., 1997, *White Dwarfs*, eds. I. Isern *et al.* (Kluwer Academic Publisher), 467

Wu Y., 1997, PhD Thesis, California Institute of Technology, Passadena, California

Wu Y., Goldreich P., 1999, submitted